Optimization of Fungal Aryl-Alcohol Oxidases for the Production of Flavor, Fragrances and Value-added Aldehydes

Inaugural-Dissertation

zur Erlangung des Doktorgrades
der Mathematisch-Naturwissenschaftlichen Fakultät
der Heinrich-Heine-Universität Düsseldorf

vorgelegt von

Nina Jankowski
aus Duisburg

Düsseldorf, September 2023

aus dem Institut für Biochemie II
der Heinrich-Heine-Universität Düsseldorf

Gedruckt mit der Genehmigung der
Mathematisch-Naturwissenschaftlichen Fakultät der
Heinrich-Heine-Universität Düsseldorf

Berichterstatter:

1. Prof. Vlada B. Urlacher

2. Apl. Prof. Martina Pohl

Tag der mündlichen Prüfung:
9. April 2024

Eidesstattliche Erklärung

Ich versichere an Eides Statt, dass die Dissertation von mir selbstständig und ohne unzulässige fremde Hilfe unter Beachtung der „Grundsätze zu Sicherung guter wissenschaftlicher Praxis an der Heinrich-Heine-Universität Düsseldorf“ erstellt worden ist.

Die Dissertation wurde in der vorgelegten oder in ähnlicher Form noch bei keiner anderen Institution eingereicht. Ich habe bisher keine erfolglosen Promotionsversuche unternommen.

Düsseldorf, den _____ _____

(Nina Jankowski)

I. List of Publications

Jankowski, N., Koschorreck, K. & Urlacher, V. B. (**2020**) High-level expression of aryl-alcohol oxidase 2 from *Pleurotus eryngii* in *Pichia pastoris* for production of fragrances and bioactive precursors. *Appl. Microbiol. Biotechnol.* 104, 9205-9218, doi:10.1007/s00253-020-10878-4

Jankowski, N., Urlacher, V. B. & Koschorreck, K. (**2021**) Two adjacent C-terminal mutations enable expression of aryl-alcohol oxidase from *Pleurotus eryngii* in *Pichia pastoris*. *Appl. Microbiol. Biotechnol.* 105, 7743-7755, doi:10.1007/s00253-021-11585-4

Lappe, A., **Jankowski, N.**, Albrecht, A. & Koschorreck, K. (**2021**) Characterization of a thermotolerant aryl-alcohol oxidase from *Moesziomyces antarcticus* oxidizing 5-hydroxymethyl-2-furancarboxylic acid. *Appl. Microbiol. Biotechnol*. 105, 8313-8327, doi:10.1007/s00253-021-11557-8

Jankowski, N. & Koschorreck, K. (**2022**) Agar plate assay for rapid screening of aryl-alcohol oxidase mutant libraries in *Pichia pastoris*. *J. Biotechnol.* 346, 47-51, doi:10.1016/j.jbiotec.2022.01.006

Jankowski, N., Koschorreck, K. & Urlacher, V. B. (**2022**) Aryl-alcohol-oxidase-mediated synthesis of piperonal and other valuable aldehydes. *Adv. Synth. Catal.* 364, 2364-2372, doi:10.1002/adsc.202200381

II. Conference Contributions

Jankowski, N. (**2018**). Characterization of a fungal aryl-alcohol oxidase from *Pleurotus eryngii* expressed in *Pichia pastoris; 9th OxiZymes Conference,* 8 - 10th July 2018, Belfast, United Kingdom (Oral presentation)

Jankowski, N. & Urlacher, V. B. (**2019**). A novel aryl-alcohol oxidase from *Pleurotus eryngii* produced in *Pichia pastoris*. *14th International Symposium on Biocatalysis and Biotransformations (BioTrans)*, 7 - 11th July 2019, Groningen, The Netherlands (Poster)

III. Table of Contents

IV. Abstract

Aryl-alcohol oxidases (AAOs) are FAD-containing fungal oxidoreductases that catalyze the oxidation of primary aromatic or allylic alcohols to the corresponding aldehyde or, if present as *gem*-diol, to the acid with the concomitant reduction of O_2 to H_2O_2. In nature, these enzymes are secreted by white-rot wood-decaying fungi and participate in the degradation of lignin, the world's second most abundant natural heteropolymer. The biotechnological exploitation of AAOs is mainly aiming at the production of valuable aldehydes such as the flavors and fragrances benzaldehyde and *trans*-2-hexenal, the production of acids such as 2,5-furandicarboxylic acid (FDCA), a precursor for polyethylene furanoate (PEF) with high prospects of substituting fossil-based polymers, or the enzymatic supply of H_2O_2 to peroxidase or peroxygenase-catalyzed reactions. Another potential application lies in the participation of AAOs in efficient lignin utilization. However, the number of characterized AAOs is still very low, because the biochemical and structural investigation of these enzymes, as well as their broader application, has been largely hampered by the low production in native fungal hosts. Moreover, the reported heterologous systems often did not lead to higher enzyme titres as compared to production by native fungal hosts. Therefore, to explore and finally utilize AAOs' full potential as biocatalysts, an efficient expression system is required to provide the recombinant enzymes at high yields and their substrate scope and catalytic potential need to be investigated.

Only a few examples of sufficient AAO expression in recombinant yeasts have been published, which urged us to search for new AAO-encoding genes for heterologous expression. The methylotrophic yeast *Pichia pastoris* (recently re-classified as *Komagataella phaffii*) was chosen as expression host, because it can efficiently produce recombinant proteins and enables

their glycosylation. The genes encoding five AAOs were heterologously expressed in *P. pastoris* (Chapter I). Two of them were produced in secreted form in fed-batch processes at high yields of 315 mg/l for *Pe*AAO2 from *Pleurotus eryngii* P34 and 750 mg/l for *Ma*AAO from *Moesziomyces antarcticus* (Chapters II and III). The thorough biochemical investigation of *Pe*AAO2 and *Ma*AAO has revealed that both enzymes are promising biocatalysts, since they are thermo- and pH stable, and convert a wide range of substrates with high activity. Moreover, a handful of previously unknown AAO substrates was identified, whose products find application as flavor and fragrance compounds or pharmaceutical building blocks.

The amino acid sequence alignment of *Pe*AAO2 and the non-expressible in *P. pastoris* *Pe*AAO1 from a different *P. eryngii* substrain showed that the two enzymes differ in only 7 amino acids in the mature protein (Chapter IV). Iterative introduction of the respective amino acids from *Pe*AAO2 into *Pe*AAO1 led to the generation of *Pe*AAO1 variant ER, which contained two adjacent amino acid exchanges (K583E/Q584R) and achieved even higher activity in cell-free supernatant than wild-type *Pe*AAO2, after expression and secretion by *P. pastoris*. The homology model of the variant ER indicated a newly formed salt bridge at position 583, which is not present in the wild-type *Pe*AAO1 and may therefore improve protein folding and stability of the respective variant.

A new agar plate based activity assay was developed for the rapid screening of *P. pastoris* mutant libraries for improved activity towards selected substrates (Chapter V). Several strains expressing *Pe*AAO1 variants and wild-type *Pe*AAO2 were used for assay validation. The correlation between the observed volumetric activity in a liquid spectrophotometric assay and the color development on the agar plate underscores the usability and reliability of this assay for the rapid identification of the AAO variants with improved activity. In directed evolution campaigns involving the introduction of multiple random

mutations and the generation of hundreds of individual *P. pastoris* transformants, the secretion and activity towards a specific substrate can be easily visualized using this agar plate based assay without the need for laborious cultivation in liquid medium, thus reducing the material, cost and time required.

Oxidation of two newly discovered AAO substrates lead to the corresponding products piperonal and *trans*-2-*cis*-6-nonadienal. Both aldehydes are of considerable interest to the flavor and fragrance industry, because they are fragrances with very pleasant odors. Produced via AAO-catalyzed reactions they can be advertised as "natural fragrance", meeting consumer demand for all-natural products. The biocatalytic production of piperonal was optimized on a small scale with respect to substrate concentration, shaking speed and temperature. The addition of catalase to degrade H_2O_2 and to re-introduce O_2 was found to be essential and resulted in almost full conversion of 300 mM substrate within 44 h under optimized conditions (Chapter VI). The reaction was then scaled up to 10 ml volume, and the preparative production of piperonal resulted in a space-time yield of 9.5 g/l/h. The product was obtained with a high product yield of 85 % and more than 99 % purity via a simple extraction with *n*-hexane. *trans*-2-*cis*-6-Nonadienal and cuminal were produced under the same optimized conditions on a small scale. Cuminal, the oxidation product of cumic alcohol, is reported to possess various therapeutic effects such as anticancer and antidiabetic. Its AAO-mediated biocatalytic production could be of interest to the pharmaceutical industry.

Taken together, the newly discovered and characterized AAOs, *Pe*AAO2 and *Ma*AAO, have demonstrated their high potential as biocatalysts with applications in the synthesis of potent pharmaceutical and flavor and fragrance compounds.

V. Zusammenfassung

Arylalkohol-Oxidasen (AAOs) sind FAD-haltige Oxidoreduktasen aus Pilzen, die die Oxidation primärer aromatischer oder allylischer Alkohole zu den entsprechenden Aldehyden oder, wenn *gem*-Diole vorliegen, zur Säuren, katalysieren, wobei gleichzeitig O_2 zu H_2O_2 reduziert wird. In der Natur werden diese Enzyme von holzzersetzenden Weißfäulepilzen ausgeschieden und sind am Abbau des Pflanzenmaterials Lignin, dem zweithäufigsten natürlichen Heteropolymer der Welt, beteiligt. Die biotechnologische Nutzung von AAOs zielt vor allem auf die Produktion von wertvollen Aldehyden wie die Aroma- und Duftstoffe Benzaldehyd und *trans*-2-Hexenal, auf die Produktion von Säuren wie 2,5-Furandicarbonsäure (FDCA), einer Vorstufe für Polyethylenfuranoat (PEF), das fossile Polymere ersetzen könnte, oder auf die enzymatische Bereitstellung von H_2O_2 für Peroxidase- oder Peroxygenase-katalysierte Reaktionen ab. Eine weitere mögliche Anwendung ist die Beteiligung von AAOs an einer effizienten Ligninverwertung. Die Zahl der charakterisierten AAOs ist jedoch noch sehr gering, da die biochemischen und strukturellen Untersuchungen dieser Enzyme sowie ihre breitere Anwendung durch die geringe Produktion in nativen Pilzwirten weitgehend beeinträchtigt wurden. Darüber hinaus führte die Produktion in heterologen Systemen oft zu kaum höheren Ausbeuten als die Produktion in nativen Pilzwirten. Um jedoch das volle Potenzial von AAOs als Biokatalysatoren erforschen und nutzen zu können, müssen die rekombinanten Enzyme mit hoher Ausbeute hergestellt, und ihr Substratspektrum sowie ihre physikalischen Eigenschaften untersucht werden.

Es wurden nur wenige Beispiele für die sekretorische Produktion mit Hefeexpressionssystemen mit ausreichend hohen Produktausbeuten veröffentlicht, was die Suche nach AAO-kodierenden Genen für die heterologe Expression veranlasste. Die

methylotrophe Hefe *Pichia pastoris* (re-klassifiziert als *Komagataella phaffii*) wurde als Expressionswirt ausgewählt, da sie effizient rekombinante Proteine herstellt und deren Glykosylierung ermöglicht. In dieser Arbeit wurden die Gene, die für fünf AAOs kodieren, rekombinant in *P. pastoris* exprimiert (Kapitel I), und zwei von ihnen wurden sezerniert und in Fed-Batch-Verfahren in hohen Ausbeuten von 315 mg/l für *Pe*AAO2 aus *Pleurotus eryngii* P34 und 750 mg/l für *Ma*AAO aus *Moesziomyces antarcticus* produziert (Kapitel II und III). Die eingehende biochemische Untersuchung von *Pe*AAO2 und *Ma*AAO ergab, dass beide Enzyme vielversprechende Biokatalysatoren sind, da sie thermo- und pH-stabil sind und ein breites Spektrum von Substraten mit hoher Aktivität umsetzen. Darüber hinaus wurde eine Handvoll bisher unbekannter AAO-Substrate identifiziert, deren Produkte als Aroma- und Duftstoffe oder pharmazeutische Bausteine Verwendung finden.

Das Aminosäuresequenz-Alignment von *Pe*AAO2 und der in *P. pastoris* nicht exprimierbaren *Pe*AAO1 aus einem anderen *P. eryngii*-Unterstamm zeigte, dass sich die beiden Enzyme in 7 Aminosäuren im reifen Protein unterscheiden (Kapitel IV). Die iterative Einführung der entsprechenden Aminosäuren aus *Pe*AAO2 in *Pe*AAO1 führte zur Erzeugung der *Pe*AAO1-Variante ER, die zwei benachbarte Aminosäureaustausche (K583E/Q584R) enthielt und im zellfreien Expressionsüberstand sogar eine höhere Aktivität als der Wildtyp *Pe*AAO2 aufwies. Das Homologiemodell der ER-Variante wies auf eine neu gebildete komplexe Salzbrücke an Position 583 hin, die sich im Wildtyp-*Pe*AAO1 nicht ausbilden kann und somit die Proteinfaltung und -stabilität der entsprechenden Variante verbessern könnte.

Es wurde ein neuer, auf Agarplatten basierender Aktivitätstest für das schnelle Screening von *P. pastoris*-Mutantenbibliotheken auf erhöhte Aktivität gegenüber ausgewählten Zielsubstraten entwickelt (Kapitel V). Zur Validierung des Assays wurden mehrere *P. pastoris* Stämme verwendet, die *Pe*AAO1-Varianten und den Wildtyp *Pe*AAO2 exprimieren. Die

Korrelation zwischen der beobachteten volumetrischen Aktivität in einem flüssigkeitsbasierten spektrophotometrischen Assay und der Farbentwicklung auf einer Agarplatte unterstreicht die Nützlichkeit und Zuverlässigkeit dieses Assays für die schnelle Identifizierung von AAO-Varianten mit höherer Aktivität. In gezielten Evolutionskampagnen, in denen mehrere Zufallsmutationen eingeführt und Hunderte von individuellen *P. pastoris*-Transformanten erzeugt werden, kann die Sekretion und Aktivität gegen ein bestimmtes Substrat mit diesem auf Agarplatten basierenden Assay leicht sichtbar gemacht werden, ohne dass eine mühsame Kultivierung in Flüssigmedium erforderlich ist, was den Material-, Kosten- und Zeitaufwand reduziert.

Unter den neu entdeckten AAO-Substraten sind die entsprechenden Produkte Piperonal und *trans*-2-*cis*-6-Nonadienal für die Aromen- und Duftstoffindustrie von großem Interesse, da es sich bei beiden um Duftstoffe mit sehr angenehmen Geruch handelt, die als "natürliche Aromen" beworben werden können und damit dem Wunsch der Verbraucher nach natürlichen Produkten entgegenkommt. Die biokatalytische Herstellung von Piperonal wurde im kleinen Maßstab hinsichtlich Substratkonzentration, Schüttelgeschwindigkeit und Temperatur optimiert. Die Zugabe von Katalase zum Abbau von H_2O_2 und zur Rückführung von O_2 erwies sich als unerlässlich und führte unter den optimierten Bedingungen zu einer nahezu vollständigen Umsetzung von 300 mM Substrat innerhalb von 44 Stunden (Kapitel VI). Die Reaktion wurde dann auf ein Reaktionsvolumen von 10 ml hochskaliert und die präparative Herstellung von Piperonal führte zu einer Raum-Zeit-Ausbeute von 9,5 g/l/h. Das Produkt wurde in einem einfachen Extraktionsschritt mit *n*-Hexan mit einer hohen Produktausbeute von 85 % und einer Reinheit von mehr als 99 % isoliert. *Trans*-2-*cis*-6-Nonadienal und Cuminal wurden unter den gleichen optimierten Bedingungen in kleinem Maßstab hergestellt. Cuminal, das Oxidationsprodukt von Cuminalalkohol, soll Berichten zufolge verschiedene

therapeutische Wirkungen, wie z. B. krebshemmend und antidiabetisch haben. Seine AAO-vermittelte biokatalytische Produktion könnte für die pharmazeutische Industrie von Interesse sein.

Insgesamt konnte das hohe Potenzial der neu entdeckten und charakterisierten AAOs, *Pe*AAO2 und *Ma*AAO, als Biokatalysatoren für die Synthese von pharmazeutisch wirksamen Verbindungen sowie von Aroma- und Duftstoffen gezeigt werden.

VI. Abbreviations

°C	degree celsius	mg	milligram
µg	microgram	min	minute
µl	microliter	ml	milliliter
µM	micromolar	mm	millimeter
5-HMF	5-hydroxymethylfurfural	mM	millimolar
A. nidulans	*Aspergillus nidulans*	MnP	manganese peroxidase
AA	auxiliary activity	*Mr*AAO3	AAO3 from *Moniliophthora roreri* MCA 2997
AAO	aryl-alcohol oxidase	NAD(P)H	Nicotinamide adenine dinucleotide (phosphate)
aao	gene encoding for an aryl-alcohol oxidase	NCBI	National Center for Biotechnology Information
AADH	aryl-alcohol dehydrogenase	NER	*Pe*AAO1 variant harboring D361N/K583E/Q584R mutations
ADP	adenosine diphosphate	ng	nanogram
AER	*Pe*AAO1 variant harboring V367A/K583E/Q584R mutations	nm	nanometer
AOX1	alcohol oxidase 1	OD_{600}	optical density at 600 nm
BMGY	buffered complex glycerol medium	*P. eryngii*	*Pleurotus eryngii*
BMMY	buffered minimal methanol medium	*P. pastoris*	*Pichia pastoris*
cDNA	complementary DNA	*P. pulmonarius*	*Pleurotus pulmonarius*
CDS	coding sequence	PAGE	polyacrylamide gel electrophoresis
cm	centimeter	P_{AOX1}	promoter of alcohol oxidase 1
Da	dalton	*Pe*AAO1	AAO from *Pleurotus eryngii* ATCC 90787
DNA	desoxyribonucleic acid	*Pe*AAO2	AAO2 from *Pleurotus eryngi*i P34
E. coli	*Escherichia coli*	PEF	polyethylene furanoate
EC	enzyme commission	PET	polyethylene terephthalate
ER	*Pe*AAO1 variant harboring K583E/Q584R mutations	*Pp*AAO1	AAO1 from *Pleurotus pulmonarius* CBS 507.8
EV	empty vector	rpm	revolutions per minute
FAD	flavin adenine dinucleotide	s	second
FDCA	2,5-furandicarboxylic acid	*S. cerevisiae*	*Saccharomyces cerevisiae*
g	gram	SDS	sodium dodecyl sulfate
GMC	glucose-methanol-choline	SN	supernatant
GMO	genetically modified organism	TCA	trichloroacetic acid
h	hour	TRIS	tris(hydroxymethyl)aminomethane
kDa	kilodalton	U	Unit, µmol/min
kV	kilovolt	U/l	volumetric activity, unit per liter
l	liter	*v/v*	volume percent
LB	lysogeny broth	VP	versatile peroxidase
LiP	lignin peroxidase	*w/v*	weight percent
LME	lignin-modifying enzymes	X	x-fold
LDA	lignin-degrading auxiliary enzymes	x *g*	centrifugal force
M	molar	Xaa	any amino acid
M. roreri	*Moniliophthora roreri*	YPDS	yeast peptone dextrose sorbitol
*Ma*AAO	AAO from *Moesziomyces antarcticus* JCM 10317	zeo	zeocin
*Ma*GMC1	former name of *Ma*AAO	ε_{310}	molar extinction coefficient at 310 nm

1. Introduction

1.1. Green Chemistry and the Role of Biocatalysis

"Green chemistry" plays an important role in tackling the growing demand for consumer materials as the world's population is rapidly increasing. The current world population reached the milestone of 8 billion as of November 2022 and is expected to further grow by another 25 % over the next 40 years, according to the United Nations.[1]

The increasing amount of chemical waste from various production routes concomitant with the increase of the world's population has led to considerable concern and environmental awareness and initiated a reassessment of traditional chemical processes in the 1980s. Instead of treatment and clarification of chemical waste produced, the emphasis was put on the urgent need of waste prevention. These considerations, among others, led to the development of the term "green chemistry" by the U.S. Environmental Protection Agency in the 1990s and the concept of green chemistry has been summarized by Roger A. Sheldon as follows:

"Green chemistry efficiently utilises (preferably renewable) raw materials, eliminates waste and avoids the use of toxic and/or hazardous reagents and solvents in the manufacture and application of chemical products."[2]

A more precise definition was manifested in the "12 Principles of Green Chemistry" (Table 1).[3] These principles cover the entire scope of a chemical process starting from the raw materials to the solvents and catalysts used, and the degradability of the final product.[4] The green chemistry approach aims at converting the entity of a chemical process to a more sustainable alternative without focusing only on certain "problems". Most dominantly, the transition to renewable feedstocks in an economy based on non-renewable fossil resources is

one of the greatest challenges of adopting green chemistry principles, and the use of renewable feedstocks would at the same time simplify the prevention of chemical waste.

The main factors that add up to the amount of chemical waste generated include the nature and amount of organic or inorganic chemicals used in a particular process. The impact of these factors can be reduced through the use of catalysis – either homologous, heterologous or biocatalysis.[3] In using catalysis, the necessary amount of a certain reagent is lowered from a stoichiometric to a catalytic amount, which is more atom- and step-economical, thus drastically reducing waste production in a given chemical process.[4,5] Among the different types of catalytic reactions, biocatalysis plays a pivotal role in the transition to a greener and more sustainable economy, and the use of biocatalytic reactions instead of classical chemical reactions is in great agreement with the principles of green chemistry (Table 1).[3]

Table 1 The 12 principles of green chemistry and the respective contribution of biocatalysis. Adapted from Sheldon and Woodley.[3]

	Green chemistry principle	**Biocatalysis**
1	Waste prevention	Significantly reduced waste
2	Atom economy	More atom- and step-economical
3	Less hazardous syntheses	Generally low toxicity
4	Design for safer products	Not relevant *
5	Safer solvents and auxiliaries	Usually performed in water
6	Energy efficiency	Mild conditions/energy-efficient
7	Renewable feedstocks	Enzymes are renewable
8	Reduced derivatization	Avoids protection/deprotection steps
9	Catalysis	Enzymes are catalysts
10	Design for degradation	Not relevant *
11	Real-time analysis	Applicability to biocatalytic processes
12	Inherently safer processes	Mild and safe conditions

* Biocatalytic product is considered, not the process itself.

Biocatalytic processes can be performed in different setups, but all processes necessitate specialized proteins, i.e. enzymes that are able to catalyze a particular biocatalytic reaction.[5] In all setups, the first step en route to a biocatalytic process starts with the growth of a microbial culture (Scheme 1), which relies on rather simple ingredients: The culture medium is composed of a carbon- and nitrogen-rich nutrient solution that contains necessary building blocks such as amino acids, carbohydrates, and sometimes buffer components to maintain an optimal pH during growth. Already during the growth of the microbial cells the conversion of a specific substrate by means of intracellularly produced enzymes can be used to produce a desired product, defined as fermentation. In addition to the use of growing cells for biocatalytic processes, cultures after growth in rich culture medium and harvest of the cells can be used as "resting" whole-cell biocatalysts or can be utilized to isolate the specific enzyme of interest (biocatalyst).[5] Isolated biocatalysts are usually applied in aqueous buffered solutions, which is preferred according to the principles of green chemistry, but quite often also tolerate organic solvents – if required for substrate solubilization. The biocatalyst itself is renewable, biodegradable, non-toxic, and non-hazardous, performs well under mild conditions and is quite often more chemo-, regio-, and stereo-selective than classical chemical catalysts, thus conforming to several of the introduced principles of green chemistry.[3,4]

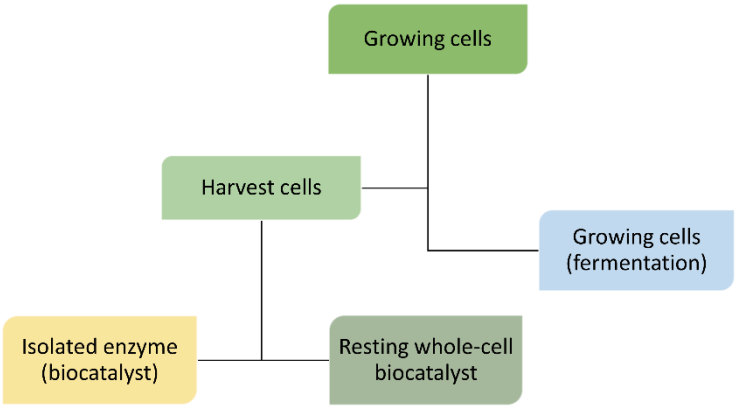

Scheme 1 Classification of biocatalytic processes. Adapted and modified from Sheldon and Brady.[5]

The application of growing cells in fermentations or the growth of cells followed by isolation of the biocatalyst is usually preceded by genetic manipulation, unless native enzymes of the microbial host are used for the biocatalytic reactions in question. Great advances in recombinant DNA technologies over the last 30 years have made it possible to produce a desired biocatalyst with acceptable yields and modified properties (see Chapter 1.2 and Chapter 1.3), which is a important prerequisite for its use in biocatalytic processes and ultimately in an industrial setting.[3]

1.2. Heterologous Production of recombinant Biocatalysts

Microorganisms can be engineered to produce a specific enzyme by introducing a (foreign) target gene, i.e. a DNA sequence encoding the desired enzyme. Through immense progress in DNA sequencing and extensive metagenomic studies, large sets of sequenced genomic material is available in databases and bioinformatic tools assist in identifying genes encoding enzymes with desired properties.[5] The introduction of a foreign gene and its subsequent production in the appropiate microbial host is called heterologous expression, which allows the production of the desired enzyme at large scale with the help of genetically modified host organisms, such as the bacterium *Escherichia coli* or the yeast *Pichia pastoris* (recently reclassified as *Komagataella phaffii*). Various methods and approaches are known to maximize the production yield of hetreologous expression of the desired biocatalyst.[6]

In fermentative biocatalytic processes, the growing genetically modified organisms (GMOs) are supplemented with a substrate in order to fuel the intracellular biocatalytic conversion to yield the desired product. A major advantage of fermentative processes is the involvement of intracellular cofactor recycling systems of the host cell, which is necessary depending on the type of biocatalyst and the catalyzed reaction, and the higher stability of the

target enzyme, as opposed to the lower stability of isolated enzymes. On the other hand, the cell membrane represents a barrier that may be insurmountable for certain substances and the intracellular native enzyme consortium may lead to undesired side reactions that are difficult to avoid.[7]

If the occurrence of side reactions renders the product recovery difficult or leads to low product yields, the alternative of using isolated enzymes for the biocatalytic process may be more promising. This involves removing the enzyme-producing GMOs from the culture medium and releasing the desired biocatalyst from the cells along with other native cellular components. Depending on the substrate specificity of the biocatalyst, crude cell extracts can be applied for biocatalytic processes after harvesting and disruption of the cells, but in most cases (partial) purification of the extract is required to avoid the aforementioned side reactions of other host enzymes present in the crude cell extract.[3,8] Secreted enzymes have significant advantages over their intracellular counterparts. These enzymes are translocated across the cell membrane and released into the medium and therefore significantly lower the amount of contaminant host enzymes. Secreted enzymes undergo proper folding and may contain post-translational modifications such as glycosylation or disulfide bond formation, which are sometimes essential for certain enzymes.[9] Suitable hosts for the secretory production are yeasts such as *Pichia pastoris* or *Saccharomyces cerevisiae.* The target gene must be cloned with a signal sequence that directs the produced enzyme into the secretory pathway and ultimately into the extracellular space. The target enzyme can then be easily removed from the medium via simple centrifugation, and quite often the cell-free supernatant shows sufficient purification degree and can be applied directly in biocatalytic processes, reducing the time and cost of cell disruption and purification steps.[9] Overall, isolated (and purified) biocatalysts may show higher productivities and fewer side reactions, but may be less stable in the reaction setup in contrast

to their use as intracellular biocatalysts[7] and the pros and cons of each approach need to be balanced for each target enzyme and reaction in question.

1.3. Protein Engineering of Biocatalysts

Recent advances in DNA-based technologies have not only simplified the production of biocatalysts with help of recombinant microbial hosts, but have also had a great impact on the modification of biocatalysts at the amino acid level. The concept of protein engineering encompasses various approaches in altering the catalytic and physical properties of enzymes, such as their activity, stability, substrate specificity, selectivity or expression yield. Lutz and Iamurri described the progression of engineering occurring in "four waves" as seen over the last two decades:[10]

i) Isolation of natural enzymes and utilizing their natural activities

ii) Introduction of rational design and directed evolution approaches

iii) Incorporation of structural information in semi-rational approaches

iv) Design of novel enzymes with non-natural activities based on directed evolution, rational and computational design

The amount of knowledge about the target protein greatly dictates the methods used for modification, and there are basically two main approaches: rational and evolutionary methods of protein engineering.[10-12] Structural and mechanistic information about the target protein enables the use of rational protein design to introduce specific mutations in certain regions of the protein with anticipated and predicted changes in protein properties. For example, the replacement of amino acids located in or near the active site of an enzyme can result in significant changes in activity, substrate specificity and selectivity, ultimately leading to the conversion of previously non-natural substrates. However, if no detailed structural or

mechanistic information is available or the rational basis for a desired altered property is unknown, a directed (random) evolutionary approach is more appropiate: random protein mutagenesis is performed on the entire amino acid sequence or on certain regions, resulting in a large variety of protein mutants with unforeseen changed properties.[12] As an example: The production of the anti-diabetic drug sitagliptin can be realized via transamination of prositagliptin, the corresponding ketone.[13] Due to steric hindrances the bulky prositagliptin is not accepted as substrate by transaminases. Savile et al. used a rational computational approach to alter the lining within the binding pockets in a two-step evolution and generated an enzyme variant with initial activity towards prositagliptin. This variant required further optimization to better suit industrial process conditions, i.e. to achieve high substrate conversion under optimized reaction conditions (organic solvent up to 50 % (*v/v*), high temperature of 45 °C and pH 8.5). This was achieved using a directed evolution approach and yielded a final transaminase variant capable of efficient prositagliptin conversion under process conditions with up to 200 g/l product.[13] This example illustrates how both rational and directed evolution approaches can complement each other, but also work well when used separately. The great influence and extraordinary importance of the directed evolution approach is represented by Nobel Prize laureate Frances H. Arnold, who was awarded the 2018 Nobel Prize in Chemistry for "the directed evolution of enzymes".[14]

In all cases, a reliable screening method is indispensable, as the large number of mutants created needs to be evaluated for introduced changes.[12] The utilization of enzymatic activity assays is among the easiest and fastest methods for screening mutant libraries. Quite often surrogate substrates - rather than actual target substrates - are employed to screen for activity enhancement within enzyme mutant libraries. Activity towards these surrogate substrates is often easier to detect, for example, if the conversion product shows spectrophotometric

changes. This is particularly misleading as the activity towards a surrogate substrate does not necessarily correlate with the activity towards a target substrate. In this context, it is important to use a specific target substrate for which an improved activity is desired, rather than using surrogate substrates. Utilizing protein engineering approaches, the increasing importance of biocatalysis in otherwise classical organic syntheses is undeniable, and several hundred biocatalytic processes are in operation, mainly in the pharmaceutical industry, contributing to the transition towards a greener and more sustainable economy.[15]

1.4. Lignocellulose and ligninolytic Enzymes

Not only re-evaluation of classical chemical synthesis, such as the use of biocatalysis, but also the exploration and eventual implementation of alternatives to the use of fossil resources are required in the pursuit for transitioning to a more sustainable economy. However, these alternative resources must meet certain criteria, such as not competing with food production, being CO_2 neutral, and being renewable.[16] Lignocellulose, the main component of the cell walls of woody plants, is a remarkably suitable candidate: it consists of inedible plant material, is widely available, and is constantly produced.[17]

Lignocellulose is composed of three quite distinct components with varying relative proportions: cellulose (40-50 %), hemicellulose (25-30 %) and lignin (10-30 %) (Figure 1A).[18] Crystalline cellulose fibers consist exclusively of β-1,4-linked D-glucose units of up to 10,000 monomers and are the most abundant natural polymer. These fibers are embedded in a matrix consisting of hemicellulose, composed of various branched pentose and hexose sugars, and lignin, a cross-linked heteropolymer composed of phenolic units.[16,18,19] These components are tightly packed and arranged into microfibrils. These microfibrils are in turn grouped into macrofibrils, which are the major component of the plant cell wall (Figure 1A).[20] These

structures provide a strong, rigid barrier against microbial degradation, while also exhibiting unique structural properties that allow the plant to remain flexible as it grows, support its own weight, and enable the transport of water without swelling of the plant material.[17]

Lignin, the second most abundant natural polymer and the most recalcitrant and disordered component of lignocellulosic biomass, is composed of three phenolic subunits called monolignols, which differ only in the number of substituent methoxy groups: *p*-coumaryl alcohol (H), coniferyl alcohol (G) and sinapyl alcohol (S) (Figure 1B).[19] The highly irregular pattern of cross-linked monolignol units is established by free radical formation and yields a plethora of different C-C and C-O bonds, such as β-O-4 aryl ethers, β-β resinol bonds or 5-5 biphenyl bonds.[19,21]

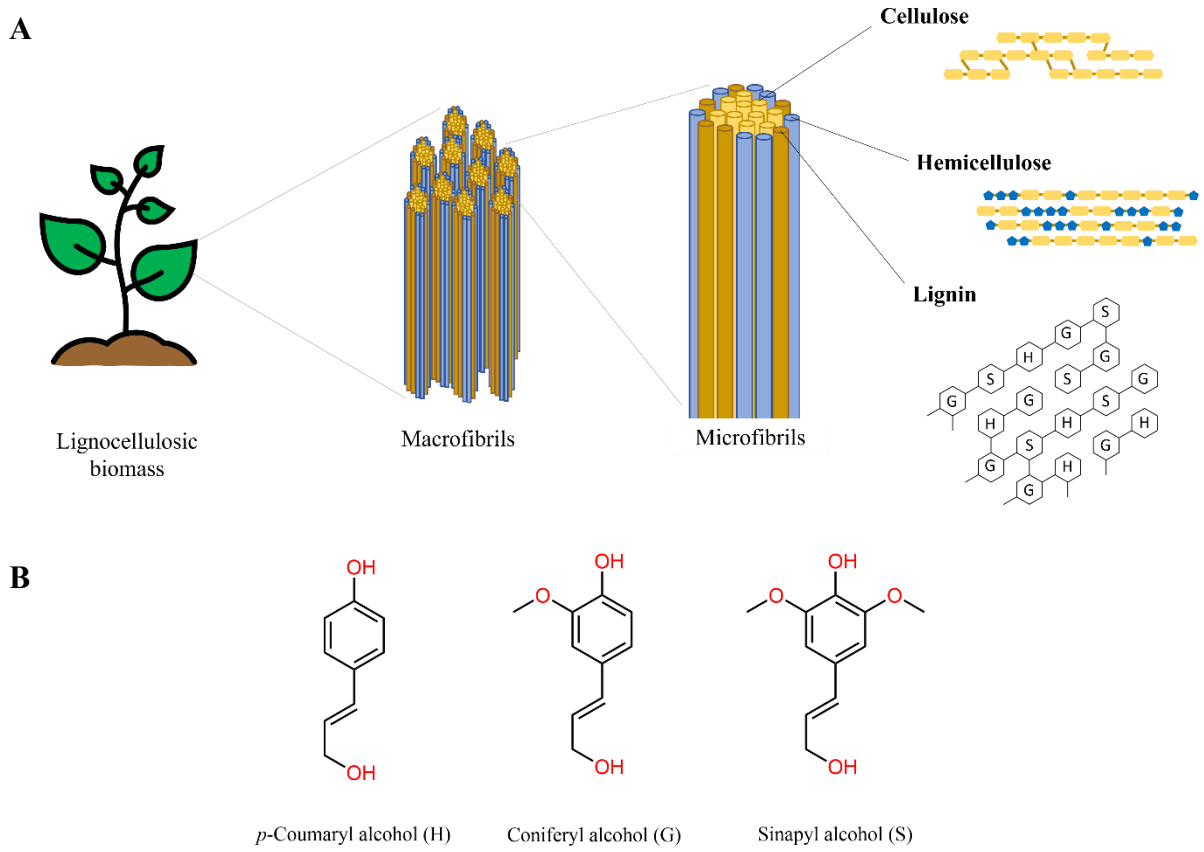

Figure 1 Composition of lignocellulosic biomass. **(A)** Microfibrils are composed of crystalline cellulose and hemicellulose fibers, surrounded by the cross-linked heteropolymer lignin, which in turn are grouped as macrofibrils. Lignin units: *p*-coumaryl alcohol (H), coniferyl alcohol (G) and sinapyl alcohol (S). Adapted from Streffer et al. and Bertella et al.[18,20] **(B)** Structures of the three monolignols representing the building blocks of lignin.

Wood-decaying fungi have specialized pathways to efficiently break down and utilize the different components of lignocellulose, in particular lignin, by secreting an "enzymatic cocktail" tailored to the particular lignocellulose composition.[19] Two main types of fungi have evolved to degrade lignocellulosic biomass: White-rot and brown-rot fungi. Brown-rot fungi preferentially degrade the sugary components, leaving the brownish lignin mostly behind, while two distinct groups of white-rot fungi have evolved to either convert lignin, leaving the whitish cellulose and hemicellulose untouched, or to convert all lignocellulose components simultaneously.[19,21]

The ligninolytic cocktail of white-rot fungi comprises of several oxidative activities and can be divided into two subgroups: lignin-modifying enzymes (LMEs) and lignin-degrading auxiliary enzymes (LDAs).[17] LMEs are capable of directly attacking the lignin polymer and include lignin peroxidases (LiP; EC 1.11.1.14), manganese peroxidases (MnP; EC 1.11.1.13), versatile peroxidases (VP; EC 1.11.1.16), and laccases (EC 1.10.3.2) (Figure 2).[17,19]

Peroxidases require H_2O_2 as a co-substrate, which is provided by members of the LDA subgroup. This subgroup includes oxidases active on lignin metabolites or other small molecules, like aryl-alcohol oxidases (AAO; EC 1.1.3.7), glyoxal oxidases (EC 1.2.3.5), pyranose 2-oxidases (EC 1.1.3.10), cellobiose dehydrogenases (EC 1.1.99.18), and glucose oxidases (EC 1.1.3.4).[17] In particular, AAOs oxidize aromatic alcohols in a cycling reaction with intracellular aryl-alcohol dehydrogenases (AADH; EC 1.1.1.90) and ultimately yield H_2O_2, which is consumed by peroxidases of the LME subgroup. In a second application, the H_2O_2 produced is involved in the generation of reactive hydroxyl species via the Fenton reaction, which are capable of directly attacking the lignin heteropolymer (Figure 2).[17,22]

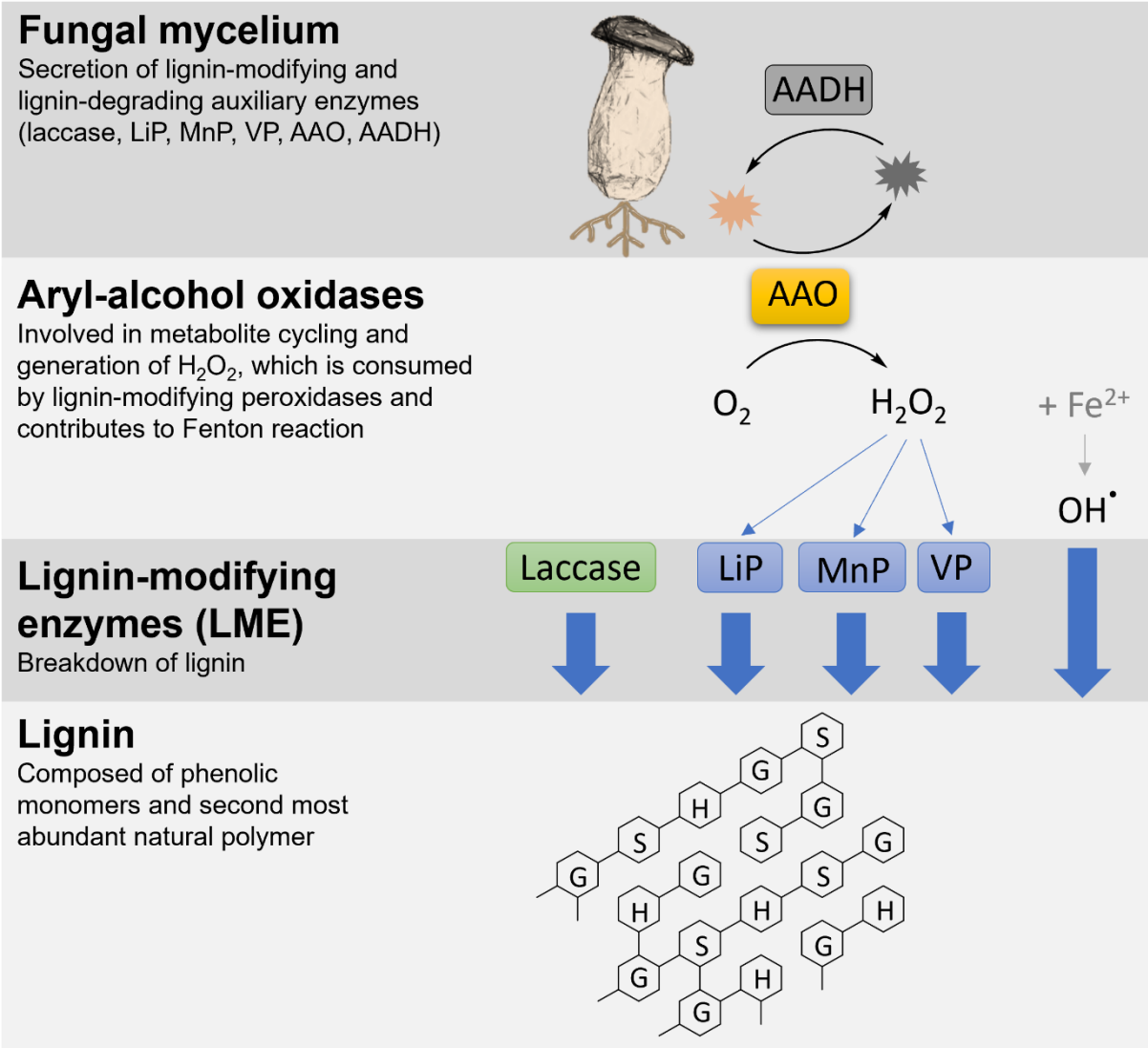

Figure 2 Fungal enzymes involved in lignocellulose breakdown. Lignin-modifying enzymes (LMEs) such as laccases and peroxidases (LiP, MnP, VP) are capable of direct attack on the lignin polymer. Peroxidases are fuelled by H_2O_2 producing enzymes categorized as lignin-degrading auxiliary enzymes (LDAs) like aryl-alcohol oxidases (AAO), which in turn oxidize fungal metabolites in conjunction with mycelium-associated aryl-alcohol dehydrogenases (AADH). The generated H_2O_2 is also used to fuel the Fenton reaction to create reactive hydroxyl species.

The use of lignocellulose on an industrial scale is mainly restricted to its use in the pulp and paper industry and for the production of bioethanol, which uses the carbohydrate-containing cellulose fraction.[16] The valorization of heteropolymeric lignin in industrial processes is hampered by its high degree of complexity and diversity of chemical bonds present, and it is therefore usually considered as a low-value by-product and burned as an energy source in the pulp and paper industry.[4] To enable the efficient utilization of lignin and to fully uncover

its potential as a renewable feedstock, processes are needed that allow the controlled and selective cleavage of the C-C and C-O bonds, which could release monomeric aromatic units and would thus render lignin a valuable and renewable source for aromatic species.[19] Much emphasis is placed on the development of effective and sustainable processes for the conversion of lignin into value-added products and the elucidation of the microbial strains and enzymes involved, as summarized and discussed in many recent reviews and book chapters.[16,21,23-26]

From a sustainability point of view, the use of a biological approach or biocatalysis to adress the problems of lignin valorization is preferred, as engineered microbial strains or recombinant enzyme cocktails can be considered as originating from renewable sources and their production reduces chemical waste. The use of engineered microbial strains and engineered metabolic pathways show promising developments and have resulted in lignin-derived products such as the flavor compound vanillin or the plastics precursor *cis,cis*-muconic acid.[27,28] One aspect towards a sustainable approach to utilize lignin is the in-depth analysis and, in addition, the high-yield heterologous production of enzymes involved in lignin degradation to enable the biocatalytic conversion of lignin preparations to eventually produce value-added products.

1.5. Fungal Aryl-Alcohol Oxidases

As previously outlined, aryl-alcohol oxidases (AAOs) play an essential role in lignin degradation. These fungal flavoenzymes are oxidoreductases active on primary aromatic or allylic hydroxyl donor groups with O_2 as the terminal electron acceptor (EC 1.1.3.7), yielding an aldehyde (or acid) and H_2O_2 as products, which in turn is required by ligninolytic peroxidases (Scheme 2).[29]

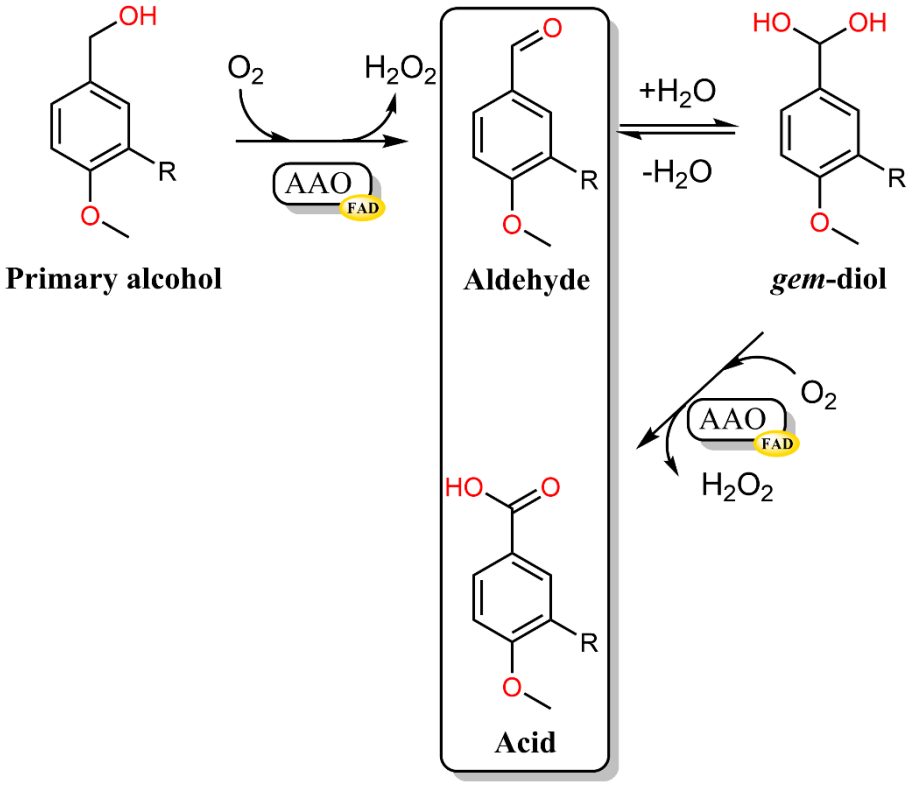

Scheme 2 Enzymatic reaction catalyzed by aryl-alcohol oxidases (AAO). The (aromatic) primary alcohol is oxidized to yield the corresponding aldehyde with concomitant reduction of O_2 to H_2O_2. If the aldehyde is present in its hydrated version (*gem*-diol) it might further serve as substrate and yield an acid as product.

1.5.1. A brief History of AAOs

The discovery of AAOs began in 1955, when Henderson observed the accumulation of aromatic aldehydes and acids after incubation of sawdust with white-rot fungus *Polystictus versicolor* (synonym of *Trametes versicolor*).[30] It was hypothesized that fungal extracellular enzymes were involved in the initial attack on lignin, as the identified compounds were thought

to be products of lignin degradation. As the insight on biological lignin degradation and enzymes involved was scarce at the time, these findings prompted further research into the extracellular enzymes of *P. versicolor*.

Farmer et al. first described the presence of an "aromatic alcohol oxidase" (i.e. AAO) in 1960 when activity towards several aromatic primary alcohols concomitant with aldehyde and H_2O_2 production was identified in the liquid medium of *P. versicolor*, marking the "birth" of AAOs.[31] In the late 1980s and early 1990s, several other reports of "aromatic alcohol oxidases" or "veratryl alcohol oxidases" emerged, all describing AAO activity in culture liquids of different fungal species, mostly representatives of the genus *Pleurotus,* including *Pleurotus sajor-caju*, *Pleurotus eryngii,* and *Pleurotus ostreatus.*[32-34] AAO activity was detected in these species, but not that of lignin peroxidases. The occurrence of both types of enzymes was first described for *Bjerkandera adusta* in 1990.[35-37]

While the first era of AAO research was focused on characterizing homologously produced AAOs in their native fungal hosts, the advent of recombinant DNA technologies led to cDNA cloning and production of recombinant proteins in heterologous expression hosts. In 1999, Varela et al. extensively characterized the cDNA sequence of the *P. eryngii aao* gene and observed a 33 % sequence identity and 51 % similarity with *Aspergillus niger* glucose oxidase.[38] Furthermore, a 27 amino acid long N-terminal signal peptide was deduced from sequencing of the protein and structural conformities with other oxidoreductases were revealed including a conserved adenosine diphosphate (ADP)-binding motif common to flavoenzymes containing a flavin adenine dinucleotide (FAD) cofactor.[38,39]

For biochemical and structural studies and ultimately biotechnological applications of a particular enzyme, sufficient amounts of the target enzyme are necessary and the production yields in their native fungal hosts are often rather low. The first report of heterologous

expression of an AAO was published in 2001, when *P. eryngii* AAO (namely *Pe*AAO) was successfully expressed in the fungus *Aspergillus nidulans* and cultures showed a 10 to 50 times higher extracellular AAO activity compared to cultures of *P. eryngii.*[40] The recombinant *Pe*AAO had identical properties to native *P. eryngii* AAO in terms of mass, p*I*, degree of glycosylation and kinetics and was therefore considered as promising candidate for further investigations. In 2006, *P. eryngii* AAO was expressed in *E. coli* for the first time and purified from inclusion bodies by in vitro refolding with yields of 45 mg of pure enzyme per liter of culture.[41] However, the recombinant *Pe*AAO was less pH and thermostable than its counterparts derived from native or recombinant fungal hosts, presumably due to the lack of glycosylation. Nevertheless, the *E. coli*-derived AAO was used for catalytic and structural examinations and led to the first protein crystal structure of an aryl-alcohol oxidase.[42,43]

In terms of gaining higher protein yields and more stable AAO variants, the first report on AAO expression using *Saccharomyces cerevisiae* as a yeast expression system was published in 2015 by Viña-Gonzalez et al.[44] The yeast-derived *Pe*AAO was over-glycosylated, resulting in higher pH and thermostability compared to non-glycosylated *E. coli Pe*AAO. However, the secretion level was still at around 2 mg/l and thus rather low for biotechnological applications. Efforts were made to generate AAO variants with optimized expression in yeast systems through structure-guided evolution and introduction of chimeric signal peptides and finally led to *Pe*AAO variant FX9, which secreted the recombinant enzyme at 25 mg/l.[45]

The solved crystal structure of *Pe*AAO paved the way for detailed follow-up studies on mechanistic properties and initiated protein engineering approaches to further extend the insights into the mode of catalysis and the extension of the substrate scope.[46-55] Computational simulations and structure-guided evolution approaches were carried out to create *Pe*AAO variants with altered substrate preferences specifically towards secondary alcohols.[54,55] The

evolved *Pe*AAO variant LanDo exhibited an 800-fold improvement in overall activity towards the model substrate and secondary alcohol 1-(*p*-methoxyphenyl)-ethanol, in contrast to its parent variant FX9, and was successfully applied in chiral de-racemization of racemic 1-(*p*-methoxyphenyl)-ethanol.[54] In addition, combinatorial saturation mutagenesis at two defined positions in the active site cavity allowed the identification of mutations to generate the *Pe*AAO variant Bantha, which was able to completely convert 5-hydroxymethylfurfural (5-HMF) to 2,5-furandicarboxylic acid (FDCA), a building block for bio-based polymers.[56]

1.5.2. Classification and Structure

AAOs are classified as members of the AA3 subgroup according to the Carbohydrate-Active enZyme (CAZy) database (http://www.cazy.org/). This database categorizes several different enzyme classes active on glycosidic bonds into different families, i.e. glycoside hydrolases and polysaccharide lyases.[57] These enzymes catalyze reactions including the degradation, modification, and formation of glycosidic bonds, and classes are based on amino acid sequence similarities, protein folding, and catalytic properties and may still group together enzymes with different substrate specificities.[57] Additional to these classes that directly modify glycosidic bonds, a new class of enzymes with "auxiliary activities" (AA) has been introduced. Most of these enzymes are not active on carbohydrates themselves, but on lignin and act in conjunction with other CAZymes.[58] These AA enzymes are further subdivided into 10 families of ligninolytic enzymes and of lytic polysaccharide mono-oxygenases.[58] The ligninolytic "cocktail" secreted by wood-decaying fungi consists of different enzymes as described earlier (see Chapter 1.4) with different catalytic features and properties, such as copper-containing laccases (CAZy group AA1), heme-peroxidases like manganese, versatile, and lignin peroxidases (group AA2), and cellobiose dehydrogenase, glucose oxidase, alcohol oxidase, pyranose oxidase, and aryl-alcohol oxidases (group AA3). While members of groups AA1 and

AA2 are directly involved in breakdown of lignin to yield various degradation products, members of subgroup AA3 play pivotal roles in supporting the lignin-degrading enzymes in subgroup AA2 by providing of H_2O_2.

Furthermore, all members of group AA3 including aryl-alcohol oxidases, belong to the superfamily of the glucose-methanol-choline (GMC) oxidoreductases. In 2000, Varela and colleagues performed a sequence analysis of AAO from *Pleurotus eryngii* ATCC 90787 (*Pe*AAO) and found highly homologous regions with members of the GMC oxidoreductase superfamily.[39] This family of enzymes was first described in 1992 and groups together enzymes with different catalytic properties based on similar structural folds and motifs.[59] The name-giving representatives of the GMC superfamily, namely glucose oxidase, glucose dehydrogenase, methanol oxidase and choline dehydrogenase are flavoenzymes containing FAD as cofactor and accept different substrates and subsequently yield different products. Despite their differences in catalytic activity, these enzymes have high amino acid sequence similarities and share a major conserved structural element: an N-terminal βαβ fold, also known as Rossmann fold, which represents the dinucleotide binding site necessary for interaction with the ADP moiety in the FAD cofactor.[59] Further, these enzymes contain a C-terminal substrate binding domain, which shows greater sequence variance as it significantly determines the catalytic activity of the respective enzyme.[60] AAOs contain both the Rossmann fold and the highly variable C-terminal substrate binding domain, which is common to all GMC members, and AAOs have therefore been assigned to this superfamily.

The first crystal structure of an AAO was solved in 2009 by Fernández et al. using *Pe*AAO expressed and purified from inclusion bodies in *E. coli.*[42] The resolution of the structure revealed that AAOs are monomeric enzymes, and as expected from sequence similarities among GMC enzymes, contain a two-domain structure: a flavin-binding domain and a

substrate-binding domain. The central core of the flavin-binding domain consists of a five-stranded parallel β-sheet surrounded by three α-helices containing the previously described βαβ Rossmann fold to which the dinucleotide ADP of the FAD cofactor is non-covalently bound. The binding of FAD is realized by a network of hydrogen bonds, including several interactions with the main chain atoms of residues Asn12 and with the carboxyl group of Glu33, both part of the Rossmann fold.[42] The C-terminal part contains the substrate binding domain with the active site, whose central core consists of a six-stranded antiparallel β-sheet and two long α-helices. The two domains are linked by three segments spanning from one domain to the other and by two two-stranded parallel β-sheets at their interface.[42]

A rather unique feature of the AAO structure is a funnel-shaped tunnel decorated with aromatic amino acid side chains from loop Gln395 to Thr404, which creates a hydrophobic environment and connects the solvent region with the active site and the buried FAD cofactor.[42,61] Together with a platform above the active site and in front of the FAD, consisting of two elements (a 14-amino acid long unstructured insertion and a 30-amino acid insertion that folds into three α-helices), these two features regulate the access to the substrate binding site. Three other aromatic residues (Tyr92, Phe397 and Phe501) act as bottleneck of this tunnel and further limit the accessibility of the active site.[42,61]

1.5.3. Architecture of the Active Site

The architecture of the active site and the catalytic cycle of aryl-alcohol oxidases have been analyzed in several in-depth studies using *Pleurotus eryngii Pe*AAO employing site-directed mutagenesis and computational simulations.[42,48,51,53,61-63] The active site of *Pe*AAO (Figure 3) is located on the *re* side of the isoalloxazine ring of FAD, as molecular docking simulations with different AAO substrates revealed the *re* side as a preferred position and in close proximity to two catalytically active histidine residues.[42,62] His502 and His546 have been

identified as catalytically active residues in site-directed mutagenesis studies by replacement with either leucine, serine or arginine[62], or with alanine[48], where all mutations led to a strong decrease in substrate oxidation rates, demonstrating the importance of the two histidine residues in catalysis. The protonation states of His502 and His546 were analyzed using quantum mechanics/molecular mechanics and molecular docking simulations and revealed that His502 acts as catalytic base and His546 is involved in substrate stabilization.[48] The active site is present in a pre-organized state and catalysis only requires the approach of the hydride donor and acceptor via the substrate access channel.[51]

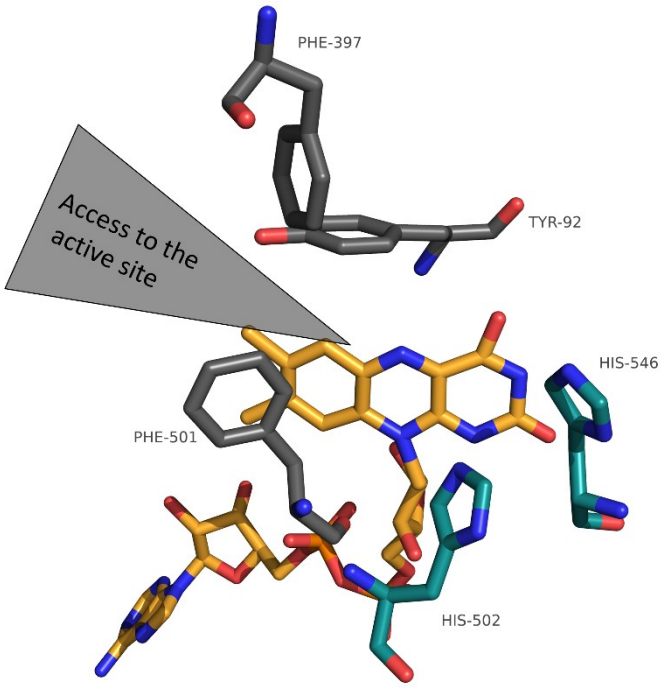

Figure 3 Active site of *Pe*AAO (PDB entry 3FIM). Catalytic active residues His502 and His546 (teal), FAD cofactor (orange), and Tyr92, Phe397 and Phe501 (grey), which form the hydrophobic bottleneck (depicted as grey wedge) and limit the accessibility to the active site. Adapted and modified from Fernández et al.[42]

For an alcohol substrate to enter the active site, structural motions must to be performed to accommodate for a migrating substrate as the access channel is too narrow.[61] Protein energy landscape studies have been performed and have shown that oscillating motions of residues within the loop Gln395 to Thr404 are strictly necessary for substrate diffusion through the

access channel.[63] Once the alcohol substrate reaches the active site the alcohol hydroxyl hydrogen is positioned towards the N-ε of deprotonated His502 and one of the C-α hydrogen atoms is positioned towards the N-5 of the FAD isoalloxazine ring at distances of 2.4 – 2.5 Å.[63]

1.5.4. Catalytic Cycle

The catalytic cycle of AAOs is divided into a reductive and an oxidative half-reaction (Figure 4).[63] In the reductive half-reaction (top to right in Figure 4) the substrate is two-electron oxidized as a hydride from the pro-R-α position is transferred to the N-5 atom of the flavin, yielding reduced $FADH_2$.[49] At the same time, the catalytic base His502, with the assistance of His546, withdraws the alcohol hydroxyl proton to yield the aldehyde product. Both proton and hydride transfer occur in a concerted fashion with no stable intermediates observable.[47,48]

During the oxidative half-reaction (bottom to left in Figure 4) the co-substrate O_2 freely diffuses through the substrate access channel and is guided by Phe501 to a catalytically relevant position in close proximity to the flavin C-4-α and H-ε of His502.[63] O_2 is then two-electron reduced by $FADH_2$, which generates the superoxide anion radical and transforms into a neutral semi-quinone.[64] In a stepwise fashion, a hydrogen atom from the flavin N-5 atom and a proton from the solvent or exchangeable His502 are transferred to superoxide, releasing H_2O_2 and oxidized flavin (FAD).[53] The oxidation of aromatic aldehydes via the same mechanism described requires their presence in hydrated form (*gem*-diol) and ultimately yields an acid.[46]

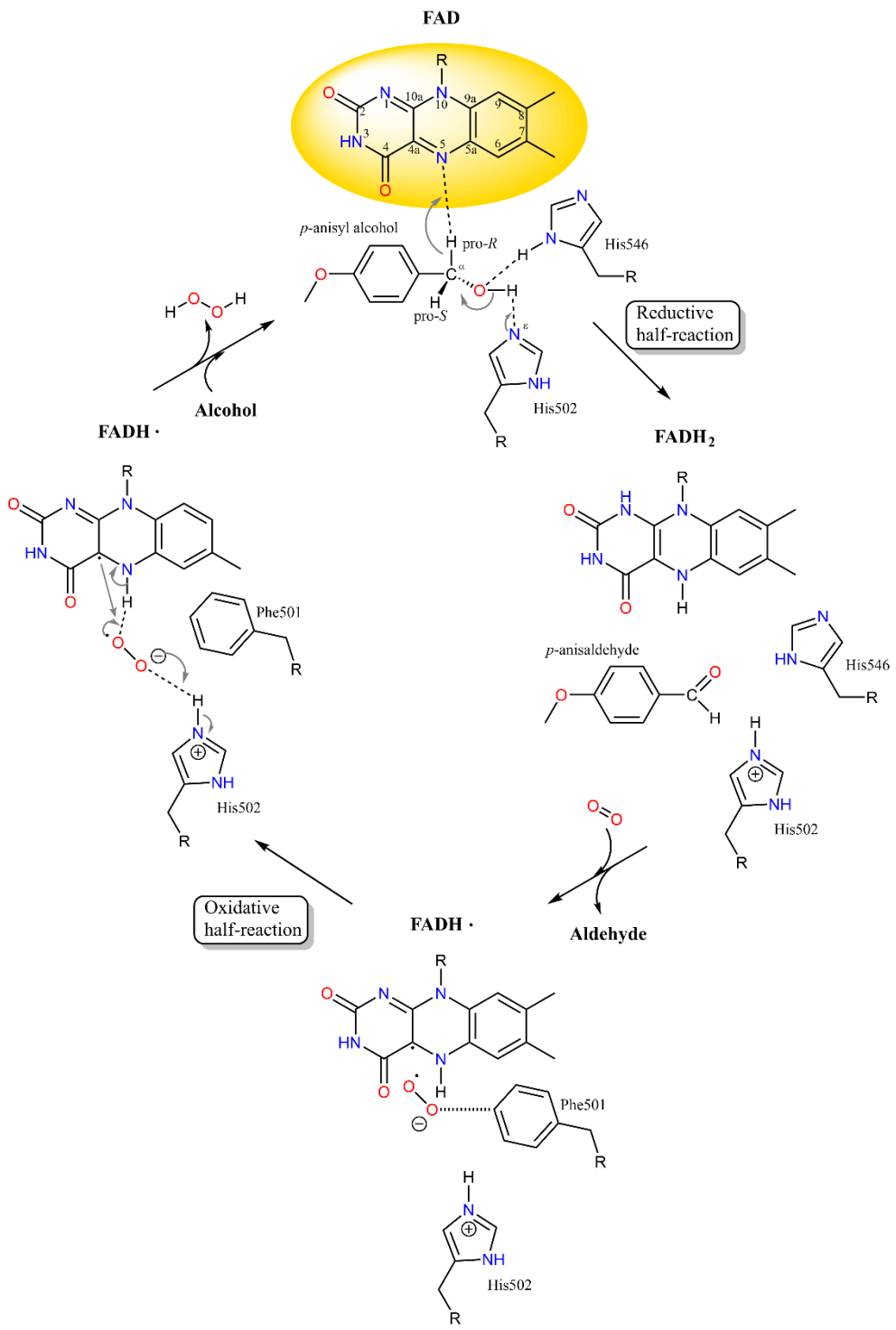

Figure 4 Catalytic cycle of *Pe*AAO` oxidation of model substrate *p*-anisyl alcohol. The reaction is composed of two half-reactions: reductive (right side) and oxidative (left side). Adapted from Carro et al.[53]

1.5.5. Biotechnological Application

As the reaction products of AAO' activity are predominantly aromatic aldehydes, these substances are receiving considerable attention in various parts of the biotechnology industry, with the flavor and fragrance industry being a major area of interest. Flavor and fragrances produced via biocatalysis can be classified as "natural", which meets the growing consumer's demand for all-natural products.[65,66] Van Schie et al. demonstrated the biocatalytic production of the fresh fragrance "Green Note" *trans*-2-hexenal in a continuous flow reactor using recombinant *Pe*AAO from *P. eryngii* ATCC 90787.[67] The yield was further optimized in a two-phase system, yielding 2.6 M of product and reaching a turnover number of 2.2 million.[68]

Another application of AAOs as biocatalysts comprises the production of a bio-based precursor for polyethylene furanoate (PEF). The precursor 2,5-furandicarboxylic acid (FDCA) could be produced from 5-hydroxymethylfurfural (5-HMF) after reaction optimization by recombinant *Pe*AAO.[69] Another approach involved the generation of the evolved *Pe*AAO variant Bantha via combinatorial saturation mutagenesis and comparison with another GMC enzyme, HMF-oxidase, in which the Phe501 in the active site next to the catalytically active His base, was replaced by a Trp residue, resulting in a 6-fold improvement in the overall conversion of 5-HMF to FDCA.[56] However, further reaction optimization is required, as the reported FDCA yield was still modest at only 3 % FDCA starting with 5-HMF as substrate. Bio-based PEF is an interesting alternative to fossil-based polyethylene terephthalate (PET) and is already produced on a ton-scale via chemical catalytic steps, and the transition to a biocatalytic production route would be desirable to implement the "green chemistry" approach.[70]

To extend the substrate scope of AAOs towards secondary alcohols, a mixed approach of directed and structure-guided evolution was employed to engineer *Pe*AAO for the oxidation of secondary alcohols.[54,55] The engineered enzyme variant *Pe*AAO LanDo allows the chiral deracemization of racemic 1-(*p*-methoxyphenyl)-ethanol as only the *S*-enantiomer is oxidized. This substrate was previously not accepted by *Pe*AAO, opening up new paths for the use of AAOs as biocatalysts.[54]

Next to the application of AAOs for production of valuable aldehydes, their action as H_2O_2 donors in combination with H_2O_2-consuming enzymes such as peroxidases and peroxygenases is conceivable, essentially extending the use of AAOs to a plethora of different biocatalytic routes. The valorization of lignin with a set of recombinant ligninolytic enzymes (including AAOs) would boost the importance of this natural resource and contribute to the transition towards a more sustainable economy. As with all industrially relevant biocatalysts, these enzymes need to be produced in sufficiently large amounts, with at best simple purification steps to keep the share of biocatalyst costs as low as possible in the overall costs of a bioprocess.

1.6. Aim of this work

The application of biocatalysts in all areas of biotechnology requires sufficient amounts of enzyme and in-depth understanding of their catalytic activity, substrate scope, and stability parameters. The reported yields for heterologously expressed AAOs are quite low, which is a limitation for the use of these enzymes as biocatalysts. Furthermore, the often applied intracellular production of AAOs in *E. coli* led to formation of inclusion bodies, which hinders easy and rapid enzyme purification. Eukaryotic expression systems that enable the secretion of a target enzyme provide several advantages: The level of contamination with endogenous proteins is significantly reduced, and in addition, post-translational glycosylation may confer higher enzyme stability. The published studies regarding the substrate spectra of AAOs rely on a narrow range of substances, and the discovery of "new" substrates with biotechnological potential has stagnated. Finally, biocatalytic application of AAOs for the production of valuable products at gram-scale has not been explored yet. To adress these challenges in the use of AAOs as biocatalysts and to demonstrate their biocatalytic potential, this work aimed at different aspects of aforementioned problems.

i. Identification and high-yield heterologous expression of suitable AAO-encoding genes in the yeast *P. pastoris* and development of secretion-optimized enzyme variants using site-directed mutagenesis;
ii. Thorough biochemical characterization of the respective recombinant AAOs with special emphasis on elucidation of their substrate spectra and stability characteristics;
iii. Development of an easy and rapid assay for screening of AAO mutant libraries for improved enzymatic activity;
iv. Application of a recombinant AAO to produce value-added products at the gram-scale with potential in various areas of biotechnological industry

2. Results

The experimental results obtained during the work on this thesis are divided into six chapters, of which chapters II to VI have been published in peer-reviewed journals. The own contribution to each publication is given in relative percentage. The full extent of this work includes the search for suitable genes encoding aryl-alcohol oxidases (AAO), the production and characterization of the respective recombinant enzymes, enzyme engineering, and finally the biotechnological application of an AAO as a biocatalyst and the development of an agar plate assay for screening of AAO mutant libraries for improved enzymatic activity.

In a broader context, all chapters pursue the same goal: a biocatalytically manufactured product (Scheme 3). The first part covers the biocatalyst itself: its selection, production and characterization and (if necessary) its engineering. The second step deals with the bioprocess, process optimization and finally the product isolation. The contents of all six chapters are briefly summarized below.

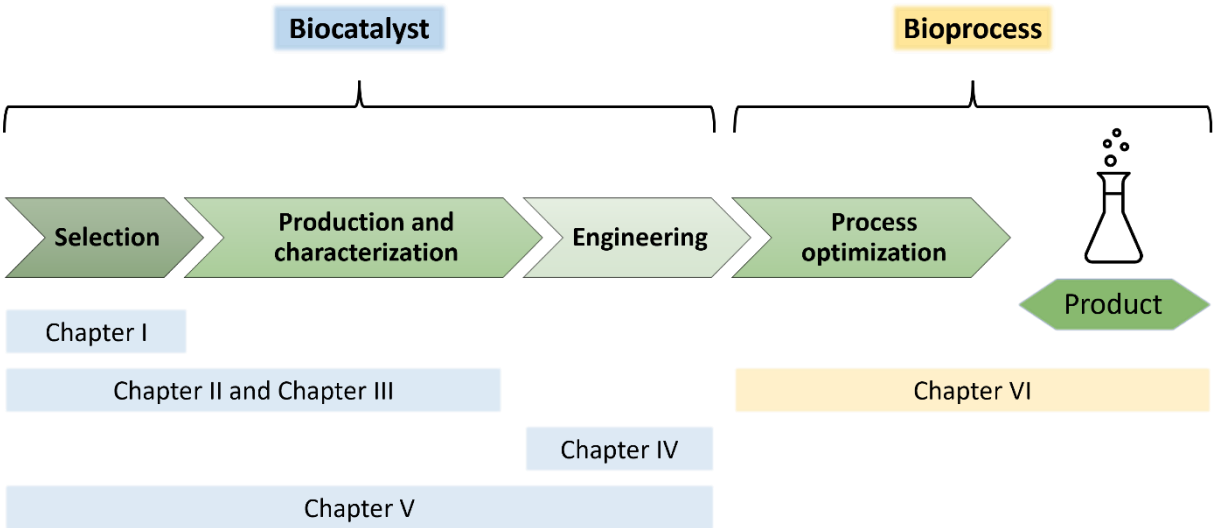

Scheme 3 Steps towards a biocatalytically manufactured product and the respective chapters in this thesis.

Chapter I: Expanding the toolbox of recombinant AAOs (2.1) describes the research work on the selection of fungal *aao* genes and their initial heterologous expression in *P. pastoris* and sets the foundation for the following chapters.

Chapter II: Biochemical characterization of *PeAAO2* from *Pleurotus eryngii* P34 and Chapter III: Biochemical characterization of *Ma*AAO from *Moesziomyces antarcticus* (2.2 and 2.3): The two aryl-alcohol oxidases *Pe*AAO2 from *Pleurotus eryngii* P34 and *Ma*AAO (originally annotated as *Ma*GMC1) from *Moesziomyces antarcticus,* which showed promising results in the initial expression experiments in Chapter I, are thoroughly characterized in terms of their biochemical properties with special emphasis on their substrate spectra.

Chapter IV: Protein engineering of *PeAAO* to enable expression in *P. pastoris* (2.4): Site-directed mutagenesis based on sequence comparison with the expressible *Pe*AAO2 described in Chapter II was employed to generate enzyme variants of the originally non-expressible in *P. pastoris Pe*AAO from *P. eryngii* ATCC 90787.

Chapter V: Novel agar plate assay for screening of AAO mutant libraries (2.5): A new generic agar plate based activity assay was developed to easily visualize *P. pastoris* transformants expressing active AAOs and variants thereof based on a colorimetric reaction, which is suitable for screening large mutant libraries for improved activity towards any substrate.

Chapter VI: Biocatalytic applicability of *PeAAO2* (2.6): The biotechnological applicability of *Pe*AAO2 was demonstrated based on the biocatalytic production of valuable aldehydes at milligram-scale with primary focus on the fragrance compound piperonal.

2.1. Chapter I: Expanding the toolbox of recombinant AAOs

2.1.1. Introduction

In 2017, the number of characterized and heterologously expressed aryl-alcohol oxidases (AAOs) was still modest despite their interesting biocatalytic properties. The ability of AAOs to oxidize bio-based 5-hydroxymethylfurfural (5-HMF) to the polymer precursor 2,5-furandicarboxylic acid (FDCA) was demonstrated in 2014 for a coupled system consisting of an AAO and an unspecific peroxygenase, stimulating interest in AAOs as biocatalysts.[71] However, the employed aryl-alcohol oxidase *Pe*AAO from *Pleurotus eryngii* was expressed in *Escherichia coli* and re-folded from inclusion bodies with low yield[41], which is not an ideal prerequisite for a biotechnological process. Significant efforts were made in 2015 to generate *Pe*AAO variants with chimeric signal peptides that showed slightly higher expression in the yeast *Saccharomyces cerevisiae* than in *E. coli.*[44] Later, an AAO from the phytopathogen *Ustilago maydis* (*Um*AAO) was successfully expressed and secreted with an outstanding yield of 1 g per liter of culture using the methylotrophic yeast *Pichia pastoris.*[72]

As this was the first report of heterologous expression of an AAO using the secretion pathway of the yeast *P. pastoris,* we aimed to further expand the toolbox of heterologously produced AAOs using *P. pastoris* and started with genome mining of *aao* genes from available databases. The amino acid sequences of the above-mentioned recombinant AAOs were used as query and database entries within the NCBI database with high amino acid identities were selected for the expression experiments. A selection of codon-optimized gene sequences was ordered with their native signal sequences to enable secretion in the yeast, which should facilitate easy and rapid analysis of expression success and subsequent purification of the recombinant enzyme.

2.1.2. Experimental procedures

2.1.2.1. Genome mining of *aao* genes

Employing the National Center for Biotechnology Information (NCBI) database (https://www.ncbi.nlm.nih.gov/gene) and using the amino acid sequences of *Pe*AAO[38] and *Um*AAO[72] as query in protein BLAST search, several *aao* genes from different fungal sources were retrieved from the database (Table 2).

Table 2 List of selected genes from the NCBI database encoding for four AAOs and one GMC oxidoreductase.

Name	Organism/Strain	NCBI Accession No.	Note/Publication
*Pe*AAO	*Pleurotus eryngii* ATCC 90787	AF064069	Published. Wild-type expressed in *A. nidulans*[40] and *E. coli*[41], variants expressed in *S. cerevisiae*[44]
*Pe*AAO2	*Pleurotus eryngii* P34	GU444001	Unpublished. Annotated as AAO. High amino acid identity (99 %) with *Pe*AAO sequence as query
*Pp*AAO1	*Pleurotus pulmonarius* CBS 507.85	AF143814	Published. Wild-type expressed homologously in *P. pulmonarius*[73]. High amino acid identity (95 %) with *Pe*AAO sequence as query
*Mr*AAO3	*Moniliophthora roreri* MCA 2997	AWSO01000287, locus tag Moror_4538[1]	Unpublished. Annotated as AAO. Highest amino acid identity (49 %) with *Pe*AAO sequence as query within the genome of *M. roreri* MCA 2997
*Ma*GMC1	*Moesziomyces antarcticus* JCM 10317	XM_014798063	Unpublished. Annotated as GMC oxidoreductase. High amino acid identity (86 %) with *Um*AAO expressed in *P. pastoris*[72] as query

[1] The coding sequence (CDS) of this gene was derived from a whole genome shotgun sequencing project. The preliminary NCBI record of the gene (XM_007850085.1) was discontinued.

The selected genes were codon optimized using JCat (http://www.jcat.de/)[74] for expression in *Saccharomyces cerevisiae*, as both *S. cerevisiae* and *P. pastoris* share a similar codon usage (see Supplemental Information 2.1.5.1). TAA was added as a stop codon and the

restriction sites EcoRI and NotI were included for restriction and ligation into the vector pPICZA. The vector harbors the strong methanol inducible alcohol oxidase 1 (*AOX1*) promoter (P_{AOX1}) upstream of the *aao* genes and allows for induction of *aao* gene expression upon addition of methanol. The antibiotic resistance marker conferring resistance to zeocin was employed for selection. The gene synthesis as well as the cloning steps were carried out by BioCat GmbH (Heidelberg, Germany).

2.1.2.2. Generation of recombinant *P. pastoris* strains for expression of selected genes

The readily cloned pPICZA-constructs were used for transformation of chemically competent *Escherichia coli* DH5α cells and transformants were selected on low salt lysogeny broth agar plates (LB, 1% peptone, 0.5% yeast extract, 0.5% NaCl, 1.5% agar) with 25 µg/ml zeocin (InvivoGen, San Diego, USA). The plates were incubated at 37 °C overnight and transformants were used to inoculate 5 ml of LB_{zeo} medium for plasmid amplification (37 °C, 180 rpm, overnight). The plasmids were isolated using the ZR Plasmid Miniprep Kit (Zymo Research, Irvine, USA) according to the manufacturer's instructions and eluted in 30 µl of ultra-pure water.

Approximately 10 µg of linearized plasmid DNA is required for transformation of electro-competent *P. pastoris* X-33 cells to obtain a sufficiently high transformation rate. Plasmid linearization was carried out using the FastDigest MssI restriction enzyme (Thermo Fisher Scientific, Waltham, USA): 30 µl of purified plasmid DNA (around 300-500 ng/µl), 5 µl of MssI, 10 µl of 10X FastDigest Buffer and 55 µl ultra-pure water were mixed and incubated at 37 °C for 2 h. The linearized plasmid DNA was purified and concentrated employing the DNA Clean & Concentrate Kit from Zymo Research and eluted in 12 µl ultra-pure water.

The linearized plasmid DNA was mixed with 40 µl of electro-competent *P. pastoris* X-33 cells, transferred to pre-chilled electroporation cuvettes (2 mm gap, 400 µl, VWR, Darmstadt, Germany) and incubated on ice for 5 min. The pre-set program "Pic" (2.0 kV, 1 pulse) of the MicroPulser Electroporator (Bio-Rad, Hercules, USA) was used for electroporation. After the pulse, the cells were immediately mixed with 1 ml of 1 M sorbitol, transferred to a 15-ml reaction tube and incubated at 30 °C for 2 h without shaking. 100 and 200 µl of cells were then spread on yeast peptone dextrose sorbitol agar plates (YPDS, 1% yeast extract, 2% peptone, 2% dextrose, 1 M sorbitol, 2% agar) with 100 µg/ml zeocin and incubated at 30 °C until formation of colonies.

2.1.2.3. Expression of selected genes in *P. pastoris*

Up to four transformants for each recombinant strain (i.e. each new gene) were used for expression analysis. Precultures of each transformant were grown in 10 ml of buffered complex glycerol medium (BMGY, 1% yeast extract, 2% peptone, 100 mM potassium phosphate buffer pH 6.0, 1.34% yeast nitrogen base without amino acids, 4 × 10−5% biotin, 1% glycerol) overnight (30 °C, 200 rpm). For the main culture, preculture at an OD_{600} value of 1 was used to inoculate 10 ml of buffered complex methanol medium (BMMY, same as BMGY but without glycerol) and incubated for two days (25 °C, 200 rpm). Every 24 h 0.5 % (*v/v*) methanol was added to maintain induction of gene expression.

2.1.2.4. Analysis of produced AAOs

Gene expression was analyzed via SDS-polyacrylamide gel electrophoresis (SDS-PAGE) with 12.5 % resolving gel.[75] The gel was stained with Coomassie Brilliant Blue R-250. To visualize intracellular proteins, main culture samples diluted to an OD_{600} = 0.5 were taken and centrifuged (1500 x *g*, 15 min, 4 °C). The resulting cell pellet was dissolved in 10 µl of 5X

SDS-sample buffer (62.5 mM TRIS-HCl pH 6.8, 30 % (*w/v*) glycerol, 4 % (*w/v*) SDS, 0.05 % (*w/v*) bromophenol blue, 10 % (*v/v*) β-mercaptoethanol) and 40 µl of ultra-pure water, boiled at 95 °C for 20 min to yield the total cell extract and applied on a SDS gel.

To obtain the cell-free supernatant, the main cultures were transferred to 15-ml reaction tubes and harvested (1500 x *g*, 15 min, 4 °C). The supernatant was used for activity assays (2.1.2.5) and an aliquot was precipitated with trichloroacetic acid (TCA) for analysis of the supernatant on SDS-gel. For this, 250 µl of 100 % (*w/v*) TCA solution was mixed with 1 ml of supernatant, incubated on ice for 2 h and centrifuged to pellet denatured proteins (18,000 x g, 15 min, 4 °C). The supernatant was discarded, the pellet dissolved in 200 µl of ice-cold acetone and centrifuged (18,000 x g, 15 min, 4 °C). The acetone wash step was repeated and finally the pellet was dried at room temperature under the fume hood for 1 h to dry off residual acetone. The dried pellet was dissolved in 15 µl of 5X SDS-sample buffer, boiled at 95 °C for 10 min and directly loaded onto the SDS-gel.

2.1.2.5. Determination of AAO activity in the supernatant

The cell-free supernatant was tested for activity towards the commonly used AAO substrate veratryl alcohol (3,4-dimethoxybenzyl alcohol) in a standard activity assay.[29] The conversion to the aldehyde veratraldehyde was followed spectrophotometrically at 310 nm. For this, 800 µl of 100 mM sodium phosphate buffer pH 6.0 was mixed with 100 µl of a 50 mM veratryl alcohol solution (in ultra-pure water, end concentration of 5 mM) in a standard 1-ml cuvette. The reaction was started by addition of 100 µl of cell-free supernatant and the change of absorption at 310 nm was followed in a Ultrospec 7000 photometer (GE Healthcare, Chicago, USA). For calculation of volumetric activity [U/l], the molar extinction coefficient of veratraldehyde (ε_{310} = 9.3 mM^{-1} cm^{-1}) was used.[29]

2.1.3. Results and Discussion

Five (putative) *aao* genes were selected for heterologous production in *P. pastoris* and analyzed regarding the presence of protein bands in total cell extract and cell-free supernatant samples on SDS-polyacrylamide gels, and the presence of AAO activity in the supernatant.

The gene encoding for *Pe*AAO from *Pleurotus eryngii* ATCC 90787 was selected as it represents the model enzyme for the group of aryl-alcohol oxidases and was used for the majority of biochemical and structural research conducted on AAOs.[29,33,38-43,46-53,62-64,76] However, there have been no reports on successful expression of the wild-type enzyme in *Pichia pastoris.* The selected gene *peaao2* is annotated to encode for an AAO from a closely related strain of *P. eryngii*, namely P34, and shows a very high amino acid identity of 99 % to *Pe*AAO. Further, an AAO from *P. pulmonarius* CBS 507.85 (*Pp*AAO1) was selected, which has been produced and characterized from homologous expression in *P. pulmonarius*[73], but no reports on heterologous expression are available. *Pp*AAO1 also shows high amino acid identity to *Pe*AAO with 95 %.

The gene encoding for *Mr*AAO3 from *Moniliophthora roreri* MCA 2997 was chosen as research on other ligninolytic enzymes derived from *M. roreri* were conducted at the Institute of Biochemistry II.[77,78] Within this project one aim was to combine a set of heterologously produced ligninolytic enzymes from *M. roreri* (i.e., laccase, peroxidase and eventually aryl-alcohol oxidase) to promote the degradation of lignocellulosic biomass in vitro. Among several *aao* genes within the genome of *M. roreri*, the one with the highest amino acid identity to *Pe*AAO of 49 % was chosen. Further, a gene annotated to encode for a glucose-methanol-choline (GMC)-oxidoreductase from *Moesziomyces antarcticus* was selected based on its high

amino acid identity to *Um*AAO (86 %), which was successfully expressed in *P. pastoris* and originally annotated as GMC-oxidoreductase as well.[72]

The molecular properties of the five target proteins are summarized below (Table 3). For all target proteins, a signal peptide between 18 and 23 amino acids in length was predicted, indicating the possibility of secretion of the recombinant enzyme into the supernatant if the signal peptide is recognized by *P. pastoris*' secretion machinery. For instance, the experimental data for *Pe*AAO showed that the signal peptide is 27 amino acids in length but only 21 amino acids based on in silico prediction. The expected molecular weights of the respective AAOs were calculated from the amino acid sequences of the mature proteins (processed signal peptide) and of the preproteins (unprocessed signal peptide). Furthermore, the presence of *N*-glycosylation sequons (Asn-Xaa-Ser/Thr, where Xaa is any amino acid except for Pro)[79] was evaluated, ranging from five sequons in *Ma*GMC1 to eight in *Pe*AAO2 and *Pp*AAO1.

The mere presence of *N*-glycosylation sequons does not imply that every sequon will eventually be glycosylated. In fact, the structural environment of each sequon plays a significant role in potential *N*-glycosylation, so that, for example, only surface-lying sequons may be glycosylated and would reflect a true *N*-glycosylation site. Nevertheless, the evaluation of *N*-glycosylation sequons aids in estimating the expected *N*-glycosylation degree and ultimately in identifying the protein bands on SDS gel as the apparent molecular weight of glycosylated proteins will be higher than the expected molecular weight.

Table 3 Molecular properties of target proteins. The signal peptide was predicted using SignalP 6.0 (https://services.healthtech.dtu.dk/service.php?SignalP)[80] and the molecular weight was calculated using ProtParam (https://web.expasy.org/protparam/)[81]. The number of *N*-glycosylation sequons was determined using the NetNGlyc server (https://services.healthtech.dtu.dk/service.php?NetNGlyc-1.0).[82]

Protein	Length of signal peptide in amino acids	Expected molecular weight [kDa]		Number of *N*-glycosylation sequons[2]
		Processed signal peptide	Unprocessed signal peptide	
***Pe*AAO**	21 (27)[1]	61.5 (60.9)[1]	63.7	7
***Pe*AAO2**	21	61.4	63.6	8
***Pp*AAO1**	23	61.3	63.6	8
***Mr*AAO3**	20	64.8	67.0	8
***Ma*GMC1**	18	67.0	68.6	5

[1] Values in brackets represent experimentally derived data on signal peptide length.[38]

[2] Number of *N*-glycosylation sequons was determined based on target proteins with processed signal peptides.

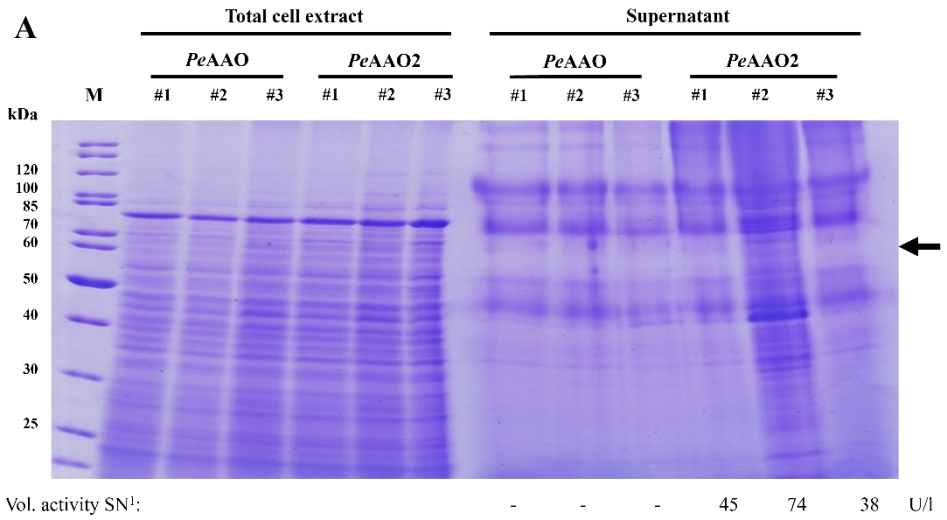

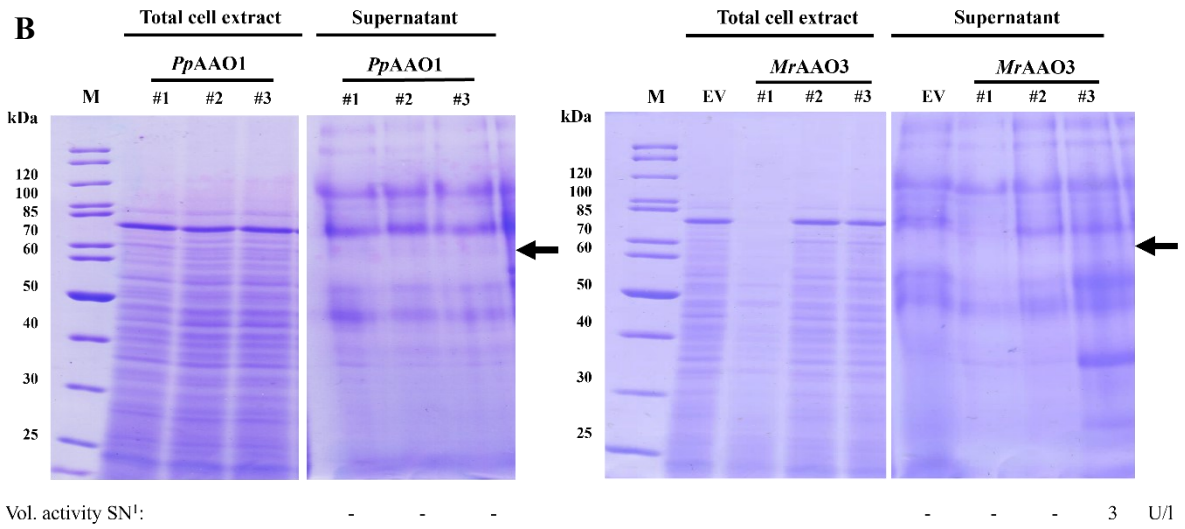

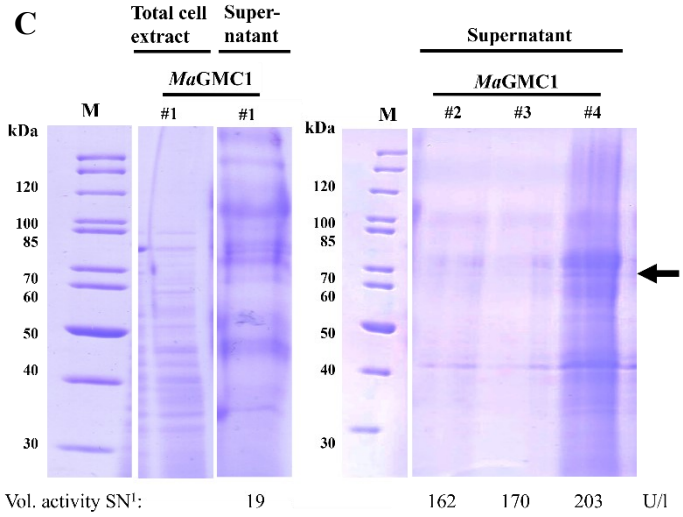

Figure 5 SDS-PAGE analysis and volumetric activity of up to four transformants (numbered #1-4) of *Pe*AAO and *Pe*AAO2 (**A**), *Pp*AAO1 and *Mr*AAO3 (**B**), and *Ma*GMC1 (**C**) after expression in *P. pastoris* X-33. Total cell extract samples derived from samples equal to OD_{600}=0.5 and 1 ml of TCA precipitated supernatant after 48 h were applied. M: PageRuler Unstained Protein Ladder. EV: control strain with empty vector. [1] = Volumetric activity [U/l] in cell-free supernatant (SN) was determined towards 5 mM of veratryl alcohol with standard assay. The arrow indicates the expected molecular weight of the processed recombinant enzymes.

After 48 h of *Pe*AAO expression, no activity towards veratryl alcohol was observed in the supernatant (A in Figure 5) of three individual *P. pastoris* transformants. At the same time no distinct protein band corresponding to the size of mature *Pe*AAO (60.9 kDa, Table 3) was visible on SDS gel in the supernatant or of unprocessed *Pe*AAO (63.7 kDa, Table 3) in the total cell extract. The sequence of *Pe*AAO contains seven *N*-glycosylation sequons (Table 3) and would indicate that the secreted enzyme contains attached glycan chains, resulting in a higher apparent molecular weight. Taking into account possible glycosylation, no protein band could be attributed to *Pe*AAO that was not already present in the empty vector (EV) control (B in Figure 5). Therefore, the expression of *Pe*AAO was not successful.

On the contrary, transformants expressing the closely related *Pe*AAO2, which shares 99 % amino acid identity with *Pe*AAO and differs in only seven amino acid positions (Table 2 and Figure 6), showed activity towards veratryl alcohol in the supernatant with values ranging from 38 and 74 U/l for three individual transformants (A in Figure 5). The expected size of

mature *Pe*AAO2 without glycosylation is 61.4 kDa, but since there are eight *N*-glycosylation sequons in the sequence (Table 3), a certain degree of glycosylation was expected. In contrast to the supernatant of *Pe*AAO and the EV control, a darker protein smear above 100 kDa was visible on SDS gel (A in Figure 5), which was attributed to secreted active *Pe*AAO2.

Transformants expressing the *Pp*AAO1 did not show any activity in the supernatant or any distinct protein bands corresponding to the size of mature *Pp*AAO1 in the supernatant or of unprocessed protein in the total cell extract (61.3 and 63.6 kDa, respectively, Table 3) (B in Figure 5). Considering the eight *N*-glycosylation sequons (Table 3), which are mostly identical to those in *Pe*AAO2 (Figure 6), no protein bands of higher molecular weight were visible on SDS gel either. The expression of *Pp*AAO1 was therefore considered unsuccessful.

The amino acid sequence alignment of the three *Pleurotus* AAOs, *Pe*AAO, *Pe*AAO2 and *Pp*AAO1 (Figure 6), illustrates the high degree of identity between these selected proteins in terms of total protein length, signal peptide length and presence of *N*-glycosylation sequons, despite their high variance in the outcome of heterologous expression and secretion in *P. pastoris*. As the only activity for *Pleurotus* AAOs was measured in cell-free supernatant after expression of *Pe*AAO2, which differs from *Pe*AAO in seven amino acids, the positive expression result is thought to correlate with the presence of one of the seven differing amino acids in *Pe*AAO2.

```
                                 21 23    27
                                  |  |     |
PeAAO       MSFGALRQLLLIACLALPSLAATNLPTADFDYVVVGAGNAGNVVAARLTEDPDVSVLVLE 60
PeAAO2      MSFGALRQLLLIACLALPSLAATNLPTADFDYVVVGAGNAGNVVAARLTEDPDVSVLVLE 60
PpAAO1      MSFSALRQLLLIACLALPSLAAANLPTADFDYIVVGAGNAGNVVAARLTEDPNVSVLVLE 60
            ***.******************:*********:********************:*******

PeAAO       AGVSDENVLGAEAPLLAPGLVPNSIFDWNYTTTAQAGYNGRSIAYPRGRMLGGSSSVHYM 120
PeAAO2      AGVSDENVLGAEAPLLAPGLVPNSIFDWNYTTTAQAGYNGRSIAYPRGRMLGGSSSVHYM 120
PpAAO1      AGVSDENVLGAEAPLLAPGLVPNSIFDWNYTTTAQAGYNGRSIAYPRGRMLGGSSSVHYM 120
            ************************************************************

PeAAO       VMMRGSTEDFDRYAAVTGDEGWNWDNIQQFVRKNEMVVPPADNHNTSGEFIPAVHGTNGS 180
PeAAO2      VMMRGSTEDFDRYAAVTGDEGWNWDNIQQFVGKNEMVVPPADNHNTSGEFIPAVHGTNGS 180
PpAAO1      VMMRGSIEDFDRYAAVTGDDGWNWDNIQQFVRKNEMVVPPADNHNTSGEFIPAVHGTNGS 180
            ****** ************:*********** ****************************

PeAAO       VSISLPGFPTPLDDRVLATTQEQSEEFFFNPDMGTGHPLGISWSIASVGNGQRSSSSTAY 240
PeAAO2      VSISLPGFPTPLDDRVLATTQEQSEEFFFNPDMGTGHPLGISWSIASVGNGQRSSSSTAY 240
PpAAO1      VSISLPGFPTPLDDRVLATTQEQSEEFFFNPDMGTGHPLGISWSIASVGNGQRSSSSTAY 240
            ************************************************************

PeAAO       LRPAQSRPNLSVLINAQVTKLVNSGTTNGLPAFRCVEYAEQEGAPTTTVCAKKEVVLSAG 300
PeAAO2      LRPAQSRPNLSVLINAQVTKLVNSGITNGLPAFRCVEYAEQEGAPTTTVCAKKEVVLSAG 300
PpAAO1      LRPAQSRPNLSVLINAQVTKLVNSGTTNGLPAFRCVEYAEREGAPTTTVCANKEVVLSAG 300
            ************************* **************:***********:********

PeAAO       SVGTPILLQLSGIGDENDLSSVGIDTIVNNPSVGRNLSDHLLLPAAFFVNSNQTFDNIFR 360
PeAAO2      SVGTPILLQLSGIGDENDLSSVGIDTIVNNPSVGRNLSDHLLLPAAFFVNSNQTFDNIFR 360
PpAAO1      SVGTPILLQLSGIGDQSDLSAVGIDTIVNNPSVGRNLSDHLLLPATFFVNNNQSFDNLFR 360
            ***************:.***:************************:****.**:***:**

PeAAO       DSSEFNVDLDQWTNTRTGPLTALIANHLAWLRLPSNSSIFQTFPDPAAGPNSAHWETIFS 420
PeAAO2      NSSEFNADLDQWTNTRTGPLTALIANHLAWLRLPSNSSIFQTFPDPAAGPNSAHWETIFS 420
PpAAO1      DSSEFNADLDQWTNTRTGPLTALIANHLAWLRLPSNSSIFQSVPDPAAGPNSAHWETIFS 420
            :*****.**********************************:.*****************

PeAAO       NQWFHPAIPRPDTGSFMSVTNALISPVARGDIKLATSNPFDKPLINPQYLSTEFDIFTMI 480
PeAAO2      NQWFHPAIPRPDTGSFMSVTNALISPVARGDIKLATSNPFDKPLINPQYLSTEFDIFTMI 480
PpAAO1      NQWFHPALPRPDTGNFMSVTNALIAPVARGDIKLATSNPFDKPLINPQYLSTEFDIFTMI 480
            *******:******.*********:**********************************

PeAAO       QAVKSNLRFLSGQAWADFVIRPFDPRLRDPTDDAAIESYIRDNANTIFHPVGTASMSPRG 540
PeAAO2      QAVKSNLRFLSGQAWADFVIRPFDPRLRDPTNDAAIESYIRDNANTIFHPVGTASMSPRG 540
PpAAO1      QAVKSNLRFLSGQAWADFVIRPFDARLSDPTNDAAIEWNIRDNANTIFHPVGTASMSPRG 540
            ************************ ** ***:*****  ********************

PeAAO       ASWGVVDPDLKVKGVDGLRIVDGSILPFAPNAHTQGPIYLVGKQGADLIKADQ 593
PeAAO2      ASWGVVDPDLKVKGVDGLRIVDGSILPFAPNAHTQGPIYLVGERGADLIKADQ 593
PpAAO1      ASWGVVDPDLKVKGVDGLRIVDGSILPFAPNAHTQGPIYLVGERGADLIKADQ 593
            *****************************************::*********
```

Figure 6 Sequence alignment of *Pleurotus* AAOs. Amino acid sequences of *Pe*AAO (AF064069), *Pe*AAO2 (GU444001) and *Pp*AAO1 (AF143814) were aligned using the Clustral Omega tool (https://www.ebi.ac.uk/Tools/msa/clustalo/)[83]. Light blue box: (predicted) signal peptide with numbering of amino acid positions; yellow box: *N*-glycosylation sequons; letters in red: variations in amino acid sequences among *Pleurotus* AAOs.

Out of the three transformants expressing the *M. roreri* derived *Mr*AAO3, only #3 showed measurable activity towards veratryl alcohol with 3 U/l (B in Figure 5). The protein bands in the supernatant of this transformant also showed the highest overall intensity of the three transformants tested, but not at the expected molecular weight of 64.8 kDa for mature protein or higher, as the protein sequence contains eight *N*-glycosylation sequons (Table 3). Instead, two distinct protein bands at approximately 25 and 35 kDa were visible on SDS gel and might be due to proteolytic cleavage resulting in smaller protein fragments, as both fragments were not visible in the empty vector control. This indicates that *Mr*AAO3 was expressed and active in the supernatant, but presumably not under optimal conditions resulting in protein degradation.

All transformants expressing the GMC oxidoreductase *Ma*GMC1 from *M. antarcticus* showed AAO activity in the supernatant ranging from 19 to 203 U/l, and thus the highest detected activity so far (C in Figure 5). However, there was no distinct band of the expected molecular weight of 67.0 kDa for the mature protein and the visible protein pattern resembles the EV control (Table 3). Nevertheless, the observed activity towards veratryl alcohol indicates a successful heterologous expression of *Ma*GMC1 in *P. pastoris* X-33.

2.1.4. Summary and Outlook

In summary, the expression of three out of five selected genes resulted in measurable AAO activity in the cell-free culture supernatant. For *Pe*AAO2 and *Ma*GMC1, all tested *P. pastoris* transformants showed volumetric activities of up to 200 U/l. Only one *Mr*AAO3 transformant exhibiting rather low activity of 3 U/l and an unexpected protein fragment pattern in the supernatant makes the expression of the intact and active form of recombinant *Mr*AAO3 questionable.

These findings set the foundation for the following chapters of this thesis, as two AAOs have been successfully expressed in the yeast *P. pastoris*. In order to fully evaluate the potential of *Pe*AAO2 and *Ma*GMC1, both enzymes will be produced in fed-batch fermentations, purified, and biochemically characterized with special emphasis on their substrate scopes.

2.1.5. Supplemental Information

2.1.5.1. Codon-optimized gene and amino acid sequences

The selected genes (Table 2) were codon-optimized using the JCat online tool (http://www.jcat.de/) and the codon usage information of *Saccharomyces cerevisiae.* The optimized genes were flanked by *Eco*RI (5' GAATTC) and *Not*I (5' GCGGCCGC) restriction sites, and a TAA stop codon was included.

***Pe*AAO optimized gene sequence**

```
ATGTCTTTCGGTGCTTTGAGACAATTGTTGTTGATCGCTTGTTTGGCTTT     50
GCCATCTTTGGCTGCTACTAACTTGCCAACTGCTGACTTCGACTACGTTG     100
TTGTTGGTGCTGGTAACGCTGGTAACGTTGTTGCTGCTAGATTGACTGAA     150
GACCCAGACGTTTCTGTTTTGGTTTTGGAAGCTGGTGTTTCTGACGAAAA     200
CGTTTTGGGTGCTGAAGCTCCATTGTTGGCTCCAGGTTTGGTTCCAAACT     250
CTATCTTCGACTGGAACTACACTACTACTGCTCAAGCTGGTTACAACGGT     300
AGATCTATCGCTTACCCAAGAGGTAGAATGTTGGGTGGTTCTTCTTCTGT     350
TCACTACATGGTTATGATGAGAGGTTCTACTGAAGACTTCGACAGATACG     400
CTGCTGTTACTGGTGACGAAGGTTGGAACTGGGACAACATCCAACAATTC     450
GTTAGAAAGAACGAAATGGTTGTTCCACCAGCTGACAACCACAACACTTC     500
TGGTGAATTTATCCCAGCTGTTCACGGTACTAACGGTTCTGTTTCTATCT     550
CTTTGCCAGGTTTCCCAACTCCATTGGACGACAGAGTTTTGGCTACTACT     600
CAAGAACAATCTGAAGAATTTTTCTTCAACCCAGACATGGGTACTGGTCA     650
CCCATTGGGTATCTCTTGGTCTATCGCTTCTGTTGGTAACGGTCAAAGAT     700
CTTCTTCTTCTACTGCTTACTTGAGACCAGCTCAATCTCGTCCAAACTTG     750
TCTGTTTTGATCAACGCTCAAGTTACTAAGTTGGTTAACTCTGGTACTAC     800
TAACGGTTTGCCAGCTTTCAGATGTGTTGAATACGCTGAACAAGAAGGTG     850
CTCCAACTACTACTGTTTGTGCTAAGAAGGAAGTTGTTTTGTCTGCTGGT     900
TCTGTTGGTACTCCAATCTTGTTGCAATTGTCTGGTATCGGTGACGAAAA     950
CGACTTGTCTTCTGTTGGTATCGACACTATCGTTAACAACCCATCTGTTG     1000
GTAGAAACTTGTCTGACCACTTGTTGTTGCCAGCTGCTTTCTTCGTTAAC     1050
TCTAACCAAACTTTCGACAACATCTTCAGAGACTCTTCTGAATTTAACGT     1100
TGACTTGGACCAATGGACTAACACTAGAACTGGTCCATTGACTGCTTTGA     1150
TCGCTAACCACTTGGCTTGGTTGAGATTGCCATCTAACTCTTCTATCTTC     1200
CAAACTTTCCCAGACCCAGCTGCTGGTCCAAACTCTGCTCACTGGGAAAC     1250
TATCTTCTCTAACCAATGGTTCCACCCAGCTATCCCAAGACCAGACACTG     1300
GTTCTTTCATGTCTGTTACTAACGCTTTGATCTCTCCAGTTGCTAGAGGT     1350
GACATCAAGTTGGCTACTTCTAACCCATTCGACAAGCCATTGATCAACCC     1400
ACAATACTTGTCTACTGAATTTGACATCTTCACTATGATCCAAGCTGTTA     1450
AGTCTAACTTGAGATTCTTGTCTGGTCAAGCTTGGGCTGACTTCGTTATC     1500
AGACCATTCGACCCAAGATTGAGAGACCCAACTGACGACGCTGCTATCGA     1550
ATCTTACATCAGAGACAACGCTAACACTATCTTCCACCCAGTTGGTACTG     1600
CTTCTATGTCTCCAAGAGGTGCTTCTTGGGGTGTTGTTGACCCAGACTTG     1650
```

```
AAGGTTAAGGGTGTTGACGGTTTGAGAATCGTTGACGGTTCTATCTTGCC     1700
ATTCGCTCCAAACGCTCACACTCAAGGTCCAATCTACTTGGTTGGTAAGC     1750
AAGGTGCTGACTTGATCAAGGCTGACCAATAA
```

*Pe*AAO amino acid sequence

```
        10         20         30         40         50         60
MSFGALRQLL LIACLALPSL AATNLPTADF DYVVVGAGNA GNVVAARLTE DPDVSVLVLE

        70         80         90        100        110        120
AGVSDENVLG AEAPLLAPGL VPNSIFDWNY TTTAQAGYNG RSIAYPRGRM LGGSSSVHYM

       130        140        150        160        170        180
VMMRGSTEDF DRYAAVTGDE GWNWDNIQQF VRKNEMVVPP ADNHNTSGEF IPAVHGTNGS

       190        200        210        220        230        240
VSISLPGFPT PLDDRVLATT QEQSEEFFFN PDMGTGHPLG ISWSIASVGN GQRSSSSTAY

       250        260        270        280        290        300
LRPAQSRPNL SVLINAQVTK LVNSGTTNGL PAFRCVEYAE QEGAPTTTVC AKKEVVLSAG

       310        320        330        340        350        360
SVGTPILLQL SGIGDENDLS SVGIDTIVNN PSVGRNLSDH LLLPAAFFVN SNQTFDNIFR

       370        380        390        400        410        420
DSSEFNVDLD QWTNTRTGPL TALIANHLAW LRLPSNSSIF QTFPDPAAGP NSAHWETIFS

       430        440        450        460        470        480
NQWFHPAIPR PDTGSFMSVT NALISPVARG DIKLATSNPF DKPLINPQYL STEFDIFTMI

       490        500        510        520        530        540
QAVKSNLRFL SGQAWADFVI RPFDPRLRDP TDDAAIESYI RDNANTIFHP VGTASMSPRG

       550        560        570        580        590
ASWGVVDPDL KVKGVDGLRI VDGSILPFAP NAHTQGPIYL VGKQGADLIK ADQ
```

*Pe*AAO2 optimized gene sequence

```
ATGTCTTTCGGTGCTTTGAGACAATTGTTGTTGATCGCTTGTTTGGCTTT     50
GCCATCTTTGGCTGCTACTAACTTGCCAACTGCTGACTTCGACTACGTTG     100
TTGTTGGTGCTGGTAACGCTGGTAACGTTGTTGCTGCTAGATTGACTGAA     150
GACCCAGACGTTTCTGTTTTGGTTTTGGAAGCTGGTGTTTCTGACGAAAA     200
CGTTTTGGGTGCTGAAGCTCCATTGTTGGCTCCAGGTTTGGTTCCAAACT     250
CTATCTTCGACTGGAACTACACTACTACTGCTCAAGCTGGTTACAACGGT     300
AGATCTATCGCTTACCCAAGAGGTAGAATGTTGGGTGGTTCTTCTTCTGT     350
TCACTACATGGTTATGATGAGAGGTTCTACTGAAGACTTCGACAGATACG     400
CTGCTGTTACTGGTGACGAAGGTTGGAACTGGGACAACATCCAACAATTC     450
GTTGGTAAGAACGAAATGGTTGTTCCACCAGCTGACAACCACAACACTTC     500
TGGTGAATTTATCCCAGCTGTTCACGGTACTAACGGTTCTGTTTCTATCT     550
CTTTGCCAGGTTTCCCAACTCCATTGGACGACAGAGTTTTGGCTACTACT     600
CAAGAACAATCTGAAGAATTTTTCTTCAACCCAGACATGGGTACTGGTCA     650
CCCATTGGGTATCTCTTGGTCTATCGCTTCTGTTGGTAACGGTCAAAGAT     700
CTTCTTCTTCTACTGCTTACTTGAGACCAGCTCAATCTCGTCCAAACTTG     750
TCTGTTTTGATCAACGCTCAAGTTACTAAGTTGGTTAACTCTGGTATCAC     800
```

```
TAACGGTTTGCCAGCTTTCAGATGTGTTGAATACGCTGAACAAGAAGGTG     850
CTCCAACTACTACTGTTTGTGCTAAGAAGGAAGTTGTTTTGTCTGCTGGT     900
TCTGTTGGTACTCCAATCTTGTTGCAATTGTCTGGTATCGGTGACGAAAA     950
CGACTTGTCTTCTGTTGGTATCGACACTATCGTTAACAACCCATCTGTTG     1000
GTAGAAACTTGTCTGACCACTTGTTGTTGCCAGCTGCTTTCTTCGTTAAC     1050
TCTAACCAAACTTTCGACAACATCTTCAGAAACTCTTCTGAATTTAACGC     1100
TGACTTGGACCAATGGACTAACACTAGAACTGGTCCATTGACTGCTTTGA     1150
TCGCTAACCACTTGGCTTGGTTGAGATTGCCATCTAACTCTTCTATCTTC     1200
CAAACTTTCCCAGACCCAGCTGCTGGTCCAAACTCTGCTCACTGGGAAAC     1250
TATCTTCTCTAACCAATGGTTCCACCCAGCTATCCCAAGACCAGACACTG     1300
GTTCTTTCATGTCTGTTACTAACGCTTTGATCTCTCCAGTTGCTAGAGGT     1350
GACATCAAGTTGGCTACTTCTAACCCATTCGACAAGCCATTGATCAACCC     1400
ACAATACTTGTCTACTGAATTTGACATCTTCACTATGATCCAAGCTGTTA     1450
AGTCTAACTTGAGATTCTTGTCTGGTCAAGCTTGGGCTGACTTCGTTATC     1500
AGACCATTCGACCCAAGATTGAGAGACCCAACTAACGACGCTGCTATCGA     1550
ATCTTACATCAGAGACAACGCTAACACTATCTTCCACCCAGTTGGTACTG     1600
CTTCTATGTCTCCAAGAGGTGCTTCTTGGGGTGTTGTTGACCCAGACTTG     1650
AAGGTTAAGGGTGTTGACGGTTTGAGAATCGTTGACGGTTCTATCTTGCC     1700
ATTCGCTCCAAACGCTCACACTCAAGGTCCAATCTACTTGGTTGGTGAAA     1750
GAGGTGCTGACTTGATCAAGGCTGACCAATAA
```

*Pe*AAO2 amino acid sequence

```
        10         20         30         40         50         60
MSFGALRQLL LIACLALPSL AATNLPTADF DYVVVGAGNA GNVVAARLTE DPDVSVLVLE

        70         80         90        100        110        120
AGVSDENVLG AEAPLLAPGL VPNSIFDWNY TTTAQAGYNG RSIAYPRGRM LGGSSSVHYM

       130        140        150        160        170        180
VMMRGSTEDF DRYAAVTGDE GWNWDNIQQF VGKNEMVVPP ADNHNTSGEF IPAVHGTNGS

       190        200        210        220        230        240
VSISLPGFPT PLDDRVLATT QEQSEEFFFN PDMGTGHPLG ISWSIASVGN GQRSSSSTAY

       250        260        270        280        290        300
LRPAQSRPNL SVLINAQVTK LVNSGITNGL PAFRCVEYAE QEGAPTTTVC AKKEVVLSAG

       310        320        330        340        350        360
SVGTPILLQL SGIGDENDLS SVGIDTIVNN PSVGRNLSDH LLLPAAFFVN SNQTFDNIFR

       370        380        390        400        410        420
NSSEFNADLD QWTNTRTGPL TALIANHLAW LRLPSNSSIF QTFPDPAAGP NSAHWETIFS

       430        440        450        460        470        480
NQWFHPAIPR PDTGSFMSVT NALISPVARG DIKLATSNPF DKPLINPQYL STEFDIFTMI

       490        500        510        520        530        540
QAVKSNLRFL SGQAWADFVI RPFDPRLRDP TNDAAIESYI RDNANTIFHP VGTASMSPRG

       550        560        570        580        590
ASWGVVDPDL KVKGVDGLRI VDGSILPFAP NAHTQGPIYL VGERGADLIK ADQ
```

*Pp*AAO1 optimized gene sequence

```
ATGTCTTTCTCTGCTTTGAGACAATTGTTGTTGATCGCTTGTTTGGCTTT     50
GCCATCTTTGGCTGCTGCTAACTTGCCAACTGCTGACTTCGACTACATCG     100
TTGTTGGTGCTGGTAACGCTGGTAACGTTGTTGCTGCTAGATTGACTGAA     150
GACCCAAACGTTTCTGTTTTGGTTTTGGAAGCTGGTGTTTCTGACGAAAA     200
CGTTTTGGGTGCTGAAGCTCCATTGTTGGCTCCAGGTTTGGTTCCAAACT     250
CTATCTTCGACTGGAACTACACTACTACTGCTCAAGCTGGTTACAACGGT     300
AGATCTATCGCTTACCCAAGAGGTAGAATGTTGGGTGGTTCTTCTTCTGT     350
TCACTACATGGTTATGATGAGAGGTTCTATCGAAGACTTCGACAGATACG     400
CTGCTGTTACTGGTGACGACGGTTGGAACTGGGACAACATCCAACAATTC     450
GTTAGAAAGAACGAAATGGTTGTTCCACCAGCTGACAACCACAACACTTC     500
TGGTGAATTTATCCCAGCTGTTCACGGTACTAACGGTTCTGTTTCTATCT     550
CTTTGCCAGGTTTCCCAACTCCATTGGACGACAGAGTTTTGGCTACTACT     600
CAAGAACAATCTGAAGAATTTTTCTTCAACCCAGACATGGGTACTGGTCA     650
CCCATTGGGTATCTCTTGGTCTATCGCTTCTGTTGGTAACGGTCAAAGAT     700
CTTCTTCTTCTACTGCTTACTTGAGACCAGCTCAATCTCGTCCAAACTTG     750
TCTGTTTTGATCAACGCTCAAGTTACTAAGTTGGTTAACTCTGGTACTAC     800
TAACGGTTTGCCAGCTTTCAGATGTGTTGAATACGCTGAAAGAGAAGGTG     850
CTCCAACTACTACTGTTTGTGCTAACAAGGAAGTTGTTTTGTCTGCTGGT     900
TCTGTTGGTACTCCAATCTTGTTGCAATTGTCTGGTATCGGTGACCAATC     950
TGACTTGTCTGCTGTTGGTATCGACACTATCGTTAACAACCCATCTGTTG     1000
GTAGAAACTTGTCTGACCACTTGTTGTTGCCAGCTACTTTCTTCGTTAAC     1050
AACAACCAATCTTTCGACAACTTGTTCAGAGACTCTTCTGAATTTAACGC     1100
TGACTTGGACCAATGGACTAACACTAGAACTGGTCCATTGACTGCTTTGA     1150
TCGCTAACCACTTGGCTTGGTTGAGATTGCCATCTAACTCTTCTATCTTC     1200
CAATCTGTTCCAGACCCAGCTGCTGGTCCAAACTCTGCTCACTGGGAAAC     1250
TATCTTCTCTAACCAATGGTTCCACCCAGCTTTGCCAAGACCAGACACTG     1300
GTAACTTCATGTCTGTTACTAACGCTTTGATCGCTCCAGTTGCTAGAGGT     1350
GACATCAAGTTGGCTACTTCTAACCCATTCGACAAGCCATTGATCAACCC     1400
ACAATACTTGTCTACTGAATTTGACATCTTCACTATGATCCAAGCTGTTA     1450
AGTCTAACTTGAGATTCTTGTCTGGTCAAGCTTGGGCTGACTTCGTTATC     1500
AGACCATTCGACGCTAGATTGTCTGACCCAACTAACGACGCTGCTATCGA     1550
ATGGAACATCAGAGACAACGCTAACACTATCTTCCACCCAGTTGGTACTG     1600
CTTCTATGTCTCCAAGAGGTGCTTCTTGGGGTGTTGTTGACCCAGACTTG     1650
AAGGTTAAGGGTGTTGACGGTTTGAGAATCGTTGACGGTTCTATCTTGCC     1700
ATTCGCTCCAAACGCTCACACTCAAGGTCCAATCTACTTGGTTGGTGAAA     1750
GAGGTGCTGACTTGATCAAGGCTGACCAATAA
```

*Pp*AAO1 amino acid sequence

```
        10         20         30         40         50         60
MSFSALRQLL LIACLALPSL AAANLPTADF DYIVVGAGNA GNVVAARLTE DPNVSVLVLE

        70         80         90        100        110        120
AGVSDENVLG AEAPLLAPGL VPNSIFDWNY TTTAQAGYNG RSIAYPRGRM LGGSSSVHYM

       130        140        150        160        170        180
VMMRGSIEDF DRYAAVTGDD GWNWDNIQQF VRKNEMVVPP ADNHNTSGEF IPAVHGTNGS

       190        200        210        220        230        240
VSISLPGFPT PLDDRVLATT QEQSEEFFFN PDMGTGHPLG ISWSIASVGN GQRSSSSTAY
```

```
        250        260        270        280        290        300
LRPAQSRPNL SVLINAQVTK LVNSGTTNGL PAFRCVEYAE REGAPTTTVC ANKEVVLSAG

        310        320        330        340        350        360
SVGTPILLQL SGIGDQSDLS AVGIDTIVNN PSVGRNLSDH LLLPATFFVN NNQSFDNLFR

        370        380        390        400        410        420
DSSEFNADLD QWTNTRTGPL TALIANHLAW LRLPSNSSIF QSVPDPAAGP NSAHWETIFS

        430        440        450        460        470        480
NQWFHPALPR PDTGNFMSVT NALIAPVARG DIKLATSNPF DKPLINPQYL STEFDIFTMI

        490        500        510        520        530        540
QAVKSNLRFL SGQAWADFVI RPFDARLSDP TNDAAIEWNI RDNANTIFHP VGTASMSPRG

        550        560        570        580        590
ASWGVVDPDL KVKGVDGLRI VDGSILPFAP NAHTQGPIYL VGERGADLIK ADQ
```

*Mr*AAO3 optimized gene sequence

```
ATGTACCCAAGAACTTTCTGGTTGGCTTTGGCTTTGTCTGCTGTTTCTAC     50
TTGTTGGGCTGCTATCTACCACGACTTGGACGCTGTTCCAAAGGACACTT     100
ACGACTTCATCGTTGCTGGTGGTGGTACTGCTGGTTTGGTTATCGCTAAC     150
AGATTGTCTGAAAACCCAAAGGTTTCTGTTTTGGTTATCGAAGCTGGTCC     200
ATCTAACGAAGGTGTTTTGAACATCGAAGTTCCATTCTACTGTACTAGAG     250
CTTCTCCAGACACTCCATACGACTGGAACTACACTACTGCTCCACAAGAA     300
ATGTTGAACGGTAGATCTTTGCCATACAACAGAGGTCACGTTTTGGGTGG     350
TTCTTCTTCTACTAACTTCATGATCTACACTAGAGGTTCTGCTGAAGACT     400
ACGACAGAATCGCTGCTGTTTCTGGTGACCCAGGTTGGTCTTGGGAAAAG     450
TTGCAACCATTCATCTTCAGAAACGAAATCGTTACTCCACCAGCTGACGG     500
TCACGACACTTCTGAACAATACGACCCAAGATTCCACGGTACTAAGGGTA     550
TCAACCCAGACTCTTTGCCAGGTTTCCCAACTCCAATCGACGACAGAATC     600
TTGGCTGCTACTCAAGAATTGTCTGACGAATTTCCATTCAACTTGGACTA     650
CAACTCTGGTTACCACTTGGGTATCGGTTGGGGTATCGCTACTATCTTCA     700
ACGGTTCTCGTTCTTCTTCTGCTACTTCTTACTTGGGTCCAAAGTACGCT     750
CAAAGAAAGAACTTGAACGTTGTTTTGAACACTAGAGTTACTAGAGTTTT     800
GCCAAAGGAAAAGGAAGACTCTGGTGACGTTACTAAGAGAGTTATCCCAA     850
GAAACAACGACAAGAAGAGAAAGTTGCACATCAACGCTATCGAAGTTGCT     900
AAGACTTCTGACGGTCCAAGAAAGCAATTCACTGCTAAGAAGGAAATCAT     950
CTTGTCTGCTGGTGCTATCGGTTCTCCACAAATCTTGTTGAACTCTGGTA     1000
TCGGTGGTTCTGAAGCTTTGTCTCAATTGGGTATCGAACCAATCTTGGAC     1050
AACCCATCTGTTGGTCAAAACTTGTCTGACCACCCAGTTTTGGGTAACTC     1100
TTGGTTCGTTAACGAAACTCAAACTTGGGAATTGATCGCTAGAAACGCTA     1150
CTTACGCTGAAGAAGTTTTGGACTTGTGGGAAACTCAAAGAGAAGGTCCA     1200
TTGGTTAACACTATCGCTACTCAATTGGGTTGGCACAGAATCCCAGACAA     1250
CTCTTCTATCTTCGAGACTCACGAAGACCCAGCTGCTGGTCCAAACACTG     1300
CTCACTACGAATTGGTTTTCGCTAACGGTTTGAGAGGTACTCCACCACCA     1350
GAAGGTAACTTCATGACTATCACTACTGCTTTGGTTTCTCCAGCTTCTCG     1400
TGGTTCTGTTACTTTGAGATCTTCTAACCCATTCGACTCTCCAATCATCG     1450
ACCCAAACTTCTTGAACTCTGAATTTGACATGTTCGTTTTGAAGTACGCT     1500
ATCCACGCTGCTAGAAGATTCGTTGCTGCTAGAGCTTTCGACGGTTACAT     1550
```

```
CTTGAGACCATTCTTCAACTCTACTACTGACGAAGAAATCGAAGAAATGA     1600
TCAGAAACACTACTAGAACTATCTACCACCCAGTTGGTACTTTGTCTATG     1650
TCTGCTAAGAACGACGCTTGGGGTGTTGTTGACCCAGACTTGTCTGTTAA     1700
GGGTGTTGAAGGTTTGAGAGTTGTTGACGCTTCTGTTTTCCCACACATCC     1750
CAACTGCTCACACTCAAGTTCCAGTTTACATCTTGGCTGAAAGAGGTTCT     1800
GACTTGATCAAGCAATCTTGGAAGTTG
```
TAA

*Mr*AAO3 amino acid sequence

```
        10         20         30         40         50         60
MYPRTFWLAL ALSAVSTCWA AIYHDLDAVP KDTYDFIVAG GGTAGLVIAN RLSENPKVSV

        70         80         90        100        110        120
LVIEAGPSNE GVLNIEVPFY CTRASPDTPY DWNYTTAPQE MLNGRSLPYN RGHVLGGSSS

       130        140        150        160        170        180
TNFMIYTRGS AEDYDRIAAV SGDPGWSWEK LQPFIFRNEI VTPPADGHDT SEQYDPRFHG

       190        200        210        220        230        240
TKGINPDSLP GFPTPIDDRI LAATQELSDE FPFNLDYNSG YHLGIGWGIA TIFNGSRSSS

       250        260        270        280        290        300
ATSYLGPKYA QRKNLNVVLN TRVTRVLPKE KEDSGDVTKR VIPRNNDKKR KLHINAIEVA

       310        320        330        340        350        360
KTSDGPRKQF TAKKEIILSA GAIGSPQILL NSGIGGSEAL SQLGIEPILD NPSVGQNLSD

       370        380        390        400        410        420
HPVLGNSWFV NETQTWELIA RNATYAEEVL DLWETQREGP LVNTIATQLG WHRIPDNSSI

       430        440        450        460        470        480
FETHEDPAAG PNTAHYELVF ANGLRGTPPP EGNFMTITTA LVSPASRGSV TLRSSNPFDS

       490        500        510        520        530        540
PIIDPNFLNS EFDMFVLKYA IHAARRFVAA RAFDGYILRP FFNSTTDEEI EEMIRNTTRT

       550        560        570        580        590        600
IYHPVGTLSM SAKNDAWGVV DPDLSVKGVE GLRVVDASVF PHIPTAHTQV PVYILAERGS


DLIKQSWKL
```

*Ma*GMC1 optimized gene sequence

```
ATGAAGGCTACTACTATCATCGCTGCTGCTGCTTTGGCTGGTTCTGTTGC     50
TGCTACTCCAGTTGCTTGGACTAAGGTTTCTCCAAGATCTGAAATGGCTG     100
CTAGAATGGCTGAAAACTCTCACTTGGCTTCTCGTGCTATCACTAACGAC     150
GCTGCTAAGTTCGTTTCTAAGCAATACGACTACGTTGTTGTTGGTGCTGG     200
TACTGCTGGTTTGGCTTTGGCTGCTAGATTGTCTGAAAACGGTAAGTACA     250
AGGTTGGTGTTTTGGAAGCTGGTGGTTCTGGTTACGGTGTTGGTATCATC     300
GACACTCCAGGTCAATTCGGTGCTGACTTGGGTACTCAATACGACTGGAA     350
CTACACTACTGTTGCTAACCCAGCTAACGGTGTTCCATCTTCTGGTTGGC     400
CAAGAGGTAGAGTTTTGGGTGGTTCTTCTGCTTTGAACTTCTTGGTTTGG     450
GACAGATCTTCTCGTTACGAAATCGACGCTTGGGAACAATTGGGTAACCC     500
```

```
AGGTTGGAACTGGAACAACTTGTACAAGGCTATGAAGAAGTCTGAAAGAT     550
TCCACGCTCCATCTCAAGAAAACGCTGACTTGTTGGGTGTTAAGCCAGTT     600
GCTTCTGACTACGGTTCTTCTGGTCCAATCCAAGTTGCTTTCCCAAACTA     650
CATCTCTCAACAAGTTAGAAGATGGATCCCAGCTTTGTTGGAATTGGGTA     700
TCCCAAAGAACGACCAACCATTGGCTGGTGAAAACGTTGGTGTTTCTCAA     750
CAACCATCTGACATCAACCCAACTAACTACACTAGATCTTACTCTGCTCC     800
AGCTTACTTGTTCCCAAACCAAGCTAGATCTAACTTGGACGTTTTGACTA     850
ACGCTTTGGCTTCTAAGGTTAACTTCGACTCTTCTTGTGGTGAATTGTGG     900
GCTAAGTCTGTTACTTTCACTAACGGTGGTAAGTCTTACACTGTTAACGC     950
TACTAAGGAAGTTATCATCTCTGCTGGTACTGTTAACACTCCACAATTGT     1000
TGGAATTGTCTGGTATCGGTTCTAAGGACGTTTTGGGTAAGGCTGGTGTT     1050
AAGGTTTTGTACGAAAACGCTAACGTTGGTGAAAACTTGCAAGACCACAC     1100
TTACTCTGCTACTGTTTACAACTTGAAGTCTGGTTTCAAGACTTTGGACT     1150
CTTTGAGATCTGACTCTACTTTCGCTGCTGAACAATTGGCTGCTTACAAG     1200
GCTAACCAAACTTCTATCTTCACTGAAACTGTTCCATCTATCTCTTACGT     1250
TTCTTTGGCTAGAGTTGTTGGTGCTGACAGAGCTAAGGCTATGATCAACG     1300
AAGTTACTCAATACGTTCAATCTTCTCGTGCTCCATACAAGGCTACTTTG     1350
AACAAGCAATTGGACTTCTTGAACAACTACCCAGACAAGGTTGGTCAAAT     1400
GGAATTGATCGGTATCGACGGTTACTTCGCTGGTACTGGTGCTCCAAAGC     1450
CAACTGAAACTTACTTCACTATCTTGGCTGCTAACCAACACTTGTTCTCT     1500
CGTGGTAACGTTCACATCCAATCTTCTGACCCAACTAAGTACCCATTGAT     1550
CGACCCAAAGTACTTCTCTGTTCCATTCGACACTGAATTGTCTACTGCTG     1600
GTACTGCTTACACTAGAAAGGTTGGTTTGTCTAAGGCTTACTCTGACATG     1650
GTTGTTGGTGAATACTGGCCAGGTAACGTTGACTTGCAAAACTACACTAA     1700
GACTACTTCTGTTACTGAATACCACCCAATCGGTACTGCTTCTATGTTGC     1750
CAAGAAACCAAGGTGGTGTTGTTGACCCATCTTTGAGAGTTTACGGTACT     1800
ACTAACTTGAGAGTTGTTGACGCTTCTATCATGCCATTGCACGTTGCTGC     1850
TCACATCCAAGCTACTATCTACGGTGTTGCTGAATACGCTGCTTCTATCA     1900
TCAAGTCTCAAGCTTAA
```

*Ma*GMC1 amino acid sequence

```
        10         20         30         40         50         60
MKATTIIAAA ALAGSVAATP VAWTKVSPRS EMAARMAENS HLASRAITND AAKFVSKQYD

        70         80         90        100        110        120
YVVVGAGTAG LALAARLSEN GKYKVGVLEA GGSGYGVGII DTPGQFGADL GTQYDWNYTT

       130        140        150        160        170        180
VANPANGVPS SGWPRGRVLG GSSALNFLVW DRSSRYEIDA WEQLGNPGWN WNNLYKAMKK

       190        200        210        220        230        240
SERFHAPSQE NADLLGVKPV ASDYGSSGPI QVAFPNYISQ QVRRWIPALL ELGIPKNDQP

       250        260        270        280        290        300
LAGENVGVSQ QPSDINPTNY TRSYSAPAYL FPNQARSNLD VLTNALASKV NFDSSCGELW

       310        320        330        340        350        360
AKSVTFTNGG KSYTVNATKE VIISAGTVNT PQLLELSGIG SKDVLGKAGV KVLYENANVG

       370        380        390        400        410        420
ENLQDHTYSA TVYNLKSGFK TLDSLRSDST FAAEQLAAYK ANQTSIFTET VPSISYVSLA

       430        440        450        460        470        480
RVVGADRAKA MINEVTQYVQ SSRAPYKATL NKQLDFLNNY PDKVGQMELI GIDGYFAGTG
```

```
        490        500        510        520        530        540
APKPTETYFT ILAANQHLFS RGNVHIQSSD PTKYPLIDPK YFSVPFDTEL STAGTAYTRK

        550        560        570        580        590        600
VGLSKAYSDM VVGEYWPGNV DLQNYTKTTS VTEYHPIGTA SMLPRNQGGV VDPSLRVYGT

        610        620        630
TNLRVVDASI MPLHVAAHIQ ATIYGVAEYA ASIIKSQA
```

2.1.5.2. Sequence alignment

Multiple sequence alignment of *Pe*AAO, *Pe*AAO2, *Pp*AAO1, *Mr*AAO3 and *Ma*GMC1 protein sequences using the Clustral Omega tool (https://www.ebi.ac.uk/Tools/msa/clustalo/) and amino acid sequences from 2.1.5.1.

```
MaGMC1      MKATTIIAAAALAGSVAATPVAWTKVSPRSEMAARMAENSHLASRAITNDAAKFVSKQYD    60
MrAAO3      -------------------------MYPRTFWLALALSAVSTCWAAIYHDLDAVPKDTYD    35
PpAAO1      ------------------------------MSFSALRQLLLIACLALPSLAAANLPTADFD    31
PeAAO       ------------------------------MSFGALRQLLLIACLALPSLAATNLPTADFD    31
PeAAO2      ------------------------------MSFGALRQLLLIACLALPSLAATNLPTADFD    31
                                                *        .          . .  :*

MaGMC1      YVVVGAGTAGLALAARLSENGKYKVGVLEAGGSGYGVGIIDTPGQ-FGADLGTQYDWNYT    119
MrAAO3      FIVAGGGTAGLVIANRLSENPKVSVLVIEAGPSNEGVLNIEVPFYCTRASPDTPYDWNYT    95
PpAAO1      YIVVGAGNAGNVVAARLTEDPNVSVLVLEAGVSDENVLGAEAPLLAPGLVPNSIFDWNYT    91
PeAAO       YVVVGAGNAGNVVAARLTEDPDVSVLVLEAGVSDENVLGAEAPLLAPGLVPNSIFDWNYT    91
PeAAO2      YVVVGAGNAGNVVAARLTEDPDVSVLVLEAGVSDENVLGAEAPLLAPGLVPNSIFDWNYT    91
            ::*.*.*.** .:* **:*: . .* *:*** *. .*   :.*        .: :*****

MaGMC1      TVANPANGVPSSGWPRGRVLGGSSALNFLVWDRSSRYEIDAWEQ-LGNPGWNWNNLYKAM    178
MrAAO3      TAPQEMLNGRSLPYNRGHVLGGSSSTNFMIYTRGSAEDYDRIAAVSGDPGWSWEKLQPFI    155
PpAAO1      TTAQAGYNGRSIAYPRGRMLGGSSSVHYMVMMRGSIEDFDRYAAVTGDDGWNWDNIQQFV    151
PeAAO       TTAQAGYNGRSIAYPRGRMLGGSSSVHYMVMMRGSTEDFDRYAAVTGDEGWNWDNIQQFV    151
PeAAO2      TTAQAGYNGRSIAYPRGRMLGGSSSVHYMVMMRGSTEDFDRYAAVTGDEGWNWDNIQQFV    151
            *. :   .  *  : **::*****: ::::  *.*  : *      *: **.*:::   :

MaGMC1      KKSERFHAPSQENADLLGVKPVASDYGSSGPIQVAFPNYISQQVRRWIPALLELG--IPK    236
MrAAO3      FRNEIVTPPADGHDTSEQYDPRF--HGTKGINPDSLPGFPTPIDDRILAATQELSDEFPF    213
PpAAO1      RKNEMVVPPADNHNTSGEFIPAV--HGTNGSVSISLPGFPTPLDDRVLATTQEQSEEFFF    209
PeAAO       RKNEMVVPPADNHNTSGEFIPAV--HGTNGSVSISLPGFPTPLDDRVLATTQEQSEEFFF    209
PeAAO2      GKNEMVVPPADNHNTSGEFIPAV--HGTNGSVSISLPGFPTPLDDRVLATTQEQSEEFFF    209
             :.* .  *:: :       *    :*:.*    ::*.: :    * : :  * .  :

MaGMC1      NDQPLAGENVGVSQQPSDINPTNYTRSYSAPAYLFPNQA-RSNLDVLTNALASKVNFDSS    295
MrAAO3      NLDYNSGYHLGIGWGIA--TIFNGSRSSSATSYLGPKYAQRKNLNVVLNTRVTRVLPKEK    271
PpAAO1      NPDMGTGHPLGISWSIA--SVGNGQRSSSSTAYLRPAQS-RPNLSVLINAQVTKLVNSGT    266
PeAAO       NPDMGTGHPLGISWSIA--SVGNGQRSSSSTAYLRPAQS-RPNLSVLINAQVTKLVNSGT    266
PeAAO2      NPDMGTGHPLGISWSIA--SVGNGQRSSSSTAYLRPAQS-RPNLSVLINAQVTKLVNSGI    266
            * :  :*  :*:.   :  .  *  ** *: :** *  : * **.*: *: .:::  .

MaGMC1      -------------------CGELWAKSVTFTNGGKSYTVNATKEVIISAGTVNTPQLLEL    336
MrAAO3      EDSGDVTKRVIPRNNDKKRKLHINAIEVAKTSDGPRKQFTAKKEIILSAGAIGSPQILLN    331
PpAAO1      TN----------------GLPAFRCVEYAEREGAPTTTVCANKEVVLSAGSVGTPILLQL    310
PeAAO       TN----------------GLPAFRCVEYAEQEGAPTTTVCAKKEVVLSAGSVGTPILLQL    310
PeAAO2      TN----------------GLPAFRCVEYAEQEGAPTTTVCAKKEVVLSAGSVGTPILLQL    310
                                  : . . :  ...    . *.**:::***::.:* :*

MaGMC1      SGIGSKDVLGKAGVKVLYENANVGENLQDHTYSATVYNLKSGFKTLDSLRSDSTFAAEQL    396
MrAAO3      SGIGGSEALSQLGIEPILDNPSVGQNLSDHPVLGNSWFVNET-QTWELIARNATYAEEVL    390
PpAAO1      SGIGDQSDLSAVGIDTIVNNPSVGRNLSDHLLLPATFFVNNN-QSFDNLFRDSSEFNADL    369
PeAAO       SGIGDENDLSSVGIDTIVNNPSVGRNLSDHLLLPAAFFVNSN-QTFDNIFRDSSEFNVDL    369
PeAAO2      SGIGDENDLSSVGIDTIVNNPSVGRNLSDHLLLPAAFFVNSN-QTFDNIFRNSSEFNADL    369
            ****... *.  *:. : :* .**.**.**      : ::.  :: : :  :::     *

MaGMC1      AAYKANQTSIFTETVPSISYVSLARVVGADRAKAMINEVTQYVQSSRAPYKATLNKQLDF    456
MrAAO3      DLWETQREGPLVNTIA------------------------TQLGWHRIPDNS------SI    420
PpAAO1      DQWTNTRTGPLTALIA------------------------NHLAWLRLPSNS------SI    399
```

```
PeAAO       DQWTNTRTGPLTALIA------------------------NHLAWLRLPSNS------SI     399
PeAAO2      DQWTNTRTGPLTALIA------------------------NHLAWLRLPSNS------SI     399
              :   : . :.  :                           :   * * ::      .:

MaGMC1      LNNYPD-----KVGQMELIGIDGYFAGTGAPKPTETYFTILAANQHLFSRGNVHIQSSDP     511
MrAAO3      FETHEDPAAGPNTAHYELVFANGLRG---TPPPEGNFMTITTALVSPASRGSVTLRSSNP     477
PpAAO1      FQSVPDPAAGPNSAHWETIFSNQWFHPALPRPDTGNFMSVTNALIAPVARGDIKLATSNP     459
PeAAO       FQTFPDPAAGPNSAHWETIFSNQWFHPAIPRPDTGSFMSVTNALISPVARGDIKLATSNP     459
PeAAO2      FQTFPDPAAGPNSAHWETIFSNQWFHPAIPRPDTGSFMSVTNALISPVARGDIKLATSNP     459
            ::.  *     : .: * :  :             .::::  *     :**.: : :*:*

MaGMC1      TKYPLIDPKYFSVPFDTELSTAGTAYTRKVGLSKAYSDMVVGEYWPGN------VDLQNY     565
MrAAO3      FDSPIIDPNFLNSEFDMFVLKYAIHAARRFVAARAFDGYILRPFFNST----TDEEIEEM     533
PpAAO1      FDKPLINPQYLSTEFDIFTMIQAVKSNLRFLSGQAWADFVIRPFDARLSDPTNDAAIEWN     519
PeAAO       FDKPLINPQYLSTEFDIFTMIQAVKSNLRFLSGQAWADFVIRPFDPRLRDPTDDAAIESY     519
PeAAO2      FDKPLINPQYLSTEFDIFTMIQAVKSNLRFLSGQAWADFVIRPFDPRLRDPTNDAAIESY     519
             . *:*:*:::.  **      .     :.  .:*: . ::  :            ::

MaGMC1      TKTTSVTEYHPIGTASMLPRNQ-GGVVDPSLRVYGTTNLRVVDASIMPLHVAAHIQATIY     624
MrAAO3      IRNTTRTIYHPVGTLSMSAKNDAWGVVDPDLSVKGVEGLRVVDASVFPHIPTAHTQVPVY     593
PpAAO1      IRDNANTIFHPVGTASMSPRGASWGVVDPDLKVKGVDGLRIVDGSILPFAPNAHTQGPIY     579
PeAAO       IRDNANTIFHPVGTASMSPRGASWGVVDPDLKVKGVDGLRIVDGSILPFAPNAHTQGPIY     579
PeAAO2      IRDNANTIFHPVGTASMSPRGASWGVVDPDLKVKGVDGLRIVDGSILPFAPNAHTQGPIY     579
             : .: * :**:** **  :.   *****.* * *. .**:**.*::*    ** *  :*

MaGMC1      GVAEYAASIIKSQA--      638
MrAAO3      ILAERGSDLIKQSWKL      609
PpAAO1      LVGERGADLIKADQ--      593
PeAAO       LVGKQGADLIKADQ--      593
PeAAO2      LVGERGADLIKADQ--      593
             :.: .:.:** .
```

2.2. Chapter II: Biochemical characterization of *Pe*AAO2 from *Pleurotus eryngii* P34

Title	High-level expression of aryl-alcohol oxidase 2 from *Pleurotus eryngii* in *Pichia pastoris* for production of fragrances and bioactive precursors
Authors	Nina Jankowski, Katja Koschorreck, Vlada B. Urlacher
Contribution	Design, planning and conduction of all experiments, evaluation of all data, drafting the manuscript. Relative contribution: 90 %
Published in	*Applied Microbiology and Biotechnology,* 104, 9205-9218 (**2020**)
DOI	10.1007/s00253-020-10878-4
Publisher	Springer Nature
Copyright	Copyright © 2020, Springer Nature

Applied Microbiology and Biotechnology (2020) 104:9205–9218
https://doi.org/10.1007/s00253-020-10878-4

BIOTECHNOLOGICALLY RELEVANT ENZYMES AND PROTEINS

High-level expression of aryl-alcohol oxidase 2 from *Pleurotus eryngii* in *Pichia pastoris* for production of fragrances and bioactive precursors

Nina Jankowski[1] · **Katja Koschorreck**[1] · **Vlada B. Urlacher**[1]

Received: 22 June 2020 / Revised: 14 August 2020 / Accepted: 2 September 2020 / Published online: 19 September 2020

Abstract

The fungal secretome comprises various oxidative enzymes participating in the degradation of lignocellulosic biomass as a central step in carbon recycling. Among the secreted enzymes, aryl-alcohol oxidases (AAOs) are of interest for biotechnological applications including production of bio-based precursors for plastics, bioactive compounds, and flavors and fragrances. Aryl-alcohol oxidase 2 (*Pe*AAO2) from the fungus *Pleurotus eryngii* was heterologously expressed and secreted at one of the highest yields reported so far of 315 mg/l using the methylotrophic yeast *Pichia pastoris* (recently reclassified as *Komagataella phaffii*). The glycosylated *Pe*AAO2 exhibited a high stability in a broad pH range between pH 3.0 and 9.0 and high thermal stability up to 55 °C. Substrate screening with 41 compounds revealed that *Pe*AAO2 oxidized typical AAO substrates like *p*-anisyl alcohol, veratryl alcohol, and *trans,trans*-2,4-hexadienol with up to 8-fold higher activity than benzyl alcohol. Several compounds not yet reported as substrates for AAOs were oxidized by *Pe*AAO2 as well. Among them, cumic alcohol and piperonyl alcohol were oxidized to cuminaldehyde and piperonal with high catalytic efficiencies of 84.1 and 600.2 mM^{-1} s^{-1}, respectively. While the fragrance and flavor compound piperonal also serves as starting material for agrochemical and pharmaceutical building blocks, various positive health effects have been attributed to cuminaldehyde including anticancer, antidiabetic, and neuroprotective effects. *Pe*AAO2 is thus a promising biocatalyst for biotechnological applications.

Key points

- *Aryl-alcohol oxidase PeAAO2 from P. eryngii was produced in P. pastoris at 315 mg/l.*
- *Purified enzyme exhibited stability over a broad pH and temperature range.*
- *Oxidation products cuminaldehyde and piperonal are of biotechnological interest.*

Keywords Aryl-alcohol oxidase · *Pichia pastoris* (*Komagataella phaffii*) · Flavoprotein · Aromatic alcohols · Fragrances · Piperonal

Introduction

The pursuit of a sustainable and bio-based society includes the search for and development of environmentally friendly production routes for fine chemicals. As a result, more and more biocatalytic processes for production of fine chemicals and valuable building blocks are coming into the focus of research and industry. In green chemistry, the use of biocatalysts has many advantages over conventional organic chemical synthesis, including mild reaction conditions (aqueous systems, ambient temperatures, atmospheric pressure), use of catalyst in non-stoichiometric quantities, and reduced waste production (Sheldon and Woodley 2018). Aryl-alcohol oxidases (AAOs, EC 1.1.3.7) are FAD-dependent oxidoreductases secreted by wood-decaying fungi as glycoproteins (Sannia et al. 1991; Varela et al. 2000a, b). They catalyze the oxidation of primary aromatic and aliphatic polyunsaturated alcohols to the corresponding aldehydes while reducing molecular O_2 to H_2O_2 (Guillén et al. 1992). In some cases, the generated aldehydes

Electronic supplementary material The online version of this article (https://doi.org/10.1007/s00253-020-10878-4) contains supplementary material, which is available to authorized users.

✉ Vlada B. Urlacher
vlada.urlacher@uni-duesseldorf.de

[1] Institute of Biochemistry, Heinrich-Heine-University Düsseldorf, Universitätsstraße 1, 40225 Düsseldorf, Germany

can be further oxidized to the aromatic acids depending on the degree of hydration via *gem*-diol formation of the aldehyde (Ferreira et al. 2010). AAOs offer great potential for application in biocatalytic processes, as they only require molecular oxygen for substrate oxidation and generate hydrogen peroxide as byproduct, without the need of added cofactors. In nature, AAOs play an essential role in degradation of lignocellulosic biomass and hence also in carbon recycling. Wood-decaying fungi secrete a whole bunch of oxidative enzymes like laccases, ligninolytic peroxidases, and aryl-alcohol oxidases in order to break down lignin, the most recalcitrant component of lignocellulose (Kirk and Farrell 1987).

While laccases (EC 1.10.3.2) and ligninolytic peroxidases (EC 1.11.1.x) have been intensively studied and applied in different fields including food, textile and cosmetics industry, biorefineries, and bioremediation (Arregui et al. 2019; Falade et al. 2016, 2018; Fillat et al. 2017; Rodríguez Couto and Toca Herrera 2006; Stanzione et al. 2020), H_2O_2-producing oxidases like aryl-alcohol oxidases only slowly step forward into biocatalytic applications. For example, an AAO from *Pleurotus eryngii* ATCC 90787 (*Pe*AAO) was studied for production of 2,5-furandicarboxylic acid (FDCA), a bio-based precursor for plastics (Carro et al. 2014; Karich et al. 2018; Serrano et al. 2019a; Viña-Gonzalez et al. 2020). Structure-guided mutagenesis was applied on *Pe*AAO to construct enzyme variants capable of selectively oxidizing secondary aromatic alcohols like (*S*)-1-(*p*-methoxyphenyl)-ethanol to the corresponding ketones (Serrano et al. 2019b; Viña-Gonzalez et al. 2019). This enables the use of AAO in kinetic deracemization of secondary alcohols and generation of enantiomer enriched preparations, which are essential building blocks in the production of pharmaceuticals (Patel 2018). The most recent studies regarding enzyme engineering of AAOs and potential applications were summarized by Viña-Gonzalez and Alcalde (2020).

In general, most oxidation products of AAO-catalyzed reactions have considerable importance for the flavor and fragrance industry. Recently, *Pe*AAO from *P. eryngii* was employed for the conversion of *trans*-2-hexenol to the aldehyde *trans*-2-hexenal, which is of interest for the flavor and fragrance industry as fresh and fruity note of different vegetables and fruits (de Almeida et al. 2019; Van Schie et al. 2018). To gain access to a wider range of pleasant-smelling aldehydes and valuable building blocks via biocatalysis, more information about the substrate scope of AAOs is needed.

One of the factors limiting a broader application and protein engineering of AAOs is their "difficult" expression in recombinant hosts. For instance, the most studied aryl-alcohol oxidase *Pe*AAO from *P. eryngii* yielded only 3 mg/l in *Aspergillus nidulans* (Ferreira et al. 2005). The same enzyme was produced in *Escherichia coli* as inclusion bodies (Ruiz-Dueñas et al. 2006) and yielded 45 mg/l after in vitro refolding. However, due to the lack of glycosylation, the *E. coli*-derived recombinant *Pe*AAO showed lower pH and thermal stability than the recombinant enzyme expressed in *A. nidulans* (Ruiz-Dueñas et al. 2006). Efforts were made to optimize *Pe*AAO for secretion in eukaryotic hosts. The optimized *Pe*AAO variant FX7 was constructed using the mutagenic organized recombination process by homologous in vivo grouping (MORPHING) for improved expression in *Saccharomyces cerevisiae* and yielded 2 mg/l of active hyperglycosylated enzyme (Viña-Gonzalez et al. 2015). This variant was further optimized by in vivo shuffling with other *Pe*AAO variants and by the targeted MORPHING of the chimeric signal peptide, which eventually led to the variant FX9. This variant was transferred to *Pichia pastoris* for high-level production, leading to 25.5 mg/l of enzyme (Viña-Gonzalez et al. 2018). Using a basidiomycete as expression host, an AAO from *Pleurotus sapidus* was heterologously produced in *Coprinopsis cinerea* with a yield of 1.4 mg/l (Galperin et al. 2016). In order to fully elucidate fungal AAOs promising properties as biocatalysts in biotechnological processes, a high-yield expression system needs to be established.

Here, we report on high-yield expression of aryl-alcohol oxidase 2 from *P. eryngii* P34 (*Pe*AAO2) in the methylotrophic yeast *P. pastoris* for biotechnological applications. *Pe*AAO2 was characterized and the activity towards a large set of aromatic, heterocyclic, and aliphatic alcohols was investigated. Several compounds not yet described as substrates for AAOs were oxidized by *Pe*AAO2 to furnish important products for the flavor and fragrance industry, and bioactive compounds like piperonal and cuminaldehyde. Furthermore, the influence of glycosylation on enzyme stability was investigated, and kinetic parameters were determined for selected substrates to assess the biotechnological potential of this AAO.

Materials and methods

Materials

All chemicals were purchased from abcr GmbH (Karlsruhe, Germany), Acros Organics (Geel, Belgium), Alfa Aesar (Kandel, Germany), AppliChem GmbH (Darmstadt, Germany), BLDpharm (Shanghai, China), Carbolution Chemicals GmbH (St. Ingbert, Germany), Carl Roth GmbH + Co. KG (Karlsruhe, Germany), Fluorochem (Hadfield, UK), J&K Scientific (Lommel, Belgium), Sigma-Aldrich (Schnelldorf, Germany), TCI Chemicals (Eschborn, Germany), and VWR (Darmstadt, Germany). Enzymes and kits were obtained from New England Biolabs (Frankfurt am Main, Germany), Thermo Fisher Scientific (Bremen, Germany), SERVA Electrophoresis GmbH (Heidelberg, Germany), and Zymo Research (Freiburg, Germany).

Bacterial and yeast strains

Escherichia coli strain DH5α used for plasmid amplification was obtained from Clontech Laboratories Inc. (Heidelberg, Germany). *Pichia pastoris* strain X-33 (recently reclassified as *Komagataella phaffii*) used for expression was purchased from Invitrogen (Carlsbad, USA).

Generation of recombinant *P. pastoris* X-33 transformants

The gene encoding for *Pe*AAO2 from the *P. eryngii* strain P34 (GenBank accession number GU444001.1) was identified by protein BLAST search, using the AAO from the *P. eryngii* strain ATCC 90787 (GenBank accession number AAC72747) as query. The gene *peaao2* was codon optimized (GenBank accession number MT711371) for the expression in *Saccharomyces cerevisiae* using the online tool JCat (Grote et al. 2005). The optimized gene carrying the native signal sequence was synthesized by BioCat GmbH (Heidelberg, Germany) and readily ligated into pPICZA vector (Invitrogen, Carlsbad, USA) employing the restriction sites *Eco*RI and *Not*I, to generate the plasmid pPICZA_*peAAO2*. Chemically competent *E. coli* DH5α cells were transformed with the desired plasmid and transformants were selected on low salt lysogeny broth agar plates (LB; 1% peptone, 0.5% yeast extract, 0.5% NaCl, 1.5% agar) containing 25 μg/ml zeocin (InvivoGen, San Diego, USA). A total of 5 ml of LB medium with 25 μg/ml zeocin was inoculated with transformed *E. coli* cells and cultivated overnight (37 °C and 180 rpm). The plasmids were isolated using the ZR Plasmid Miniprep Kit (Zymo Research, Irvine, USA) according to manufacturer's instructions.

The isolated plasmid pPICZA_*Pe*AAO2 was linearized in the 5'AOX1 region with FastDigest *Mss*I (Thermo Fisher Scientific, Waltham, USA) and used for transformation of electrocompetent *P. pastoris* X-33 cells. Recombinant *P. pastoris* X-33 cells were selected on yeast extract peptone dextrose sorbitol agar plates (YPDS; 1% yeast extract, 2% peptone, 2% dextrose, 1 M sorbitol, 2% agar) supplemented with 100 μg/ml of zeocin and grown for 4–6 days at 30 °C.

Enzyme production in shaking flasks

Several *P. pastoris* transformants with pPICZA_*peAAO2* integrated into the genome were used for expression in 100 ml shaking flasks. Precultures were grown overnight (30 °C, 200 rpm) in 10 ml of buffered complex glycerol medium (BMGY; 1% yeast extract, 2% peptone, 100 mM potassium phosphate buffer pH 6.0, 1.34% yeast nitrogen base without amino acids, 4×10^{-5}% biotin, 1% glycerol). The precultures were used to inoculate 10 ml of buffered complex methanol medium (BMMY; same as BMGY but without glycerol) to an optical density at 600 nm (OD_{600}) of 1. The cells were cultivated for 2 days (25 °C, 200 rpm) with the addition of 0.5% (v/v) methanol every 24 h. The OD_{600} and volumetric activity in the cell-free supernatant towards veratryl alcohol were assayed daily as described below.

Enzyme production in 7.5 l bioreactor

The best producing *P. pastoris* transformant was used for fed-batch cultivation in a 7.5 l bioreactor (Infors, Bottmingen, Switzerland). A total of 3 l of fermentation basal salts medium (per 1 l: 0.47 g $CaSO_4$ x 2 H_2O, 8 ml H_3PO_4 (85%), 9.1 g K_2SO_4, 4.2 g KOH, 3.66 g $MgSO_4$, 43.5 g glycerol (100%), 0.87 mg biotin, 4.35 ml *Pichia* trace metals (per 1 l of PTM_1 solution: 6 g $CuSO_4$ x 5 H_2O, 0.08 g NaI, 3 g $MnSO_4$. H_2O, 0.5 g $CoCl_2$, 20 g $ZnCl_2$, 0.02 g H_3BO_3, 0.2 g Na_2Mo_4 x 2 H_2O, 65 g $FeSO_4$, 7 H_2O, 0.2 g biotin, 5 ml H_2SO_4)) was inoculated to an OD_{600} of 0.5 from a preculture in 200 ml BMGY medium containing 100 μg/ml zeocin grown over night (30 °C, 200 rpm). For this, the necessary amount of cells was harvested from the preculture by centrifugation (1500x*g*, 5 min, 4 °C) and resuspended in sterile 0.9% sodium chloride solution for inoculation of the fermentation medium. Oxygen was supplied with a rate of 3 l/min and the stirring rate was 800 rpm. The pH was kept at pH 5.0 by titrating 10% phosphoric acid or 25% ammonium hydroxide and the temperature was set to 30 °C. After full consumption of glycerol, a pO_2-spike controlled fed-batch started with methanol as inducer and sole carbon source. Methanol was added automatically to 0.5% (v/v; with 12 g/l PTM_1 solution) when a sharp increase in pO_2 indicated depletion of the carbon source. After induction, the temperature was reduced to 25 °C and the fermentation was continued for a total of 9 days with daily sampling to monitor OD_{600}, volumetric activity towards veratryl alcohol, and protein concentration in the cell-free supernatant.

Protein purification

The collected fermentation broth was centrifuged (11,325×*g*, 15 min, 4 °C) and the cell-free supernatant was concentrated and rebuffered in 50 mM potassium phosphate pH 6.0 using tangential flow filtration (TFF) with three membranes (10 kDa molecular cut-off, Pall, Port Washington, USA).

*Pe*AAO2 was purified by three chromatographic steps. For hydrophobic interaction chromatography (HIC), 2 M of ammonium sulfate (solid) was added to 10 ml of the concentrated supernatant and dissolved at 10 °C and rotation overnight. The sample was centrifuged (18,000×*g*, 30 min, 4 °C) and filtered using a 0.45-μm pore size filter. A XK16/20 column with Butyl Sepharose HP medium (20 ml, GE Healthcare, Chicago, USA) connected to an ÄKTApurifier FPLC-system (GE Healthcare, Chicago, USA) was equilibrated with 50 mM potassium phosphate buffer pH 6.0 with 1.5 M

ammonium sulfate (eluent B). A total of 10 ml of sample was loaded onto the column and washed for two column volumes (CV) with eluent B and a flow rate of 1.5 ml/min. Proteins were eluted using a step gradient with decreasing concentrations of eluent B by mixing with 50 mM potassium phosphate buffer pH 6.0 (eluent A). Foreign proteins were removed with two CV of 70% eluent B, and PeAAO2 was eluted with three CV of 40% eluent B. Fractions showing activity towards veratryl alcohol were pooled, concentrated, and desalted using a Vivaspin Turbo 15 ultrafiltration unit (10 kDa molecular cut-off, Sartorius, Göttingen, Germany). The concentrated HIC sample was used for ion exchange chromatography (IEX) using a XK16/20 column packed with DEAE Sepharose FF medium (29 ml, GE Healthcare, Chicago, USA). The column was equilibrated with 50 mM potassium phosphate buffer pH 6.0 (eluent A) and proteins were eluted with increasing amounts of 50 mM potassium phosphate buffer pH 6.0 with 1 M sodium chloride (eluent B) at a flow rate of 1.5 ml/min. A linear gradient of 0–30% eluent B for five CV was used to elute *Pe*AAO2. Again, the active fractions were pooled and concentrated. At last, the concentrated sample was applied to a Superdex 200 Increase 10/300 GL column (24 ml, GE Healthcare, Chicago, USA) for size exclusion chromatography (SEC). Using an isocratic gradient of one CV of 50 mM potassium phosphate buffer pH 6.0 with 150 mM sodium chloride at a flow rate of 0.25 ml/min, *Pe*AAO2 was eluted and active fractions were pooled, concentrated, and desalted as described above. Purified *Pe*AAO2 was stored at 4 °C until use.

Biochemical characterization

Protein concentration was determined by the Bradford method (Bradford 1976) with bovine serum albumin (BSA) as standard.

Glycosylation extent was analyzed by employing Peptide-N-amidase PNGase F (New England Biolabs, Frankfurt am Main, Germany) to deglycosylate 20 μg of purified *Pe*AAO2 according to the manufacturer's protocol. The deglycosylation was carried out under denaturing as well as under native conditions (for up to 96 h) to investigate the influence of glycosylation on activity and thermal stability of *Pe*AAO2. The resulting deglycosylated protein was analyzed via SDS-polyacrylamide gel electrophoresis (SDS-PAGE). SDS-PAGE with purified enzyme samples was carried out following the protocol of Laemmli (1970) with 12.5% resolving gel. The gels were stained with Coomassie Brilliant Blue R250.

Spectroscopic analysis

All measurements were performed at 25 °C with 2 mg/ml purified *Pe*AAO2 in 50 mM potassium phosphate buffer pH 6.0 using a Lambda 35 spectrophotometer (Perkin Elmer, Waltham, USA). The molar extinction coefficient of *Pe*AAO2 was calculated on the basis of released FAD cofactor from the purified enzyme after heat denaturation as reported elsewhere (Aliverti et al. 1999). *Pe*AAO2 was subjected to heat denaturation for 10 min at 80 °C. Precipitated protein was removed by centrifugation and the absorbance of extracted FAD was measured. The molar extinction coefficient of *Pe*AAO2 at 463 nm was calculated on the basis of the equation $\varepsilon_{463} = \varepsilon_{FAD} * A_{463}/A_{450}$ with $\varepsilon_{FAD} = 11{,}300\ M^{-1}\ cm^{-1}$ and A_{463} being the absorbance of *Pe*AAO2 before heat denaturation and A_{450} of released FAD after heat denaturation.

Enzymatic activity assay

The routinely used assay for determination of aryl-alcohol oxidase activity was carried out with veratryl alcohol as substrate. The measurements were conducted at room temperature in triplicates using 1-ml cuvettes with 800 μl of 100 mM sodium phosphate buffer pH 6.0 and 100 μl of 50 mM veratryl alcohol. A total of 100 μl of appropriately diluted *Pe*AAO2 in 50 mM potassium phosphate buffer pH 6.0 was added to start the reaction. Formation of veratraldehyde ($\varepsilon_{310} = 9300\ M^{-1}\ cm^{-1}$) (Guillén et al. 1992) was followed at 310 nm using an Ultrospec 7000 photometer (GE Healthcare, Chicago, USA). One unit of activity is defined as the amount of enzyme that converts 1 μmol substrate per minute under the stated conditions.

Influence of pH and temperature on stability

Purified *Pe*AAO2 was incubated at different pH values ranging from pH 2.0 to 12.0 (at room temperature) using 100 mM Britton-Robinson buffer or at different temperatures between 4 and 80 °C in 50 mM potassium phosphate buffer at pH 6.0 for up to 1 h. Samples were taken after certain time points, incubated on ice for 5 min (in case of thermal stability) and the residual activity towards veratryl alcohol was determined. The activity assay was conducted in triplicates in microtiter plates with 20 μl of *Pe*AAO2 containing sample, 20 μl of 50 mM veratryl alcohol, and 160 μl of 100 mM sodium phosphate buffer pH 6.0. The product formation was followed at 310 nm using an Infinite M200 Pro plate reader (Tecan, Männedorf, Switzerland). For determination of T_{50}, the temperature at which the enzyme loses 50% of activity, *Pe*AAO2 was incubated at temperatures ranging from 45 to 75 °C for 10 min. Afterwards, the samples were cooled on ice for 10 min before measuring the residual activity towards veratryl alcohol as stated above. The resulting data set was plotted using the program OriginPro 9.0 (OriginLab Corporation, Northampton, MA, USA) and the T_{50} value was determined by fitting the data using the Boltzmann equation.

Determination of melting temperature

To identify the melting temperature (T_M) of purified and of natively *N*-deglycosylated *Pe*AAO2, the change of intrinsic FAD cofactor fluorescence was monitored in dependence of temperature as employed in the *Thermo*FAD assay (Forneris et al. 2009). *Pe*AAO2 was diluted in 50 mM potassium phosphate buffer pH 6.0 to 1 mg/ml and 25 µl of diluted sample (in triplicate) was used to monitor the fluorescence at different temperatures using qPCR cycler qTOWER^3 (Analytik Jena, Jena, Germany). Excitation wavelength was set to 470 nm and emission wavelength to 520 nm using the SYBR Green fluorescence filter. A temperature gradient from 15 to 95 °C in 0.5 °C increments after 15 s delay was used. The first derivative of the melting curve was calculated using the program OriginPro 9.0 and the T_M value was extracted as maximum of the first derivative.

Investigation of substrate spectrum

Activity of *Pe*AAO2 towards 41 compounds was tested in a coupled assay making use of the generated hydrogen peroxide as product of AAO activity. The coupled system included horseradish peroxidase (HRP, Type VI, Sigma-Aldrich, Schnelldorf, Germany) and 2,2′-azino-bis(3-ethylbenzothiazoline-6-sulphonic acid) (ABTS). The measurements were conducted in triplicates in 96-well plates in a total volume of 200 µl at room temperature. For this, 20 µl of a suitable *Pe*AAO2 dilution was mixed with 20 µl of 10 mM substrate (with residual percentage of appropriate organic solvent, see Supplemental Table S1), 20 µl of 50 mM ABTS, 20 µl of 1 mg/ml HRP, and 120 µl of 100 mM potassium phosphate buffer pH 6.0. Oxidation of ABTS by HRP in the presence of hydrogen peroxide was followed spectrophotometrically at 420 nm for 3 m ($\varepsilon_{420} = 36{,}000\ M^{-1}cm^{-1}$) (Childs and Bardsley 1975) using an Infinite M200 Pro plate reader (Tecan, Männedorf, Switzerland).

Determination of kinetic constants

Kinetic constants V_{max} and K_M were determined for selected substrates at varying concentrations at 25 °C in 100 mM sodium phosphate buffer pH 6.0 in triplicates in a UV-Star® 96-well micro titer plate (Greiner Bio-One GmbH, Frickenhausen, Germany) with 200 µl assay volume using an Infinite M200 Pro plate reader (Tecan, Männedorf, Switzerland). The tested substrates were *p*-anisyl alcohol (0.98 µM to 1 mM), benzyl alcohol (9.8 µM to 10 mM), cinnamyl alcohol (9.8 µM to 20 mM in DMSO), cumic alcohol (9.8 µM to 10 mM), *trans,trans*-2,4-hexadienol (0.98 µM to 1.75 mM), piperonyl alcohol (0.98 µM to 1 mM), and veratryl alcohol (9.8 µM to 10 mM). The molar extinction coefficients used for calculation were *p*-anisaldehyde $\varepsilon_{285} = 16{,}980\ M^{-1}\ cm^{-1}$ (Guillén et al. 1992), benzaldehyde $\varepsilon_{250} = 13{,}800\ M^{-1}\ cm^{-1}$ (Guillén et al. 1992), cinnamaldehyde $\varepsilon_{310} = 15{,}600\ M^{-1}\ cm^{-1}$ (Ferreira et al. 2005), veratraldehyde $\varepsilon_{310} = 9300\ M^{-1}\ cm^{-1}$, and *trans,trans*-2,4-hexadienal $\varepsilon_{280} = 30{,}140\ M^{-1}\ cm^{-1}$ (Ruiz-Dueñas et al. 2006). The molar extinction coefficients of cuminaldehyde ($\varepsilon_{262} = 2920\ M^{-1}cm^{-1}$) and piperonal ($\varepsilon_{317} = 8680\ M^{-1}cm^{-1}$) were determined as shown in the Supplemental Figs. S1, S2, S3 and S4. Results were analyzed using OriginPro 9.0. A non-linear regression using the Michaelis-Menten equation was conducted to yield the maximum rate V_{max} and the Michaelis constant K_M, and led to the calculation of the rate constant k_{cat} and catalytic efficiency k_{cat}/K_M based on the molar concentration as determined by using the calculated molar extinction coefficient of *Pe*AAO2.

Results

Enzyme production and purification

The *P. pastoris* (*K. phaffii*) expression vector pPICZA harboring the codon-optimized *peaao2* gene with its native signal sequence under control of the methanol inducible P_{AOX1} promoter was integrated into the genome of *P. pastoris* X-33 by homologous recombination. Six *P. pastoris* transformants were screened for secretion of active *Pe*AAO2 in BMMY medium in shaking flasks. After 2 days of expression, the volumetric activities towards veratryl alcohol ranged from 18.4 to 74.0 U/l for different transformants. The *P. pastoris* transformant with the highest volumetric activity was subsequently used for enzyme production in a 7.5-l bioreactor. After 9 days of fed-batch cultivation, the OD_{600} of the culture reached its maximum at 389 accompanied by a volumetric activity of 7250 U/l at a protein concentration of 1.4 g/l (Fig. 1).

After cell separation and supernatant concentration by tangential flow filtration (TFF), recombinant *Pe*AAO2 was purified to homogeneity in a three-step purification procedure, including hydrophobic interaction (HIC), ion exchange (IEX), and size exclusion chromatography (SEC) (Table 1). The purified enzyme showed a specific activity of 23.0 U/mg towards veratryl alcohol, and was strongly yellow in color and slightly viscous. The expression yield calculated on the basis of specific activity of *Pe*AAO2 was 315 mg/l of culture.

Native PAGE demonstrated that purified *Pe*AAO2 is present in solution as monomer (Supplemental Fig. S5). SDS-PAGE analysis of purified *Pe*AAO2 revealed a strong band at around 100 kDa (Fig. 2). The theoretical molecular weight of *Pe*AAO2 without signal peptide (first 27 amino acids; the same signal peptide as of the closely related *Pe*AAO, Varela et al. 1999) was predicted to be 60.8 kDa (using Protparam ExPAsy) (Gasteiger et al. 2005). After *N*-deglycosylation using PNGase F, a shift of mobility to around 70 kDa was

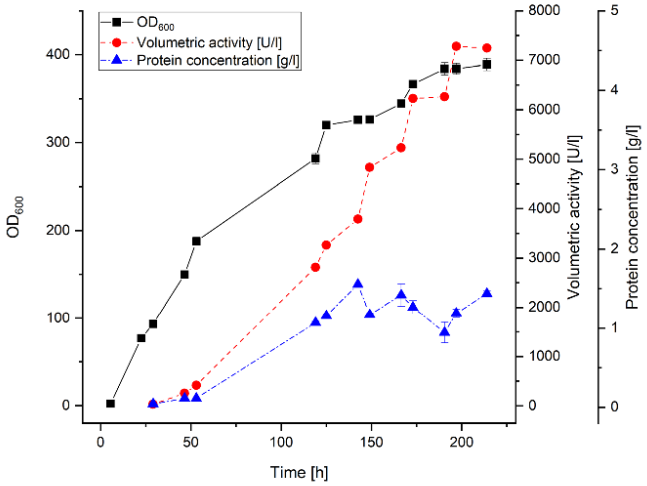

Fig. 1 Fed-batch cultivation of recombinant *P. pastoris* X-33 in a 7.5-l bioreactor to produce *Pe*AAO2. Squares: OD_{600} values; circles: volumetric activity (U/l) in cell-free supernatant; triangles: protein concentration (g/l). All measurements were done in triplicate

observed, indicating at least 30% *N*-glycosylation of heterologously expressed *Pe*AAO2 (Fig. 2).

The purified *Pe*AAO2 was analyzed in terms of its spectroscopic properties (Fig. 3). The oxidized enzyme showed two maxima at 376 nm and 463 nm. The extracted FAD showed two pronounced maxima at 376 nm and 450 nm. The estimated molar extinction coefficient of *Pe*AAO2 at 463 nm (ε_{463}) was 7029 M^{-1} cm^{-1}.

Influence of pH, temperature, and glycosylation on enzyme stability

pH stability of *Pe*AAO2 was investigated at various pH values between 2.0 and 12.0 and the enzyme remained stable over a wide range from pH 3.0 to 9.0 with residual activities of around 90% after 1 h incubation at room temperature (Fig. 4a), while a total loss of activity at pH 2.0 and pH 11.0 after 1 h incubation was observed. Thermal stability of *Pe*AAO2 was studied at temperatures between 4 and 80 °C for up to 1 h incubation at pH 6.0. *Pe*AAO2 was stable from 4 to 50 °C with residual activities of around 90%, while residual activity dropped to 70% and 10% after 1 h of incubation at 55 °C and 60 °C, respectively (Fig. 4b).

The temperatures at which half of the activity of *Pe*AAO2 was lost after 10 min of incubation (T_{50}) and the melting temperature (T_M) of *Pe*AAO2 were determined as well. *Pe*AAO2 showed a T_{50} value of 62.1 °C, while the T_M value was 65.5 °C. For natively *N*-deglycosylated *Pe*AAO2, a T_M value of 57.0 °C was measured. The deglycosylated enzyme showed a residual activity of 98.5% as compared with *Pe*AAO2 incubated under the same conditions but without PNGase F.

Table 1 Purification of recombinant *Pe*AAO2

Purification step	Total protein (mg)[c]	Total activity (U)[d]	Specific activity (U/mg)	Yield (%)[e]	Purity (x-fold)
Supernatant[a]	5030	25,400	5.0	–	1.0
TFF 1st eluate[b]	860	10,200	11.8	100	2.3
Butyl Sepharose HP	50	648	13.0	64	2.6
DEAE Sepharose HP	26.4	439	16.6	43	3.3
Superdex 200 increase	12.6	291	23.0	29	4.6

[a] Cell-free supernatant after centrifugation of fermentation broth

[b] Ultrafiltration retentate of supernatant using tangential flow filtration (TFF). Concentrated sample was collected in three steps (eluates) with different enzyme activities and protein concentrations. Only the first eluate was used for chromatographic purifications. Hence the apparent loss of activity

[c] Protein concentration was estimated by Bradford assay with BSA as standard

[d] Enzyme activity was measured with veratryl alcohol

[e] Yield based on 10 ml of the 1st eluate applied to Butyl Sepharose HP

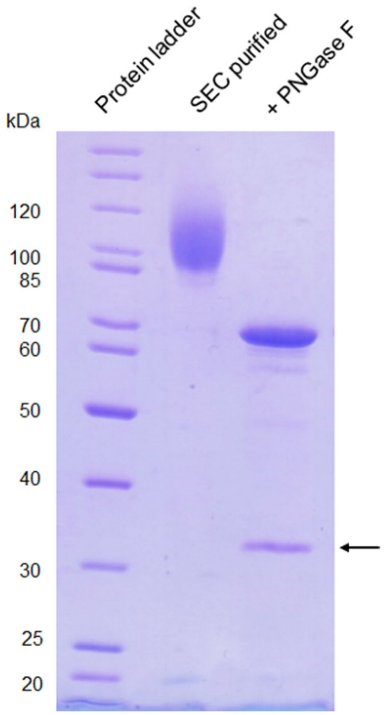

Fig. 2 SDS-PAGE analysis of purified *Pe*AAO2 and PNGase F treated *Pe*AAO2. A total of 5 μg of each sample was loaded and separated in a 12.5% resolving gel. Arrow indicates PNGase F (36 kDa)

Substrate spectrum

A coupled colorimetric assay using ABTS and HRP to measure hydrogen peroxide produced by AAO upon substrate oxidation was used to determine the substrate spectrum of *Pe*AAO2. A total of 41 compounds, some of which have been described as aryl-alcohol oxidase substrates including benzylic, other cyclic, heterocyclic, and aliphatic alcohols, were investigated (Table 2). The activity towards benzyl alcohol was set to 100%. Benzylic alcohols methoxylated in *para*-position like *p*-anisyl alcohol (647%), veratryl alcohol (322%), and isovanillyl alcohol (246%) were much better substrates than benzyl alcohol. The presence of an extended unsaturated side chain as in cinnamyl alcohol increased activity as well (442%). The enzyme showed the highest relative activity of 874% towards bicyclic 2-naphthalenemethanol, followed by the aliphatic and unsaturated *trans,trans*-2,4-hexadienol and *trans,trans*-2,4-heptadienol with 807% and 737%, respectively. Also, the heterocyclic benzodioxol derivative piperonyl alcohol was accepted by *Pe*AAO2 and oxidized with a relative activity of 301%, while with the isopropyl substituted benzylic alcohol - cumic alcohol, a relative activity of 149% was reached. All other tested compounds were "worse" substrates for *Pe*AAO2 and led to lower relative activities compared to benzyl alcohol. Amino substituted 3- and 4-aminobenzyl alcohols were oxidized with relative activities of 9.4 and 18.6%, respectively, while nitrogen-containing heterocyclic compounds like pyridine and indole derivatives were converted with relative activities of 2% or below. Among the unsaturated aliphatic alcohols, *trans*-2-hexenol (64%), *trans*-2-heptenol (32%), *trans*-2-octenol (5.2%), and *trans*-2-*cis*-6-nonadienol (3.3%) were oxidized. The investigated branched aliphatic

Fig. 3 UV-Vis spectrum of purified *Pe*AAO2. Solid line: native *Pe*AAO2 in its oxidized form; dashed line: extracted FAD after heat denaturation

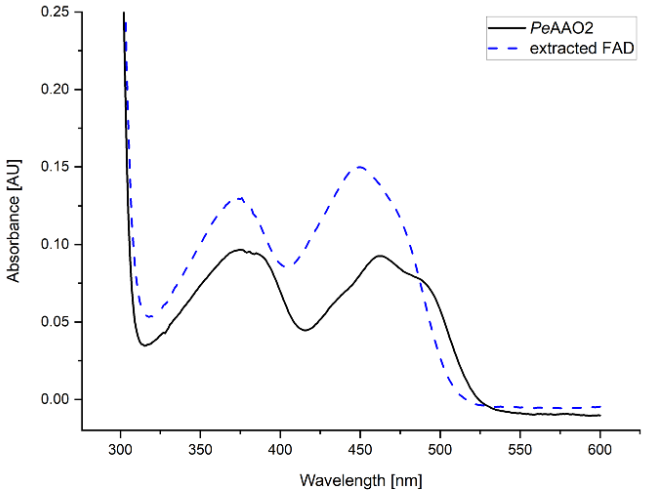

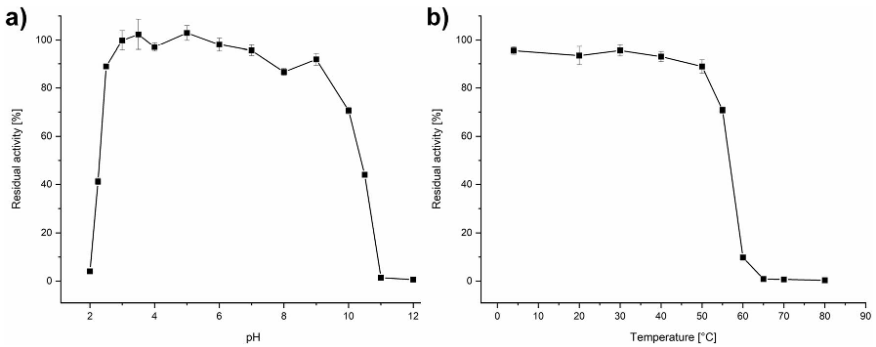

Fig. 4 Influence of pH and temperature on stability of *Pe*AAO2. **a** pH stability was determined in 100 mM Britton-Robinson buffer at the corresponding pH for 1 h at room temperature. **b** Thermal stability was investigated from 4 to 80 °C in 50 mM potassium phosphate buffer pH 6.0 for 1 h. Residual activity is given in % of initial activity without incubation

alcohols were only accepted to a very small extent as compared with benzyl alcohol, with relative activities generally below 5%.

Kinetic constants

Kinetic constants K_M, k_{cat}, and k_{cat}/K_M of *Pe*AAO2 for some of the substrates identified during substrate screening were determined at pH 6.0 (Table 3), at which *Pe*AAO2 showed the highest activity (Supplemental Fig. S6). *Pe*AAO2 showed the highest affinity (K_M) towards *p*-anisyl alcohol with 24.3 μM followed by piperonyl alcohol with 59.1 μM and the lowest affinity was found for cinnamyl alcohol with 1912 μM. The highest catalytic efficiencies (k_{cat}/K_M) with 2436 mM^{-1} s^{-1} and 600.2 mM^{-1} s^{-1} were also estimated for *p*-anisyl alcohol and piperonyl alcohol. Using cumic alcohol as substrate, the highest turnover rate (k_{cat}) was observed with 160.8 s^{-1}, which is 4-fold higher than for benzyl alcohol.

Discussion

Enzyme production and properties

The efficient utilization of AAOs in biocatalytic processes is mainly hampered due to the lack of high-yield expression systems. Our attempts to express the well-examined *Pe*AAO from *P. eryngii* ATCC 90787 in *P. pastoris* led to no detectable activity (unpublished data), while the expression level of *Pe*AAO2 from *P. eryngii P34* reached 315 mg/l and exceeded that of the in *P. pastoris* expressible and "engineered" variant *Pe*AAO FX9 with 25.5 mg/l by factor 12 (Viña-Gonzalez et al. 2018). Thus, *Pe*AAO2 is the best expressed *Pleurotus* AAO in *P. pastoris* described so far. *Pe*AAO2 and *Pe*AAO differ in seven amino acid positions located on or near the surface of the protein (Supplemental Fig. S7 and S8). The active site including the two catalytic active histidine residues (His529 and His573 (Ferreira et al. 2006)) and the hydrophobic substrate access channel (Tyr119, Phe424, and Phe528 (Fernández et al. 2009)) are identical in both enzymes, but an additional potential *N*-glycosylation site (Asn361-X-Ser) is present in *Pe*AAO2. Which of the amino acid variations leads to (high) expression of *Pe*AAO2 in *P. pastoris* as compared with *Pe*AAO remains questionable and is under further investigation.

*Pe*AAO2 contains eight potential *N*-glycosylation sites (Asn-X-Thr/Ser, where X is any amino acid except for proline) (Kukuruzinska et al. 1987) at the residues Asn89, Asn165, Asn178, Asn249, Asn336, Asn352, Asn361, and Asn396 (Supplemental Fig. S7). The discrepancy in molecular weight of *Pe*AAO2 with a theoretical molecular weight without signal peptide of 60.8 kDa and 100 kDa observed via SDS-PAGE is due to *N*- and *O*-glycosylation performed by *P. pastoris*. The *N*-deglycosylated enzyme showed a sharp band at 70 kDa, indicating 30% of *N*-glycosylation extent in recombinantly produced *Pe*AAO2, while 10% *O*-glycosylation is assumed. This value is higher than the carbohydrate content described for homologously produced *Pe*AAO with 14% (Varela et al. 2000b). Interestingly, the *Pe*AAO variant FX9 expressed in *P. pastoris* was poorly glycosylated, despite the presence of seven potential *N*-glycosylation sites (Viña-Gonzalez et al. 2018).

The *N*-deglycosylated *Pe*AAO2 retained its activity after deglycosylation, implying that glycosylation is not necessary for enzymatic activity, but rather positively affects enzyme thermostability. The glycosylated *Pe*AAO2 showed a 9 °C higher T_M value than the *N*-deglycosylated enzyme, which confirms that glycosylation enhances

Appl Microbiol Biotechnol (2020) 104:9205–9218

Table 2 Substrate scope of *Pe*AAO2. Generated H_2O_2 formed upon substrate oxidation was detected in a coupled ABTS-HRP assay. Activity towards benzyl alcohol was set to 100%

Compound	Structure	Relative activity [%]
Benzylic alcohols		
Benzyl alcohol		100.0
p-Anisyl alcohol		647.0
Veratryl alcohol		321.7
Isovanillyl alcohol		245.7
Vanillyl alcohol		2.0
3-Aminobenzyl alcohol		9.4
4-Aminobenzyl alcohol		18.6
Cumic alcohol		149.0
2-Phenylethanol		<0.1
Cinnamyl alcohol		441.9
Coniferyl alcohol	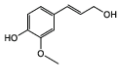	<0.1
Cyclic alcohols		
2-Naphthalenemethanol		873.9
9-Anthracenemethanol		*n. d.*
1-Pyrenemethanol	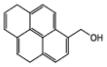	35.3
Guaiacol glyceryl ether	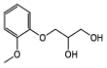	*n. d.*
Guaiacylglycerol-β-guaiacyl ether	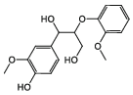	<0.1
Veratrylglycerol-β-guaiacyl ether	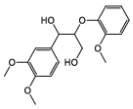	1.7
Heterocyclic alcohols		
Furfuryl alcohol		7.5
5-Hydroxymethylfural		4.8
5-Hydroxymethylthiazole		<0.1
2-Thiophenemethanol		15.8
2-Pyridinemethanol		0.8
3-Pyridinemethanol		0.5
4-Pyridinemethanol		0.3
3-Indolemethanol		2.0
Piperonyl alcohol		301.4
Aliphatic alcohols		
Isoamyl alcohol		0.3
Prenol		4.6
Geraniol	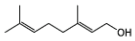	0.4
Nerol	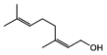	0.3
2,6-Dimethyl-5-heptenol	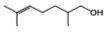	*n. d.*
Farnesol	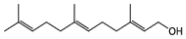	*n. d.*
trans-2-Hexenol		63.9
trans-3-Hexenol		*n. d.*
trans-4-Hexenol		*n. d.*
trans,trans-2,4-Hexadienol		807.0
1-Heptanol	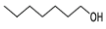	*n. d.*
trans-2-Heptenol	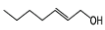	31.9
trans,trans-2,4-Heptadienol	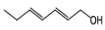	736.7
trans-2-Octenol	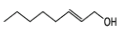	5.2
trans-2-*cis*-6-Nonadienol	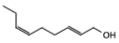	3.3

n. d. = not detected (no change in color detected or high background activity)

Table 3 Kinetic constants of *Pe*AAO2 compared with those of other AAOs

		*Pe*AAO2 from *P. eryngii* expressed in *P. pastoris*[a]	*Pe*AAO from *P. eryngii* expressed in *A. nidulans*[b]	*Pe*AAO FX9 variant from *P. eryngii* expressed in *P. pastoris*[c]
p-Anisyl alcohol	K_M (μM)	24.3 ± 0.8	27	37
	k_{cat} (s^{-1})	59.2 ± 0.04	142	70
	k_{cat}/K_M (mM^{-1} s^{-1})	2436	5230	1909
Benzyl alcohol	K_M (μM)	599.6 ± 18.7	632	440
	k_{cat} (s^{-1})	12.8 ± 0.01	30	34
	k_{cat}/K_M (mM^{-1} s^{-1})	21.39	47	78
Cinnamyl alcohol	K_M (μM)	2740 ± 103	*n.d.*	*n.d.*
	k_{cat} (s^{-1})	125.5 ± 0.1	*n.d.*	*n.d.*
	k_{cat}/K_M (mM^{-1} s^{-1})	45.80	*n.d.*	*n.d.*
Cumic alcohol	K_M (μM)	1912 ± 42.4	*n.d.*	*n.d.*
	k_{cat} (s^{-1})	160.8 ± 0.1	*n.d.*	*n.d.*
	k_{cat}/K_M (mM^{-1} s^{-1})	84.1	*n.d.*	*n.d.*
trans,trans-2,4-hexadienol	K_M (μM)	143.6 ± 11.5	94	106
	k_{cat} (s^{-1})	68.8 ± 0.05	119	89
	k_{cat}/K_M (mM^{-1} s^{-1})	479.3	1270	840
Piperonyl alcohol	K_M (μM)	59.1 ± 3.0	*n.d.*	*n.d.*
	k_{cat} (s^{-1})	35.5 ± 0.02	*n.d.*	*n.d.*
	k_{cat}/K_M (mM^{-1} s^{-1})	600.2	*n.d.*	*n.d.*
Veratryl alcohol	K_M (μM)	446.6 ± 7.5	540	410
	k_{cat} (s^{-1})	47.2 ± 0.03	114	57
	k_{cat}/K_M (mM^{-1} s^{-1})	105.7	210	139

n.d. not determined

[a] (This study), 100 mM sodium phosphate buffer pH 6.0. 25 °C, all measurements in triplicate

[b] (Ferreira et al. 2006), 100 mM sodium phosphate buffer pH 6.0, 24 °C

[c] (Viña-Gonzalez et al. 2018), 100 mM sodium phosphate buffer pH 6.0, 25 °C

thermostability (Wang et al. 1996). Indeed, the glycosylated *Pe*AAO2 exhibited 90% of residual activity after 1 h incubation at 50 °C and showed a T_{50} value of 62.1 °C, which is comparable with that of hyperglycosylated *Pe*AAO variant FX9 expressed in *S. cerevisiae* (63.0 °C) (Viña-Gonzalez et al. 2018). In contrast, *Pe*AAO purified from inclusion bodies from *E. coli* lacks glycosylation and shows a much lower thermostability compared to *Pe*AAO2 and *Pe*AAO variant FX9 with around 20% of residual activity after 50 min incubation at 50 °C and a T_{50} of 47.5 °C (Ruiz-Dueñas et al. 2006; Viña-Gonzalez et al. 2015). *Pe*AAO2 showed high stability within a wide pH range between pH 3.0 and 9.0, which is similar to another glycosylated *Pleurotus* AAO (Viña-Gonzalez et al. 2015). Since the *E. coli*-derived *Pe*AAO showed considerably lower pH stability, especially at pH 3.0 and above pH 9.0 (Viña-Gonzalez et al. 2015), we assume that high pH stability of AAOs is also attributed to glycosylation.

Substrate scope of *Pe*AAO2

*Pe*AAO2 was found to oxidize a broad range of chemically diverse primary alcohols, including compounds not yet reported as substrates for AAOs. The substrate preference was dependent on the present aromatic substitution groups and the number of conjugated double bonds, as reported also for other *Pleurotus* AAOs (Bourbonnais and Paice 1988; Guillén et al. 1992). A methoxy-group at the *para*-position of the aromatic ring seems to be crucial for efficient substrate oxidation as shown for *p*-anisyl alcohol, veratryl alcohol, and isovanillyl alcohol when compared with the non-substituted benzyl alcohol. A *para*-isopropyl group in cumic alcohol had also a beneficial effect leading to a 1.5-times higher relative activity than with benzyl alcohol. These results allow to suggest that the presence of an electron-donating group at *para*-position had a positive effect on enzyme activity. Presumably, enhanced electron density at the aromatic ring facilitates oxidation of the primary alcohol group. The presence of an amino group

in *para*-position in 4-aminobenzyl alcohol reduced substrate acceptance by a factor of 5, which might be explained by its protonated state at neutral pH, which makes this group electron-withdrawing. The presence of unsaturated bonds in the side chains of (aryl) alkyl alcohols, and thus extension of the conjugated double bond system as in cinnamyl alcohol had tremendous effects on substrate oxidation resulting in 4-times higher relative activity compared to benzyl alcohol. Although coniferyl alcohol contains an unsaturated side chain, its oxidation was barely detectable as was also seen for the *meta*-methoxy-*para*-hydroxy substituted vanillyl alcohol. In both substrates, a methoxy-group at *meta*-position of the aromatic ring act as electron-withdrawing group. Interestingly, the presence of a *para*-hydroxyl group has been previously reported to negatively influence the oxidation reaction by an AAO (Guillén et al. 1992). Obviously, the influence of the substrate binding site on substrate specificity and enzyme activity should be considered as well.

Expansion of the aromatic system to two condensed aromatic rings in 2-naphthalenemethanol led to the highest activity detected among all substrates, which is in accordance with activity of *Pe*AAO (Guillén et al. 1992). However, further extension of the ring system as in the tricyclic 9-anthracenemethanol did not result in detectable substrate oxidation, while the four-membered ring of 1-pyrenemethanol was oxidized with one third of activity as compared with benzyl alcohol. The acceptance of 9-anthracenemethanol by *Pe*AAO could be affected by steric hindrances: The primary alcohol group is located in a less exposed position as compared with 2-naphthalenemethanol or 1-pyrenemethanol, thereby not reaching into the active site cavity.

Various heterocyclic compounds derived from benzodioxole, furan, indole, pyridine, and thiophene were tested as substrates and were accepted by *Pe*AAO2 at least to some extent. Most remarkably, the benzodioxole derivative piperonyl alcohol was oxidized with a 3-times higher relative activity than benzyl alcohol. As described for veratryl alcohol (Guillén et al. 1992), the oxygen atoms in piperonyl alcohol most likely produce an electron-donating effect, leading to a higher electron density at the primary hydroxyl group, resulting in favored oxidation of the primary alcohol group. *Pe*AAO2's activity was rather low towards the furan-derived 5-hydroxymethylfurfural (5-HMF) which has been investigated in several studies as starting material for the production of bio-based 2,5-furandicarboxylic acid (FDCA) as precursor for plastics with involvement of an AAO (Carro et al. 2014; Karich et al. 2018; Serrano et al. 2019a; Viña-Gonzalez et al. 2020). The sulfur-containing 2-thiophenemethanol was converted with a relative activity of 16% and was the first described sulfuric compound accepted by an AAO. Several nitrogen-containing heterocyclic compounds including indole and pyridine derivatives were converted by *Pe*AAO2 only to less than 2%. Even though the substrate oxidation was rather low with some of these heterocyclic compounds, the results show that *Pe*AAO2 is capable of oxidizing chemically diverse primary alcohols.

Linear primary alcohols can serve as AAO substrates, if the alcohol group is in conjugation with double bonds, like in *trans,trans*-2,4-hexadienol (Guillén et al. 1992) or *trans,trans*-2,4-heptadienol, which led to the second and third highest relative activity of all tested compounds. The reduction of number of conjugated double bonds as in *trans*-2-hexenol and *trans*-2-heptenol resulted in 12-fold and 23-fold lower relative activity than with their counterparts *trans,trans*-2,4-hexadienol and *trans,trans*-2,4-heptadienol. The elongation of the linear unsaturated alcohol to C8 and C9 as in *trans*-2-octenol and *trans*-2-*cis*-6-nonadienol reduced enzyme activity further. Nevertheless, oxidation of the latter substrate results in "the violet leaf aldehyde" or "cucumber aldehyde," which is the major aroma component in fresh cucumber (Schieberle et al. 1990) and among the most potent fragrance compounds (Surburg and Panten 2006). This volatile compound is also present in different plant materials including extracts of violet leafs and fruits such as cherry and mango (Pino and Mesa 2006; Schmid and Grosch 1986). Several other aliphatic alcohols like geraniol, nerol, and prenol were accepted by *Pe*AAO2 and converted with activities below 5%, possibly due to steric limitations caused by their branched aliphatic structure.

Substrate affinities of *Pe*AAO2 for *p*-anisyl alcohol, benzyl alcohol, *trans,trans*-2,4-hexadienol, and veratryl alcohol were in the same range as for the closely related *P. eryngii Pe*AAO expressed in *A. nidulans* and its FX9 variant expressed in *P. pastoris* (Table 2). All three enzymes showed the highest catalytic efficiency for *p*-anisyl alcohol. Glycosylated wild-type *Pe*AAO with 14% carbohydrate content, expressed in *A. nidulans* (Varela et al. 2001), showed higher catalytic efficiencies for most substrates compared to *Pe*AAO2 with 30% carbohydrate content and the poorly glycosylated *Pe*AAO variant FX9 (Viña-Gonzalez et al. 2018). Lower activity of variant FX9 compared to *Pe*AAO might be caused by introduced mutations. On the other hand, it has been shown that non-glycosylated *Pe*AAO derived from *E. coli* showed lower catalytic efficiencies than glycosylated *Pe*AAO (Ruiz-Dueñas et al. 2006). Besides having a positive effect on pH and thermal stability, catalytic efficiency of AAOs seems to be positively influenced by glycosylation as well. Other AAOs that have been expressed in *P. pastoris* include *Coprinopsis cinerea* (*Cc*AAO) (Tamaru et al. 2018) and *Ustilago maydis* AAO (*Um*AAO) (Couturier et al. 2016). *Um*AAO exhibited the highest catalytic efficiency towards *p*-anisyl alcohol similar to *Pleurotus* AAOs, while for *Cc*AAO, the highest catalytic efficiency was described for benzyl alcohol. These results indicate different substrate specificities among different fungal AAOs.

As far as to our knowledge, the acceptance of piperonyl alcohol and cumic alcohol, as well as of amino-substituted and thiophene-derived primary alcohols and 1-pyrenemethanol, has not been reported for AAOs so far, and extends our knowledge of the substrate scope of aryl-alcohol oxidases. The second highest catalytic efficiency of *Pe*AAO2 was observed with piperonyl alcohol, proving that this compound is a promising substance for biocatalytic conversions, as its aldehyde is the fragrance compound piperonal used in cosmetics, and flavor and fragrance industry. Piperonal has a sweet-flowery and spicy odor and is present in essential oils of flowers of the *Heliotropium* genus (Bellardita et al. 2014; Santos et al. 2003) and thus also termed as "heliotropin". Due to its benzodioxole functionality, it also serves as intermediate for several products of industrial importance, such as insecticides, pesticides, and pharmaceutical products, e.g., used in the synthesis of new drugs against Alzheimer's disease (Brum et al. 2019; Santos et al. 2004; Wang et al. 2019).

The highest turnover rate for *Pe*AAO2 was observed for cumic alcohol oxidation to the bioactive compound cuminaldehyde, a major constituent of seed oil of *Cuminum cyminum* plant (Lee 2005; Li and Jiang 2004). Beyond the use of *C. cyminum* seeds as spice in traditional cuisines, different beneficial effects have been attributed to its use, including anticancer, antidiabetic, and neuroprotective effects that have been linked to cuminaldehyde as its active ingredient (Lee 2005; Morshedi et al. 2015; Patil et al. 2013; Tsai et al. 2016). The biocatalytic production of cuminaldehyde has not been described yet and the oxidation of cumic alcohol to cuminaldehyde using *Pe*AAO2 seems to be a feasible route.

In summary, high-yield production of *Pe*AAO2 in *P. pastoris* together with its broad substrate spectrum and high stability renders this enzyme a promising candidate for biotechnological applications. Additionally, the production of piperonal and cuminaldehyde by *Pe*AAO2 further expands the use of this biocatalyst for the production of intermediates for pharmaceutical products, as well as of flavors and fragrances.

Authors' contributions NJ designed and conducted the experiments, evaluated the results, and drafted the manuscript. KK and VBU gave advices in the research work, helped in drafting the manuscript, and revised the manuscript. All authors read and approved the final manuscript.

Funding Open Access funding provided by Projekt DEAL. The scientific activities of the Bioeconomy Science Center were financially supported by the Ministry of Innovation, Science and Research within the framework of the North Rhine-Westphalia, Germany, NRW-Strategieprojekt BioSC (No. 313/323-400-002 13).

Data availability All data on which the conclusions were drawn are presented in this study.

Compliance with ethical standards

Conflict of interest The authors declare that they have no conflict of interest.

Ethical approval This article does not contain any studies with human participants or animals performed by any of the authors.

Consent to participate Not applicable.

Consent for publication Not applicable.

References

Aliverti A, Curti B, Vanoni MA (1999) Identifying and quantitating FAD and FMN in simple and in iron-sulfur-containing flavoproteins. In: Chapman SK, Reid GA (eds) Flavoprotein Protocols. Humana Press, Totowa, pp 9–23

Arregui L, Ayala M, Gómez-Gil X, Gutiérrez-Soto G, Hernández-Luna CE, Herrera de Los Santos M, Levin L, Rojo-Domínguez A, Romero-Martínez D, Saparrat MCN, Trujillo-Roldán MA, Valdez-Cruz NA (2019) Laccases: structure, function, and potential application in water bioremediation. Microb Cell Factories 18(1):200. https://doi.org/10.1186/s12934-019-1248-0

Bellardita M, Loddo V, Palmisano G, Pibiri I, Palmisano L, Augugliaro V (2014) Photocatalytic green synthesis of piperonal in aqueous TiO2 suspension. Appl Catal B 144:607–613. https://doi.org/10.1016/j.apcatb.2013.07.070

Bourbonnais R, Paice MG (1988) Veratryl alcohol oxidases from the lignin-degrading basidiomycete *Pleurotus sajor-caju*. Biochem J 255(2):445–450. https://doi.org/10.1042/bj2550445

Bradford MM (1976) A rapid and sensitive method for the quantitation of microgram quantities of protein utilizing the principle of protein-dye binding. Anal Biochem 72:248–254. https://doi.org/10.1016/0003-2697(76)90527-3

Brum JOC, Neto DCF, de Almeida JSFD, Lima JA, Kuca K, França TCC, Figueroa-Villar JD (2019) Synthesis of new quinoline-piperonal hybrids as potential drugs against Alzheimer's disease. Int J Mol Sci 20(16):3944. https://doi.org/10.3390/ijms20163944

Carro J, Ferreira P, Rodríguez L, Prieto A, Serrano A, Balcells B, Ardá A, Jiménez-Barbero J, Gutiérrez A, Ullrich R, Hofrichter M, Martínez AT (2014) 5-hydroxymethylfurfural conversion by fungal aryl-alcohol oxidase and unspecific peroxygenase. FEBS J 282:3218–3229. https://doi.org/10.1111/febs.13177

Childs BRE, Bardsley WG (1975) The steady-state kinetics of peroxidase with 2,2′-azino-di-(3-ethylbenzthiazoline-6-sulphonic acid) as chromogen. Biochem J 145:93–103. https://doi.org/10.1042/bj1450093

Couturier M, Mathieu Y, Li A, Navarro D, Drula E, Haon M, Grisel S, Ludwig R, Berrin JG (2016) Characterization of a new aryl-alcohol oxidase secreted by the phytopathogenic fungus *Ustilago maydis*. Appl Microbiol Biotechnol 100:697–706. https://doi.org/10.1007/s00253-015-7021-3

de Almeida TP, van Schie MMCH, Ma A, Tieves F, Younes SHH, Fernández-Fueyo E, Arends IWCE, Riul A, Hollmann F (2019) Efficient aerobic oxidation of *trans*-2-hexen-1-ol using the aryl alcohol oxidase from *Pleurotus eryngii*. Adv Synth Catal 361:2668–2672. https://doi.org/10.1002/adsc.201801312

Falade AO, Nwodo UU, Iweriebor BC, Green E, Mabinya LV, Okoh AI (2016) Lignin peroxidase functionalities and prospective applications. Microbiologyopen 6:1–14. https://doi.org/10.1002/mbo3.394

Falade AO, Mabinya LV, Okoh AI, Nwodo UU (2018) Ligninolytic enzymes: versatile biocatalysts for the elimination of endocrine-disrupting chemicals in wastewater. Microbiologyopen 7(6): e00722. https://doi.org/10.1002/mbo3.722

Fernández IS, Ruíz-Duëas FJ, Santillana E, Ferreira P, Martínez MJ, Martínez ÁT, Romero A (2009) Novel structural features in the GMC family of oxidoreductases revealed by the crystal structure of fungal aryl-alcohol oxidase. Acta Crystallogr Sect D Biol Crystallogr 65:1196–1205. https://doi.org/10.1107/S0907444909035860Ferreira

Ferreira P, Medina M, Guillén F, Martínez MJ, Van Berkel WJH, Martínez AT (2005) Spectral and catalytic properties of aryl-alcohol oxidase, a fungal flavoenzyme acting on polyunsaturated alcohols. Biochem J 389:731–738. https://doi.org/10.1042/BJ20041903

Ferreira P, Ruiz-Dueñas FJ, Martínez MJ, Van Berkel WJH, Martínez AT (2006) Site-directed mutagenesis of selected residues at the active site of aryl-alcohol oxidase, an H_2O_2-producing ligninolytic enzyme. FEBS J 273:4878–4888. https://doi.org/10.1111/j.1742-4658.2006.05488.x

Ferreira P, Hernández-Ortega A, Herguedas B, Rencoret J, Gutiérrez A, Martínez MJ, Jiménez-Barbero J, Medina M, Martínez ÁT (2010) Kinetic and chemical characterization of aldehyde oxidation by fungal aryl-alcohol oxidase. Biochem J 425:585–593. https://doi.org/10.1042/BJ20091499

Fillat Ú, Ibarra D, Eugenio M, Moreno A, Tomás-Pejó E, Martín-Sampedro R (2017) Laccases as a potential tool for the efficient conversion of lignocellulosic biomass: a review. Fermentation 3(2):17. https://doi.org/10.3390/fermentation3020017

Forneris F, Orru R, Bonivento D, Chiarelli LR, Mattevi A (2009) *Thermo*FAD, a *Thermofluor*®-adapted flavin ad hoc detection system for protein folding and ligand binding. FEBS J 276:2833–2840. https://doi.org/10.1111/j.1742-4658.2009.07006.x

Galperin I, Javeed A, Luig H, Lochnit G, Rühl M (2016) An aryl-alcohol oxidase of *Pleurotus sapidus:* heterologous expression, characterization, and application in a 2-enzyme system. Appl Microbiol Biotechnol 100:8021–8030. https://doi.org/10.1007/s00253-016-7567-8

Gasteiger E, Hoogland C, Gattiker A, Duvaud S, Wilkins MR, Appel RD, Bairoch A (2005) Protein identification and analysis tools on the ExPASy server. In: Walker JM (ed) The proteomics protocols handbook. Humana Press, Totowa, pp 571–607

Grote A, Hiller K, Scheer M, Münch R, Nörtemann B, Hempel DC, Jahn D (2005) JCat: a novel tool to adapt codon usage of a target gene to its potential expression host. Nucleic Acids Res 33:526–531. https://doi.org/10.1093/nar/gki376

Guillén F, Martínez AT, Martínez MJ (1992) Substrate specificity and properties of the aryl-alcohol oxidase from the ligninolytic fungus *Pleurotus eryngii*. Eur J Biochem 209:603–611. https://doi.org/10.1111/j.1432-1033.1992.tb17326.x

Karich A, Kleeberg S, Ullrich R, Hofrichter M (2018) Enzymatic preparation of 2,5-furandicarboxylic acid (FDCA)—a substitute of terephthalic acid—by the joined action of three fungal enzymes. Microorganisms 6(1):5. https://doi.org/10.3390/microorganisms6010005

Kirk TK, Farrell RL (1987) Enzymatic "combustion": the microbial degradation of lignin. Annu Rev Microbiol 41:465–505. https://doi.org/10.1146/annurev.mi.41.100187.002341

Kukuruzinska MA, Bergh MLE, Jackson BJ (1987) Protein glycosylation in yeast. Annu Rev Biochem 56:915–944. https://doi.org/10.1146/annurev.bi.56.070187.004411

Laemmli UK (1970) Cleavage of structural proteins during assembly of head of bacteriophage-T4. Nature 227:680–685. https://doi.org/10.1038/227680a0

Lee HS (2005) Cuminaldehyde: aldose reductase and α-glucosidase inhibitor derived from *Cuminum cyminum* L. seeds. J Agric Food Chem 53(7):2446–2450. https://doi.org/10.1021/jf048451g

Li R, Jiang ZT (2004) Chemical composition of the essential oil of *Cuminum cyminum* L. from China. Flavour Fragr J 19(4):311–313. https://doi.org/10.1002/ffj.1302

Morshedi D, Aliakbari F, Tayaranian-Marvian A, Fassihi A, Pan-Montojo F, Pérez-Sánchez H (2015) Cuminaldehyde as the major component of *Cuminum cyminum*, a natural aldehyde with inhibitory effect on alpha-synuclein fibrillation and cytotoxicity. J Food Sci 80(10):H2336–H2345. https://doi.org/10.1111/1750-3841.13016

Patel RN (2018) Biocatalysis for synthesis of pharmaceuticals. Bioorg Med Chem 26(7):1252–1274. https://doi.org/10.1016/j.bmc.2017.05.023

Patil SB, Takalikar SS, Joglekar MM, Haldavnekar VS, Arvindekar AU (2013) Insulinotropic and β-cell protective action of cuminaldehyde, cuminol and an inhibitor isolated from *Cuminum cyminum* in streptozotocin-induced diabetic rats. Br J Nutr 110(8): 1434–1443. https://doi.org/10.1017/S0007114513000627

Pino JA, Mesa J (2006) Contribution of volatile compounds to mango (*Mangifera indica* L.) aroma. Flavour Fragr J 21(2):207–213. https://doi.org/10.1002/ffj.1703

Rodríguez Couto S, Toca Herrera JL (2006) Industrial and biotechnological applications of laccases: a review. Biotechnol Adv 24:500–513. https://doi.org/10.1016/j.biotechadv.2006.04.003

Ruiz-Dueñas FJ, Ferreira P, Martínez MJ, Martínez AT (2006) *In vitro* activation, purification, and characterization of *Escherichia coli* expressed aryl-alcohol oxidase, a unique H_2O_2-producing enzyme. Protein Expr Purif 45(1):191–199. https://doi.org/10.1016/j.pep.2005.06.003

Sannia G, Limongi P, Cocca E, Buonocore F, Nitti G, Giardina P (1991) Purification and characterization of a veratryl alcohol oxidase enzyme from the lignin degrading basidiomycete *Pleurotus ostreatus*. Biochim Biophys Acta 1073:114–119. https://doi.org/10.1016/0304-4165(91)90190-R

Santos AS, Pereira N, Da Silva IM, Sarquis MIM, Antunes OAC (2003) Microbiologic oxidation of isosafrole into piperonal. Appl Biochem Biotechnol 105-108:649–657. https://doi.org/10.1385/abab:107:1-3:649

Santos AS, Pereira N, Da Silva IM, Sarquis MIM, Antunes OAC (2004) Peroxidase catalyzed microbiological oxidation of isosafrol into piperonal. Process Biochem 39(12):2269–2275. https://doi.org/10.1016/j.procbio.2003.11.019

Schieberle P, Ofner S, Grosch W (1990) Evaluation of potent odorants in cucumbers (*Cucumis sativus*) and muskmelons (*Cucumis melo*) by aroma extract dilution analysis. J Food Sci 55(1):193–195. https://doi.org/10.1111/j.1365-2621.1990.tb06050.x

Schmid W, Grosch W (1986) Quantitative Analyse flüchtiger Aromastoffe mit hohen Aromawerten in Sauerkirschen (*Prunus cerasus* L.), Süßkirschen (*Prunus avium* L.) und Kirschkonfitüren. Z Lebensm Unters Forsch 183(1):39–44. https://doi.org/10.1007/BF01027592

Serrano A, Calviño E, Carro J, Sánchez-Ruiz MI, Cañada FJ, Martínez AT (2019a) Complete oxidation of hydroxymethylfurfural to

furandicarboxylic acid by aryl-alcohol oxidase. Biotechnol Biofuels 12:217. https://doi.org/10.1186/s13068-019-1555-z

Serrano A, Sancho F, Viña-González J, Carro J, Alcalde M, Guallar V, Martínez AT (2019b) Switching the substrate preference of fungal aryl-alcohol oxidase: towards stereoselective oxidation of secondary benzyl alcohols. Catal Sci Technol 9:833–841. https://doi.org/10.1039/C8CY02447B

Sheldon RA, Woodley JM (2018) Role of biocatalysis in sustainable chemistry. Chem Rev 118(2):801–838. https://doi.org/10.1021/acs.chemrev.7b00203

Stanzione I, Pezzella C, Giardina P, Sannia G, Piscitelli A (2020) Beyond natural laccases: extension of their potential applications by protein engineering. Appl Microbiol Biotechnol 104:915–924. https://doi.org/10.1007/s00253-019-10147-z

Surburg H, Panten J (2006) Common fragrance and flavor materials, 5th edn. Wiley-VCH, Weinheim

Tamaru Y, Umezawa K, Yoshida M (2018) Characterization of an aryl-alcohol oxidase from the plant saprophytic basidiomycete *Coprinopsis cinerea* with broad substrate specificity against aromatic alcohols. Biotechnol Lett 40(7):1077–1086. https://doi.org/10.1007/s10529-018-2534-3

Tsai KD, Liu YH, Chen TW, Yang SM, Wong HY, Cherng J, Chou KS, Cherng JM (2016) Cuminaldehyde from *Cinnamomum verum* induces cell death through targeting topoisomerase 1 and 2 in human colorectal adenocarcinoma COLO 205 cells. Nutrients 8(6):318. https://doi.org/10.3390/nu8060318

Van Schie MMCH, De Almeida TP, Laudadio G, Tieves F, Fernández-Fueyo E, Noël T, Arends IWCE, Hollmann F (2018) Biocatalytic synthesis of the Green Note *trans*-2-hexenal in a continuous-flow microreactor. Beilstein J Org Chem 14:697–703. https://doi.org/10.3762/bjoc.14.58

Varela E, Martínez AT, Martínez MJ (1999) Molecular cloning of aryl-alcohol oxidase from the fungus *Pleurotus eryngii*, an enzyme involved in lignin degradation. Biochem J 341:113. https://doi.org/10.1042/0264-6021:3410113

Varela E, Böckle B, Romero A, Martínez AT, Martínez MJ (2000a) Biochemical characterization, cDNA cloning and protein crystallization of aryl-alcohol oxidase from *Pleurotus pulmonarius*. Biochim Biophys Acta 1476:129–138. https://doi.org/10.1016/S0167-4838(99)00227-7

Varela E, Martínez MJ, Martínez AT (2000b) Aryl-alcohol oxidase protein sequence: a comparison with glucose oxidase and other FAD oxidoreductases. Biochim Biophys Acta 1481:202–208. https://doi.org/10.1016/S0167-4838(00)00127-8

Varela E, Guillén F, Martínez ÁT, Martínez MJ (2001) Expression of *Pleurotus eryngii* aryl-alcohol oxidase in *Aspergillus nidulans*: purification and characterization of the recombinant enzyme. Biochim Biophys Acta 1546:107–113. https://doi.org/10.1016/S0167-4838(00)00301-0

Viña-Gonzalez J, Alcalde M (2020) Directed evolution of the aryl-alcohol oxidase: beyond the lab bench. Comput Struct Biotechnol J 18:1800–1810. https://doi.org/10.1016/j.csbj.2020.06.037

Viña-Gonzalez J, Martinez AT, Guallar V, Alcalde M (2020) Sequential oxidation of 5-hydroxymethylfurfural to furan-2,5-dicarboxylic acid by an evolved aryl-alcohol oxidase. Biochim Biophys Acta 1868(1):140293. https://doi.org/10.1016/j.bbapap.2019.140293

Viña-Gonzalez J, Gonzalez-Perez D, Ferreira P, Martinez AT, Alcalde M (2015) Focused directed evolution of aryl-alcohol oxidase in *Saccharomyces cerevisiae* by using chimeric signal peptides. Appl Environ Microbiol 81(18):6451–6462. https://doi.org/10.1128/AEM.01966-15

Viña-Gonzalez J, Elbl K, Ponte X, Valero F, Alcalde M (2018) Functional expression of aryl-alcohol oxidase in *Saccharomyces cerevisiae* and *Pichia pastoris* by directed evolution. Biotechnol Bioeng 115(7):1666–1674. https://doi.org/10.1002/bit.26585

Viña-Gonzalez J, Jimenez-Lalana D, Sancho F, Serrano A, Martinez AT, Guallar V, Alcalde M (2019) Structure-guided evolution of aryl alcohol oxidase from *Pleurotus eryngii* for the selective oxidation of secondary benzyl alcohols. Adv Synth Catal 361:2514–2525. https://doi.org/10.1002/adsc.201900134

Wang C, Eufemi M, Turano C, Giartosio A (1996) Influence of the carbohydrate moiety on the stability of glycoproteins. Biochemistry 35(23):7299–7307. https://doi.org/10.1021/bi9517704

Wang S, Bao L, Song D, Wang J, Cao X (2019) Heterocyclic lactam derivatives containing piperonyl moiety as potential antifungal agents. Bioorg Med Chem Lett 29(20):126661. https://doi.org/10.1016/j.bmcl.2019.126661

2.2.1. Supplemental Information

Applied Microbiology and Biotechnology Jankowski et al. (2020)

ELECTRONIC SUPPLEMENTARY MATERIAL

High-level expression of aryl-alcohol oxidase 2 from *Pleurotus eryngii* in *Pichia pastoris* for production of fragrances and bioactive precursors

Nina Jankowski [1], Katja Koschorreck[1], Vlada B. Urlacher [1#]

[1] Institute of Biochemistry at Heinrich-Heine-University Düsseldorf, Universitätsstraße 1, 40225 Düsseldorf, Germany

[#]Address correspondence to

Vlada B. Urlacher

vlada.urlacher@uni-duesseldorf.de

Supplementary Materials and Methods

Compounds and solvents used in substrate screening

In total, 41 different benzylic, cyclic, heterocyclic and aliphatic alcohols were used at 1 mM final concentration in the coupled ABTS-HRP assay. The solutions of tested compounds were prepared using the following solvents (Table S1).

Table S1 Compounds used in substrate screening

	Substrate	**Manufacturer**	**Solvent for 10 mM Stock**
Benzylic alcohols	3-Aminobenzyl alcohol	TCI	ddH_2O
	4-Aminobenzyl alcohol	TCI	10 % DMSO
	p-Anisyl alcohol	Sigma-Aldrich	ddH_2O
	Benzyl alcohol	AppliChem	ddH_2O
	Cinnamyl alcohol	Acros Organics	10 % DMSO
	Coniferyl alcohol	Sigma-Aldrich	10 % DMSO
	Cumic alcohol	Acros Organics	10 % DMSO
	Isovanillyl alcohol	BLDpharm	10 % DMSO
	2-Phenylethanol	Carl Roth	10 % DMSO
	Vanillyl alcohol	Acros Organics	10 % DMSO
	Veratryl alcohol	Acros Organics	ddH_2O
Cyclic alcohols	9-Anthracenemethanol	BLDpharm	100 % DMSO *
	2-Naphthalenemethanol	Acros Organics	10 % DMSO
	1-Pyrenemethanol	TCI	100 % DMSO *
	Guaiacol glyceryl ether	Sigma-Aldrich	ddH_2O
	Guaiacylglycerol-β-guaiacyl ether	abcr	10 % DMSO
	Veratrylglycerol-β-guaiacyl ether	abcr	10 % DMSO
Heterocyclic alcoshols	Furfuryl alcohol	Sigma-Aldrich	ddH_2O
	5-Hydroxymethylfural	Carbolutions	ddH_2O
	5-Hydroxymethylthiazole	J&K	10 % DMSO
	3-Indolemethanol	J&K	100 % DMSO
	Piperonyl alcohol	J&K	10 % DMSO
	2-Pyridinemethanol	J&K	ddH_2O
	3-Pyridinemethanol	J&K	ddH_2O
	4-Pyridinemethanol	Acros Organics	ddH_2O
	2-Thiophenemethanol	Sigma-Aldrich	10 % DMSO
Aliphatic alcohols	Farnesol	Acros Organics	10 % DMSO
	Geraniol	Sigma-Aldrich	100 % ethanol

2,6-Dimethyl-5-heptenol	Sigma-Aldrich	10 % DMSO
1-Heptanol	Acros Organics	10 % DMSO
trans-2-Heptenol	TCI	10 % DMSO
trans,trans-2,4-Heptadienol	Alfa Aesar	10 % DMSO
trans-2-Hexenol	Alfa Aesar	10 % DMSO
trans-3-Hexenol	Alfa Aesar	10 % DMSO
trans-4-Hexenol	Fluorochem	10 % DMSO
trans,trans-2,4-Hexadienol	Acros Organics	ddH_2O
Isoamyl alcohol	TCI	100 % ethanol
Nerol	Sigma-Aldrich	100 % ethanol
trans-2-*cis*-6-Nonadienol	Sigma-Aldrich	10 % DMSO
trans-2-Octenol	Alfa Aesar	10 % DMSO
Prenol	TCI	10 % DMSO

* for 9-anthracenemethanol and 1-pyrenemethanol the final DMSO concentration was 20 % in the assay mixture as additional 10 % of DMSO was added to the 10 % from 10 mM stock (in 100 % DMSO) solutions for final concentration of 1 mM

Determination of molar extinction coefficients for cuminaldehyde and piperonal

Cumic alcohol (Acros Organics), cuminaldehyde (J&K Scientific), piperonyl alcohol (J&K Scientific) and piperonal (Sigma-Aldrich) were prepared as stock solutions at 10 mM in 100 mM sodium phosphate buffer pH 6.0 and dissolved by gentle shaking and warming of the solutions. For recording of the spectra, all samples were diluted in the same buffer as mentioned. The spectra were recorded from 200 to 400 nm in a Quartz cuvette using a Lambda 35 spectrophotometer (Perkin Elmer, Waltham, USA) at 25 °C. The absorption maxima of alcohol and aldehyde were extracted from the obtained spectra.

For measurements of absorbance at the corresponding maxima of the aldehydes, further dilutions were prepared: Cuminaldehyde dilutions ranged from 0.2 mM to 0.02 mM, and piperonal dilutions ranged from 0.1 to 0.01 mM in 100 mM sodium phosphate buffer pH 6.0. The respective absorption maxima were determined and plotted against the concentration of cuminaldehyde or piperonal. A linear fit of the data was conducted using the program OriginPro 9.0 (OriginLab Corporation, Northampton, USA) and the molar extinction coefficient was deduced from the fitted data as slope of the regression curve. According to Lambert-Beer-Law with $A = \varepsilon * c * d$, where A is absorbance, ε is the molar extinction coefficient, c is the concentration and d is the path length (1 cm). In a plot with A vs. c, the extinction coefficient is described as the $slope = \varepsilon * d$.

Native PAGE of purified *Pe*AAO2

Blue native PAGE of 5 µg of purified *Pe*AAO2 was carried out using the SERVA*Gel* N Native starter kit (SERVA Electrophoresis GmbH, Heidelberg, Germany) with 4-16 % gel according to the manufacturer's protocol. The gel was stained with Coomassie Brilliant Blue R250.

Influence of pH on enzyme activity

The effect of pH on activity towards *p*-anisyl alcohol, benzyl alcohol, cinnamyl alcohol, cumic alcohol, *trans,trans*-2,4-hexadienol, piperonyl alcohol and veratryl alcohol was investigated in 100 mM Britton-Robinson buffer with pH in the range of 2.0 to 10.0. The assay was conducted at room temperature using 1-ml cuvettes with 800 µl of 100 mM Britton-Robinson buffer, 100 µl of 50 mM substrate (10 mM for cumic alcohol) and 100 µl of appropriately diluted *Pe*AAO2. The change of absorbance during product formation was followed using an Ultrospec 7000 photometer (GE Healthcare, Chicago, USA). The corresponding molar extinction coefficients used for calculation were as follows: *p*-anisaldehyde $\varepsilon_{285} = 16{,}980\ \mathrm{M^{-1}\ cm^{-1}}$ (Guillén et al. 1992), benzaldehyde $\varepsilon_{250} = 13{,}800\ \mathrm{M^{-1}\ cm^{-1}}$ (Guillén et al. 1992), cinnamaldehyde $\varepsilon_{310} = 15{,}600\ \mathrm{M^{-1}\ cm^{-1}}$ (Ferreira et al. 2005), cuminaldehyde $\varepsilon_{262} = 2{,}920\ \mathrm{M^{-1}\ cm^{-1}}$ (this work), piperonal $\varepsilon_{317} = 8{,}680\ \mathrm{M^{-1}\ cm^{-1}}$ (this work), veratraldehyde $\varepsilon_{310} = 9{,}300\ \mathrm{M^{-1}\ cm^{-1}}$ (Guillén et al. 1992) and *trans,trans*-2,4-hexadienal $\varepsilon_{280} = 30{,}140\ \mathrm{M^{-1}\ cm^{-1}}$ (Ruiz-Dueñas et al. 2006).

Sequence alignment and homology modelling

The protein sequences of *Pe*AAO (accession number AAC72747) and *Pe*AAO2 (accession number ADD14021) were aligned using the multiple sequence alignment tool Clustal Omega (https://www.ebi.ac.uk/Tools/msa/clustalo/).

Using the homology-modelling server SWISS-MODEL (Waterhouse et al. 2018) and the crystal structure of *Pe*AAO expressed in *E. coli* (Protein data bank (PDB) entry 3FIM, Fernández et al. 2009), a homology model of *Pe*AAO2 was created and the PyMOL Molecular Graphics System (https://pymol.org/2/) was used for visualization.

Supplementary Results

Molar extinction coefficient of cuminaldehyde

The spectra of cumic alcohol and cuminaldehyde were recorded from 200 to 400 nm (Fig. S1).

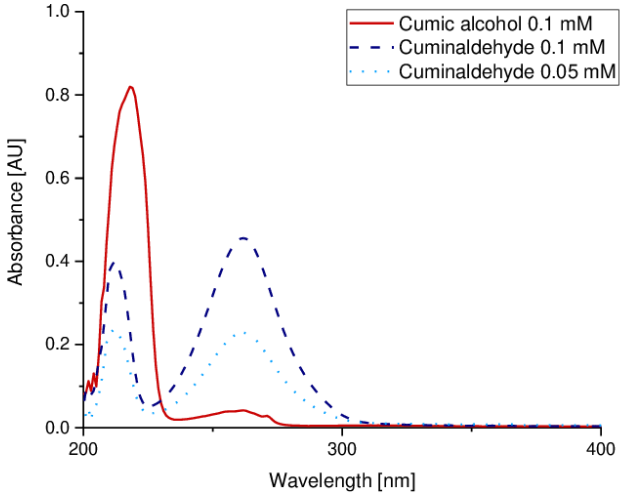

Fig. S1 UV-Vis spectra of cumic alcohol (red, solid line), cuminaldehyde at 0.1 mM (dark blue, dashed line) and cuminaldehyde at 0.05 mM (light blue, dotted line) were recorded in 100 mM sodium phosphate buffer pH 6.0 at 25 °C

The substrate cumic alcohol showed one major absorbance maximum at 218 nm and a minor maximum at 262 nm, whereas the product cuminaldehyde showed a more pronounced absorbance maximum at 262 nm and a second maximum at 212 nm. Therefore, the maximum at 262 nm was used for determination of the molar extinction coefficient of cuminaldehyde.

The absorbance at 262 nm for different cuminaldehyde concentrations was measured (Fig. S2).

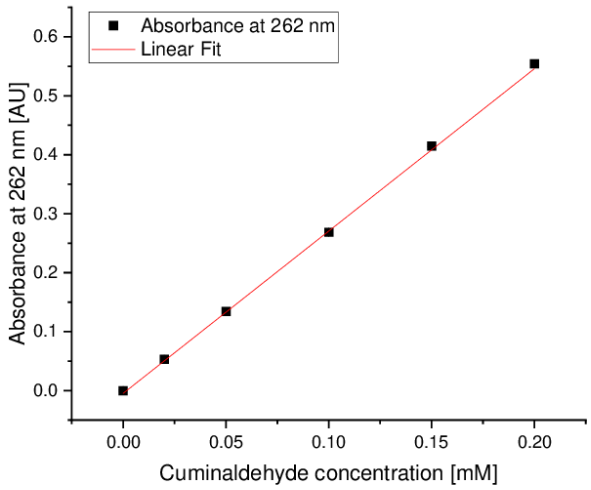

Fig. S2 Correlation of absorbance at 262 nm with cuminaldehyde concentration. The slope of the linear fit represents the molar extinction coefficient ε_{262} in mM^{-1} cm^{-1}. Measurements were done in triplicate from three individual cuminaldehyde stock solutions

The absorbance at 262 nm correlates with the concentration of cuminaldehyde. Using the Lambert-Beer-Law, the molar extinction coefficient ε_{262} of cuminaldehyde under the stated conditions was determined to be $\varepsilon_{262} = 2.92\ mM^{-1}\ cm^{-1}$.

Molar extinction coefficient of piperonal

The spectra of piperonyl alcohol and piperonal were recorded from 250 to 400 nm (Fig. S3).

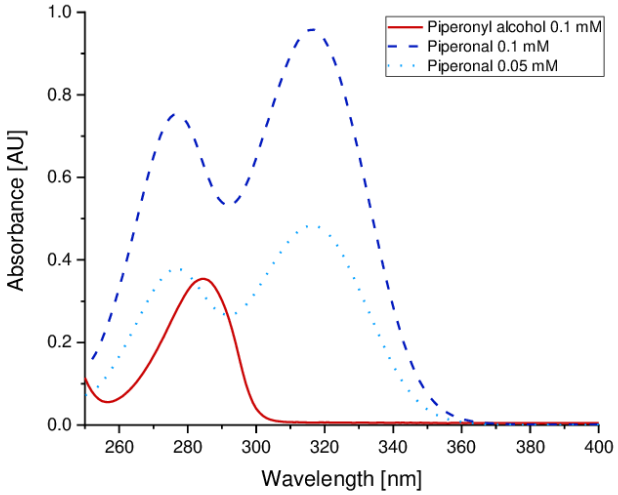

Fig. S3 UV-Vis spectra of piperonyl alcohol (red, solid line), piperonal at 0.1 mM (dark blue, dashed line) and piperonal at 0.05 mM (light blue, dotted line) were recorded in 100 mM sodium phosphate buffer pH 6.0 at 25 °C

The substrate piperonyl alcohol showed a maximum at 285 nm, while the product piperonal showed two strong maxima at 275 and 317 nm. The molar extinction coefficient for piperonal was determined at 317 nm as the absorbance at this wavelength is solely attributed to the aldehyde.

The absorbance at 317 nm for different piperonal concentrations was measured (Fig. S4).

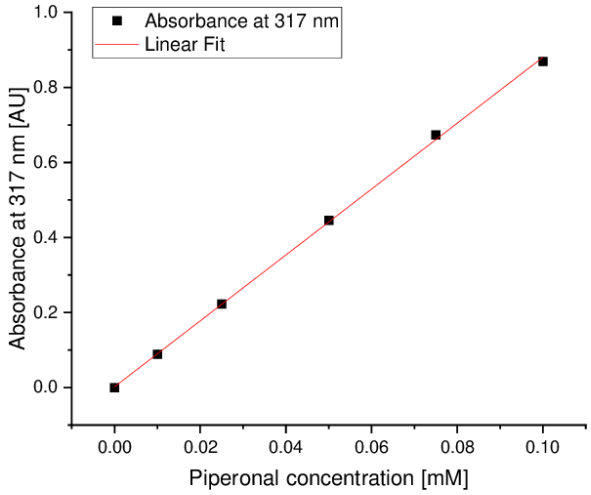

Fig. S4 Correlation of absorbance at 317 nm with piperonal concentration. The slope of the linear fit represents the molar extinction coefficient ε_{317} in mM^{-1} cm^{-1}. Measurements were done in triplicate from three individual piperonal stock solutions

The absorbance at 317 nm correlates with the concentration of piperonal. The molar extinction coefficient for piperonal was determined as described previously for cuminaldehyde. The molar extinction coefficient ε_{317} of piperonal under the stated conditions was determined to be $\varepsilon_{317} = 8.68\, mM^{-1}\, cm^{-1}$.

Native PAGE of purified *Pe*AAO2

The purified *Pe*AAO2 was investigated under non-denaturing conditions in a blue native PAGE (Fig. S5).

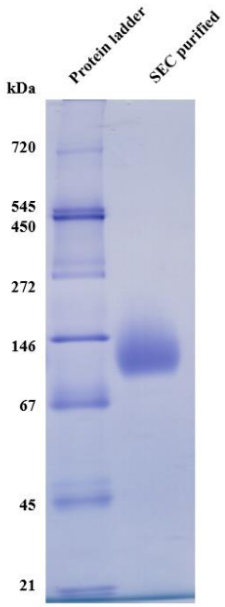

Fig. S5 Gel after Blue Native PAGE of purified *Pe*AAO2. 5 µg of sample were loaded and separated in a 4-16 % gel

Recombinant *Pe*AAO2 moved as a single band between 67 and 146 kDa, and therefore indicates that *Pe*AAO2 is present in a monomeric form.

Influence of pH on activity of *Pe*AAO2

The routinely used buffer in the AAO activity assay mixture was exchanged for 100 mM Britton-Robinson buffer at different pH values. The activity of *Pe*AAO2 towards several substrates at different pH was measured (Fig. S6).

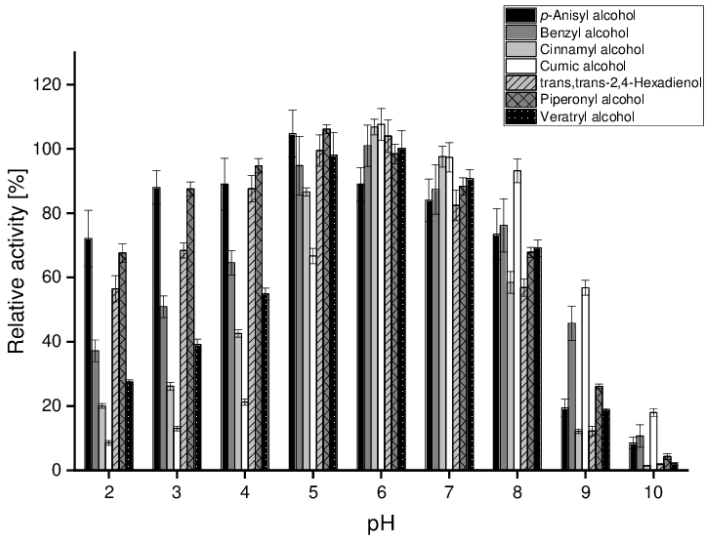

Fig. S6 Influence of pH on activity of *Pe*AAO2. 100 mM Britton-Robinson buffer at the corresponding pH was used instead of the assay buffer - 100 mM sodium phosphate pH 6.0. Values were put in relation to the control experiment with assay buffer. All measurements were done in triplicate

*Pe*AAO2 converted the substrates benzyl alcohol, cinnamyl alcohol, cumic alcohol, *trans,trans*-2,4-hexadienol and veratryl alcohol best at pH 6.0, while for *p*-anisyl alcohol and piperonyl alcohol a slightly more acidic pH 5.0 was best. Relative activities towards *p*-anisyl alcohol and piperonyl alcohol at lower pH were higher compared with other substrates. Overall, the pH activity profile for *p*-anisyl alcohol and piperonyl alcohol appeared shifted towards more acidic pH.

Sequence alignment and homology model

The two *P. eryngii* derived AAOs *Pe*AAO und *Pe*AAO2 differ only in seven amino acid positions (Fig. S7). One of these positions is a potential *N*-glycosylation site (motif Asn-X-Thr/Ser, where X is any amino acid except for proline) in *Pe*AAO2 (residue Asn361), whereas *Pe*AAO lacks this site as an aspartic acid is present instead of asparagine. The catalytically active histidine residues His529 and His573 as well as the main residues involved in regulating substrate accessibility to the active site (Tyr119, Phe424 and Phe528, as described for *Pe*AAO in Fernández et al. 2009) are conserved in both aryl-alcohol oxidases.

```
                    Signal peptide
PeAAO     MSFGALRQLLLIACLALPSLAATNLPTADFDYVVVGAGNAGNVVAARLTEDPDVSVLVLE    60
PeAAO2    MSFGALRQLLLIACLALPSLAATNLPTADFDYVVVGAGNAGNVVAARLTEDPDVSVLVLE    60
          ****************************************************************
                                 Asn89                          Tyr119
PeAAO     AGVSDENVLGAEAPLLAPGLVPNSIFDWNYTTTAQAGYNGRSIAYPRGRMLGGSSSVHYM   120
PeAAO2    AGVSDENVLGAEAPLLAPGLVPNSIFDWNYTTTAQAGYNGRSIAYPRGRMLGGSSSVHYM   120
          ****************************************************************
                                                Asn165        Asn178
PeAAO     VMMRGSTEDFDRYAAVTGDEGWNWDNIQQFVRKNEMVVPPADNHNTSGEFIPAVHGTNGS   180
PeAAO2    VMMRGSTEDFDRYAAVTGDEGWNWDNIQQFVGKNEMVVPPADNHNTSGEFIPAVHGTNGS   180
          ****************************** *************************** **

PeAAO     VSISLPGFPTPLDDRVLATTQEQSEEFFFNPDMGTGHPLGISWSIASVGNGQRSSSSTAY   240
PeAAO2    VSISLPGFPTPLDDRVLATTQEQSEEFFFNPDMGTGHPLGISWSIASVGNGQRSSSSTAY   240
          ****************************************************************
                Asn249
PeAAO     LRPAQSRENLSVLINAQVTKLVNSGTTNGLPAFRCVEYAEQEGAPTTTVCAKKEVVLSAG   300
PeAAO2    LRPAQSRENLSVLINAQVTKLVNSGITNGLPAFRCVEYAEQEGAPTTTVCAKKEVVLSAG   300
          ******************************* ********************************
                                                Asn336        Asn352
PeAAO     SVGTPILLQLSGIGDENDLSSVGIDTIVNNPSVGRNLSDHLLLPAAFFVNSNQTFDNIFR   360
PeAAO2    SVGTPILLQLSGIGDENDLSSVGIDTIVNNPSVGRNLSDHLLLPAAFFVNSNQTFDNIFR   360
          ****************************************************************
          Asn361                                Asn396
PeAAO     DSSEFNVDLDQWTNTRTGPLTALIANHLAWLRLPSNSSIFQTFPDPAAGPNSAHWETIFS   420
PeAAO2    NSSEFNADLDQWTNTRTGPLTALIANHLAWLRLPSNSSIFQTFPDPAAGPNSAHWETIFS   420
          :*****.***************************************************** *
             Phe424
PeAAO     NQWFHPAIPRPDTGSFMSVTNALISPVARGDIKLATSNPFDKPLINPQYLSTEFDIFTMI   480
PeAAO2    NQWFHPAIPRPDTGSFMSVTNALISPVARGDIKLATSNPFDKPLINPQYLSTEFDIFTMI   480
          ****************************************************************
                                                Phe528 His529
PeAAO     QAVKSNLRFLSGQAWADFVIRPFDPRLRDPTDDAAIESYIRDNANTIFHPVGTASMSPRG   540
PeAAO2    QAVKSNLRFLSGQAWADFVIRPFDPRLRDPTNDAAIESYIRDNANTIFHPVGTASMSPRG   540
          ******************************:*****************************
                                     His573
PeAAO     ASWGVVDPDLKVKGVDGLRIVDGSILPFAPNAHTQGPIYLVGKQGADLIKADQ   593
PeAAO2    ASWGVVDPDLKVKGVDGLRIVDGSILPFAPNAHTQGPIYLVGERGADLIKADQ   593
          ****************************************:::*********
```

Fig. S7 Alignment of *Pe*AAO (accession number AAC72747) and *Pe*AAO2 (accession number ADD14021). The signal peptide comprising the first 27 amino acids is indicated by the blue filled box. Residues in red show differences in both sequences. Residues in purple represent the catalytic active histidine residues His529 and His573. Residues in grey filled boxes are part of the hydrophobic bottleneck, regulating substrate accessibility with Tyr119, Phe424 and Phe528. Residues in green open boxes are possible *N*-glycosylation sites of *Pe*AAO2 with Asn89, Asn165, Asn178, Asn249, Asn336, Asn352, Asn361, Asn396.

The high similarity of both aryl-alcohol oxidases from *P. eryngii*, especially in terms of residues involved in substrate accessibility and catalytically active residues, indicate that both AAOs share similar catalytic properties.

Using the crystal structure of *Pe*AAO expressed in *E. coli* as template (PDB entry 3FIM), a homology model of *Pe*AAO2 was created and the differing residues were marked in purple (Fig. S8). The seven differing residues are located on or near the surface of the protein and the active site is conserved among both AAOs.

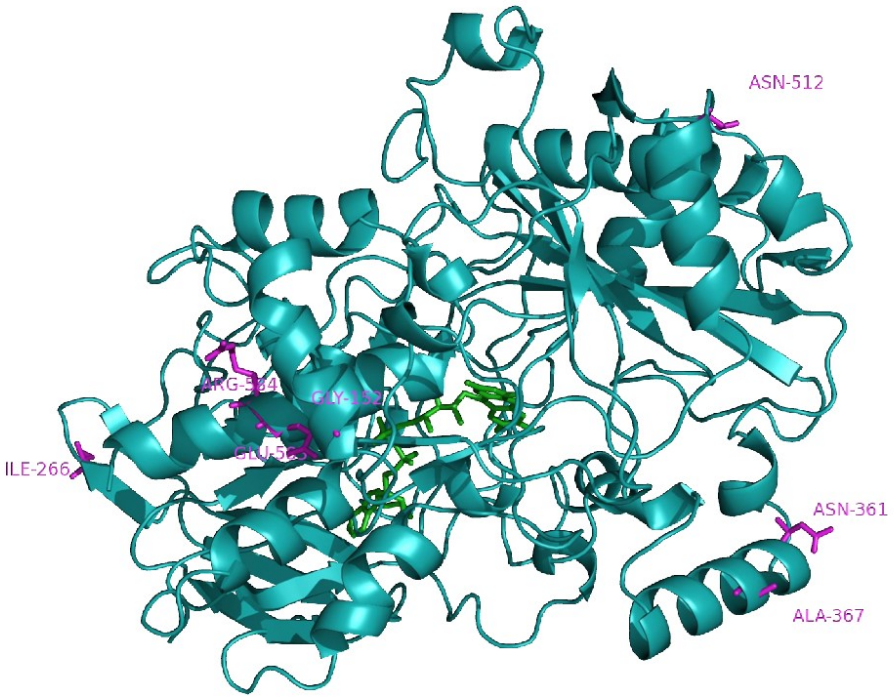

Fig. S8 Homology model of *Pe*AAO2 using the *Pe*AAO crystal structure (PDB entry 3FIM) as template. Residues in purple depict the different positions as compared to *Pe*AAO. Cofactor FAD in green. Numbering including the signal peptide.

References

Fernández IS, Ruíz-Duëas FJ, Santillana E, Ferreira P, Martínez MJ, Martínez ÁT, Romero A (2009) Novel structural features in the GMC family of oxidoreductases revealed by the crystal structure of fungal aryl-alcohol oxidase. Acta Crystallogr Sect D Biol Crystallogr 65:1196-1205. doi:10.1107/S0907444909035860

Ferreira P, Medina M, Guillén F, Martínez MJ, Van Berkel WJH, Martínez AT (2005) Spectral and catalytic properties of aryl-alcohol oxidase, a fungal flavoenzyme acting on polyunsaturated alcohols. Biochem J 389:731-738. doi:10.1042/BJ20041903

Guillén F, Martínez AT, Martínez MJ (1992) Substrate specificity and properties of the aryl-alcohol oxidase from the ligninolytic fungus *Pleurotus eryngii*. Eur J Biochem 209:603-611. doi:10.1111/j.1432-1033.1992.tb17326.x

Ruiz-Dueñas FJ, Ferreira P, Martínez MJ, Martínez AT (2006) In vitro activation, purification, and characterization of *Escherichia coli* expressed aryl-alcohol oxidase, a unique H_2O_2-producing enzyme. Protein Expr Purif 45(1):191-199. doi:10.1016/j.pep.2005.06.003

Waterhouse A, Bertoni M, Bienert S, Studer G, Tauriello G, Gumienny R, Heer FT, de Beer TAP, Rempfer C, Bordoli L, Lepore R, Schwede T (2018) SWISS-MODEL: homology modelling of protein structures and complexes. Nucleic Acids Res 46(W1):W296-W303. doi:10.1093/nar/gky427

2.3. Chapter III: Biochemical characterization of *Ma*AAO from *Moesziomyces antarcticus*

Title	Characterization of a thermotolerant aryl-alcohol oxidase from *Moesziomyces antarcticus* oxidizing 5-hydroxymethyl-2-furancarboxylic acid
Authors	Alessa Lappe, Nina Jankowski, Annemie Albrecht, Katja Koschorreck
Contribution	Cloning of *maaao* gene, correction of the first draft of the manuscript. Relative contribution: 10 %
Published in	*Applied Microbiology and Biotechnology,* 105, 8313-8327 (**2021**)
DOI	10.1007/s00253-021-11557-8
Publisher	Springer Nature
Copyright	Copyright © 2021, Springer Nature

Applied Microbiology and Biotechnology (2021) 105:8313–8327
https://doi.org/10.1007/s00253-021-11557-8

BIOTECHNOLOGICALLY RELEVANT ENZYMES AND PROTEINS

Characterization of a thermotolerant aryl-alcohol oxidase from *Moesziomyces antarcticus* oxidizing 5-hydroxymethyl-2-furancarboxylic acid

Alessa Lappe[1] · Nina Jankowski[1] · Annemie Albrecht[1] · Katja Koschorreck[1]

Received: 6 July 2021 / Revised: 23 August 2021 / Accepted: 26 August 2021 / Published online: 13 October 2021

Abstract

The development of enzymatic processes for the environmentally friendly production of 2,5-furandicarboxylic acid (FDCA), a renewable precursor for bioplastics, from 5-hydroxymethylfurfural (HMF) has gained increasing attention over the last years. Aryl-alcohol oxidases (AAOs) catalyze the oxidation of HMF to 5-formyl-2-furancarboxylic acid (FFCA) through 2,5-diformylfuran (DFF) and have thus been applied in enzymatic reaction cascades for the production of FDCA. AAOs are flavoproteins that oxidize a broad range of benzylic and aliphatic allylic primary alcohols to the corresponding aldehydes, and in some cases further to acids, while reducing molecular oxygen to hydrogen peroxide. These promising biocatalysts can also be used for the synthesis of flavors, fragrances, and chemical building blocks, but their industrial applicability suffers from low production yield in natural and heterologous hosts. Here we report on heterologous expression of a new aryl-alcohol oxidase, *Ma*AAO, from *Moesziomyces antarcticus* at high yields in the methylotrophic yeast *Pichia pastoris* (recently reclassified as *Komagataella phaffii*). Fed-batch fermentation of recombinant *P. pastoris* yielded around 750 mg of active enzyme per liter of culture. Purified *Ma*AAO was highly stable at pH 2–9 and exhibited high thermal stability with almost 95% residual activity after 48 h at 57.5 °C. *Ma*AAO accepts a broad range of benzylic primary alcohols, aliphatic allylic alcohols, and furan derivatives like HMF as substrates and some oxidation products thereof like piperonal or perillaldehyde serve as building blocks for pharmaceuticals or show health-promoting effects. Besides this, *Ma*AAO oxidized 5-hydroxymethyl-2-furancarboxylic acid (HMFCA) to FFCA, which has not been shown for any other AAO so far. Combining *Ma*AAO with an unspecific peroxygenase oxidizing HMFCA to FFCA in one pot resulted in complete conversion of HMF to FDCA within 144 h. *Ma*AAO is thus a promising biocatalyst for the production of precursors for bioplastics and bioactive compounds.

Key points

- *MaAAO from M. antarcticus was expressed in P. pastoris at 750 mg/l.*
- *MaAAO oxidized 5-hydroxymethyl-2-furancarboxylic acid (HMFCA).*
- *Complete conversion of HMF to 2,5-furandicarboxylic acid by combining MaAAO and UPO.*

Keywords Aryl-alcohol oxidase · *Pichia pastoris (Komagataella phaffii)* · 5-hydroxymethylfurfural (HMF) · 5-hydroxymethyl-2-furancarboxylic acid (HMFCA) · Bioplastics

Introduction

In times of an emerging importance of a sustainable bioeconomy, biocatalytic processes have gained more and more attention as a promising alternative to chemical synthesis by utilizing enzymes with high activity and product selectivity. Enzymes are able to convert readily available bio-based raw materials under mild reaction conditions into valuable compounds like building blocks for pharmaceuticals, flavors, and fragrances or precursors for

✉ Katja Koschorreck
Katja.Koschorreck@hhu.de

[1] Institute of Biochemistry, Heinrich-Heine University Düsseldorf, Universitätsstraße 1, 40225 Düsseldorf, Germany

polymers (Wiltschi et al. 2020). Among them, aryl-alcohol oxidases (AAOs) have emerged as promising biocatalysts. AAOs (EC 1.1.3.7) are FAD-dependent oxidoreductases that belong to the glucose-methanol-choline (GMC) oxidoreductase superfamily and play an essential role in biomass degradation as they supply peroxide-dependent ligninolytic enzymes with hydrogen peroxide. Although most AAOs described so far have been found in basidiomycetous and ascomycetous fungi, enzymes with AAO activity have been identified in bacteria, insects, and gastropods as well (Ferreira et al. 2015; Serrano et al. 2020; Urlacher and Koschorreck 2021). AAOs typically oxidize benzylic and polyunsaturated aliphatic primary alcohols to the corresponding aldehydes via hydrogen abstraction and transfer to molecular oxygen to produce hydrogen peroxide (Guillen et al. 1992). Hydrated aldehydes (*gem*-diols) can be further oxidized to the corresponding acids, but efficiencies are much lower (Ferreira et al. 2010).

Their broad range of oxidized substrates with the only need of molecular oxygen offers a huge potential of AAOs for biotechnological applications. Besides being used as hydrogen peroxide supplier for peroxide-dependent enzymes in delignification or dye decolorization processes, AAOs can be applied for the production of chemical building blocks, flavors, and fragrances (Serrano et al. 2020; Urlacher and Koschorreck 2021). *Trans*-2-hexenal, used in the flavor and fragrance industry as fresh flavor in foods, was recently produced in a two liquid phase system by selective oxidation of *trans*-2-hexen-1-ol by *P. eryngii* AAO with a turnover number of over 2 million (de Almeida et al. 2019; van Schie et al. 2018). *Pe*AAO2 from *P. eryngii* P34 was shown to oxidize piperonyl alcohol to the fragrance compound piperonal (Jankowski et al. 2020), which is also an important precursor for the synthesis of pharmaceuticals and insecticides (Brum et al. 2019; Santos et al. 2004). The biotechnological potential of AAO was further demonstrated by engineering AAO from *P. eryngii* for selective oxidation of chiral secondary benzyl alcohols (Serrano et al. 2019b; Viña-Gonzalez et al. 2019). This allows for kinetic resolution of racemic secondary alcohols used as building blocks for pharmaceuticals without the need of external cofactors.

Besides this, AAO was applied for the synthesis of 2,5-furandicarboxylic acid (FDCA), a promising renewable building block that is of special interest for the production of bio-based polyesters (polyethylene furanoate (PEF)). FDCA can be produced from 5-hydroxymethylfurfural (HMF) which is obtained from, e.g., cellulose through hydrolysis of cellulose to glucose, followed by acid-mediated isomerization of glucose to fructose, and finally acid-catalyzed dehydration of fructose to HMF (Menegazzo et al. 2018). AAO was shown to oxidize HMF predominantly to 5-formyl-2-furancarboxylic acid (FFCA) via 2,5-diformylfuran (DFF), while oxidation of FFCA to FDCA is rather low and inhibited by hydrogen peroxide formed in course of the reaction (Serrano et al. 2019a). Addition of catalase (Serrano et al. 2019a) or establishment of a three-enzyme system, consisting of AAO, unspecific peroxygenase (UPO), and galactose oxidase (GAO) (Karich et al. 2018), resulted in complete conversion of HMF to FDCA. The latter approach applied H_2O_2-dependent UPO to oxidize HMF to 5-hydroxymethyl-2-furancarboxylic acid (HMFCA) and FFCA to FDCA while AAO and GAO provided H_2O_2 for UPO by oxidizing HMF to FFCA (catalyzed by AAO) and HMFCA to FFCA (catalyzed by GAO), respectively (Fig. 1). Furthermore, combinatorial saturation mutagenesis was applied to engineer *P. eryngii* AAO for the stepwise oxidation of HMF to FDCA (Vina-Gonzalez et al. 2020). The evolved Bantha variant showed a sixfold improved production of FDCA starting from HMF compared to the wild-type.

However, despite their huge biotechnological potential, only a limited number of AAOs have been described so far and industrial processes applying AAOs have not been established yet which might be due to their difficult expression in natural and heterologous hosts suffering from low yields or requiring tedious in vitro refolding (Ruiz-Duenas et al. 2006; Vina-Gonzalez et al. 2018).

Here, we report on the heterologous expression of a new, thermotolerant AAO, *Ma*AAO from *Moesziomyces antarcticus*, at high yields in *P. pastoris* with promising biocatalytic properties. The enzyme showed a broad activity towards benzylic and polyunsaturated aliphatic primary alcohols as well as furan-derived alcohols and aldehydes which makes

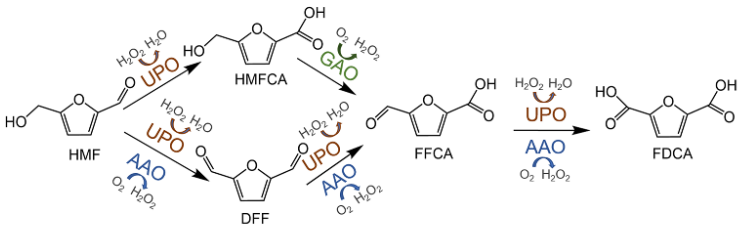

Fig. 1 Reaction scheme of HMF oxidation to FDCA employing AAO, UPO, and GAO

this enzyme a promising biocatalyst for the synthesis of bio-based polyesters, fragrances, and bioactive compounds.

Materials and methods

Strains, plasmid, and chemicals

Plasmids were propagated in *Escherichia coli* DH5α (Clontech Laboratories Inc., Heidelberg, Germany). *Pichia pastoris* strain X-33 (currently reclassified as *Komagataella phaffii*) was used for heterologous expression of *Ma*AAO and purchased from Invitrogen (Carlsbad, USA). pPICZA_*maaao* was purchased from BioCat GmbH (Heidelberg, Germany). Chemicals and enzymes were purchased from abcr GmbH (Karlsruhe, Germany), Acros Organics (Geel, Belgium), Alfa Aesar (Kandel, Germany), AppliChem GmbH (Darmstadt, Germany), BLDpharm (Shanghai, China), Carl Roth GmbH + Co. KG (Karlsruhe, Germany), Carbolution Chemicals GmbH (St. Ingbert, Germany), Fluorochem (Hadfield, UK), IoLiTec (Heidelberg, Germany), J&K Scientific (Lommel, Belgium), New England Biolabs (Frankfurt am Main, Germany), Sigma-Aldrich (Schnelldorf, Germany), Thermo Fisher Scientific (Bremen, Germany), TCI Chemicals (Eschborn, Germany), and VWR (Darmstadt, Germany).

Strain construction and expression

The gene encoding for *Ma*AAO from *Moesziomyces antarcticus* (GenBank accession number XM_014798063.1) was codon optimized by JCat (http://www.jcat.de/) for expression in *Saccharomyces cerevisiae* (GenBank accession number MZ574089). The gene was synthesized and ligated into the pPICZA vector by BioCat GmbH (Heidelberg, Germany) using restriction sites BstBI and NotI. Chemically competent *E. coli* DH5α cells were transformed with pPICZA_*maaao* and plasmid isolation was carried out using the ZR Plasmid Miniprep Kit (Zymo Research, Irvine, USA) according to the manufacturer's instructions. *P. pastoris* X-33 cells were transformed with MssI linearized pPICZA_*maaao* by electroporation. Recombinant cells were selected on yeast extract peptone dextrose sorbitol agar plates (YPDS; 10 g/l yeast extract, 20 g/l peptone, 20 g/l glucose, 1 M sorbitol, 20 g/l agar) supplemented with 100 µg/ml of Zeocin™ (InvivoGen, San Diego, USA). Cells were grown for 4 days at 30 °C. For expression of *Ma*AAO in shaking flasks, several *P. pastoris* transformants were grown in 10 ml buffered complex glycerol medium (BMGY; 10 g/l yeast extract, 20 g/l peptone, 100 mM potassium phosphate buffer pH 6.0, 13.4 g/l yeast nitrogen base without amino acids, 0.4 mg/l biotin, 10 g/l glycerol) at 30 °C and 200 rpm overnight. Precultures were used for inoculation of 100 ml buffered methanol complex medium (BMMY; same as BMGY but with 0.5% methanol instead of glycerol) or 100 ml buffered methanol minimal medium (BMM; 13.4 g/l yeast nitrogen base without amino acids, 100 mM potassium phosphate buffer pH 6.0, 0.4 mg/l biotin, 0.5% (v/v) methanol) to an optical density at 600 nm (OD_{600}) of 0.5 and cells were grown for 3 days at 25 °C and 200 rpm. Methanol (0.5% (v/v)) was added daily. Volumetric activity of the cell-free supernatants was measured daily towards veratryl alcohol. The measurements were conducted in 100 mM potassium phosphate buffer pH 6.0 with 5 mM veratryl alcohol at 25 °C. Formation of veratraldehyde ($\varepsilon_{310} = 9{,}300\ M^{-1}\ cm^{-1}$) (Guillen et al. 1992) was followed at 310 nm using an Infinite™ M200 PRO plate reader (Tecan, Männedorf, Switzerland). One unit is defined as the amount of enzyme that converts 1 µmol substrate per minute.

Fed-batch fermentation and enzyme purification

Fed-batch fermentation of the most active *P. pastoris* transformant was conducted in a 7.5 l bioreactor (Infors, Bottmingen, Switzerland) as described earlier (Jankowski et al. 2020). Samples were taken daily to monitor OD_{600}, volumetric activity towards veratryl alcohol, and protein concentration. After 8 days of cultivation, the fermentation broth was harvested by centrifugation for 15 min at 10,000 g and 4 °C. The cell-free supernatant was concentrated and rebuffered in 50 mM potassium phosphate buffer pH 6.0 by tangential flow filtration with cut-off membranes of 10 kDa (Pall, Port Washington, USA). The concentrated supernatant was supplemented with ammonium sulfate to a final concentration of 1.5 M. The sample was centrifuged for 30 min at 18,000 *g* and 4 °C and filtered using a 0.45 µm pore size filter. Five milliliters of sample was loaded onto a Butyl Sepharose HP column (GE Healthcare, Chicago, USA) on an ÄKTApurifier FPLC-system (GE Healthcare). The column was washed with two column volumes (CVs) of 50 mM potassium phosphate buffer pH 6.0 with 1.5 M ammonium sulfate and proteins were eluted with a linear gradient over 6 CVs to 100% 50 mM potassium phosphate buffer pH 6.0. Active fractions towards veratryl alcohol were pooled, concentrated, and desalted using a Vivaspin Turbo 15 ultrafiltration unit with 10 kDa cut-off (Sartorius, Göttingen, Germany). The concentrated sample was loaded onto a Superdex 200 Increase column (GE Healthcare). Proteins were eluted with one CV of 50 mM potassium phosphate buffer pH 6.0 with 150 mM sodium chloride and active fractions were pooled, concentrated, and desalted as described above. The concentrated sample was loaded onto a DEAE Sepharose FF column (GE Healthcare) equilibrated with 100 mM Tris/HCl buffer pH 8.5. Proteins were eluted with a linear gradient over 3 CVs to 50% of 100 mM Tris/HCl buffer pH 8.5 with 1 M sodium chloride. Active fractions were pooled, concentrated, and

rebuffered in 50 mM potassium phosphate buffer pH 6.0 as described above. Purified *Ma*AAO was stored at 4 °C.

Biochemical characterization

Protein concentration was determined with the Bradford assay (Bradford 1976) with bovine serum albumin (BSA) as standard. Deglycosylation of *Ma*AAO was conducted by treatment with PNGase F (New England Biolabs, Frankfurt am Main, Germany) according to the manufacturer's instructions. SDS-PAGE analysis was performed according to the protocol of Laemmli (1970). Spectroscopic analysis of *Ma*AAO was performed using a Lambda 35 spectrophotometer (Perkin Elmer, Waltham, USA). The molar extinction coefficient of purified *Ma*AAO was calculated by heat denaturation using $\varepsilon_{450} = 11{,}300\ M^{-1}\ cm^{-1}$ for the free FAD (Aliverti et al. 1999). For determination of the T_{50} value (temperature at which the enzyme loses 50% of its activity after heat incubation), purified *Ma*AAO was incubated at temperatures of 30 to 80 °C for 10 min. After cooling on ice, the residual activity towards veratryl alcohol was measured as described above. The T_{50} value was estimated by fitting the data to the Boltzmann equation.

Influence of pH, temperature, hydrogen peroxide, and cosolvents

The influence of pH on activity of *Ma*AAO towards veratryl alcohol, cinnamyl alcohol, and *trans,trans*-2,4-hexadien-1-ol (at a concentration of 5 mM each) was investigated in 100 mM Britton-Robinson buffer pH 2 to 9 at room temperature. Product formation was followed spectrophotometrically using an Infinite™ M200 PRO plate reader. Enzyme activity was calculated by using the molar extinction coefficient of veratraldehyde ($\varepsilon_{310} = 9{,}300\ M^{-1}\ cm^{-1}$) (Guillen et al. 1992), cinnamaldehyde ($\varepsilon_{310} = 15{,}600\ M^{-1}\ cm^{-1}$) (Ferreira et al. 2005), and *trans,trans*-2,4-hexadienal ($\varepsilon_{280} = 30{,}140\ M^{-1}\ cm^{-1}$) (Ruiz-Duenas et al. 2006). pH stability of *Ma*AAO was determined by incubating the purified enzyme in 100 mM Britton-Robinson buffer pH 2 to 9 at room temperature for 48 h. Thermal stability of *Ma*AAO was determined by incubating the purified enzyme at temperatures of 30 to 80 °C in 50 mM potassium phosphate buffer pH 6.0 for 48 h. Samples were taken at certain time points and residual activity towards veratryl alcohol was measured as described above. The influence of increasing concentrations of hydrogen peroxide (H_2O_2) on the activity of *Ma*AAO was investigated by measuring the activity towards veratryl alcohol in the presence of 0 to 500 mM H_2O_2. Stability towards H_2O_2 was determined by incubating the enzyme in 50 mM potassium phosphate buffer pH 6.0 with 0 to 500 mM H_2O_2 for up to 48 h. Samples were taken at certain time points and residual activity towards veratryl alcohol was measured as described above. Activity of *Ma*AAO in the presence of up to 40% of dimethyl sulfoxide (DMSO), 2-methyltetrahydrofuran (MeTHF), choline acetate, and choline dihydrogen phosphate towards veratryl alcohol was determined as described above. Stability of *Ma*AAO towards up to 20% of dimethyl sulfoxide (DMSO), 40% of choline acetate, and 40% of choline dihydrogen phosphate was determined by incubating *Ma*AAO in 50 mM potassium phosphate buffer pH 7.5 with the respective cosolvent for 24 h at 25 °C. Residual activity towards veratryl alcohol was measured as described above. All measurements were done in triplicate.

Substrate screening

Activity of *Ma*AAO towards benzyl alcohol, 4-hydroxybenzyl alcohol, *m*-anisyl alcohol, *p*-anisyl alcohol, veratryl alcohol, isovanillyl alcohol, vanillyl alcohol, 2,4-dimethoxybenzyl alcohol, 3-aminobenzyl alcohol, 4-aminobenzyl alcohol, cumic alcohol, piperonyl alcohol, 1-phenylethanol, 2-naphthalenemethanol, 1-pyrenemethanol, cinnamyl alcohol, coniferyl alcohol, sinapyl alcohol, furfuryl alcohol, furfural, 2,5-diformylfuran (DFF), 5-hydroxymethylfurfural (HMF), 5-hydroxymethyl-2-furancarboxylic acid (HMFCA), 5-formyl-2-furancarboxylic acid (FFCA), prenol, *trans,trans*-2,4-hexadien-1-ol, *trans,trans*-2,4-heptadien-1-ol, 2-thiophenemethanol, 2-pyridinemethanol, (*S*)-perillyl alcohol, eugenol, benzaldehyde, and vanillin was determined by using a coupled assay for detection of H_2O_2 generated in course of substrate oxidation via horseradish peroxidase-(HRP, Type VI, Sigma-Aldrich, Schnelldorf, Germany) catalyzed H_2O_2-dependent oxidation of 2,6-dimethoxyphenol (2,6-DMP) to coerulignone. Stock solutions of substrates were prepared in 100 mM potassium phosphate buffer pH 6.0 and dimethyl sulfoxide, respectively, at a concentration of 50 and 500 mM, respectively. The measurements were conducted in 100 mM potassium phosphate buffer pH 6.0 with 5 mM substrate, 5 mM 2,6-DMP, 100 µg/ml HRP, and 0.02 µM of purified *Ma*AAO in a total volume of 200 µl at 25 °C. Formation of coerulignone ($\varepsilon_{468} = 49{,}600\ M^{-1}\ cm^{-1}$) was followed at 468 nm using an Infinite™ M200 PRO plate reader. All measurements were conducted in triplicates.

Determination of kinetic constants

V_{max} and K_M values were determined for selected substrates in 100 mM potassium phosphate buffer pH 6.0 at 25 °C using an Infinite™ M200 PRO plate reader. Substrate concentrations ranged from 1 µM up to 10 mM (dependent on the substrate). All measurements were done in triplicate. Product formation was followed at 314 nm for *m*-anisaldehyde ($\varepsilon_{314} = 2{,}540\ M^{-1}\ cm^{-1}$) (Guillen et al. 1992), at 285 nm for *p*-anisaldehyde ($\varepsilon_{285} = 16{,}980\ M^{-1}\ cm^{-1}$) (Guillen et al.

1992), at 250 nm for benzaldehyde ($\varepsilon_{250} = 13{,}800\ M^{-1}\ cm^{-1}$) (Guillen et al. 1992), at 310 nm for cinnamaldehyde ($\varepsilon_{310} = 15{,}600\ M^{-1}\ cm^{-1}$) (Ferreira et al. 2005), at 314 nm for 2,4-dimethoxy benzaldehyde ($\varepsilon_{314} = 8{,}840\ M^{-1}\ cm^{-1}$) (Guillen et al. 1992), at 280 nm for *trans,trans*-2,4-hexadienal ($\varepsilon_{280} = 30{,}140\ M^{-1}\ cm^{-1}$) (Ruiz-Duenas et al. 2006), at 307 nm for isovanillin ($\varepsilon_{307} = 7{,}383\ M^{-1}\ cm^{-1}$) (Ferreira et al. 2005), at 317 nm for piperonal ($\varepsilon_{317} = 8{,}680\ M^{-1}\ cm^{-1}$) (Jankowski et al. 2020), and at 309 nm for vanillin ($\varepsilon_{309} = 8{,}332\ M^{-1}\ cm^{-1}$) (Ferreira et al. 2005). For 3-aminobenzyl alcohol, HMF and (*S*)-perillyl alcohol the coupled 2,6-DMP-HRP assay was applied for determination of kinetic constants as described above. Data were fitted to the Michaelis–Menten equation or substrate excess inhibition equation ($v = V_{max}*[S]/(K_M + [S]*(1 + [S]/K_i))$ using OriginPro 9.0. k_{cat} values were calculated based on the molar concentration of *Ma*AAO determined by using the molar extinction coefficient.

Oxidation of HMF and its oxidized derivatives

HMF, DFF, HMFCA, and FFCA, respectively, were incubated at a concentration of 2 mM in 100 mM sodium acetate buffer pH 5.0 and 100 mM sodium phosphate buffer pH 6.0, respectively, with 2 µM *Ma*AAO in a total volume of 200 µl at 25 °C under shaking conditions for up to 6 days. Samples were taken in course of reaction. Reactions were stopped by adding 10 µl 6 M HCl. 2-furoic acid was added as internal standard at a final concentration of 2 mM. Samples were extracted two times with 200 µl methyl *tert*-butyl ether (MTBE), dried over $MgSO_4$, evaporated, resuspended in *N,O*-bis(trimethylsilyl)trifluoroacetamide (BSTFA) for derivatization, and incubated for 15 min at 30 °C prior to GCMS analysis.

The two-enzyme setup for HMF conversion consisted of 2 mM HMF in 100 mM sodium phosphate buffer pH 6.0 with 2 µM *Ma*AAO and 2 µM UPO (see supplemental material for description of enzyme preparation) in a total volume of 200 µl. The reaction was shaken at 25 °C for up to 6 days and analyzed as described above.

GCMS analysis

Oxidation of HMF and its oxidized derivatives was analyzed on a GC–MS-QP-2010 Plus (Shimadzu, Tokyo, Japan) equipped with a FS-Supreme-5 ms column (CS Chromatographie Service GmbH, Langerwehe, Germany) and helium as carrier gas. The injection temperature was 250 °C, the interface was set to 285 °C, and the ion source was set to 200 °C. The column temperature was set to 110 °C, kept for 2 min at this temperature, and ramped to 300 °C at a rate of 20 °C/min. Compounds were identified by comparing the acquired mass spectra with authentic samples or with the NIST 08 database.

Results

Heterologous expression of *Ma*AAO

The gene encoding the putative AAO from *M. antarcticus* (XP_014653549.1), annotated as GMC oxidoreductase, was integrated into the genome of *P. pastoris* X-33 (reclassified as *Komagataella phaffii*) under control of the methanol inducible P_{AOX1} promoter. The putative AAO was designated *Ma*AAO. Nine *P. pastoris* transformants were screened for secretion of *Ma*AAO in BMMY and BMM medium in shaking flasks using veratryl alcohol as substrate. The best performing transformant yielded a volumetric activity towards veratryl alcohol of 150 U/l after 2 days of expression in BMM medium and was subsequently used for enzyme production in a 3 l fed-batch fermentation process. After 8 days of fed-batch cultivation, the volumetric activity reached 19,200 U/l at an OD_{600} of 394.

Structural and spectroscopic properties of *Ma*AAO

Purified *Ma*AAO showed a specific activity towards veratryl alcohol of 25.7 U/mg which gave a calculated expression yield of 750 mg/l after 8 days of fed-batch fermentation. *Ma*AAO runs as a single band on SDS-PAGE with a molecular mass of around 75 kDa (Figure S1). After *N*-deglycosylation with PNGase F, the band shifted to around 67 kDa, the calculated theoretical molecular mass of *Ma*AAO which corresponds to 11% of *N*-glycosylation.

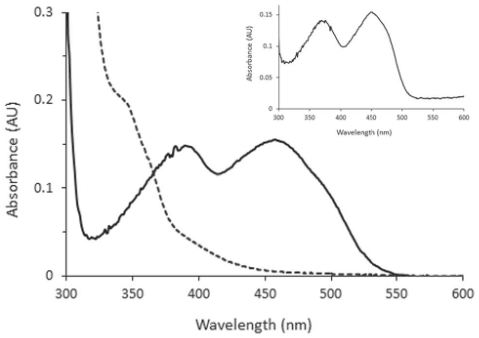

Fig. 2 Absorbance spectrum of purified *Ma*AAO. Solid line: oxidized form; dashed line: reduced form after reduction with 1 mM *p*-anisyl alcohol. The inset shows the UV/Vis spectrum of FAD extracted from *Ma*AAO after heat denaturation

Spectroscopic analysis of the yellow enzyme solution revealed two absorbance maxima at 389 nm and 458 nm, typical for flavoproteins (Fig. 2). Upon heat denaturation, an FAD spectrum with absorbance maxima at 376 nm and 450 nm was obtained. The estimated molar extinction coefficient of purified *Ma*AAO at 458 nm was 8,556 M^{-1} cm^{-1}.

Influence of pH, temperature, H_2O_2, and cosolvents on enzyme activity and stability

Activity of *Ma*AAO towards veratryl alcohol, cinnamyl alcohol, and *trans,trans*-2,4-hexadien-1-ol at pH 2 to 9 was determined. All substrates were oxidized by *Ma*AAO at the investigated pH values. pH optimum of *Ma*AAO for all substrates was at pH 6.0 (Fig. 3A). Stability of *Ma*AAO at pH values of 2 to 9 was investigated. *Ma*AAO retained around 85% of its initial activity after 48 h incubation under neutral, basic, and even acidic conditions (Fig. 3B). Thermal stability of *Ma*AAO was investigated by incubating the enzyme between 30 and 80 °C at pH 6.0 for up to 48 h. *Ma*AAO was stable up to 57.5 °C with almost 95% residual activity after 48 h (Fig. 4). At 70 °C, a residual activity of 60% was found after 3 h of incubation and after 24 h residual activity dropped to 33%. The T_{50} value of *Ma*AAO (the temperature at which half of the enzyme activity is lost after 10 min of incubation) was 74 °C.

The influence of increasing concentrations of H_2O_2 on activity and stability of *Ma*AAO was investigated (Fig. 5). Up to 100 mM H_2O_2 had a marginal effect on activity of *Ma*AAO (90% of initial activity), but 500 mM H_2O_2 resulted in 50% decrease in initial activity. Stability of *Ma*AAO was not affected by incubation with 5 or 10 mM H_2O_2 for 48 h (around 90% residual activity) but residual activity dropped to 53% and 13%, respectively, after 48 h incubation with 50 and 100 mM H_2O_2, while at 500 mM H_2O_2 only 10% residual activity was left after 3 h of incubation.

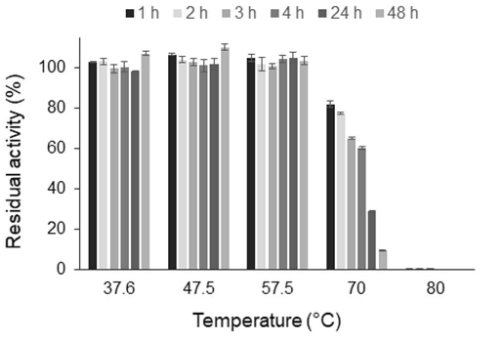

Fig. 4 Thermal stability of *Ma*AAO. Residual activity of *Ma*AAO after different times of incubation at 37.6 °C, 47.5 °C, 57.5 °C, 70 °C, and 80 °C in 50 mM potassium phosphate buffer pH 6.0. Initial activity without incubation was set to 100%

Activity and stability of *Ma*AAO in presence of two organic solvents (DMSO and 2-methyltetrahydrofuran (MeTHF)) and two ionic liquids (choline acetate and choline dihydrogen phosphate) were determined. Activity of *Ma*AAO was reduced in the presence of DMSO (Fig. 6A). At 10% DMSO activity dropped to 54% and at 40% DMSO only 24% of its initial activity remained. MeTHF had a more severe effect with 7% of remaining activity at 1% of solvent. Choline acetate and choline dihydrogen phosphate (up to 10%) hardly influenced activity of *Ma*AAO. At 40% choline acetate 74% activity remained while with choline dihydrogen phosphate activity of *Ma*AAO increased to 132% at 40% of the cosolvent. On the other hand, *Ma*AAO was quite

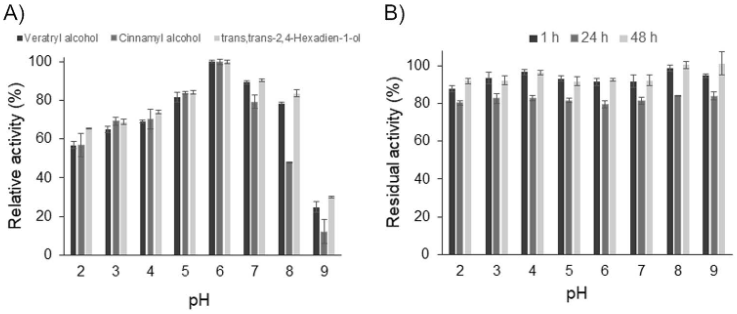

Fig. 3 Influence of pH on activity and stability of *Ma*AAO. **A** pH optimum of *Ma*AAO using veratryl alcohol (black bar), cinnamyl alcohol (dark gray bar), and *trans,trans*-2,4-hexadien-1-ol (light gray bar) as substrates determined in 100 mM Britton-Robinson buffer at pH 2–9. Activity at pH 6.0 was set to 100%. **B** pH stability of *Ma*AAO measured after incubation for 1 h (black bar), 24 h (dark gray bar), and 48 h (light gray bar) in 100 mM Britton-Robinson buffer at the corresponding pH value at 25 °C. Initial activity without incubation was set to 100%

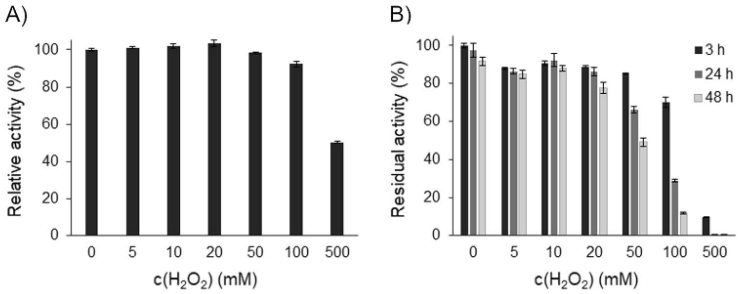

Fig. 5 Influence of hydrogen peroxide on activity and stability of *Ma*AAO. **A** Activity of *Ma*AAO towards veratryl alcohol in the presence of 0–500 mM hydrogen peroxide. Relative activity is given in % of enzyme activity without addition of hydrogen peroxide. **B** Residual activity of *Ma*AAO after 3 h (black bar), 24 h (dark gray bar), and 48 h (light gray bar) of incubation with 0-500 mM hydrogen peroxide in 50 mM potassium phosphate buffer pH 6.0 at 25 °C. Initial activity without incubation was set to 100%

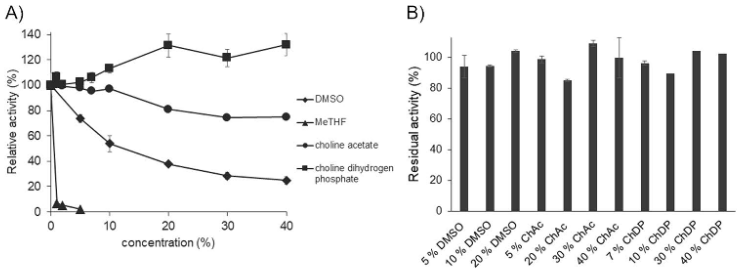

Fig. 6 Influence of cosolvents on activity and stability of *Ma*AAO. **A** Activity of *Ma*AAO towards veratryl alcohol in the presence of 0–40% of DMSO (diamonds), MeTHF (triangles), choline acetate (circles), and choline dihydrogen phosphate (squares). Relative activity is given in % of enzyme activity without cosolvents. **B** Residual activity of *Ma*AAO after 24 h incubation with DMSO, choline acetate (ChAc), and choline dihydrogen phosphate (ChDP), respectively, at different concentrations in 50 mM potassium phosphate buffer pH 7.5 at 25 °C. Activity was measured with veratryl alcohol as substrate under standard assay conditions. Initial activity without incubation was set to 100%

stable in presence of DMSO (up to 20%), choline acetate, and choline dihydrogen phosphate (up to 40%) with over 80% remaining activity after 24 h of incubation (Fig. 6B).

Substrate spectrum of *Ma*AAO

A broad range of primary alcohols and some aldehydes were tested as substrates for *Ma*AAO. For this purpose, a coupled colorimetric assay using 2,6-DMP and horseradish peroxidase to follow hydrogen peroxide production in course of substrate oxidation by *Ma*AAO was applied. The activity towards benzyl alcohol was set to 100%. All benzylic alcohols tested were accepted as substrates with relative activities of up to 250% for veratryl alcohol except for 1-phenylethanol which was not oxidized at all (Table 1). Benzylic alcohols with a methoxy- or amino-substituent at the *meta*- or *para*-position were oxidized equally well (similar relative activity of vanillyl and isovanillyl alcohol and of 3- and 4-amino benzyl alcohol), except for *m*- and *p*-anisyl alcohol with 139% and 219% relative activity, respectively. An extended unsaturated side chain as in cinnamyl alcohol increased activity to 231% as compared to benzyl alcohol, while for coniferyl alcohol activity dropped to 23% and sinapyl alcohol was not oxidized at all. *Ma*AAO showed the highest relative activity of 282% towards the aliphatic alcohol *trans,trans*-2,4-hexadien-1-ol followed by piperonyl alcohol (252%), a benzodioxol derivative. Other tested benzylic alcohols were oxidized as well but with lower activity compared to benzyl alcohol. All furan derivatives tested were oxidized by *Ma*AAO with HMF leading to the highest relative activity of 176%. HMFCA was oxidized by *Ma*AAO with a relative activity of 20%. *Ma*AAO showed a high activity towards (*S*)-perillyl alcohol (185%) while eugenol, a typical substrate of vanillyl alcohol oxidases, was hardly

8320 Applied Microbiology and Biotechnology (2021) 105:8313–8327

Table 1 Substrate spectrum of *Ma*AAO. Hydrogen peroxide formed in course of substrate oxidation was detected in a coupled 2,6-DMP-HRP assay. Substrates were used at 5 mM final concentration in 100 mM potassium phosphate buffer pH 6.0. Activity towards benzyl alcohol was set to 100%

Compound	Structure	Relative activity (%)
Benzyl alcohol		100
4-Hydroxybenzyl alcohol	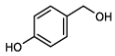	155
m-Anisyl alcohol		139
p-Anisyl alcohol	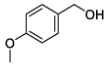	219
Veratryl alcohol	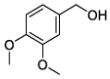	250
Isovanillyl alcohol	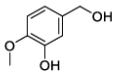	211
Vanillyl alcohol	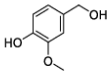	212
2,4-Dimethoxybenzyl alcohol	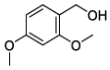	180
3-Aminobenzyl alcohol		170
4-Aminobenzyl alcohol	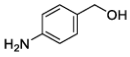	162
Cumic alcohol	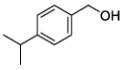	164
Piperonyl alcohol	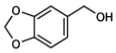	252
1-Phenylethanol		0
2-Naphthalenemethanol	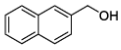	97
1-Pyrenemethanol	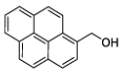	15
Cinnamyl alcohol	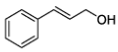	231

Applied Microbiology and Biotechnology (2021) 105:8313–8327 8321

Table 1 (continued)

Coniferyl alcohol	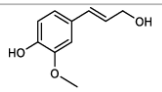	29
Sinapyl alcohol	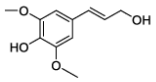	0
Furfuryl alcohol		75
Furfural		6
DFF		68
HMF	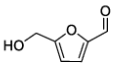	176
HMFCA	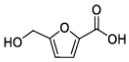	20
FFCA	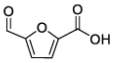	10
Prenol		74
trans,trans-2,4-Hexadien-1-ol	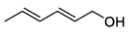	282
trans,trans-2,4-Heptadien-1-ol	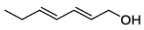	232
2-Thiophenemethanol		42
2-Pyridinemethanol		44
(*S*)-Perillyl alcohol	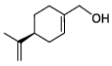	185
Eugenol	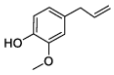	5
Benzaldehyde		23
Vanillin	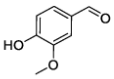	7

converted (5% relative activity). Aldehydes were oxidized to a much lesser extent than the corresponding alcohols (e.g., 7% relative activity with vanillin compared to 212% with vanillyl alcohol). No activity towards GMC oxidoreductase substrates such as D-glucose, D-galactose, maltose, lactose, methanol, or ethanol was found.

For some of the tested substrates, K_M and k_{cat} values of *Ma*AAO were determined (Table 2). While k_{cat} values were in the same range for all tested substrates, K_M values ranged from 1.74 µM for 3-aminobenzyl alcohol to 582 µM for 2,4-dimethoxybenzyl alcohol. Highest affinities and catalytic activities were found for 3-aminobenzyl alcohol, *m*-anisyl alcohol, and *p*-anisyl alcohol. For substrates with K_M values below 15 µM like 3-aminobenzyl alcohol, *p*- and *m*-anisyl alcohol, and benzyl alcohol, a strong decrease in enzymatic activity was observed at increased substrate concentrations. The data fitted well to the Michaelis–Menten equation derived for excess-substrate inhibition (Figure S2). The calculated K_{IU} values are app. 500 times higher than the corresponding K_M values (Table S1). Substrates with K_M values between 15 and 100 µM showed moderate inhibition, except for cinnamyl alcohol (no inhibition observed), and no inhibition was detected for substrates with K_M values above 100 µM. The catalytic efficiency of *Ma*AAO ranged from 15.7 mM^{-1} s^{-1} for HMF to 3670 mM^{-1} s^{-1} for monosubstituted benzylic alcohols. The catalytic efficiency of *Ma*AAO for the non-aromatic (*S*)-perillyl alcohol (387 mM^{-1} s^{-1}) was similar to the aromatic vanillyl alcohol (354 mM^{-1} s^{-1}).

Oxidation of HMF and its derivatives

Conversion of HMF and its oxidized derivatives DFF, HMFCA, and FFCA by *Ma*AAO was conducted at pH 5 and 6 for 6 days. HMF and DFF were oxidized equally well at both pH values and complete conversion to FFCA was reached after 24 h (Table 3). However, only minor amounts of FDCA with 1% or below were detected even after 6 days of reaction. HMFCA was oxidized best at pH 5 by *Ma*AAO with 60% conversion to FFCA within 24 h, while at pH 6.0 only 25% FFCA was formed after 24 h (data not shown). After 6 days of reaction, full conversion of HMFCA to FFCA was observed. Again, only marginal amounts of FDCA with less than 1% were detected. Oxidation of FFCA by *Ma*AAO was lowest among all tested furan derivatives. After 24 h, only 1% FDCA was detected at all while after 6 days of reaction at pH 6.0 40% FDCA was formed. At pH 5, no oxidation products were detected. Due to the high activity of *Ma*AAO towards HMFCA, a two-enzyme approach consisting of *Ma*AAO and an unspecific peroxygenase was applied for HMF oxidation. With this setup complete conversion of HMF to FDCA was obtained within 6 days.

Discussion

The implementation of AAOs as biocatalysts for the production of precursors for bio-based polymers, flavors, fragrances, or pharmaceutical compounds is hampered by the low expression level of most of these enzymes and the limited number of AAOs described and characterized so far. The latter one might also be caused by the limited availability of these enzymes. For instance, heterologous expression of *P. eryngii* AAO (*Pe*AAO) in *P. pastoris* required directed evolution of this enzyme and eventually yielded 25.5 mg/l of *Pe*AAO variant FX9 in *P. pastoris* (Vina-Gonzalez et al. 2018). Recently, *Pe*AAO2 from *P. eryngii* P34 was heterologously expressed in *P. pastoris* at 315 mg/l (Jankowski et al. 2020). The putative AAO, *Ma*AAO from *M. antarcticus*, was expressed with its native signal peptide for secretion in *P. pastoris* at 750 mg/l, which is one of the highest reported yields of AAOs so far.

Identified by BLASTp searches using several known AAO sequences, *Ma*AAO annotated as GMC oxidoreductase was identified. *Ma*AAO contains the two catalytic histidines (His575 and His618 in *Ma*AAO) highly conserved among AAOs as was shown by multiple sequence alignments (Figure S3). As in other AAOs, the substrate access channel is formed by three aromatic amino acid residues (Phe147, Phe476, and Tyr574), that vary among AAOs. *Pe*AAO possesses, for example, Tyr92, Phe397, and Phe501 at the corresponding positions (Fig. 7).

Spectroscopic analysis of native and heat-treated enzyme confirmed that *Ma*AAO contains a non-covalently bound FAD cofactor typically for AAOs. *Ma*AAO has a theoretical molecular mass of 67 kDa (without its predicted N-terminal signal peptide) and possesses six potential *N*-glycosylation sites. The enzyme was expressed with around 11% *N*-glycosylation extent in *P. pastoris*. In comparison, *Pe*AAO variant FX9 with seven potential *N*-glycosylation sites was only poorly glycosylated when expressed in *P. pastoris* (Vina-Gonzalez et al. 2018), while recombinantly expressed *Pe*AAO2 from *P. eryngii* P34 with eight potential *N*-glycosylation sites showed 30% *N*-glycosylation (Jankowski et al. 2020). Viña-Gonzalez and colleagues showed that *N*-glycosylation has a positive effect on thermostability of *Pe*AAO when compared to non-glycosylated *Pe*AAO expressed in *E. coli* (Vina-Gonzalez et al. 2015). Thermostability of *Ma*AAO was quite high with 60% remaining activity after 3 h of incubation at 70 °C while activity of similarly glycosylated *Pe*AAO expressed in *Aspergillus nidulans* dropped to ~ 10% after 40 min incubation at 65 °C (Ruiz-Duenas et al. 2006) and *Mt*AAOx from *Thermothelomyces thermophilus* M77 remained only ~ 10% of its activity after 2 h incubation at 70 °C in the presence of calcium (Kadowaki et al. 2020). Moreover, the T_{50} value of *Ma*AAO (74 °C) is the highest of

Applied Microbiology and Biotechnology (2021) 105:8313–8327 8323

Table 2 Kinetic constants of *Ma*AAO and of other AAOs

		*Ma*AAO from *M. antarcticus*[a]	*Pe*AAO2 from *P. eryngii* P34[b]	*Pe*AAO from *P. erygnii*[c]	r*Cc*AAO from *C. cinerea*[d]	BAO from *B. cinerea*[e]	*Um*AAO from *U. maydis*[f]
3-Aminobenzyl alcohol[g]	K_M (μM)	1.74 ± 0.24	n.d	n.d	n.d	n.d	n.d
	k_{cat} (s^{-1})	6.4	n.d	n.d	n.d	n.d	n.d
	k_{cat}/K_M (mM^{-1} s^{-1})	3670	n.d	n.d	n.d	n.d	n.d
m-Anisyl alcohol	K_M (μM)	4.43 ± 2.65	n.d	227	3.96 ± 1.14	156 ± 5	n.d
	k_{cat} (s^{-1})	12.2	n.d	15	7.66	54	n.d
	k_{cat}/K_M (mM^{-1} s^{-1})	2754	n.d	65	1940	349	n.d
p-Anisyl alcohol	K_M (μM)	3.54 ± 0.66	24.3 ± 0.8	27	11.6 ± 1.0	187 ± 16	4.8 ± 0.4
	k_{cat} (s^{-1})	10.2	59.2	142	12.5	121	45
	k_{cat}/K_M (mM^{-1} s^{-1})	2869	2436	5233	1080	646	9380
Benzyl alcohol	K_M (μM)	< 15.0	599.6 ± 18.7	632	1.21 ± 0.27	329 ± 15	n.d
	k_{cat} (s^{-1})	11.2	12.8	30	6.13	6	n.d
	k_{cat}/K_M (mM^{-1} s^{-1})	745	21.39	47	5060	18	n.d
Cinnamyl alcohol	K_M (μM)	26.9	2740 ± 103	708	n.d	73 ± 3	35 ± 2
	k_{cat} (s^{-1})	8.9	125.5	65	n.d	22	88
	k_{cat}/K_M (mM^{-1} s^{-1})	332	45.80	78	n.d	305	2510
2,4-Dimethoxy-benzyl alcohol	K_M (μM)	582	n.d	n.d	n.d	n.d	1820 ± 150
	k_{cat} (s^{-1})	5.9	n.d	n.d	n.d	n.d	30
	k_{cat}/K_M (mM^{-1} s^{-1})	35.2	n.d	n.d	n.d	n.d	16.5
trans,trans-2,4-Hexadien-1-ol	K_M (μM)	26.5 ± 1.7	143.6 ± 11.5	94	15.6 ± 0.8	521 ± 27	15 ± 1
	k_{cat} (s^{-1})	11.5	68.8 ± 0.05	119	48.3	97	64
	k_{cat}/K_M (mM^{-1} s^{-1})	435	479.3	1271	3100	186	4270
HMF[g]	K_M (μM)	341 ± 20	n.d	1600 ± 200[h]	n.d	n.d	n.d
	k_{cat} (s^{-1})	5.4	n.d	0.67[h]	n.d	n.d	n.d
	k_{cat}/K_M (mM^{-1} s^{-1})	15.7	n.d	0.42[h]	n.d	n.d	n.d
Isovanillyl alcohol	K_M (μM)	60.9 ± 6.7	n.d	831	42 ± 0.9	1115 ± 35	n.d
	k_{cat} (s^{-1})	9.6	n.d	127	7.02	56	n.d
	k_{cat}/K_M (mM^{-1} s^{-1})	158	n.d	152	167	51	n.d
(*S*)-Perillyl alcohol[g]	K_M (μM)	23.7 ± 1.7	n.d	n.d	n.d	n.d	n.d
	k_{cat} (s^{-1})	9.2	n.d	n.d	n.d	n.d	n.d
	k_{cat}/K_M (mM^{-1} s^{-1})	387	n.d	n.d	n.d	n.d	n.d
Piperonyl alcohol	K_M (μM)	12.2 ± 1.0	59.1 ± 3.0	n.d	n.d	n.d	n.d
	k_{cat} (s^{-1})	11.3	35.5	n.d	n.d	n.d	n.d
	k_{cat}/K_M (mM^{-1} s^{-1})	926	600.2	n.d	n.d	n.d	n.d
Vanillyl alcohol	K_M (μM)	30.0 ± 2.4	n.d	n.d	6.27 ± 0.43	1404.0 ± 77	n.d
	k_{cat} (s^{-1})	10.6	n.d	n.d	14.7	44	n.d
	k_{cat}/K_M (mM^{-1} s^{-1})	354	n.d	n.d	2350	31	n.d
Veratryl alcohol	K_M (μM)	119.0 ± 7.0	446.6 ± 7.5	540	48.3 ± 6.1	2094 ± 114	120 ± 10
	k_{cat} (s^{-1})	11.7	47.2	114	13.2	47	53
	k_{cat}/K_M (mM^{-1} s^{-1})	98	105.7	210	273	22	440

n.d. not determined

[a]This study, 100 mM sodium phosphate buffer pH 6.0, 25 °C

[b]Jankowski et al. (2020), 100 mM sodium phosphate buffer pH 6.0, 25 °C

[c]Ferreira et al. (2006), 100 mM sodium phosphate buffer pH 6.0, 24 °C

[d]Tamaru et al. (2018), 50 mM potassium phosphate buffer pH 7.0, 25 °C

[e]Goetghebeur et al. (1992), 100 mM sodium phosphate buffer, pH 6.0, 24 °C

[f]Couturier et al. (2016), measured with coupled ABTS-HRP assay in 100 mM McIlvaine buffer pH 6.0, at 30 °C

[g]Measured with coupled 2,6-DMP-HRP assay in 50 mM potassium phosphate buffer pH 6.0, at 25 °C

[h]Values taken from Vina-Gonzalez et al. (2020)

Table 3 Molar percentages after treatment of HMF, DFF, HMFCA, and FFCA, respectively, with *Ma*AAO for 24 h and 144 h. Reactions were performed with 2 mM substrate and 2 µM *Ma*AAO in 100 mM sodium phosphate buffer pH 6.0. HMF was additionally treated with 2 µM *Ma*AAO and 2 µM UPO

Substrate	Enzyme	Time (h)	Molar percentages (%)				
			HMF	DFF	HMFCA	FFCA	FDCA
HMF	*Ma*AAO	24	0	0	0	99.6	0.4
	*Ma*AAO	144	0	0	0	99	1
	*Ma*AAO + UPO	24	0	0	21	61	18
	*Ma*AAO + UPO	144	0	0	0	0	100
DFF	*Ma*AAO	24	-	0	0	99.6	0.4
	*Ma*AAO	144	-	0	0	99	1
HMFCA[a]	*Ma*AAO	24	-	-	39.4	60	0.4
	*Ma*AAO	144	-	-	0	99.2	0.8
FFCA	*Ma*AAO	24	-	-	-	99	1
	*Ma*AAO	144	-	-	-	60	40

[a]Reaction was conducted in 100 mM sodium acetate buffer, pH 5.0

an AAO reported so far and much higher than that of heavily glycosylated *Pe*AAO (58.8 °C) expressed in *S. cerevisiae* (Vina-Gonzalez et al. 2015) or *Pe*AAO2 (62.1 °C) expressed in *P. pastoris* (Jankowski et al. 2020). Glycosylated *Ma*AAO also showed high stability from pH 2 to 9 and is more stable under acidic conditions compared to other AAOs (Jankowski et al. 2020; Vina-Gonzalez et al. 2015). Besides this, *Ma*AAO was quite active and stable in the presence of the ionic liquids (ILs) choline acetate and choline dihydrogen phosphate. ILs are salts that exist in liquid form often below 100 °C. They have gained increasing attention over the last years and become promising reaction media for biocatalytic reactions (Elgharbawy et al. 2020). ILs have not been investigated as cosolvents in AAO-catalyzed reactions so far. However, the positive effect of the bio-based IL choline dihydrogen phosphate on enzyme activity and stability has been already described by Galai and coworkers for *Trametes versicolor* laccase (Galai et al. 2015). The high pH and thermal stability together with its high activity and stability in the presence of ILs and hydrogen peroxide makes this enzyme a promising biocatalyst for application in synthesis of value-added compounds.

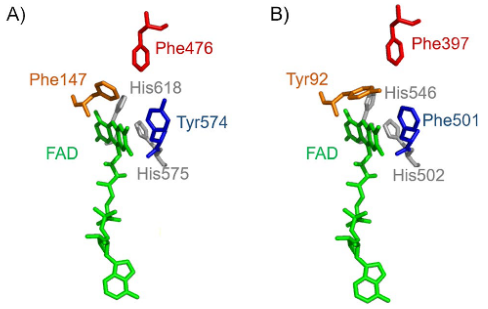

Fig. 7 Comparison of the active site of *Ma*AAO (**A**, 3D homology model) and *Pe*AAO (**B**, PDB entry 3FIM) drawn with PyMOL. The FAD molecule (in green), the catalytic histidines (in gray), and the aromatic amino acid residues forming the substrate access channel (in blue, red, and orange) of *Ma*AAO and *Pe*AAO are shown

The substrate spectrum of *Ma*AAO is quite broad and comprises a large number of benzylic alcohols, aliphatic allylic primary alcohols as well as furan derivates, and heterocyclic alcohols. Oxidation of aldehydes was much lower compared to the corresponding alcohols as described for other AAOs (Ferreira et al. 2010; Serrano et al. 2020). Furthermore, activity of *Ma*AAO towards eugenol, a typical substrate of vanillyl alcohol oxidases, was negligible and no activity towards sugars was found, confirming the classification of *Ma*AAO to AAOs (EC 1.1.3.7).

Activity of *Ma*AAO was generally enhanced towards hydroxy-, methoxy-, or amino-substituted benzylic alcohols as compared to benzyl alcohol while, for example, activity of *Pe*AAO2 from *P. eryngii* P34 towards amino-substituted benzylic alcohols was 5 to 10 times lower as compared to benzyl alcohol (Jankowski et al. 2020). Furthermore, *Ma*AAO oxidized benzylic alcohols substituted with a methoxy group at the *meta*- or *para*-position of the aromatic ring equally well as was shown for some other AAOs like r*Cc*AAO from *Coprinopsis cinerea*, BAO from *Botrytis cinerea*, and AOx from *Aspergillus terreus* (Urlacher and Koschorreck 2021). Other AAOs, like the well-studied *Pe*AAO, showed higher activity towards benzylic alcohols with methoxy-substitution in *para*-position than in *meta*-position.

*Ma*AAO accepts both, phenolic and non-phenolic substrates, while, e.g., vanillyl alcohol oxidase oxidizes 4-hydroxybenzylic compounds (Ewing et al. 2020). Phenolic vanillyl alcohol and non-phenolic veratryl alcohol were even oxidized at similar turnover numbers by *Ma*AAO as was shown for some other AAOs (Goetghebeur et al. 1992; Romero et al. 2009; Tamaru et al. 2018).

K_M and k_{cat} values of *Ma*AAO for the investigated substrates were quite similar to r*Cc*AAO from *C. cinerea*

(Tamaru et al. 2018), but lower as compared to those of *Pe*AAO, *Pe*AAO2, and BAO. Concerning the catalytic constants and the substrate specificity, *Ma*AAO resembles more r*Cc*AAO than other AAOs, although the amino acid sequence identity of both AAOs is only 31%. Enzyme inhibition at substrate excess has, however, not been reported for r*Cc*AAO as was observed for *Ma*AAO with some of the investigated substrates. Only for *Um*AAO substrate inhibition for some compounds with a very low K_M value has been described (Couturier et al. 2016).

*Ma*AAO was also active towards cumic alcohol. The oxidation product, cuminaldehyde, is the major component of essential oils obtained from cumin seeds and showed antimicrobial and anti-biofilm effects against *Staphylococcus aureus* and *E. coli* (Monteiro-Neto et al. 2020). Oxidation of cumic alcohol to cuminaldehyde was recently described for *Pe*AAO2 with a slightly lower relative activity (149%) than *Ma*AAO (167%) (Jankowski et al. 2020). Piperonyl alcohol was the best substrate among the benzylic alcohols tested for *Ma*AAO with 2.5-times faster conversion compared to benzyl alcohol. The oxidation product piperonal, also known as heliotropin, is used in the fragrance and flavor industry due to its vanilla-like aroma and serves as intermediate for the production of insecticides and pharmaceuticals (Brum et al. 2019; Santos et al. 2004; Wang et al. 2019). Surprisingly, the non-aromatic primary alcohol (*S*)-perillyl alcohol was accepted as substrate by *Ma*AAO and oxidized almost two times better than benzyl alcohol. The oxidation product of the reaction, perillaldehyde, is used as flavoring ingredient to add spiciness to foods and shows several health-promoting properties like antioxidative, antibacterial, anti-inflammatory, and antiallergic effects (Ahmed 2018; Fuyuno et al. 2018; Uemura et al. 2018). Oxidation of this monocyclic monoterpene by an AAO has to the best of our knowledge not been described so far and further expands the substrate scope of AAOs.

The oxidation of HMF and its derivatives makes *Ma*AAO quite interesting for application as biocatalyst in enzymatic synthesis of FDCA. While the chemical route to FDCA requires high temperature and pressure, organic solvents, and metal catalysts (Sajid et al. 2018), some enzymes were shown to catalyze one or more of the individual reaction steps under mild reaction conditions without cosolvents (Carro et al. 2015; Daou et al. 2019; Dijkman and Fraaije 2014; Karich et al. 2018; Mathieu et al. 2020; Vinambres et al. 2020). For example, 5-hydroxymethylfurfural oxidase (HMFO) from *Methylovorus* sp. strain MP688 was shown to oxidize HMF to FDCA via DFF and FFCA, but conversion was not complete (Dijkman and Fraaije 2014). *Pe*AAO oxidized HMF predominantly to FFCA due to hydrogen peroxide formation inhibiting further oxidation of FFCA to FDCA (Serrano et al. 2019a). Among the tested furan derivatives, *Ma*AAO showed highest activity towards HMF and the catalytic efficiency of *Ma*AAO for HMF is in the same range or even higher compared to other AAOs and HMF-oxidizing enzymes (Carro et al. 2015; Daou et al. 2019; Dijkman and Fraaije 2014; Mathieu et al. 2020; Vinambres et al. 2020). However, although FFCA was slowly oxidized to FDCA by *Ma*AAO, only trace amounts of FDCA were detected when starting from HMF. Remarkably, *Ma*AAO was able to completely oxidize HMFCA to FFCA which has not been shown for any other AAO so far. Conversion of HMFCA to FFCA enables the use of a two-enzyme system for synthesis of FDCA, employing UPO for FDCA production from FFCA, while *Ma*AAO supplies UPO with hydrogen peroxide and re-introduces HMFCA, formed by UPO from HMF, back into the reaction as FFCA. This simplifies AAO/UPO-reaction cascades for the production of FDCA relying on a third enzyme like galactose oxidase to oxidize UPO-formed HMFCA to FFCA (Karich et al. 2018). The two-enzyme system enabled complete conversion of HMF to FDCA and optimization of the reaction conditions to improve the conversion rate is under investigation yet. The construction of *Ma*AAO/UPO fusion enzymes might further enhance FDCA production and lead to promising biocatalysts for the synthesis of bioplastic precursors, pharmaceuticals, and other value-added compounds as was recently shown by the use of an evolved peroxygenase-AAO fusion for the synthesis of dextrorphan (de Santos et al. 2020).

In summary, *Ma*AAO from *M. antarcticus* is a new AAO with promising properties that is expressed at high levels in *P. pastoris*. Its broad substrate spectrum and high thermal as well as pH stability render this enzyme a highly attractive biocatalyst for biotechnological applications. Oxidation products of *Ma*AAO-catalyzed reactions can be applied, for example, as precursors for bioplastics, flavors, fragrances, and intermediates for pharmaceuticals. Implementation of AAO-mediated reactions in biotechnological processes will thus contribute to the development of environmentally friendly production routes of value-added compounds.

Supplementary Information The online version contains supplementary material available at https://doi.org/10.1007/s00253-021-11557-8.

Author contribution All authors contributed to research design. AL conducted the experiments, analyzed the data, and evaluated the results. Data on solvent stability were collected, analyzed, and evaluated by AA. NJ gave advice in research work. KK conceived and designed the study and drafted the manuscript. All authors read and approved the final manuscript.

Funding Open Access funding enabled and organized by Projekt DEAL. This study was supported by the Bioeconomy Science Center (BioSC) through the Ministry of Innovation, Science and Research

within the framework of the NRW-Strategieprojekt BioSC (No. 313/323–400-002 13).

Availability of data and material The data that support the findings of this study are available from the corresponding author upon reasonable request.

Code availability Not applicable.

Declarations

Ethics approval Not applicable.

Consent to participate Not applicable.

Consent for publication Not applicable.

Conflict of interest The authors declare no competing interests.

References

Ahmed HM (2018) Ethnomedicinal, phytochemical and pharmacological investigations of *Perilla frutescens* (L.) Britt. Molecules 24(1):102. https://doi.org/10.3390/molecules24010102

Aliverti A, Curti B, Vanoni M, Antonietta (1999) Identifying and quantitating FAD and FMN in simple and in iron-sulfur-containing flavoproteins. In: Chapman SK, Reid GA (eds) Flavoprotein protocols, vol 131. Humana Press, Totowa pp 9-23

Bradford MM (1976) Rapid and sensitive method for quantitation of microgram quantities of protein utilizing principle of protein-dye binding. Anal Biochem 72(1–2):248–254

Brum JdOC, Neto DCF, de Almeida JSFD, Lima JA, Kuca K, França TCC, Figueroa-Villar JD (2019) Synthesis of new quinoline-piperonal hybrids as potential drugs against Alzheimer's disease. Int J Mol Sci 20(16):3944. https://doi.org/10.3390/ijms20163944

Carro J, Ferreira P, Rodriguez L, Prieto A, Serrano A, Balcells B, Arda A, Jimenez-Barbero J, Gutierrez A, Ullrich R, Hofrichter M, Martinez AT (2015) 5-hydroxymethylfurfural conversion by fungal aryl-alcohol oxidase and unspecific peroxygenase. FEBS J 282(16):3218–3229. https://doi.org/10.1111/febs.13177

Couturier M, Mathieu Y, Li A, Navarro D, Drula E, Haon M, Grisel S, Ludwig R, Berrin JG (2016) Characterization of a new aryl-alcohol oxidase secreted by the phytopathogenic fungus *Ustilago maydis*. Appl Microbiol Biotechnol 100(2):697–706. https://doi.org/10.1007/s00253-015-7021-3

Daou M, Yassine B, Wikee S, Record E, Duprat F, Bertrand E, Faulds CB (2019) *Pycnoporus cinnabarinus* glyoxal oxidases display differential catalytic efficiencies on 5-hydroxymethylfurfural and its oxidized derivatives. Fungal Biol Biotechnol 6:4. https://doi.org/10.1186/s40694-019-0067-8

de Almeida TP, van Schie MMCH, Ma A, Tieves F, Younes SHH, Fernandez-Fueyo E, Arends IWCE, Riul A, Hollmann F (2019) Efficient aerobic oxidation of *trans*-2-hexen-1-ol using the aryl alcohol oxidase from *Pleurotus eryngii*. Adv Synth Catal 361(11):2668–2672. https://doi.org/10.1002/adsc.201801312

de Santos PG, Lazaro S, Vina-Gonzalez J, Hoang MD, Sanchez-Moreno I, Glieder A, Hollmann F, Alcalde M (2020) Evolved peroxygenase-aryl alcohol oxidase fusions for self-sufficient oxyfunctionalization reactions. ACS Catal 10(22):13524–13534. https://doi.org/10.1021/acscatal.0c03029

Dijkman WP, Fraaije MW (2014) Discovery and characterization of a 5-hydroxymethylfurfural oxidase from *Methylovorus* sp. strain MP688. Appl Environ Microbiol 80(3):1082–1090. https://doi.org/10.1128/aem.03740-13

Elgharbawy AAM, Moniruzzaman M, Goto M (2020) Recent advances of enzymatic reactions in ionic liquids: Part II. Biochem Eng J 154:107426. https://doi.org/10.1016/j.bej.2019.107426

Ewing TA, Gygli G, Fraaije MW, van Berkel WJH (2020) Vanillyl Alcohol Oxidase. Enzymes 47:87–116. https://doi.org/10.1016/bs.enz.2020.05.003

Ferreira P, Medina M, Guillen F, Martinez MJ, Van Berkel WJH, Martinez AT (2005) Spectral and catalytic properties of aryl-alcohol oxidase, a fungal flavoenzyme acting on polyunsaturated alcohols. Biochem J 389:731–738. https://doi.org/10.1042/Bj20041903

Ferreira P, Ruiz-Duenas FJ, Martinez MJ, van Berkel WJH, Martinez AT (2006) Site-directed mutagenesis of selected residues at the active site of aryl-alcohol oxidase, an H_2O_2-producing ligninolytic enzyme. FEBS J 273(21):4878–4888. https://doi.org/10.1111/j.1742-4658.2006.05488.x

Ferreira P, Hernandez-Ortega A, Herguedas B, Rencoret J, Gutierrez A, Martinez MJ, Jimenez-Barbero J, Medina M, Martinez AT (2010) Kinetic and chemical characterization of aldehyde oxidation by fungal aryl-alcohol oxidase. Biochem J 425:585–593. https://doi.org/10.1042/Bj20091499

Ferreira P, Carro J, Serrano A, Martinez AT (2015) A survey of genes encoding H_2O_2-producing GMC oxidoreductases in 10 Polyporales genomes. Mycologia 107(6):1105–1119. https://doi.org/10.3852/15-027

Fuyuno Y, Uchi H, Yasumatsu M, Morino-Koga S, Tanaka Y, Mitoma C, Furue M (2018) Perillaldehyde inhibits AHR signaling and activates NRF2 antioxidant pathway in human keratinocytes. Oxid Med Cell Longev 2018:9524657. https://doi.org/10.1155/2018/9524657

Galai S, de los Rios AP, Hernandez-Fernandez FJ, Kacem SH, Tomas-Alonso F (2015) Over-activity and stability of laccase using ionic liquids: screening and application in dye decolorization. RSC Adv 5(21):16173–16189. https://doi.org/10.1039/c4ra07351g

Goetghebeur M, Nicolas M, Brun S, Galzy P (1992) Purification and properties of benzyl alcohol oxidase from *Botrytis cinerea*. Biosci Biotechnol Biochem 56(2):298–303. https://doi.org/10.1271/bbb.56.298

Guillen F, Martinez AT, Martinez MJ (1992) Substrate-specificity and properties of the aryl-alcohol oxidase from the ligninolytic fungus *Pleurotus eryngii*. Eur J Biochem 209(2):603–611. https://doi.org/10.1111/j.1432-1033.1992.tb17326.x

Jankowski N, Koschorreck K, Urlacher VB (2020) High-level expression of aryl-alcohol oxidase 2 from *Pleurotus eryngii* in *Pichia pastoris* for production of fragrances and bioactive precursors. Appl Microbiol Biotechnol 104(21):9205–9218. https://doi.org/10.1007/s00253-020-10878-4

Kadowaki MAS, Higasi PMR, de Godoy MO, de Araujo EA, Godoy AS, Prade RA, Polikarpov I (2020) Enzymatic versatility and

thermostability of a new aryl-alcohol oxidase from *Thermothelomyces thermophilus* M77. Biochim Biophys Acta Gen Subj 1864(10):129681. https://doi.org/10.1016/j.bbagen.2020.129681

Karich A, Kleeberg SB, Ullrich R, Hofrichter M (2018) Enzymatic preparation of 2,5-furandicarboxylic acid (FDCA)-a substitute of terephthalic acid-by the joined action of three fungal enzymes. Microorganisms 6(1):12. https://doi.org/10.3390/microorganisms6010005

Laemmli UK (1970) Cleavage of structural proteins during assembly of head of bacteriophage-T4. Nature 227(5259):680–685. https://doi.org/10.1038/227680a0

Mathieu Y, Offen WA, Forget SM, Ciano L, Viborg AH, Blagova E, Henrissat B, Walton PH, Davies GJ, Brumer H (2020) Discovery of a fungal copper radical oxidase with high catalytic efficiency toward 5-hydroxymethylfurfural and benzyl alcohols for bioprocessing. ACS Catal 10(5):3042–3058. https://doi.org/10.1021/acscatal.9b04727

Menegazzo F, Ghedini E, Signoretto M (2018) 5-Hydroxymethylfurfural (HMF) production from real biomasses. Molecules 23(9):2201. https://doi.org/10.3390/molecules23092201

Monteiro-Neto V, de Souza CD, Gonzaga LF, da Silveira BC, Sousa NCF, Pontes JP, Santos DM, Martins WC, Pessoa JFV, Carvalho Junior AR, Almeida VSS, de Oliveira NMT, de Araujo TS, Maria-Ferreira D, Mendes SJF, Ferro TAF, Fernandes ES (2020) Cuminaldehyde potentiates the antimicrobial actions of ciprofloxacin against *Staphylococcus aureus* and *Escherichia coli*. PLoS One 15(5):e0232987. https://doi.org/10.1371/journal.pone.0232987

Romero E, Ferreira P, Martinez AT, Martinez MJ (2009) New oxidase from *Bjerkandera* arthroconidial anamorph that oxidizes both phenolic and nonphenolic benzyl alcohols. Biochim Biophys Acta Proteins Proteomics 1794(4):689–697. https://doi.org/10.1016/j.bbapap.2008.11.013

Ruiz-Duenas FJ, Ferreira P, Martinez MJ, Martinez AT (2006) In vitro activation, purification, and characterization of *Escherichia coli* expressed aryl-alcohol oxidase, a unique H_2O_2-producing enzyme. Protein Expr Purif 45(1):191–199. https://doi.org/10.1016/j.pep.2005.06.003

Sajid M, Zhao XB, Liu DH (2018) Production of 2,5-furandicarboxylic acid (FDCA) from 5-hydroxymethylfurfural (HMF): recent progress focusing on the chemical-catalytic routes. Green Chem 20(24):5427–5453. https://doi.org/10.1039/c8gc02680g

Santos AS, Pereira N, da Silva IM, Sarquis MIM, Antunes OAC (2004) Peroxidase catalyzed microbiological oxidation of isosafrol into piperonal. Process Biochem 39:2269–2275. https://doi.org/10.1016/j.procbio.2003.11.019

Serrano A, Calvino E, Carro J, Sanchez-Ruiz MI, Canada FJ, Martinez AT (2019a) Complete oxidation of hydroxymethylfurfural to furandicarboxylic acid by aryl-alcohol oxidase. Biotechnol Biofuels 12(1):217. https://doi.org/10.1186/s13068-019-1555-z

Serrano A, Sancho F, Vina-Gonzalez J, Carro J, Alcalde M, Guallar V, Martinez AT (2019b) Switching the substrate preference of fungal aryl-alcohol oxidase: towards stereoselective oxidation of secondary benzyl alcohols. Catal Sci Technol 9(3):833–841. https://doi.org/10.1039/c8cy02447b

Serrano A, Carro J, Martinez AT (2020) Reaction mechanisms and applications of aryl-alcohol oxidase. Enzymes 47:167–192. https://doi.org/10.1016/bs.enz.2020.05.005

Tamaru Y, Umezawa K, Yoshida M (2018) Characterization of an aryl-alcohol oxidase from the plant saprophytic basidiomycete *Coprinopsis cinerea* with broad substrate specificity against aromatic alcohols. Biotechnol Lett 40(7):1077–1086. https://doi.org/10.1007/s10529-018-2534-3

Uemura T, Yashiro T, Oda R, Shioya N, Nakajima T, Hachisu M, Kobayashi S, Nishiyama C, Arimura GI (2018) Intestinal anti-inflammatory activity of perillaldehyde. J Agric Food Chem 66(13):3443–3448. https://doi.org/10.1021/acs.jafc.8b00353

Urlacher VB, Koschorreck K (2021) Pecularities and applications of aryl-alcohol oxidases from fungi. Appl Microbiol Biotechnol 105(10):4111–4126. https://doi.org/10.1007/s00253-021-11337-4

van Schie MMCH, de Almeida TP, Laudadio G, Tieves F, Fernandez-Fueyo E, Noel T, Arends IWCE, Hollmann F (2018) Biocatalytic synthesis of the Green Note *trans*-2-hexenal in a continuous-flow microreactor. Beilstein J Org Chem 14:697–703. https://doi.org/10.3762/bjoc.14.58

Vina-Gonzalez J, Gonzalez-Perez D, Ferreira P, Martinez AT, Alcalde M (2015) Focused directed evolution of aryl-alcohol oxidase in *Saccharomyces cerevisiae* by using chimeric signal peptides. Appl Environ Microbiol 81(18):6451–6462. https://doi.org/10.1128/Aem.01966-15

Vina-Gonzalez J, Elbl K, Ponte X, Valero F, Alcalde M (2018) Functional expression of aryl-alcohol oxidase in *Saccharomyces cerevisiae* and *Pichia pastoris* by directed evolution. Biotechnol Bioeng 115(7):1666–1674. https://doi.org/10.1002/bit.26585

Vina-Gonzalez J, Jimenez-Lalana D, Sancho F, Serrano A, Martinez AT, Guallar V, Alcalde M (2019) Structureguided evolution of aryl alcohol oxidase from Pleurotus eryngii for the selective oxidation of secondary benzyl alcohols. Adv Synth Catal 361(11):2514–2525. https://doi.org/10.1002/adsc.201900134

Vina-Gonzalez J, Martinez AT, Guallar V, Alcalde M (2020) Sequential oxidation of 5-hydroxymethylfurfural to furan-2,5-dicarboxylic acid by an evolved aryl-alcohol oxidase. Biochim Biophys Acta Proteins Proteomics 1868(1):140293. https://doi.org/10.1016/j.bbapap.2019.140293

Vinambres M, Espada M, Martinez AT, Serrano A (2020) Screening and evaluation of new hydroxymethylfurfural oxidases for furandicarboxylic acid production. Appl Environ Microbiol 86(16):e00842-e920. https://doi.org/10.1128/AEM.00842-20

Wang S, Bao L, Song D, Wang J, Cao X (2019) Heterocyclic lactam derivatives containing piperonyl moiety as potential antifungal agents. Bioorg Med Chem Lett 29:126661. https://doi.org/10.1016/j.bmcl.2019.126661

Wiltschi B, Cernava T, Dennig A, Galindo Casas M, Geier M, Gruber S, Haberbauer M, Heidinger P, Herrero Acero E, Kratzer R, Luley-Goedl C, Muller CA, Pitzer J, Ribitsch D, Sauer M, Schmolzer K, Schnitzhofer W, Sensen CW, Soh J, Steiner K, Winkler CK, Winkler M, Wriessnegger T (2020) Enzymes revolutionize the bioproduction of value-added compounds: From enzyme discovery to special applications. Biotechnol Adv 40:107520. https://doi.org/10.1016/j.biotechadv.2020.107520

2.3.1. Supplemental Information

SUPPLEMENTARY MATERIAL

Characterization of a thermotolerant aryl-alcohol oxidase from *Moesziomyces antarcticus* oxidizing 5-hydroxymethyl-2-furancarboxylic acid

Alessa Lappe [1], Nina Jankowski [1], Annemie Albrecht [1], Katja Koschorreck [1,*]

[1] Institute of Biochemistry, Heinrich-Heine University Düsseldorf, Universitätsstraße 1, 40225 Düsseldorf, Germany

[*] Corresponding Author:

Katja Koschorreck

E-Mail: Katja.Koschorreck@hhu.de

ORCID ID 0000-0001-9689-9863

SUPPLEMENTARY MATERIAL AND METHODS

Expression and purification of UPO

The gene encoding for the unspecific peroxygenase *Aae*UPO form *Agrocybe aegerita* (GenBank accession number FM872458.1) containing additional mutations of *Aae*UPO variant PaDa-I (Molina-Espeja et al. 2014) was synthesized and ligated into the pPICZB vector by BioCat GmbH (Heidelberg, Germany) using restriction sites EcoRI and NotI. *P. pastoris* X-33 cells were transformed with MssI linearized pPICZB_*upo* by electroporation. Recombinant cells were selected on yeast extract peptone dextrose sorbitol agar plates (YPDS; 10 g/l yeast extract, 20 g/l peptone, 20 g/l glucose, 1 M sorbitol, 20 g/l agar) supplemented with 100 µg/ml of Zeocin™ (InvivoGen, San Diego, USA). Cells were grown for four days at 30 °C. For expression of UPO in shaking flasks *P. pastoris* transformants were grown in 10 ml buffered complex glycerol medium (BMGY; 10 g/l yeast extract, 20 g/l peptone, 100 mM potassium phosphate buffer pH 6, 13.4 g/l yeast nitrogen base without amino acids, 0.4 mg/l biotin, 10

g/l glycerol) at 30 °C and 200 rpm overnight. Precultures were used for inoculation of 10 ml buffered methanol minimal medium (BMM; 13.4 g/l yeast nitrogen base without amino acids, 100 mM potassium phosphate buffer pH 6, 0.4 mg/l biotin, 0.5 % (v/v) methanol) to an optical density at 600 nm (OD_{600}) of 0.5 and 10 µM hemin was added. Cells were grown for 3 days at 25 °C and 200 rpm. Methanol (0.5 % (v/v)) was added daily. Volumetric activity of the cell-free supernatants was measured daily towards 2,2'-azino-bis(3-ethylbenzthiazoline-6-sulfonic acid) (ABTS) at a concentration of 0.5 mM in 100 mM sodium citrate buffer pH 4.4 with 1.2 mM H_2O_2. Oxidation of ABTS was followed at 420 nm.

Fed-batch fermentation of the most active *P. pastoris* transformant was conducted in a 7.5 l bioreactor (Infors, Bottmingen, Switzerland) as described earlier (Jankowski et al. 2020). Additionally, hemin was added to a final concentration of 10 µM at the time of induction. Samples were taken daily to monitor OD_{600} and volumetric activity towards ABTS. After eight days of cultivation the fermentation broth was harvested by centrifugation for 15 min at 10,000 *g* and 4 °C. The cell-free supernatant was concentrated and rebuffered in 50 mM potassium phosphate buffer pH 7.0 by tangential flow filtration with cut-off membranes of 10 kDa (Pall, Port Washington, USA). Two ml of concentrated supernatant was loaded onto a Butyl Sepharose HP medium (20 ml, GE Healthcare, Chicago, USA) connected to an ÄKTApurifier FPLC-system (GE Healthcare, Chicago, USA). The column, equilibrated with 50 mM potassium phosphate buffer pH 7.0 with 1.5 M ammonium sulfate (eluent B), was washed with four column volumes (CV) with eluent B at a flow rate of 2 ml/min. Proteins were eluted with 75 % of eluent B (eluent A was 50 mM potassium phosphate buffer pH 7.0) for two CV, followed by 35 % of eluent B for two CV to elute UPO. Fractions with a strong absorbance at 418 nm were pooled, concentrated and rebuffered in 50 mM potassium phosphate buffer pH 7.0. Purified UPO was stored at 4 °C.

SUPPLEMENTARY RESULTS

TABLE S1 Kinetic constants K_M, k_{cat}, k_{cat}/K_M and K_{IU} of *Ma*AAO

Substrate	K_M [µM]	k_{cat} [s^{-1}]	k_{cat}/K_M [mM^{-1} s^{-1}]	K_{IU} [mM]
3-Aminobenzyl alcohol	1.74 ± 0.24	6.4	3690	3.27 ± 0.98
***m*-Anisy alcohol**	4.43 ± 2.65	12.3	2769	2.09 ± 0.33
***p*-Anisyl alcohol**	3.54 ± 0.66	10.2	2884	4.28 ± 0.62
Benzyl alcohol	< 15.0	11.2	749	1.39 ± 0.35

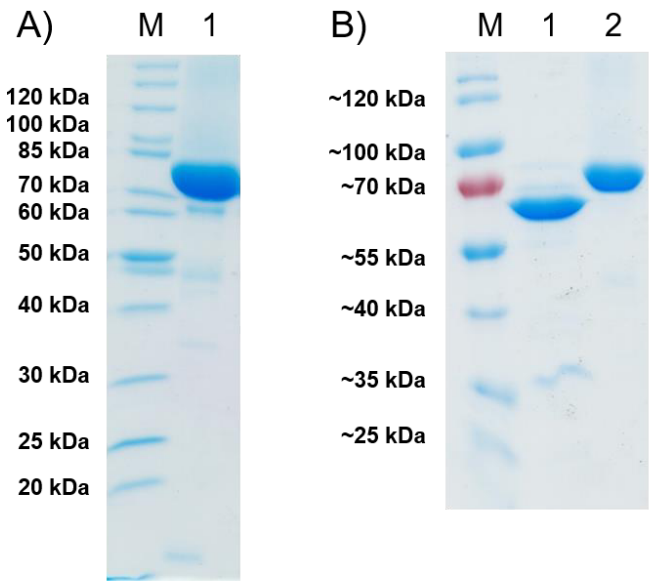

Figure S1. SDS-PAGE analysis of purified *Ma*AAO (lane 1 in A and lane 2 in B) and *Ma*AAO after PNGase F treatment (lane 1 in B). 5 µg of sample was loaded onto the gel. M = Protein ladder.

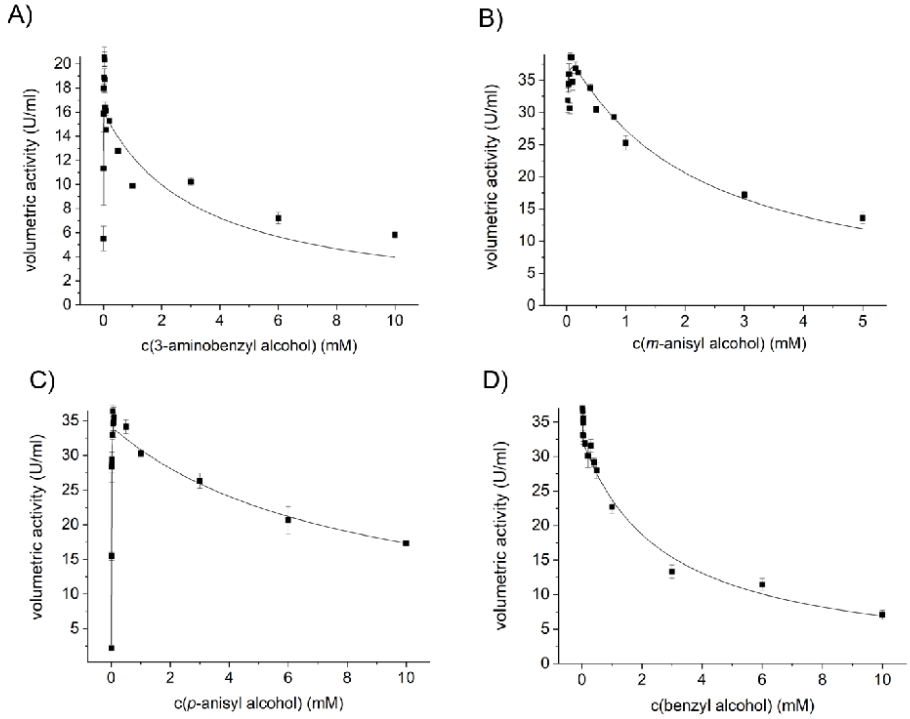

Figure S2. Kinetic analysis of *Ma*AAO for 3-aminobenzyl alcohol (A), *m*-anisyl alcohol (B), *p*-anisyl alcohol (C) and benzyl alcohol (D).

```
AOx        ------------------------------------------------------------    0
MtAAOx     -----------------------------MGF----LAATLVSCAALASAASIPRPHAKR    27
MaAAO      MKATTIIAAAALAGSVAATPVAWTKVSPRSEMAARMAENSHLASRAI-TNDA--------    51
UmAAO      MKTTTLVAAATLAGAVAANPIAWSKVSPRSEFAARMAENSHIAARSI-SSDA--------    51
CcAAO      ---------------------------------------------ALLTDPS--------    7
PeAAO      ----------------------------MSFGA-LRQLLLIACLALPSLAA--------    22
PsAAO      ----------------------------MSFSA-LRQLLFIACLALPSLAA--------    22

AOx        --MTIPDEVDIIICGGGSSGCVPAGRLANLDPSLSVLLIEAGEDNLNNPWVYRPGIYPRN    58
MtAAOx     QVSQLRDDYDFVIVGGGTSGLTVADRLTEAFPAKNVLVIEYGDVHYAPGTFDPPTDWITP    87
MaAAO      -AKFVSKQYDYVVVGAGTAGLALAARLSENGK-YKVGVLEAGGSGYGVGIIDTP-----G    104
UmAAO      -AKFSSKQYDYLVVGAGTAGLAVAARLSESGK-YKVGVLEAGGNGFGVGIIDTP-----G    104
CcAAO      -QLRGDRTYDYVIVGAGNAGNVIAERISAGPHPKSVLVLEAGVSDEGVLAAQVPFLGPTL    66
PeAAO      -TNLPTADFDYVVVGAGNAGNVVAARLTEDPD-VSVLVLEAGVSDENVLGAEAPLLAPGL    80
PsAAO      -ANLPTADFDYIVVGAGNAGNVVAARLTEDPN-VSVLVLEAGVSDENVVGAEAPLLAPGL    80
                    * :: *.*.:* . * *::      .* ::* *           *

AOx        M---KLDSKTASFYYSRPSEHLDGRRAIVPCANILGGGSSINFMMYTRASASDYDDFQ--    113
MtAAOx     QP----DAPPSWSFNSLPNPDMANTTAFVLAGQVVGGSSAVNGMFFDRASRHDYDAWTAV    143
MaAAO      QFGADLGTQYDWNYTTVANPANGVPSSGWPRGRVLGGSSALNFLVWDRSSRYEIDAWE-Q    163
UmAAO      QFGADLGTIYDWNYTTV--PQNGVPAVGWPRGKVLGGSSALNFLVWDRSSRHEIDAWE-Q    161
CcAAO      TPGTFRRTPFDWNYTVAPQEGLDGRTFPFPRGKMLGGCSSVNYMVHHFGSSEDYNKLARD    126
PeAAO      VP----NSIFDWNYTTTAQAGYNGRSIAYPRGRMLGGSSSVHYMVMMRGSTEDFDRYAAV    136
PsAAO      VP----NSIFDWNYTTTAQAGYNGRSIAYPRGRMLGGSSSVHYMVMMRGSIEDFDRYAAV    136
                  :     :                  ..::** *::: :.   .*  : :

AOx        --------AEGWKTKDLVPLMRKHETYQRACNNREL----------HGFD-GPIKVSFGN    154
MtAAOx     GGSGFEQSSHKWDWEGLFPFFQKSVTFTEPPADIVQKYHYTWDLSAYGNGSTPIYSSYPV    203
MaAAO      LG------NPGWNWNNLYKAMKKSERFHAPSQENADLLGVKPVASDYGSS-GPIQVAFPN    216
UmAAO      LG------NPGWNWNNLYSAMKKSEKFHAPSQENADLLGVKPVASDYGSS-GPIQVAFPN    214
CcAAO      SG------DNGWSWSSIKKYIFKHEKIVPPADNSDTDGKF--LPQFHGTG-GTVSVSLPG    177
PeAAO      TG------DEGWNWDNIQQFVRKNEMVVPPADNHNTSGEF--IPAVHGTN-GSVSISLPG    187
PsAAO      TG------DDGWNWDNIQQFVRKNEMVVPPADNHNTSGEF--IPAVHGTN-GSVSISLPG    187
                     *. ..:   . *        :             :* .   :  :

AOx        YTYPIMRDFLRAAESQDIPITDDLQDLKTGHGAEHWLKWI----NRDTGRRSDAAHAYVH    210
MtAAOx     FQWADQPL----LNQAWQEMGINP-VTECAGGDKEGVCWVPASQHPVTARRSHAGLGHYA    258
MaAAO      YISQQVRRWIPALLELGIPKNDQP-L----AGENVGVSQQPSDINPTNYTRSYSAPAYLF    271
UmAAO      YISQQVRRWIPALSELGIPKNDQP-L----AGQNVGVSQQPSNINPSNYTRSYSAPAYLF    269
CcAAO      NSQSIDAKVIATTDEL-PEFPFNP-DQGHGNGQVLGMGWTQN--SIGEGARSSSSTTYLK    233
PeAAO      FPTPLDDRVLATTQEQSEEFFFNP-DMG--TGHPLGISWSIA--SVGNGQRSSSSTAYLR    242
PsAAO      FPTPLDDRVLATTQEQSEEFFFNP-DMG--TGHPLGISWSIA--SVGNGQRSSSSTAYLR    242
                       .       :        *    :             ** :.  :

AOx        STRAKQSNLHLKCNTKVDKVIIENGRAVGVATVPSKPL-DGHDPPRKIFRARKQIIISSG    269
MtAAOx     DVL-PRANYDLLVQHQVVRVVFPNGPSHGPPLVEARS---LADNHLFNVTVKGEVIISAG    314
MaAAO      PNQ-ARSNLDVLTNALASKVNFDS-S-CGELWAKSVTFT--NGGKSYTVNATKEVIISAG    326
UmAAO      PNQ-ARPNLDVLTDALVSKVNFDI-E-CGELSANGVTFI--SNGQTYTVNATKEVILSGG    324
CcAAO      EAL-KRPHVDVLINAHVTKLVTTRKK-RGRPVFDKVQFASGPGAPVTTVTARREIILSAG    291
PeAAO      PAQ-SRPNLSVLINAQVTKLVNSGTT-NGLPAFRCVEYAEQEGAPTTTVCAKKEVVLSAG    300
PsAAO      PAQ-SRPNLSVLINAQVTKLVNSGTT-NGLPAFRCVEYAEREGAPTTTVCAKKEVVLSAG    300
                : :  :  :  . ::        *             .     . .  ::::*.*

AOx        TLSSPLILQRSGIGDPEKLRAAGIRPLMNLPGVGRNFQDHYLTFSVFRAKPDVES---FD    326
MtAAOx     ALHTPTVLQRSGIGPASFLDDAGIPVTLDLPGVGANLQDHCGPPVTWNYTEPYTGFFPLP    374
MaAAO      TVNTPQLLELSGIGSKDVLGKAGVKVLYENANVGENLQDHTYSATVYNLKSGFKT----L    382
UmAAO      TVNTPQILELSGIGSKDVLSKAGVKVLYENANVGENLQDHTYSATVYKLKPGFPT----L    380
CcAAO      AFGTPQILLLSGIGPKTDLDVLGIPTVIHNPSVGQNLSDHVLLPNIFNVRGQDTL----D    347
PeAAO      SVGTPILLQLSGIGDENDLSSVGIDTIVNNPSVGRNLSDHLLLPAAFFVNSNQTF----D    356
PsAAO      SVGTPILLQLSGIGDQSDLSAVGIDTIVNNPSVGRNLSDHLLLPATFFVNNNQSF----D    356
           :. :* :*  ****    *   *:    .  .** *:.**      :

AOx        DFVRGDPEVQKKVFDEWNLK-GTGPLATNGIDAGV----------------KIRPTEK--    367
MtAAOx     SEMVNNATFKAEAITGFDEVPARGPYTLAGGNNAIFVSLPHLTADYGAITAKIRAMVADG    434
MaAAO      DSLRSDSTFAAEQLAAYKAN-QTSIFTETV-PSISYVSLARVVGAD---RA--KAMIN--    433
UmAAO      DSLRSNTTFAAEQAAAYKAN-QSSILTETV-PSISYVSLARVVGDK---RA--KAMIA--    431
CcAAO      QIIRGDPNVVPGVLDQWTTS-RSGP-----------------------------LAN--    374
PeAAO      NIFRDSSE-FNVDLDQWTNT-RTGP-----------------------------LTA--    382
PsAAO      NLFRDSSE-FNADLDQWTNT-RTGP-----------------------------LTA--    382
           . . ..          :      .
```

```
AOx        ELEEM---KKWPTPEFVDGWET-------YFKN------KPDKPVMHYSVIAGWFGDHML    411
MtAAOx     TAASYLAADVRTIPGMVAGYEAQ----LLVLADLLD---NPEAPSLET----PWAT----    479
MaAAO      EVTQYVQ-------SSRAPYKATLNKQLDFLNNYPD-----KVGQMELIGIDGYFAGTGA    481
UmAAO      EVAKYVG-------ASRAPYKATLKKQLDFLIQYPD-----KIGQMELIGIDGYFAGTGA    479
CcAAO      GVTNNLG-------FFRLPANSS------IFNSVSDPATGPTASHWEMIVINFYLNPFGP    421
PeAAO      LIANHLA-------WLRLPSNSS------IFQTFPDPAAGPNSAHWETIFSNQWFHPAI-    428
PsAAO      LIANHLA-------WLRLPSNSS------IFQSVPDPAAGPNSAHWETIFSNQWFHPAL-    428
              .                ::        :               .      :

AOx        --MPPGKFFTMFHFLEYPFSRGFTHVKSADPYGNPDFDAGFMNDKRDMAAMVWGYIKSRE    469
MtAAOx     --SEAPQTSSVLAFLLHPLSRGSVRLNLSDPLAQPVLDYRSGSNPVDIDLHLAHVRFLRG    537
MaAAO      PKPTE-TYFTILAANQHLFSRGNVHIQSSDPTKYPLIDPKYFSVPFDTELSTAGTAYTRK    540
UmAAO      PKPDE-TYFTILAANQHLFSRGNIHITSNDATKYPSIDAKYFDVPFDLEISTAGTNYTRK    538
CcAAO      PIPPAGTFMTLISALISPTSRGFVRLASADPFTAPIIDPKFLTTQFDIFALREAVRATKR    481
PeAAO      PRPDTGSFMSVTNALISPVARGDIKLATSNPFDKPLINPQYLSTEFDIFTMIQAVKSNLR    488
PsAAO      PRPDTGNFMSVTNALIAPVARGDIKLATSNPFDKPLINPQYLSTEFDIFTMIQAVKSNLR    488
                   ::        :**  ::   :    * ::        *

AOx        TARRMSSYAGEVTAMHPHFAYDSPARAFDLDLETTKAYAGPNHITAGIQHGSWSHPLEKG    529
MtAAOx     ------------------------------LLDTPTMQARG-------ALETAP-----    554
MaAAO      ------------------------------VGLSKAYSDMV-------VGEYWP-----    557
UmAAO      ------------------------------IGLGKTYSDMV-------DSEYWP-----    555
CcAAO      ------------------------------FVTASVWNDYV-------ISPWGG-----    498
PeAAO      ------------------------------FLSGQAWADFV-------IRPFDP-----    505
PsAAO      ------------------------------FLSGQAWADFV-------IRPFDA-----    505
                                            .    .

AOx        NPSLETHLNSHRQDTRNELQYSNEDIKHIEKWVQRHVE-TTWHSLGTCSMAPREGNSLTK    588
MtAAOx     ---------------GSAVA---DSDEALGEYVRSHSTLSFMHPCCTAAMLPEDR-----    591
MaAAO      ------------------------GNVDLQNYTKTTSV-TEYHPIGTASMLPRNQ-----    587
UmAAO      ------------------------GNVDIQEYTKTTSV-TEYHPIGTASMLPRKQ-----    585
CcAAO      ---------------LAQ-----TSDEGIDAYVRQQST-TVYHPVGTAAISPRGA-----    532
PeAAO      ---------------RLRDP---TDDAAIESYIRDNAN-TIFHPVGTASMSPRGA-----    541
PsAAO      ---------------RLSDP---TNDAAIESYIRDNAN-TIFHPVGTASMSPRGA-----    541
                                  .   :  : :     :  *   *.:: *.

AOx        HGGVVDERLNVHGVEGLKVCDLSICPDNVGCNTFSTALLIGEKCAMLVAEDLGYSGAALE    648
MtAAOx     -GGVVGPDLKVHGAEGLRVVDMSVMPLLPGAHLSATAYAVGEKAADIIIQEWMDKEQ---    647
MaAAO      -GGVVDPSLRVYGTTNLRVVDASIMPLHVAAHIQATIYGVAEYAASIIKSQA--------    638
UmAAO      -GGVVDPSLRVYGTSNLRVVDASIIPLHVAAHIQATIYGVAEYAAKIIKSQA--------    636
CcAAO      NYGVVDPDLKLKGAEGVRIADASVWPFLPNAHTQGPVYLLAERAADLILGRA--------    584
PeAAO      SWGVVDPDLKVKGVDGLRIVDGSILPFAPNAHTQGPIYLVGKQGADLIKADQ--------    593
PsAAO      SWGVVDPDLKVKGVDGLRIVDGSILPFAPNAHTQGPIYLVGERGADLIKADQ--------    593
             ***.  *.: *. .::: * *: *    .:  .    :.:  * ::

AOx        MKVPTYHAPGEFTGLARL    666
MtAAOx     ------------------    647
MaAAO      ------------------    638
UmAAO      ------------------    636
CcAAO      ------------------    584
PeAAO      ------------------    593
PsAAO      ------------------    593
```

Figure S3. Sequence alignment of *Ma*AAO and other AAOs. The catalytic histidines are highlighted in blue, the aromatic amino acid residues forming the substrate access channel are highlighted in brown. AOx from *A. terreus* (GenBank accession number AFP17823.1), *Mt*AAOx from *T. thermophilus* (GenBank accession number AEO55678.1), *Ma*AAO from *M. antarcticus* (NCBI reference sequence XP_014653549.1), *Um*AAO from *U. maydis* (GenBank accession number KIS68002.1), *Cc*AAO from

C. cinerea (GenBank accession number BBC20609.1), *Pe*AAO from *P. eryngii* (GenBank accession number AAC72747.1) and *Ps*AAO from *P. sapidus* (GenBank accession number AMW87253.1).

SUPPLEMENTAL REFERENCES

Jankowski N, Koschorreck K, Urlacher VB (2020) High-level expression of aryl-alcohol oxidase 2 from *Pleurotus eryngii* in *Pichia pastoris* for production of fragrances and bioactive precursors. Appl Microbiol Biotechnol 104(21):9205-9218. doi:10.1007/s00253-020-10878-4

Molina-Espeja P, Garcia-Ruiz E, Gonzalez-Perez D, Ullrich R, Hofrichter M, Alcalde M (2014) Directed evolution of unspecific peroxygenase from *Agrocybe aegerita*. Appl Environ Microbiol 80(11):3496-507. doi:10.1128/AEM.00490-14

2.4. Chapter IV: Protein engineering of *Pe*AAO to enable expression in *P. pastoris*

Title Two adjacent C-terminal mutations enable expression of aryl-alcohol oxidase from *Pleurotus eryngii* in *Pichia pastoris*

Authors Nina Jankowski, Vlada B. Urlacher, Katja Koschorreck

Contribution Design and planning of all experiments, conducting most of the experiments, evaluation of all data, drafting the manuscript. Relative contribution: 90 %

Published in *Applied Microbiology and Biotechnology,* 105, 7743–7755 (**2021**)

DOI 10.1007/s00253-021-11585-4

Publisher Springer Nature

Applied Microbiology and Biotechnology (2021) 105:7743–7755
https://doi.org/10.1007/s00253-021-11585-4

BIOTECHNOLOGICALLY RELEVANT ENZYMES AND PROTEINS

Two adjacent C-terminal mutations enable expression of aryl-alcohol oxidase from *Pleurotus eryngii* in *Pichia pastoris*

Nina Jankowski[1] · Vlada B. Urlacher[1] · Katja Koschorreck[1]

Received: 9 July 2021 / Revised: 23 August 2021 / Accepted: 26 August 2021 / Published online: 21 September 2021

Abstract
Fungal aryl-alcohol oxidases (AAOs) are attractive biocatalysts because they selectively oxidize a broad range of aromatic and aliphatic allylic primary alcohols while yielding hydrogen peroxide as the only by-product. However, their use is hampered by challenging and often unsuccessful heterologous expression. Production of *Pe*AAO1 from *Pleurotus eryngii* ATCC 90787 in *Pichia pastoris* failed, while *Pe*AAO2 from *P. eryngii* P34 with an amino acid identity of 99% was expressed at high yields. By successively introducing mutations in *Pe*AAO1 to mimic the sequence of *Pe*AAO2, the double mutant *Pe*AAO1 ER with mutations K583E and Q584R was constructed, that was successfully expressed in *P. pastoris*. Functional expression was enhanced up to 155 U/l via further replacements D361N (variant NER) or V367A (variant AER). Fed-batch cultivation of recombinant *P. pastoris* yielded up to 116 mg/l of active variants. Glycosylated *Pe*AAO1 variants demonstrated high stability and catalytic efficiencies similar to *Pe*AAO2. Interestingly, *P. pastoris* expressing *Pe*AAO1 variant ER contained roughly 13 gene copies but showed similar volumetric activity as NER and AER with one to two gene copies and four times lower mRNA levels. Additional H-bonds and salt bridges introduced by mutations K583E and Q584R might facilitate heterologous expression by enhanced protein folding.

Key points
- *PeAAO1 not expressed in P. pastoris and PeAAO2 well-expressed in Pichia differ at 7 positions.*
- *Expression of PeAAO1 in P. pastoris achieved through mutagenesis based on PeAAO2 sequence.*
- *Combination of K583E and Q584R is essential for expression of PeAAO1 in P. pastoris.*

Keywords *Pichia pastoris* (*Komagataella phaffii*) · Aryl-alcohol oxidase · *Pleurotus eryngii* · Site-directed mutagenesis · Salt bridges · Gene copy number

Introduction

Flavin-dependent oxidases build a diverse group of enzymes that have been successfully used in biocatalysis and biosensors (Dijkman et al. 2013). An important prerequisite for the application of these enzymes is their availability at high quantities. In this regard, heterologous expression in microbial hosts has been recognized as the most efficient approach which on the one hand, opens the way to high-scale processes and, on the other hand, when combined with protein engineering enables production and screening of mutants or mutant libraries to "tailor" the optimal biocatalyst for a specific purpose (Li and Cirino 2014). Aryl-alcohol oxidases (AAOs, EC 1.1.3.7) belong to flavin-dependent oxidases (Serrano et al. 2020). They contain a non-covalently bound FAD and catalyze the oxidation of primary aromatic and aliphatic allylic alcohols to the corresponding aldehydes, and if the *gem*-diol is formed, also to the corresponding acids (Ferreira et al. 2010; Guillén et al. 1992). AAOs are predominantly produced in wood-decaying fungi and secreted as glycoproteins. For their reactions, AAOs require only molecular oxygen and release hydrogen peroxide as the by-product (Guillén et al. 1992). Various studies have demonstrated the potential of AAOs for biotechnology (Urlacher and Koschorreck 2021). The most studied representative of this group is the AAO from *Pleurotus eryngii* ATCC 90787 (further designated as *Pe*AAO1), that among others

✉ Katja Koschorreck
Katja.Koschorreck@hhu.de

[1] Institute of Biochemistry, Heinrich-Heine-University Düsseldorf, Universitätsstraße 1, 40225 Düsseldorf, Germany

was applied for the production of the flavor and fragrance compound *trans*-2-hexenal (de Almeida et al. 2019; van Schie et al. 2018). This enzyme was also used for the conversion of 5-hydroxymethylfurfural to 2,5-furandicarboxylic acid as precursor for bioplastics in multi-enzyme cascades (Carro et al. 2014; Serrano et al. 2019a). Furthermore, *Pe*AAO1 was engineered to oxidize secondary alcohols to facilitate kinetic deracemization (Serrano et al. 2019b; Viña-Gonzalez et al. 2019). *Pe*AAO1 has served as a model enzyme for numerous investigations providing insights into substrate spectrum, structural, and mechanistic properties of AAOs (Carro et al. 2017, 2018; Fernández et al. 2009; Ferreira et al. 2009, 2010; Guillén et al. 1992; Hernández-Ortega et al. 2012a, 2012b). However, heterologous expression of *Pe*AAO1 and AAOs in general is quite challenging and often unsuccessful or leads to only low amounts of active enzyme (Urlacher and Koschorreck 2021). For example, heterologous expression of *Pe*AAO1 in *Aspergillus nidulans* yielded 3 mg/l of active enzyme, while expression in *Escherichia coli* led to the formation of inclusion bodies and required time-consuming refolding of *Pe*AAO1 which was less stable than the native enzyme due to the lack of glycosylation (Ferreira et al. 2005; Ruiz-Dueñas et al. 2006). Aiming at enhanced expression in *Saccharomyces cerevisiae* and *Pichia pastoris*, *Pe*AAO1 was subjected to protein engineering using in vivo DNA shuffling and the mutagenic organized recombination process by homologous in vivo grouping (MORPHING) (Viña-Gonzalez et al. 2015, 2018). As result, two *Pe*AAO1 variants, FX7 and FX9, were constructed and expressed at concentrations of up to 25 mg/l. A recent review summarized different approaches of directed evolution to unlock *Pe*AAO1's full potential for biotechnological purposes aiming at enhanced expression or acceptance of new substrates (Viña-Gonzalez and Alcalde 2020).

Recently, we cloned an aryl-alcohol oxidase *Pe*AAO2 from *P. eryngii* P34 in *P. pastoris* and produced it in a fed-batch process at a concentration of 315 mg/l (Jankowski et al. 2020). Interestingly, the protein sequences of *Pe*AAO2 and *Pe*AAO1 differ only in seven amino acid residues. Our efforts to actively express *Pe*AAO1 in *P. pastoris* failed and an explanation why the highly similar *Pe*AAO2 was expressed at high yields remained elusive. Here, we investigate the effect of the seven different amino acid residues on expression of *Pe*AAO1 in *P. pastoris*. A set of single, double and triple mutants of *Pe*AAO1 were generated and their expression levels were examined. The most active variants were produced in a fed-batch process, purified, and characterized. Homology models of the active variants were created in order to rationalize the effect of the mutations based on the structural changes. The gene copy numbers and mRNA levels of recombinant *P. pastoris* expressing *Pe*AAO1 variants were investigated by real-time PCR to determine the effects of these parameters on enzyme expression.

Materials and methods

Chemicals

All chemicals were of analytical grade or higher and purchased from Acros Organics (Geel, Belgium), AppliChem GmbH (Darmstadt, Germany), BD (Heidelberg, Germany), Carl Roth GmbH + Co. KG (Karlsruhe, Germany), J&K Scientific (Lommel, Belgium), and Sigma-Aldrich (Schnelldorf, Germany).

Strains and plasmids

For all cloning procedures, chemically competent *Escherichia coli* DH5α cells were used (Clontech Laboratories Inc., Heidelberg, Germany). The expression of the *Pe*AAO1 variants was carried out using *P. pastoris* X-33 (recently reclassified as *Komagataella phaffii*) cells transformed with pPICZA-based plasmids containing the methanol inducible *AOX1*-promoter (Invitrogen, Carlsbad, USA).

Site-directed mutagenesis

The gene *peaao1* encoding for *P. eryngii* ATCC 90787 aryl-alcohol oxidase 1 (GenBank accession number AF064069) was synthesized and cloned into pPICZA vector by BioCat GmbH (Heidelberg, Germany) in a codon optimized version (GenBank accession number MZ246833) for expression in yeast (JCat online tool) (Grote et al. 2005). The resulting plasmid pPICZA_*Pe*AAO1 was used as template for site-directed mutagenesis using the QuikChange protocol with the primers listed in Supplemental Table S1. First, seven single mutants, R152G, T265I, D361N, V367A, D512N, K583E, and Q584R, were generated according to the following procedure. One nanogram of pPICZA_*Pe*AAO1 was mixed with 500 nM each forward and reverse primer, 200 µM of each dNTP, 1 × high-fidelity buffer, 3% dimethyl sulfoxide (DMSO), and 0.02 U/µl Phusion High-Fidelity DNA-polymerase (Thermo Fisher Scientific, Bremen, Germany) in a total volume of 50 µl. Using a thermocycler, following cycling protocol was used: initial denaturation at 98 °C for 30 s, 16 times cycling of denaturation at 98 °C for 10 s, annealing for 30 s, extension at 72 °C for 75 s, followed by a final extension at 72 °C for 10 min, and a hold at 10 °C. The annealing temperature for each primer pair was calculated using the T_m calculator of Thermo Fisher Scientific.

To remove the parental plasmid, the reaction mixture was digested with FastDigest *Dpn*I (Thermo Fisher Scientific). Chemically competent *E. coli* DH5α cells were transformed

with the digested sample and plated on selective LB agar plates (1% peptone, 0.5% yeast extract, 0.5% NaCl, 1.5% agar) containing 25 µg/ml Zeocin™ (InvivoGen, San Diego, USA). Up to five randomly selected colonies were used to inoculate 5 ml of LB medium with 25 µg/ml Zeocin™ and incubated overnight (37 °C, 180 rpm). Plasmid isolation was carried out using the ZR Plasmid Miniprep Kit (Zymo Research, Freiburg, Germany) following the manufacturer's instructions. Introduction of mutations was verified through DNA sequencing by Eurofins Genomics Germany GmbH (Ebersberg, Germany). Once all seven single mutants were generated and evaluated regarding enzyme activity (see below), pPICZA_*Pe*AAO1_K583E was used as plasmid template to generate six double mutants (R152G/K583E, T265I/K583E, D361N/K583E, V367A/K583E, D512N/K583E, and K583E/Q584R) as described above. Finally, single mutations D361N and V367A were introduced in the double mutant K583E/Q584R (variant ER) using pPICZA_*Pe*AAO1_K583E/Q584R as template to construct the two triple mutants D361N/K583E/Q584R (variant NER) and V367A/K583E/Q584R (variant AER), respectively.

All generated pPICZA-based plasmids were linearized in the 5'*AOX1* region employing the FastDigest *Mss*I enzyme (Thermo Fisher Scientific). Electrocompetent *P. pastoris* X-33 cells were transformed with the linearized plasmids, plated on YPDS agar plates (1% yeast extract, 2% peptone, 2% dextrose, 1 M sorbitol, 2% agar) containing 100 µg/ml Zeocin™ and incubated at 30 °C until the formation of colonies.

Enzyme production and purification

A number of *P. pastoris* transformants expressing either the mutants K583E/Q584R (variant ER), D361N/K583E/Q584R (variant NER) or V367A/K583E/Q584R (variant AER) were cultivated in 10 ml BMGY medium (1% yeast extract, 2% peptone, 100 mM potassium phosphate buffer pH 6, 1.34% yeast nitrogen base without amino acids, 4×10^{-5}% biotin, 1% glycerol) in 100-ml shaking flasks overnight (30 °C, 200 rpm) and used to inoculate 10 ml of the expression medium BMMY (1% yeast extract, 2% peptone, 100 mM potassium phosphate buffer pH 6, 1.34% yeast nitrogen base without amino acids, 4×10^{-5}% biotin and 0.5% (v/v) methanol) to an OD_{600} of 1. The expression was carried out for up to 48 h (25 °C, 200 rpm) and methanol was added every 24 h at 0.5% (v/v). OD_{600} value and volumetric activity were monitored daily and used to identify the best performing recombinant *Pichia* transformants.

Fed-batch cultivation of the selected *P. pastoris* transformants expressing ER, NER, and AER with glycerol as carbon source during the batch phase and 0.5% (v/v) methanol with 12 g/l *Pichia* trace metals (PTM_1) solution during the fed-batch phase were carried out as described previously (Jankowski et al. 2020). Daily sampling was done to monitor cell growth, extracellular protein concentration, and volumetric activity. After 8 or 9 days of cultivation, the cells were harvested via centrifugation (11,325 × *g*, 15 min, 4 °C). The cell-free supernatant was concentrated and rebuffered using tangential flow filtration (TFF) and subsequently purified via three chromatographic steps, as described before for *Pe*AAO2 (Jankowski et al. 2020). In short, 5 ml of the first eluate from TFF was applied to a hydrophobic interaction chromatography column (Butyl Sepharose HP, GE Healthcare, Freiburg, Germany) and eluted with decreasing ammonium sulfate concentration. Active fractions were pooled, desalted, and loaded onto an anion exchange chromatography column (DEAE Sepharose FF, GE Healthcare) and eluted with increasing sodium chloride concentration. Again, active fractions were pooled and finally loaded onto a size exclusion chromatography column (Superdex 200 Increase 10/300 GL, GE Healthcare). The most active and purest fractions were concentrated, desalted, and stored at 4 °C until use. The production and chromatographic purification of *Pe*AAO2 were carried out as described before (Jankowski et al. 2020).

Enzyme activity assay

The standard assay to assess AAO activity in the culture supernatant or of purified enzyme was carried out with veratryl alcohol as substrate at room temperature. 5 mM of veratryl alcohol was mixed with 100 mM sodium phosphate buffer pH 6, and the reaction was initiated with culture supernatant or an appropriate dilution of AAO containing sample in a 1-ml cuvette. The change of absorbance at 310 nm as a result of veratraldehyde formation $\left(\varepsilon_{310} = 9,300\ M^{-1}cm^{-1}\right)$ (Guillén et al. 1992) was followed using an Ultrospec 7000 photometer (GE Healthcare). Initial reaction rates were calculated according to Lambert–Beer law. Under the stated conditions, one unit of activity is defined as the amount of enzyme that converts 1 µmol substrate per minute.

Protein quantification and *N*-deglycosylation

To determine protein concentrations at different steps of enzyme purification, the Bradford method was used employing bovine serum albumin as standard protein (Bradford 1976). The measurements were carried out at room temperature in 96-well micro titer plates using an Infinite M200 Pro plate reader (Tecan, Männedorf, Switzerland). The molar extinction coefficients of purified *Pe*AAO1 variants were calculated after heat denaturation of the samples and detection of released FAD as described for *Pe*AAO2 wild-type (Jankowski et al. 2020) and used for determination of molar enzyme concentrations. Latter ones were used to calculate enzyme concentration in

fermentation supernatant, specific activities of purified enzymes, and kinetic constants.

N-Deglycosylation was performed using 20 µg of purified enzymes and peptide-*N*-amidase PNGase F (New England Biolabs, Frankfurt am Main, Germany) under denaturing conditions. For this, the samples were boiled at 100 °C for 10 min in the presence of SDS prior to deglycosylation with PNGase F. An aliquot of the deglycosylated samples as well as of the purified enzymes (each 5 µg) were loaded onto a 12.5% resolving gel and SDS-PAGE was conducted according to the protocol of Laemmli (1970).

pH activity, stability, and melting temperature

The activity of *Pe*AAO1 variants ER, NER, and AER and *Pe*AAO2 wild-type towards the substrates *p*-anisyl alcohol and veratryl alcohol was determined in 100 mM Britton-Robinson buffer (consisting of 100 mM each boric acid, phosphoric acid, acetic acid) at different pH values ranging from pH 2 to 10 at room temperature. To determine the pH stability, the enzymes were incubated for up to 24 h in 100 mM Britton-Robinson buffer at pH 2 to 10 at room temperature. After certain time points, samples were taken and the relative activity towards veratryl alcohol was determined as described in the standard assay.

The melting temperature (T_M) of the *Pe*AAO1 variants ER, NER, and AER was determined by the *Thermo*FAD assay (Forneris et al. 2009). The temperature at which 50% of the enzymatic activity is retained (T_{50}) was determined for the *Pe*AAO1 variants as previously described (Jankowski et al. 2020).

Specific activities

The activity of purified *Pe*AAO1 variants ER, NER, and AER as well as of *Pe*AAO2 was determined towards several AAO substrates at a final concentration of 5 mM in 100 mM sodium phosphate buffer pH 6 at room temperature. The assay was performed in 96-well UV-Star® micro titer plates (Greiner Bio-One GmbH, Frickenhausen, Germany). The conversion of the selected alcohols to their corresponding aldehydes was followed spectrophotometrically using the Infinite M200 Pro plate reader (Tecan): $p-$anisyl alcohol $\left(\varepsilon_{285} = 16,980\ \mathrm{M^{-1}cm^{-1}}\right)$ (Guillén et al. 1992), benzyl alcohol $\left(\varepsilon_{250} = 13,800\ \mathrm{M^{-1}cm^{-1}}\right)$ (Guillén et al. 1992), piperonyl alcohol $\left(\varepsilon_{317} = 8,680\ \mathrm{M^{-1}cm^{-1}}\right)$ (Jankowski et al. 2020), veratryl alcohol $\left(\varepsilon_{310} = 9,300\ \mathrm{M^{-1}cm^{-1}}\right)$ (Guillén et al. 1992), and *trans,trans*-2,4-hexadienol $\left(\varepsilon_{280} = 30,140\ \mathrm{M^{-1}cm^{-1}}\right)$ (Ruiz-Dueñas et al. 2006).

Determination of kinetic parameters

The kinetic parameters of the oxidation of *p*-anisyl alcohol (0.98 to 1,000 µM) and veratryl alcohol (9.8 to 10,000 µM) with the purified *Pe*AAO1 variants ER, NER, and AER were determined in 96-well UV-Star® micro titer plates at 25 °C using an Infinite M200 Pro plate reader (Tecan). An appropriate stock solution of purified enzyme was mixed with 100 mM sodium phosphate buffer pH 6 and substrate stocks with varying concentrations. Using the program OriginPro 2019 (OriginLab Corporation, Northampton, MA, USA), a non-linear fit according to the Michaelis–Menten equation was calculated and the parameters V_{max} and K_M were extracted and used for calculation of k_{cat} and k_{cat}/K_M values.

Real-time PCR to determine gene copy numbers and mRNA levels

For extraction of genomic DNA (gDNA) in order to determine the gene copy numbers, precultures of recombinant *P. pastoris* transformants expressing different *Pe*AAO1 variants were cultivated in 10 ml BMGY medium overnight (30 °C, 200 rpm). The gDNA was extracted using the *Quick*-DNA Fungal/Bacterial Miniprep Kit (Zymo Research, Freiburg, Germany) according to the manufacturer's protocol and eluted in 50 µl of ultra-pure water. The precultures were used to inoculate 10 ml of BMM medium (100 mM potassium phosphate buffer pH 6, 1.34% yeast nitrogen base without amino acids, 4×10^{-5}% biotin, and 0.5% (v/v) methanol) to an OD_{600} of 1, and cultures were incubated for 48 h (25 °C, 200 rpm). Samples diluted to an OD_{600} of 1 were used for total RNA extraction using the RNeasy Mini Kit (Qiagen, Hilden, Germany) according to the manufacturer's protocol. On-column digestion of residual DNA with RNase-free DNase set (Qiagen) during purification was implemented. gDNA and RNA concentrations were measured spectrophotometrically using the NanoQuant™ Plate with the Infinite M200 Pro plate reader (Tecan) by determining the 260 nm absorbance and 260/280 nm ratio. One hundred nanograms of total RNA was used for cDNA synthesis using SuperScript™ III Reverse Transcriptase (Invitrogen) with 2.5 µM Oligo$(dT)_{18}$ primers (Thermo Fisher Scientific) as described in the manufacturer's protocol. The resulting cDNA was diluted 1:4 with ultra-pure water.

Real-time-PCR reactions were set up with innuMIX qPCR DSGreen Standard Mix (AnalytikJena, Jena, Germany) according to the manufacturer's protocol and conducted on real-time PCR cycler qTOWER^3 *touch* (AnalytikJena). Either 2 ng of gDNA or 2 µl of diluted cDNA sample was used in triplicate. The cycling protocol was as followed: initial denaturation at 95 °C for 120 s, followed by 40 cycles of denaturation at 95 °C for 30 s, and combined annealing and detection at 60 °C for 45 s. A melting curve

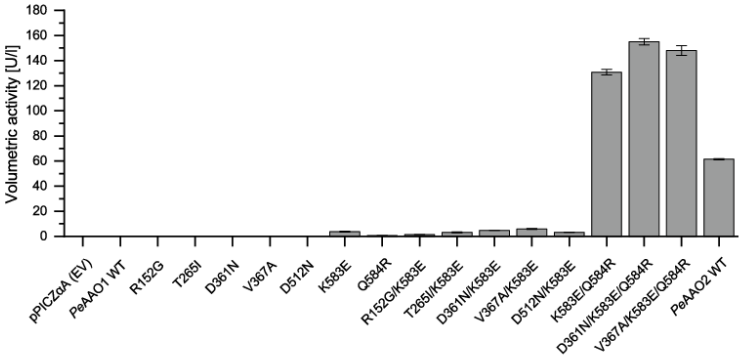

Fig. 1 Volumetric activities [U/l] of *Pe*AAO2 wild-type and *Pe*AAO1 variants in the supernatant of small-scale expressions of recombinant *P. pastoris* towards veratryl alcohol (5 mM). Empty vector pPICZαA (EV) was used as negative control. Activities were measured after 48 h of cultivation in BMMY medium (25 °C and 200 rpm) with 0.5% (v/v) methanol added daily

analysis was included after the PCR run from 60 to 95 °C in 0.5 °C increments.

For amplification of target *peaao* genes, specific primers 1qPCR_fw (5'-3': TCCAGTTGCTAGAGGTGACATC) and 1qPCR_rev (5'-3': TGGGTCGAATGGTCTGATAACG) were used, while actin was used as reference gene with primers Actin_fw (5'-3': GGTATTGCTGAGCGTATGCAAA) and Actin_rev (5'-3': CCACCGATCCATACGGAGTACT). Optimal primer concentrations were determined by titrating forward and reverse primers at 100 to 300 nM each, and combinations yielding no amplification in the no-template control were used. Primer efficiencies for both pairs at optimal concentrations were calculated using dilution series of gDNA. The results of gene copy number and mRNA level determination were analyzed using the software qPCRsoft 4.1 (AnalytikJena) employing the primer efficiency corrected Pfaffl method and actin as reference gene (Pfaffl 2001).

Homology modelling

The crystal structure of *Pe*AAO1 wild-type (PDB entry 3FIM) (Fernández et al. 2009) was used as template to generate homology models of *Pe*AAO1 variants ER, NER, and AER using the online tool SWISS-MODELL (Waterhouse et al. 2018) and the program PyMOL for visualization.

Results

Effect of mutations on *Pe*AAO1 expression

To study the effect of the seven amino acid residues which differ in the highly expressed *Pe*AAO2 and *Pe*AAO1, not expressed in *P. pastoris*, at first, seven single mutants of *Pe*AAO1 with the substitutions R152G, T265I, D361N, V367A, D512N, K583E, and Q584R were created. The corresponding *P. pastoris* transformants were screened for AAO activity after expression in BMMY medium in shaking flasks. Both AAOs, *Pe*AAO1, and *Pe*AAO2 have been reported to catalyze the oxidation of veratryl alcohol to veratraldehyde (Guillén et al. 1992; Jankowski et al. 2020). Thus, conversion of veratryl alcohol by samples taken from the supernatant after expression and cell centrifugation was used for expression verification. Out of the seven single mutants, activity was only detectable for the K583E variant and reached 3.7 U/l (Fig. 1).

Despite the low volumetric activity of *Pe*AAO1 variant K583E compared to *Pe*AAO2 wild-type with 61 U/l, the successful expression of this variant in *P. pastoris* was a good starting point for further mutagenesis. In the next step, six *Pe*AAO1 double mutants were created by introducing mutations R152G, T265I, D361N, V367A, D512N, and Q584R, respectively, into the *Pe*AAO1 variant K583E and screened for improved volumetric activity towards veratryl alcohol. Remarkably, the double mutant K583E/Q584R reached a volumetric activity of up to 131 U/l (Fig. 1), which is roughly 35 times higher than that of the variant K583E and even surpasses the volumetric activity of *Pe*AAO2 wild-type by factor 2. The double mutants D361N/K583E and

V367A/K583E showed slightly increased activities (up to 4.7 U/l and 5.9 U/l, respectively) compared to the starting variant K583E (3.7 U/l), indicating a beneficial effect of the mutations D361N and V367A on expression and/or enzyme activity. Mutations D361N and V367A, respectively, were introduced into the best double mutant K583E/Q584R yielding two triple mutants. An alignment of *Pe*AAO1 and *Pe*AAO2 wild-type and of *Pe*AAO1 variants is given in Supplemental Fig. S1. After expression in *P. pastoris*, a volumetric activity of up to 155 U/l for the variant *Pe*AAO1 D361N/K583E/Q584R was achieved (Fig. 1), which is 1.2-fold higher than the parental double mutant K583E/Q584R and 2.5-fold higher than *Pe*AAO2 wild-type. The *Pe*AAO1 mutant V367A/K583E/Q584R was expressed in *P. pastoris* leading to a similar volumetric activity of 148 U/l. The *Pe*AAO1 variants K583E/Q584R (ER), D361N/K583E/Q584R (NER), and V367A/K583E/Q584R (AER) were selected for production at a larger scale and characterization.

Production in a bioreactor and purification of active *Pe*AAO1 variants

The fed-batch cultivation of recombinant *P. pastoris* to produce *Pe*AAO1 variants ER, NER, and AER was conducted for 8 to 9 days. *Pe*AAO1 variant ER was produced at a volumetric activity of 4898 U/l after 160 h (Table 1). At around the same time, NER reached 5263 U/l and AER yielded 5734 U/l. All enzymes were purified to homogeneity following the established three-step purification protocol (see the experimental section). Purified *Pe*AAO1 NER exhibited the highest specific activity towards veratryl alcohol with 48.4 U/mg, followed by AER with 45.6 U/mg. *Pe*AAO1 ER showed a slightly lower specific activity with 42.4 U/mg

Table 1 Activity and enzyme production during fed-batch cultivation and properties of the purified *Pe*AAO1 variants and *Pe*AAO2 wild-type

Enzyme	*Pe*AAO1 ER	*Pe*AAO1 NER	*Pe*AAO1 AER	*Pe*AAO2 WT
Volumetric activity after ~ 160 h [U/l][a]	4898 (160 h)	5263 (159 h)	5734 (160 h)	5229 (167 h)
Enzyme concentration [mg/l][b]	116 (160 h)	113 (183 h)	98 (179 h)	169 (214 h)
Specific activity [U/mg][c]	42.4	48.4	45.6	43.0
Absorbance maxima [nm]	463, 383	463, 383	463, 383	463, 376 [d]
ε_{463} extinction coefficient [M^{-1} cm^{-1}]	8687	8608	8432	7029 [d]

[a]For comparison, volumetric activities after roughly 160 h (time of harvest for *Pe*AAO1 ER) are shown. Enzymatic activity was determined with 5 mM veratryl alcohol in 100 mM sodium phosphate buffer pH 6

[b]Enzyme concentration calculated based on molar protein concentration of purified enzyme. Time of harvest is given in parenthesis

[c]Specific activity of purified enzyme towards veratryl alcohol based on molar protein concentrations

[d]Values from (Jankowski et al. 2020)

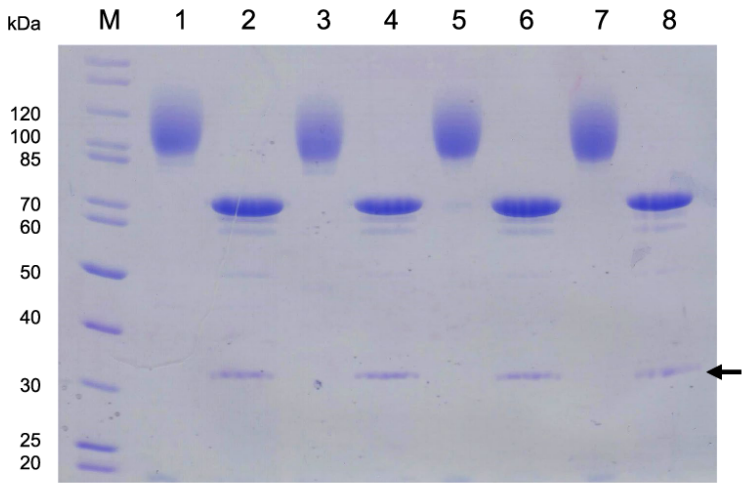

Fig. 2 SDS-PAGE analysis of purified and *N*-deglycosylated *Pe*AAO2 wild-type and *Pe*AAO1 variants. M, PageRuler™ marker; 1, native *Pe*AAO2; 2, deglycosylated *Pe*AAO2; 3, native *Pe*AAO1 ER; 4, deglycosylated *Pe*AAO1 ER; 5, native *Pe*AAO1 NER; 6, deglycosylated *Pe*AAO1 NER; 7, native *Pe*AAO1 AER; 8, deglycosylated *Pe*AAO1 AER. Arrow indicates PNGase F (36 kDa). 5 µg of each sample was loaded and the gel was stained with Coomassie Brilliant Blue R250

similar to *Pe*AAO2 wild-type with 43 U/mg. Molar protein concentrations calculated after purification revealed that the *Pe*AAO1 variant ER was produced at a level of 116 mg/l, followed by 113 mg/l for NER and 98 mg/l for AER.

To elucidate the reasons for different expression yields of the *Pe*AAO1 variants, their properties were investigated. All *Pe*AAO1 mutants exhibited absorption spectra typical for flavoproteins with two absorbance maxima at 463 nm and 383 nm. The molar extinction coefficients were calculated based on absorbance of the released FAD after heat precipitation of the apoprotein and ranged between 8400 and 8700 M^{-1} cm^{-1} (Table 1).

Purified *Pe*AAO2 wild-type and *Pe*AAO1 variants exhibited similar apparent molecular masses of around 100 kDa according to SDS-PAGE (lanes 1, 3, 5, and 7 in Fig. 2), while the theoretical molecular weight (without the predicted signal peptide) was 61 kDa for *Pe*AAO2 and *Pe*AAO1 variants. After *N*-deglycosylation sharp bands at 70 kDa appeared for all enzymes (lanes 2, 4, 6, and 8 in Fig. 2), indicating 30% of *N*-glycosylation of recombinantly produced *Pe*AAO1 variants and *Pe*AAO2 wild-type.

pH activity and stability

Regarding pH optimum, activity of *Pe*AAO2 wild-type and *Pe*AAO1 variants towards *p*-anisyl alcohol and veratryl alcohol was highest at slightly acidic pH values. The highest activity towards *p*-anisyl alcohol was at pH 5 for *Pe*AAO2 wild-type and *Pe*AAO1 NER, while pH 6 was best for *Pe*AAO1 ER and AER (Supplemental Fig. S2a). *Pe*AAO2 wild-type and all *Pe*AAO1 variants showed the highest activity at pH 6 with veratryl alcohol (Supplemental Fig. S2b).

Table 2 Melting temperature (T_M) and TT_{50} value of *Pe*AAO1 variants and *Pe*AAO2 wild-type

Enzyme	*Pe*AAO1 ER	*Pe*AAO1 NER	*Pe*AAO1 AER	*Pe*AAO2 WT [a]
T_M [°C]	65.5	65.0	64.5	65.5
T_{50} [°C]	61.5	61.6	61.7	62.1

[a]Values from (Jankowski et al. 2020)

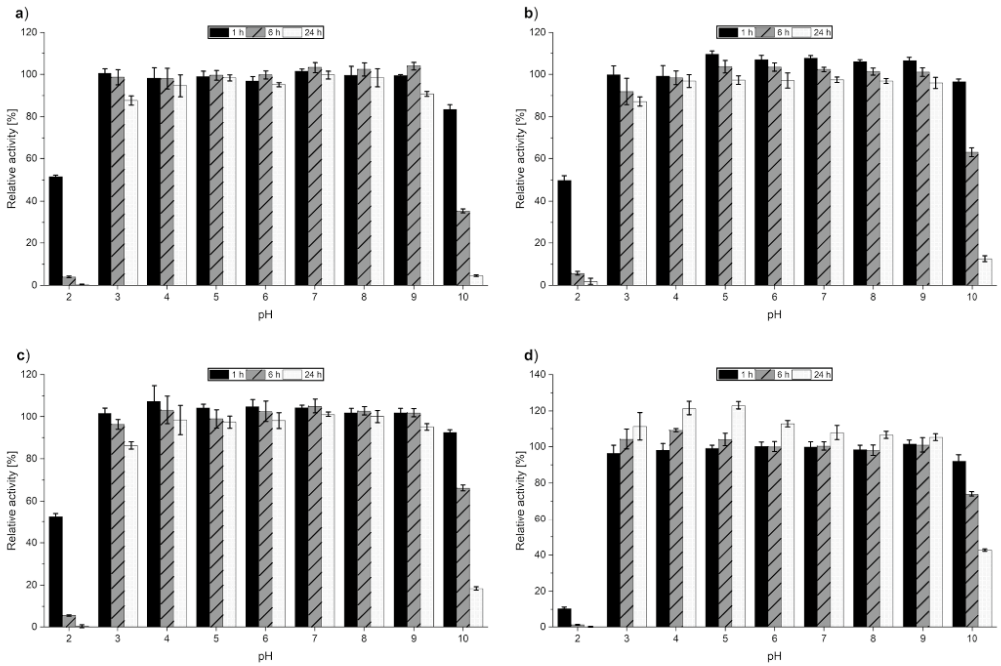

Fig. 3 pH stability profile of *Pe*AAO1 variants **a** ER, **b** NER, **c** AER, and **d** *Pe*AAO2 wild-type after incubation in 100 mM Britton-Robinson buffer pH 2 to 10 for up to 24 h. After 1 h: black, filled; after 6 h: gray, striped; after 24 h: white, dotted. Initial activity without incubation was set to 100%

High pH stability was found for all three *Pe*AAO1 variants ER, NER and AER with relative activities of over 85% after 24 h of incubation at pH ranging from 3 to 9 (Fig. 3a, b, and c). After 24 h incubation at pH 10, activities dropped, and completely vanished after incubation at pH 2. *Pe*AAO2 wild-type showed up to 130% increased relative activities after 24 h incubation between pH 3 and 6 (Fig. 3d). Incubation at pH 2 for 1 h seemed to have a more adverse effect on *Pe*AAO2 wild-type as on the *Pe*AAO1 variants, while *Pe*AAO2 wild-type remained more active after incubation at pH 10 with 40% relative activity as compared to the *Pe*AAO1 variants.

Thermal stability

The melting temperature T_M was determined by measuring the FAD fluorescence during unfolding of the proteins at increasing temperatures. The T_M values for all *Pe*AAO1 variants as well as for *Pe*AAO2 wild-type were at around 65 °C (Table 2), while the T_{50} value at which half of the enzymatic activity lost after 10 min incubation was roughly 3 to 4 °C lower for all enzymes at around 61.5 °C.

Specific activities and kinetic parameters

Next, the specific activity of *Pe*AAO1 variants towards *p*-anisyl alcohol, benzyl alcohol, *trans*,*trans*-2,4-hexadienol, piperonyl alcohol, and veratryl alcohol was determined. In general, specific activities of the *Pe*AAO1 variants and *Pe*AAO2 wild-type were in the same range when using the same substrate (Supplemental Fig. S3). The highest specific activity was reached with *trans*,*trans*-2,4-hexadienol of up to 89 U/mg for AER, followed by *p*-anisyl alcohol with up to 67 U/mg (NER). The lowest specific activities of 13 U/mg or below were observed during the oxidation of benzyl alcohol.

Kinetic measurements for the oxidation of *p*-anisyl alcohol and veratryl alcohol catalyzed by *Pe*AAO1 variants were conducted at pH 6. The *Pe*AAO1 variant NER showed the highest k_{cat} values with 87.9 s^{-1} and 68.2 s^{-1} for *p*-anisyl alcohol and veratryl alcohol, respectively, and also reached the highest catalytic efficiencies with 1975 mM^{-1} s^{-1} and 124.7 mM^{-1} s^{-1}, respectively, among the three *Pe*AAO1 variants (Table 3). The K_M values for *p*-anisyl alcohol for the *Pe*AAO1 variants were in the range from 39.2 µM for ER to 48.8 µM for AER. The K_M values for veratryl alcohol were roughly 10 times higher than for *p*-anisyl alcohol and ranged from 541.9 µM for AER to 549.0 µM for ER. *Pe*AAO2 wild-type showed the lowest K_M values with 24.3 µM and 446.6 µM for *p*-anisyl alcohol and veratryl alcohol, respectively, and in case of *p*-anisyl alcohol also the highest overall catalytic efficiency with 2436 mM^{-1} s^{-1}.

Table 3 Kinetic parameters of *Pe*AAO1 variants and *Pe*AAO2 wild-type towards the substrates *p*-anisyl alcohol and veratryl alcohol in 100 mM sodium phosphate buffer pH 6 at 25 °C

Substrate	Enzyme	K_M [µM]	k_{cat} [s^{-1}]	k_{cat}/K_M [mM^{-1} s^{-1}]
p-Anisyl alcohol	*Pe*AAO1 ER	39.2 ± 1.9	73.8 ± 0.03	1883
	*Pe*AAO1 NER	44.5 ± 1.5	87.9 ± 0.06	1975
	*Pe*AAO1 AER	48.8 ± 1.5	78.2 ± 0.05	1602
	*Pe*AAO2 WT [a]	24.3	59.2	2436
Veratryl alcohol	*Pe*AAO1 ER	549.0 ± 12.6	54.9 ± 0.02	100.0
	*Pe*AAO1 NER	546.7 ± 5.8	68.2 ± 0.05	124.7
	*Pe*AAO1 AER	541.9 ± 6.4	58.5 ± 0.03	108.0
	*Pe*AAO2 WT [a]	446.6	47.2	105.7

[a] Values from (Jankowski et al. 2020)

Gene copy number and mRNA levels

Gene copy number and mRNA level of the target *peaao* genes of the most active *P. pastoris* transformant each expressing *Pe*AAO1 wild-type, *Pe*AAO1 variants K583E, Q584R, K583E/Q584R (ER), D361N/K583E (NE), V367A/K583E (AE), NER, AER, and *Pe*AAO2 wild-type, respectively, were determined (Fig. 4). The number of integrated genes varied between one for *Pe*AAO1 wild-type and roughly 14 for *Pe*AAO2 wild-type. The mRNA level increased with increasing gene copy number. However, although the volumetric activity was highest for *Pe*AAO1 variants NER and AER with 56 and 52 U/l, respectively, the detected gene copy numbers and mRNA levels were roughly between one and two and thus among the lowest detected values. Interestingly, the *P. pastoris* transformant expressing *Pe*AAO1 variant ER contained roughly 13 gene copies but showed a similar volumetric activity of 45 U/l as NER and AER with one to two gene copies and 3–4 times lower mRNA levels.

Discussion

The sequence of *Pe*AAO2 was mimicked by mutating *Pe*AAO1 in a successive manner. Out of seven single *Pe*AAO1 mutants, only the mutation K583E led to measurable activity towards veratryl alcohol after expression in *P. pastoris*. By combining the mutations K583E and Q584R, volumetric activity increased from 3.7 to 131 U/l, even though no functional expression was achieved for the single mutant Q584R. Here, we observe a synergistic positive effect of these two mutations on heterologous expression.

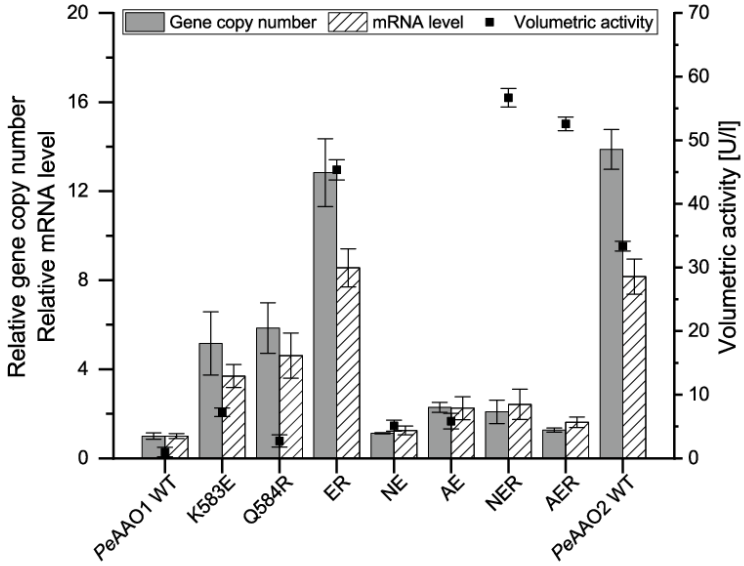

Fig. 4 Relative gene copy number and mRNA level determination in correlation to volumetric activity [U/l] of *Pe*AAO1 variants and *Pe*AAO2 wild-type. Actin was used as reference gene and values are depicted as ratio of target gene and reference gene. Volumetric activity after 48 h expression in BMM medium (25 °C, 200 rpm) was determined towards 5 mM veratryl alcohol in 100 mM sodium phosphate buffer pH 6. Relative gene copy number: gray column, filled; relative mRNA level: white column, striped; volumetric activity: black squares. ER: double mutant K583E/Q584R; NE: double mutant D361N/K583E; AE: double mutant V367A/K583E; NER: triple mutant D361N/K583E/Q584R; AER: triple mutant V367A/K583E/Q584R

The introduction of either the mutation D361N or V367A further increased volumetric activities of the respective *Pe*AAO1 variants NER and AER to 155 and 148 U/l.

In an attempt to rationalize the positive effect of the four mutations on expression in *P. pastoris*, the *Pe*AAO1 variants were investigated at different levels. First, homology models constructed for the *Pe*AAO1 variants revealed that the neighboring mutations K583E and Q584R in the variant ER are located in the C-terminal α-helix close to the surface of the enzyme (Fig. 5a). At position 583, the positively charged lysine in *Pe*AAO1 wild-type (Lys583 in Fig. 5b) was replaced by the negatively charged glutamate (Glu583 in Fig. 5a), while at position 584, a polar glutamine (Gln584) was substituted with a positively charged arginine (Arg584). The introduction of Glu583 enables polar interactions with Arg47 and Lys153, both located less than 4 Å away from Glu583 (Fig. 5c). Barlow and Thornton investigated the distance distribution of ion pairs in 38 structures of proteins and defined the distance of ≤ 4 Å between two charged residues as criterion to form an ion pair (Barlow and Thornton 1983). It was shown that close-range electrostatic interactions between charged amino acid residues as in salt bridges contribute, among others, to protein folding and stability (Kumar and Nussinov 2002).

The positive charge of the guanidine moiety in Arg47 is delocalized among the three nitrogen atoms, which increases the probability to form ion pairs with suitable oppositely charged residues like Glu583 (Barlow and Thornton 1983). The ε-amino group of Lys153 is also only 3.7 Å away from Glu583 and thus can also be involved in salt bridge formation. Musafia et al. performed an extended structure-based analysis of simple and complex salt bridges in 94 proteins and concluded that a central negatively charged glutamate residue can interact with an arginine via one or two bonds and additionally with a lysine via one bond, given that all charged groups are within the appropriate distance (Musafia et al. 1995). Thus, the mutation K583E might be involved in a new complex salt bridge formation with Arg47 and Lys153 in the C-terminal α-helix of the enzyme and might thereby influence the expression of *Pe*AAO1 in *P. pastoris* by enhancing protein folding. *Pe*AAO1 variant ER containing the additional mutation Q584R showed a dramatic enhancement of volumetric activity in comparison to K583E by factor 35, although the mutation Q584R alone did not lead to any observable expression. The homology model indicates that Arg584 is not in the ideal proximity to form salt bridges with other charged residues but might establish hydrogen bonds with main chain carbonyl groups of Asn146 and/or Gly141 with distances between 2.4 and 3.8 Å, respectively (Fig. 5a). It has been proposed that arginine is able to participate in several hydrogen bonds with main chain carbonyl oxygens and thereby connect different structural elements, enhancing protein stability as well (Borders et al. 1994). Apparently both mutations K583E and Q584R have a synergistic effect on expression, probably due to improved folding or protein stability during processing which might positively influence protein translocation, FAD incorporation, or protein glycosylation. Possibly, once

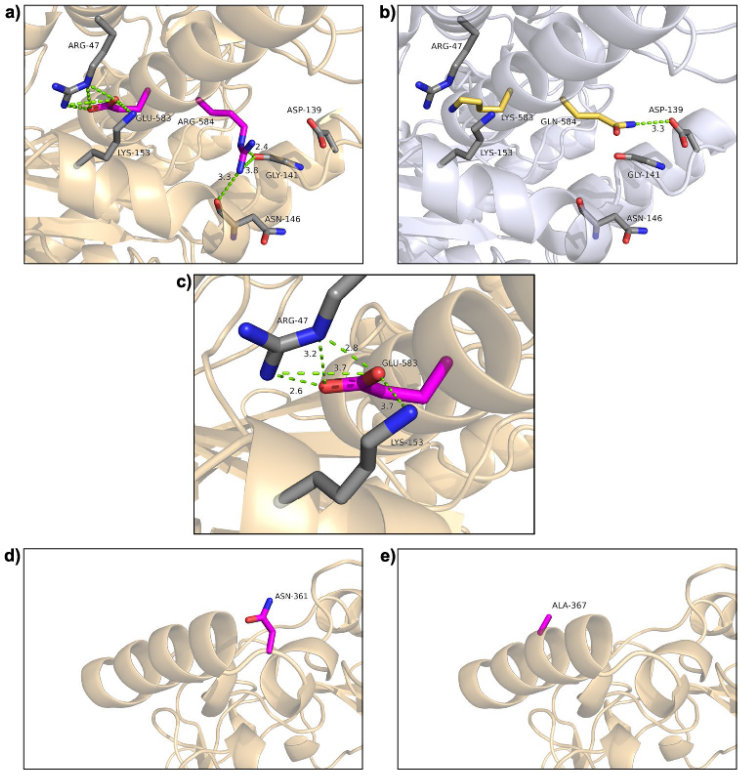

Fig. 5 Location of mutations K583E/Q584R in **a** *Pe*AAO1 variant ER and **b** the same positions in wild-type *Pe*AAO1; **c** close-up on possible polar contacts of variant ER; **d** mutation D361N in *Pe*AAO1 NER and **e** mutation V367A in *Pe*AAO1 AER. The two introduced mutations leading to Glu583 and Arg584 are depicted in pink; amino acid residues and backbone atoms in close proximity to form polar contacts (Arg47, Lys153, Asn146, Gly141, Asp139) are depicted in gray (**a**). View of the same positions in wild-type *Pe*AAO1 with Lys583 and Gln584 depicted in yellow (**b**). Close-up on possible polar contacts in variant ER at position 583 (**c**). The introduced mutations D361N and V367A in variants NER and AER are depicted in pink (**d** and **e**). The homology models of *Pe*AAO1 variants ER, NER, and AER were created using the crystal structure of *P. eryngii* AAO (wild-type *Pe*AAO1) (PDB entry 3FIM) as template. The possible polar contacts are colored in green and predicted distances are given in Å

the mutation Q584R is introduced to generate variant ER, the protein folding is slightly altered and the proposed salt bridges of Glu583 can be formed which eventually leads to the increased expression of this enzyme variant. It is important to point out that all assumptions are based on homology models built on the basis of the crystal structure of the non-glycosylated holoprotein *Pe*AAO1, crystallized after expression and refolding from inclusion bodies in *E. coli* (Fernández et al. 2009). Glycan moieties present in the three *Pe*AAO1 variants might influence folding of the enzymes so that crystal structures might differ from the predicted ones. Moreover, the mutations introduced in *Pe*AAO1 could have an impact on FAD binding as the position Arg47 involved in the hypothesized salt bridge is located in an N-terminal helix closely located to the highly conserved dinucleotide-binding motif (Fernández et al. 2009). Crystal structures of the glycosylated *Pe*AAO2 and the *Pe*AAO1 variants expressed in *P. pastoris* could provide more insight into possible structural changes induced by the introduced mutations. However, due to the heterogeneity caused by attached glycan moieties, crystallization of glycoproteins is a challenging task (Chang et al. 2007) and up to now has only been described for one glycosylated AAO - *Mt*AAOx from *Thermothelomyces thermophilus* (Kadowaki et al. 2020).

The additionally introduced mutations D361N or V367A are located in a surface exposed α-helix on the enzyme surface (Fig. 5d and e), which is unique for AAOs in comparison to other family members of the glucose-methanol-choline (GMC) oxidoreductase superfamily (Fernández et al. 2009). While no direct conclusion for the effect of the mutation V367A can be drawn based on structure-related changes, the mutation D361N introduces a new potential *N*-glycosylation site with the general motif of Asn-X-Ser/Thr, where X is any amino acid except for proline (Kukuruzinska et al. 1987). Glycosylation may assist various processes like protein folding (Helenius and Aebi 2004), stabilization of mature protein structures (Imperiali and O'Connor 1999; Wormald and Dwek 1999; Wyss and Wagner 1996), and thermostability of the protein (Wang et al. 1996). With the newly introduced *N*-glycosylation site, *Pe*AAO1 variant NER contains a total of eight potential sites which are identical to *Pe*AAO2 wild-type (Jankowski et al. 2020). All three

*Pe*AAO1 variants and *Pe*AAO2 wild-type exhibit highly similar molecular weights and *N*-glycosylation contents according to SDS-PAGE and PNGase F treatment as well as similar high pH and thermostability. The high pH stability of all variants is comparable to that observed for *Pe*AAO1 variant FX7 expressed in *S. cerevisiae*, which contained 50% glycosylation content (Viña-Gonzalez et al. 2015). It should be noted that most likely not all predicted *N*-glycosylation sites are in fact glycosylated. A database-survey focused on glycoproteins revealed that on average only two thirds of *N*-glycosylation sites are occupied (Apweiler et al. 1999). For example, the *Mt*AAOx from *T. thermophilus* contains six predicted *N*-glycosylation sites and X-ray structure elucidation revealed that four of them were glycosylated while one of them presents the major *N*-glycosylation site (Kadowaki et al. 2020). Interestingly, the previously reported optimized FX9 variant of *Pe*AAO1 expressed in *P. pastoris* was poorly glycosylated despite the presence of seven predicted *N*-glycosylation sites (Viña-Gonzalez et al. 2018), identical to the ones present in *Pe*AAO1 ER and AER. Maybe Asn361 in NER is only slightly *N*-glycosylated and therefore only marginal differences in glycan pattern of NER and the other variants exist that are not detectable via SDS-PAGE. In this case, the additional *N*-glycosylation in variant NER (and NE) could positively affect protein folding and/or secretion of the enzyme leading to enhanced volumetric activities. Stabilities of the purified *Pe*AAO1 variants and *Pe*AAO2 wild-type were comparable and showed no major differences: all *Pe*AAO1 variants exhibited high pH stabilities with roughly 90% of activity after incubation at pH 3 to 9 for 24 h, T_M values at around 65 °C, and T_{50} values between 61.5 and 62 °C.

The gene copy numbers and mRNA levels varied among the recombinant *P. pastoris* strains. Most strikingly, strains expressing the variants AER and NER demonstrated only one to two gene copies and similar high mRNA levels while exhibiting the highest observed volumetric activities. By comparing these data with the strain expressing the double mutant ER, which contained roughly 13 copies and showed a slightly lower volumetric activity than the triple mutants, our results indicate that the same (or even higher) level of volumetric AAO activity can be achieved with the triple mutants likely due to lower metabolic burden with just one to two gene copies. Overall, the real-time PCR results indicate that the observed higher volumetric activity of variants NER and AER can be solely attributed to effects of the mutations rather than multiple integration of the *aao* genes.

Since volumetric activity is dependent on enzyme concentration, on the one hand, and on catalytic properties of this enzyme, on the other hand, it is important to compare the catalytic parameters of the mutants. In general, catalytic activity of all *Pe*AAO1 variants was higher compared to *Pe*AAO2 wild-type. Thereby, mutations D361N and V367A seem to have a stimulating effect on catalytic activity when combined with ER mutations. The specific activities of the *Pe*AAO1 variants NER and AER measured for several substrates were slightly higher than those of *Pe*AAO1 ER and even *Pe*AAO2 wild-type. The α-helix which harbors both positions is the most external structural element in proximity to the catalytic pocket and might therefore influence substrate access to the active site. Interestingly, *Pe*AAO2 wild-type showed lowest K_M values for *p*-anisyl alcohol and veratryl alcohol (Jankowski et al. 2020). *Pe*AAO1 variant NER showed the highest k_{cat} value among all *Pe*AAO1 variants and *Pe*AAO2 wild-type, followed by variant AER, which could explain, at least to some extent, their increased volumetric activities after expression compared to *Pe*AAO2.

Comparison of catalytic properties of the *Pe*AAO1 variants with other AAOs showed that catalytic efficiencies of the *Pe*AAO1 variants are in the same range as compared to the poorly glycosylated *Pe*AAO1 variant FX9 expressed in *P. pastoris* with efficiencies of 1909 mM^{-1} s^{-1} (*p*-anisyl alcohol) and 139 mM^{-1} s^{-1} (veratryl alcohol) (Viña-Gonzalez et al. 2018). Interestingly, *Pe*AAO1 wild-type expressed in *A. nidulans* showed higher catalytic efficiencies with 5233 mM^{-1} s^{-1} (*p*-anisyl alcohol) and 210 mM^{-1} s^{-1} (veratryl alcohol) and up to two times higher k_{cat} values with 142 s^{-1} and 114 s^{-1} for *p*-anisyl alcohol and veratryl alcohol, respectively (Ferreira et al. 2006). While *Um*AAO from *Ustilago maydis* expressed in *P. pastoris* exhibited higher catalytic efficiencies towards *p*-anisyl alcohol (9380 mM^{-1} s^{-1}) and veratryl alcohol (440 mM^{-1} s^{-1}) (Couturier et al. 2016), than the *Pe*AAO1 variants, r*Cc*AAO from *Coprinopsis cinerea* expressed in *P. pastoris* showed a lower catalytic efficiency for conversion of *p*-anisyl alcohol with 1077 mM^{-1} s^{-1} (Tamaru et al. 2018). On the other hand, r*Cc*AAO showed an up to two times higher catalytic efficiency towards veratryl alcohol and a higher substrate affinity with K_M of 48.3 µM as compared to 446 to 549 µM for the *Pe*AAO1 variants. *Mt*AAOx from *T. thermophilus* showed quite low catalytic efficiencies with only 0.007 mM^{-1} s^{-1} and 0.011 mM^{-1} s^{-1} towards *p*-anisyl alcohol and veratryl alcohol, respectively (Kadowaki et al. 2020).

In conclusion, site-directed mutagenesis of *P. eryngii* *Pe*AAO1 led to the generation of three active and readily expressible enzyme variants with expression levels exceeding those of the already described *Pe*AAO1 variants. Up to now, the highest expression reported for the FX9 variant of *Pe*AAO1 in *P. pastoris* was 25.5 mg/l (Viña-Gonzalez et al. 2018). Here, *Pe*AAO1 variants ER, NER, and AER were constructed and expressed at four to fivefold higher concentrations ranging between 98 and 116 mg/l, accompanied by high volumetric activities. All enzymes could be produced in a bioreactor at 3 l scale, purified, and characterized.

The synergistic stabilizing effect caused by the introduced mutations K583E and Q584R is hypothesized. The

introduced mutations also slightly affected the catalytic properties of the enzyme variants. In future studies, the beneficial effect of mutations K583E/Q584R on *Pe*AAO1 expression could be combined with the reported mutations affecting enzyme selectivity and activity, such as in the oxidation of secondary benzylic alcohols (Viña-Gonzalez et al. 2019). This way, enzyme variants with new or improved catalytic activities and enhanced expression yields could become easily accessible for large-scale biocatalytic applications.

Supplementary Information The online version contains supplementary material available at https://doi.org/10.1007/s00253-021-11585-4.

Acknowledgements We thank Vanessa Göttfert for contribution to production and purification of *Pe*AAO1 variants, and collection of data for thermal stability experiments.

Author contribution NJ designed and conducted the experiments, analyzed the data, evaluated the results, and drafted the manuscript. KK and VBU gave advice in the research work, interpretation of data and helped in drafting and writing of the manuscript. All authors approved the manuscript.

Funding Open Access funding enabled and organized by Projekt DEAL. This work was financially supported by Bioeconomy Science Center supported by the Ministry of Innovation, Science and Research within the frame- work of the North Rhine-Westphalia, Germany, NRW-Strategieprojekt BioSC (Grant No. 313/323–400-002 13).

Data availability All data on which the conclusions were drawn are presented in this study.

Code availability Not applicable.

Declarations

Ethical approval This article does not contain any studies with human participants or animals performed by any of the authors.

Competing interests The authors declare no competing interests.

References

Apweiler R, Hermjakob H, Sharon N (1999) On the frequency of protein glycosylation, as deduced from analysis of the SWISS-PROT database. Biochim Biophys Acta 1473(1):4–8. https://doi.org/10.1097/00013611-198607000-00004

Barlow DJ, Thornton JM (1983) Ion-pairs in proteins. J Mol Biol 168(4):867–885. https://doi.org/10.1016/s0022-2836(83)80079-5

Borders CL, Broadwater JA, Bekeny PA, Salmon JE, Lee AS, Eldridge AM, Pett VB (1994) A structural role for arginine in proteins: multiple hydrogen bonds to backbone carbonyl oxygens. Protein Sci 3(4):541–548. https://doi.org/10.1002/pro.5560030402

Bradford MM (1976) A rapid and sensitive method for the quantitation of microgram quantities of protein utilizing the principle of protein-dye binding. Anal Biochem 72:248–254. https://doi.org/10.1016/0003-2697(76)90527-3

Carro J, Ferreira P, Martínez ÁT, Gadda G (2018) Stepwise hydrogen atom and proton transfers in dioxygen reduction by aryl-alcohol oxidase. Biochemistry 57(11):1790–1797. https://doi.org/10.1021/acs.biochem.8b00106

Carro J, Ferreira P, Rodríguez L, Prieto A, Serrano A, Balcells B, Ardá A, Jiménez-Barbero J, Gutiérrez A, Ullrich R, Hofrichter M, Martínez ÁT (2014) 5-Hydroxymethylfurfural conversion by fungal aryl-alcohol oxidase and unspecific peroxygenase. FEBS J 282:3218–3229. https://doi.org/10.1111/febs.13177

Carro J, Martínez M, Medina M, Martínez ÁT, Ferreira P (2017) Protein dynamics promote hydride tunnelling in substrate oxidation by aryl-alcohol oxidase. Phys Chem Chem Phys 19:28666–28675. https://doi.org/10.1039/C7CP05904C

Chang VT, Crispin M, Aricescu AR, Harvey DJ, Nettleship JE, Fennelly JA, Yu C, Boles KS, Evans EJ, Stuart DI, Dwek RA, Jones EY, Owens RJ, Davis SJ (2007) Glycoprotein structural genomics: solving the glycosylation problem. Structure 15(3):267–273. https://doi.org/10.1016/j.str.2007.01.011

Couturier M, Mathieu Y, Li A, Navarro D, Drula E, Haon M, Grisel S, Ludwig R, Berrin JG (2016) Characterization of a new aryl-alcohol oxidase secreted by the phytopathogenic fungus *Ustilago maydis*. Appl Microbiol Biotechnol 100(2):697–706. https://doi.org/10.1007/s00253-015-7021-3

de Almeida TP, van Schie MMCH, Ma A, Tieves F, Younes SHH, Fernández-Fueyo E, Arends IWCE, Riul A, Hollmann F (2019) Efficient aerobic oxidation of *trans*-2-hexen-1-ol using the aryl alcohol oxidase from *Pleurotus eryngii*. Adv Synth Catal 361:2668–2672. https://doi.org/10.1002/adsc.201801312

Dijkman WP, de Gonzalo G, Mattevi A, Fraaije MW (2013) Flavoprotein oxidases: classification and applications. Appl Microbiol Biotechnol 97:5177–5188. https://doi.org/10.1007/s00253-013-4925-7

Fernández IS, Ruíz-Dueñas FJ, Santillana E, Ferreira P, Martínez MJ, Martínez ÁT, Romero A (2009) Novel structural features in the GMC family of oxidoreductases revealed by the crystal structure of fungal aryl-alcohol oxidase. Acta Crystallogr Sect D Biol Crystallogr 65:1196–1205. https://doi.org/10.1107/S0907444909035860

Ferreira P, Hernández-Ortega A, Herguedas B, Martínez ÁT, Medina M (2009) Aryl-alcohol oxidase involved in lignin degradation. A mechanistic study based on steady and pre-steady state kinetics and primary and solvent isotope effects with two alcohol substrates. J Biol Chem 284:24840–24847. https://doi.org/10.1074/jbc.M109.011593

Ferreira P, Hernández-Ortega A, Herguedas B, Rencoret J, Gutiérrez A, Martínez MJ, Jiménez-Barbero J, Medina M, Martínez ÁT (2010) Kinetic and chemical characterization of aldehyde oxidation by fungal aryl-alcohol oxidase. Biochem J 425:585–593. https://doi.org/10.1042/BJ20091499

Ferreira P, Medina M, Guillén F, Martínez MJ, van Berkel WJH, Martínez AT (2005) Spectral and catalytic properties of aryl-alcohol oxidase, a fungal flavoenzyme acting on polyunsaturated alcohols. Biochem J 389:731–738. https://doi.org/10.1042/BJ20041903

Ferreira P, Ruiz-Dueñas FJ, Martínez MJ, Van Berkel WJH, Martínez AT (2006) Site-directed mutagenesis of selected residues at the active site of aryl-alcohol oxidase, an H_2O_2-producing ligninolytic enzyme. FEBS J 273:4878–4888. https://doi.org/10.1111/j.1742-4658.2006.05488.x

Forneris F, Orru R, Bonivento D, Chiarelli LR, Mattevi A (2009) ThermoFAD, a Thermofluor®-adapted flavin ad hoc detection system for protein folding and ligand binding. FEBS J 276:2833–2840. https://doi.org/10.1111/j.1742-4658.2009.07006.x

Grote A, Hiller K, Scheer M, Münch R, Nörtemann B, Hempel DC, Jahn D (2005) JCat: A novel tool to adapt codon usage of a target gene to its potential expression host. Nucleic Acids Res 33:526–531. https://doi.org/10.1093/nar/gki376

Guillén F, Martínez ÁT, Martínez MJ (1992) Substrate specificity and properties of the aryl-alcohol oxidase from the ligninolytic fungus *Pleurotus eryngii*. Eur J Biochem 209:603–611. https://doi.org/10.1111/j.1432-1033.1992.tb17326.x

Helenius A, Aebi M (2004) Roles of N-linked glycans in the endoplasmic reticulum. Annu Rev Biochem 73:1019–1049. https://doi.org/10.1146/annurev.biochem.73.011303.073752

Hernández-Ortega A, Ferreira P, Merino P, Medina M, Guallar V, Martínez ÁT (2012a) Stereoselective hydride transfer by aryl-alcohol oxidase, a member of the GMC superfamily. ChemBioChem 13:427–435. https://doi.org/10.1002/cbic.201100709

Hernández-Ortega A, Lucas F, Ferreira P, Medina M, Guallar V, Martínez ÁT (2012b) Role of active site histidines in the two half-reactions of the aryl-alcohol oxidase catalytic cycle. Biochemistry 51:6595–6608. https://doi.org/10.1021/bi300505z

Imperiali B, O'Connor SE (1999) Effect of N-linked glycosylatian on glycopeptide and glycoprotein structure. Curr Opin Chem Biol 3(6):643–649. https://doi.org/10.1016/S1367-5931(99)00021-6

Jankowski N, Koschorreck K, Urlacher VB (2020) High-level expression of aryl-alcohol oxidase 2 from Pleurotus eryngii in Pichia pastoris for production of fragrances and bioactive precursors. Appl Microbiol Biotechnol 104(21):9205–9218. https://doi.org/10.1007/s00253-020-10878-4

Kadowaki MAS, Higasi PMR, de Godoy MO, de Araujo EA, Godoy AS, Prade RA, Polikarpov I (2020) Enzymatic versatility and thermostability of a new aryl-alcohol oxidase from *Thermothelomyces thermophilus* M77. Biochim Biophys Acta 10:129681. https://doi.org/10.1016/j.bbagen.2020.129681

Kukuruzinska MA, Bergh MLE, Jackson BJ (1987) Protein glycosylation in yeast. Annu Rev Biochem 56:915–944. https://doi.org/10.1146/annurev.bi.56.070187.004411

Kumar S, Nussinov R (2002) Close-range electrostatic interactions in proteins. ChemBioChem 3(7):604–617. https://doi.org/10.1002/1439-7633(20020703)3:7%3c604::AID-CBIC604%3e3.0.CO;2-X

Laemmli UK (1970) Cleavage of structural proteins during assembly of head of bacteriophage-T4. Nature 227:680–685. https://doi.org/10.1038/227680a0

Li Y, Cirino PC (2014) Recent advances in engineering proteins for biocatalysis. Biotechnol Bioeng 111(7):1273–1287. https://doi.org/10.1002/bit.25240

Musafia B, Buchner V, Arad D (1995) Complex salt bridges in proteins: statistical analysis of structure and function. J Mol Biol 254(4):761–770. https://doi.org/10.1006/jmbi.1995.0653

Pfaffl MW (2001) A new mathematical model for relative quantification in real-time RT–PCR. Nucleic Acids Res 29(9):e45. https://doi.org/10.1111/j.1365-2966.2012.21196.x

Ruiz-Dueñas FJ, Ferreira P, Martínez MJ, Martínez AT (2006) In vitro activation, purification, and characterization of *Escherichia coli* expressed aryl-alcohol oxidase, a unique H_2O_2-producing enzyme. Protein Expression Purif 45(1):191–199. https://doi.org/10.1016/j.pep.2005.06.003

Serrano A, Calviño E, Carro J, Sánchez-Ruiz MI, Cañada FJ, Martínez AT (2019a) Complete oxidation of hydroxymethylfurfural to furandicarboxylic acid by aryl-alcohol oxidase. Biotechnol Biofuels 12:217. https://doi.org/10.1186/s13068-019-1555-z

Serrano A, Carro J, Martínez ÁT (2020) Reaction mechanisms and applications of aryl-alcohol oxidase. In: Chaiyen P, Tamanoi F (eds) The Enzymes. Flavin-Dependent Enzymes: Mechanisms, Structures and Applications, Vol 47, 2020 edn. Elsevier, pp 167–192

Serrano A, Sancho F, Viña-González J, Carro J, Alcalde M, Guallar V, Martínez ÁT (2019b) Switching the substrate preference of fungal aryl-alcohol oxidase: towards stereoselective oxidation of secondary benzyl alcohols. Catal Sci Technol 9:833–841. https://doi.org/10.1039/C8CY02447B

Tamaru Y, Umezawa K, Yoshida M (2018) Characterization of an aryl-alcohol oxidase from the plant saprophytic basidiomycete *Coprinopsis cinerea* with broad substrate specificity against aromatic alcohols. Biotechnol Lett 40(7):1077–1086. https://doi.org/10.1007/s10529-018-2534-3

Urlacher VB, Koschorreck K (2021) Pecularities and applications of aryl-alcohol oxidases from fungi. Appl Microbiol Biotechnol 105:4111–4126. https://doi.org/10.1007/s00253-021-11337-4

van Schie MMCH, de Almeida TP, Laudadio G, Tieves F, Fernández-Fueyo E, Noël T, Arends IWCE, Hollmann F (2018) Biocatalytic synthesis of the green note trans-2-hexenal in a continuous-flow microreactor. Beilstein J Org Chem 14:697–703. https://doi.org/10.3762/bjoc.14.58

Viña-Gonzalez J, Alcalde M (2020) Directed evolution of the aryl-alcohol oxidase: beyond the lab bench. Comput Struct Biotechnol J 18:1800–1810. https://doi.org/10.1016/j.csbj.2020.06.037

Viña-Gonzalez J, Elbl K, Ponte X, Valero F, Alcalde M (2018) Functional expression of aryl-alcohol oxidase in Saccharomyces cerevisiae and Pichia pastoris by directed evolution. Biotechnol Bioeng 115(7):1666–1674. https://doi.org/10.1002/bit.26585

Viña-Gonzalez J, Gonzalez-Perez D, Ferreira P, Martínez ÁT, Alcalde M (2015) Focused directed evolution of aryl-alcohol oxidase in Saccharomyces cerevisiae by using chimeric signal peptides. Appl Environ Microbiol 81(18):6451–6462. https://doi.org/10.1128/AEM.01966-15

Viña-Gonzalez J, Jimenez-Lalana D, Sancho F, Serrano A, Martínez ÁT, Guallar V, Alcalde M (2019) Structure-guided evolution of aryl alcohol oxidase from *Pleurotus eryngii* for the selective oxidation of secondary benzyl alcohols. Adv Synth Catal 361:2514–2525. https://doi.org/10.1002/adsc.201900134

Wang C, Eufemi M, Turano C, Giartosio A (1996) Influence of the carbohydrate moiety on the stability of glycoproteins. Biochemistry 35(23):7299–7307. https://doi.org/10.1021/bi9517704

Waterhouse A, Bertoni M, Bienert S, Studer G, Tauriello G, Gumienny R, Heer FT, de Beer TAP, Rempfer C, Bordoli L, Lepore R, Schwede T (2018) SWISS-MODEL: homology modelling of protein structures and complexes. Nucleic Acids Res 46(W1):W296–W303. https://doi.org/10.1093/nar/gky427

Wormald MR, Dwek RA (1999) Glycoproteins: glycan presentation and protein-fold stability. Structure 7(7):155–160. https://doi.org/10.1016/S0969-2126(99)80095-1

Wyss DF, Wagner G (1996) The structural role of sugars in glycoproteins. Curr Opin Biotechnol 7(4):409–416. https://doi.org/10.1016/S0958-1669(96)80116-9

2.4.1. Supplemental Information

Applied Microbiology and Biotechnology Jankowski et al. (2021)

SUPPLEMENTARY INFORMATION

on

Two adjacent C-terminal mutations enable expression of aryl-alcohol oxidase from *Pleurotus eryngii* in *Pichia pastoris*

Nina Jankowski [a], Vlada B. Urlacher [a], Katja Koschorreck [a]

[a] Institute of Biochemistry, Heinrich-Heine-University Düsseldorf, Universitätsstraße 1, 40225 Düsseldorf, Germany

For correspondence:

Katja Koschorreck

Tel. +49 211 81-10749

Fax +49 211 81-13117

Katja.Koschorreck@hhu.de

ORCID ID 0000-0001-9689-9863

Table S1 Primers used for site-directed mutagenesis of *Pe*AAO1. The triplets introducing the mutations are shown in *italics*

Primer name	Sequence (5' to 3')
***Pe*AAO1_R152G_fw**	CAACAATTCGTT*GGT*AAGAACGAAATGG
***Pe*AAO1_R152G_rev**	CCATTTCGTTCTT*ACC*AACGAATTGTTG
***Pe*AAO1_T265I_fw**	GGTTAACTCTGGT*ATC*ACTAACGGTTTGC
***Pe*AAO1_T265I_rev**	GCAAACCGTTAGT*GAT*ACCAGAGTTAACC
***Pe*AAO1_D361N_fw**	GACAACATCTTCAGA*AAC*TCTTCTGAATTTAACG
***Pe*AAO1_D361N_rev**	CGTTAAATTCAGAAGA*GTT*TCTGAAGATGTTGTCG
***Pe*AAO1_V367A_fw**	GACTCTTCTGAATTTAAC*GCT*GACTTGGACCAATGG
***Pe*AAO1_V367A_rev**	CCATTGGTCCAAGTC*AGC*GTTAAATTCAGAAGAGTC
***Pe*AAO1_D512N_fw**	GAGACCCAACT*AAC*GACGCTGCTATCGAATC
***Pe*AAO1_D512N_rev**	GATTCGATAGCAGCGTC*GTT*AGTTGGGTCTC
***Pe*AAO1_K583E_fw**	CCAATCTACTTGGTTGGT*GAA*CAAGGTGCTGACTTG
***Pe*AAO1_K583E_rev**	CAAGTCAGCACCTTG*TTC*ACCAACCAAGTAGATTGG
***Pe*AAO1_Q584R_fw**	CTACTTGGTTGGTAAG*AGA*GGTGCTGACTTGATC
***Pe*AAO1_Q584R_rev**	GATCAAGTCAGCACC*TCT*CTTACCAACCAAGTAG
***Pe*AAO1_K583E/Q584R_fw**	TTGGT*GAA*AGAGGTGCTGACTTGATCAAGGCTG
***Pe*AAO1_K583E/Q584R_rev**	CAGCACCTCT*TTC*ACCAACCAAGTAGATTGG

Applied Microbiology and Biotechnology Jankowski et al. (2021)

```
PeAAO1 WT     MSFGALRQLLLIACLALPSLAATNLPTADFDYVVVGAGNAGNVVAARLTEDPDVSVLVLE    60
PeAAO1 ER     MSFGALRQLLLIACLALPSLAATNLPTADFDYVVVGAGNAGNVVAARLTEDPDVSVLVLE    60
PeAAO1 NER    MSFGALRQLLLIACLALPSLAATNLPTADFDYVVVGAGNAGNVVAARLTEDPDVSVLVLE    60
PeAAO1 AER    MSFGALRQLLLIACLALPSLAATNLPTADFDYVVVGAGNAGNVVAARLTEDPDVSVLVLE    60
PeAAO2 WT     MSFGALRQLLLIACLALPSLAATNLPTADFDYVVVGAGNAGNVVAARLTEDPDVSVLVLE    60
              ************************************************************

PeAAO1 WT     AGVSDENVLGAEAPLLAPGLVPNSIFDWNYTTTAQAGYNGRSIAYPRGRMLGGSSSVHYM   120
PeAAO1 ER     AGVSDENVLGAEAPLLAPGLVPNSIFDWNYTTTAQAGYNGRSIAYPRGRMLGGSSSVHYM   120
PeAAO1 NER    AGVSDENVLGAEAPLLAPGLVPNSIFDWNYTTTAQAGYNGRSIAYPRGRMLGGSSSVHYM   120
PeAAO1 AER    AGVSDENVLGAEAPLLAPGLVPNSIFDWNYTTTAQAGYNGRSIAYPRGRMLGGSSSVHYM   120
PeAAO2 WT     AGVSDENVLGAEAPLLAPGLVPNSIFDWNYTTTAQAGYNGRSIAYPRGRMLGGSSSVHYM   120
              ************************************************************
                                        R152
PeAAO1 WT     VMMRGSTEDFDRYAAVTGDEGWNWDNIQQFVRKNEMVVPPADNHNTSGEFIPAVHGTNGS   180
PeAAO1 ER     VMMRGSTEDFDRYAAVTGDEGWNWDNIQQFVRKNEMVVPPADNHNTSGEFIPAVHGTNGS   180
PeAAO1 NER    VMMRGSTEDFDRYAAVTGDEGWNWDNIQQFVRKNEMVVPPADNHNTSGEFIPAVHGTNGS   180
PeAAO1 AER    VMMRGSTEDFDRYAAVTGDEGWNWDNIQQFVRKNEMVVPPADNHNTSGEFIPAVHGTNGS   180
PeAAO2 WT     VMMRGSTEDFDRYAAVTGDEGWNWDNIQQFVGKNEMVVPPADNHNTSGEFIPAVHGTNGS   180
              ************************************************************

PeAAO1 WT     VSISLPGFPTPLDDRVLATTQEQSEEFFFNPDMGTGHPLGISWSIASVGNGQRSSSSTAY   240
PeAAO1 ER     VSISLPGFPTPLDDRVLATTQEQSEEFFFNPDMGTGHPLGISWSIASVGNGQRSSSSTAY   240
PeAAO1 NER    VSISLPGFPTPLDDRVLATTQEQSEEFFFNPDMGTGHPLGISWSIASVGNGQRSSSSTAY   240
PeAAO1 AER    VSISLPGFPTPLDDRVLATTQEQSEEFFFNPDMGTGHPLGISWSIASVGNGQRSSSSTAY   240
PeAAO2 WT     VSISLPGFPTPLDDRVLATTQEQSEEFFFNPDMGTGHPLGISWSIASVGNGQRSSSSTAY   240
              ************************************************************
                                   T265
PeAAO1 WT     LRPAQSRPNLSVLINAQVTKLVNSGTTNGLPAFRCVEYAEQEGAPTTTVCAKKEVVLSAG   300
PeAAO1 ER     LRPAQSRPNLSVLINAQVTKLVNSGTTNGLPAFRCVEYAEQEGAPTTTVCAKKEVVLSAG   300
PeAAO1 NER    LRPAQSRPNLSVLINAQVTKLVNSGTTNGLPAFRCVEYAEQEGAPTTTVCAKKEVVLSAG   300
PeAAO1 AER    LRPAQSRPNLSVLINAQVTKLVNSGTTNGLPAFRCVEYAEQEGAPTTTVCAKKEVVLSAG   300
PeAAO2 WT     LRPAQSRPNLSVLINAQVTKLVNSGITNGLPAFRCVEYAEQEGAPTTTVCAKKEVVLSAG   300
              ************************* ***********************************

PeAAO1 WT     SVGTPILLQLSGIGDENDLSSVGIDTIVNNPSVGRNLSDHLLLPAAFFVNSNQTFDNIFR   360
PeAAO1 ER     SVGTPILLQLSGIGDENDLSSVGIDTIVNNPSVGRNLSDHLLLPAAFFVNSNQTFDNIFR   360
PeAAO1 NER    SVGTPILLQLSGIGDENDLSSVGIDTIVNNPSVGRNLSDHLLLPAAFFVNSNQTFDNIFR   360
PeAAO1 AER    SVGTPILLQLSGIGDENDLSSVGIDTIVNNPSVGRNLSDHLLLPAAFFVNSNQTFDNIFR   360
PeAAO2 WT     SVGTPILLQLSGIGDENDLSSVGIDTIVNNPSVGRNLSDHLLLPAAFFVNSNQTFDNIFR   360
              ************************************************************
              D361  V367
PeAAO1 WT     DSSEFNVDLDQWTNTRTGPLTALIANHLAWLRLPSNSSIFQTFPDPAAGPNSAHWETIFS   420
PeAAO1 ER     DSSEFNVDLDQWTNTRTGPLTALIANHLAWLRLPSNSSIFQTFPDPAAGPNSAHWETIFS   420
PeAAO1 NER    NSSEFNVDLDQWTNTRTGPLTALIANHLAWLRLPSNSSIFQTFPDPAAGPNSAHWETIFS   420
PeAAO1 AER    DSSEFNADLDQWTNTRTGPLTALIANHLAWLRLPSNSSIFQTFPDPAAGPNSAHWETIFS   420
PeAAO2 WT     NSSEFNADLDQWTNTRTGPLTALIANHLAWLRLPSNSSIFQTFPDPAAGPNSAHWETIFS   420
              :*****.************************************************************

PeAAO1 WT     NQWFHPAIPRPDTGSFMSVTNALISPVARGDIKLATSNPFDKPLINPQYLSTEFDIFTMI   480
PeAAO1 ER     NQWFHPAIPRPDTGSFMSVTNALISPVARGDIKLATSNPFDKPLINPQYLSTEFDIFTMI   480
PeAAO1 NER    NQWFHPAIPRPDTGSFMSVTNALISPVARGDIKLATSNPFDKPLINPQYLSTEFDIFTMI   480
PeAAO1 AER    NQWFHPAIPRPDTGSFMSVTNALISPVARGDIKLATSNPFDKPLINPQYLSTEFDIFTMI   480
PeAAO2 WT     NQWFHPAIPRPDTGSFMSVTNALISPVARGDIKLATSNPFDKPLINPQYLSTEFDIFTMI   480
              ************************************************************
                                        D512
PeAAO1 WT     QAVKSNLRFLSGQAWADFVIRPFDPRLRDPTDDAAIESYIRDNANTIFHPVGTASMSPRG   540
PeAAO1 ER     QAVKSNLRFLSGQAWADFVIRPFDPRLRDPTDDAAIESYIRDNANTIFHPVGTASMSPRG   540
PeAAO1 NER    QAVKSNLRFLSGQAWADFVIRPFDPRLRDPTDDAAIESYIRDNANTIFHPVGTASMSPRG   540
PeAAO1 AER    QAVKSNLRFLSGQAWADFVIRPFDPRLRDPTDDAAIESYIRDNANTIFHPVGTASMSPRG   540
PeAAO2 WT     QAVKSNLRFLSGQAWADFVIRPFDPRLRDPTNDAAIESYIRDNANTIFHPVGTASMSPRG   540
              ******************************:*****************************
                                                K583/Q584
PeAAO1 WT     ASWGVVDPDLKVKGVDGLRIVDGSILPFAPNAHTQGPIYLVGKQGADLIKADQ      593
PeAAO1 ER     ASWGVVDPDLKVKGVDGLRIVDGSILPFAPNAHTQGPIYLVGERGADLIKADQ      593
PeAAO1 NER    ASWGVVDPDLKVKGVDGLRIVDGSILPFAPNAHTQGPIYLVGERGADLIKADQ      593
PeAAO1 AER    ASWGVVDPDLKVKGVDGLRIVDGSILPFAPNAHTQGPIYLVGERGADLIKADQ      593
PeAAO2 WT     ASWGVVDPDLKVKGVDGLRIVDGSILPFAPNAHTQGPIYLVGERGADLIKADQ      593
              ****************************************:::*********
```

Fig. S1 Protein sequence alignment of *Pe*AAO1 and *Pe*AAO2 wild-type (Accession numbers AAC72747 and ADD14021) and of *Pe*AAO1 variants ER, NER and AER. Orange boxes with red labeling refer to the seven differing amino acid positions in *Pe*AAO1 and *Pe*AAO2 wild-type. Amino acids present in *Pe*AAO2 are shown in bold black. Mutated amino acids in *Pe*AAO1 variants ER, NER and AER are shown in bold blue

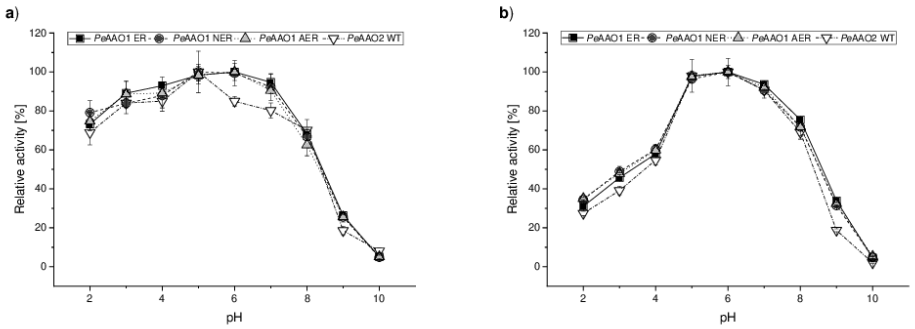

Fig. S2 pH activity profile of *Pe*AAO1 variants and *Pe*AAO2 wild-type towards **a)** *p*-anisyl alcohol and **b)** veratryl alcohol. 5 mM substrate and 100 mM Britton-Robinson buffer were used. *Pe*AAO1 ER: black squares, solid line; *Pe*AAO1 NER: dark grey circles, dashed line; *Pe*AAO1 AER: light grey triangles, dotted line; *Pe*AAO2 wild-type: white triangles, dashed-dotted line. Highest activity was set to 100 %. Data for *Pe*AAO2 wild-type taken from Jankowski et al. 2020

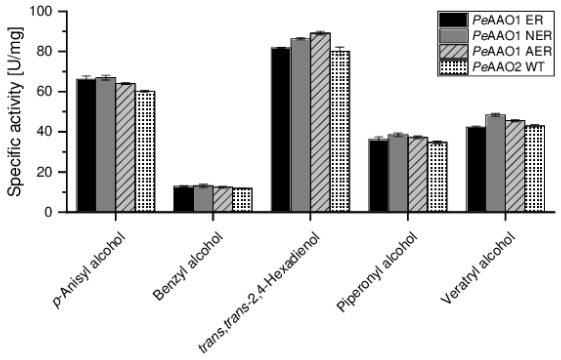

Fig. S3 Specific activities [U/mg] of *Pe*AAO1 variants and *Pe*AAO2 wild-type towards several substrates. 5 mM of each substrate was used in 100 mM sodium phosphate buffer pH 6. *Pe*AAO1 ER: black, filled; *Pe*AAO1 NER: grey, filled; *Pe*AAO1 AER: grey, striped; *Pe*AAO2 wild-type: white, dotted

References

Jankowski N, Koschorreck K, Urlacher VB (2020) High-level expression of aryl-alcohol oxidase 2 from *Pleurotus eryngii* in *Pichia pastoris* for production of fragrances and bioactive precursors. Appl Microbiol Biotechnol 104(21):9205-9218. doi:10.1007/s00253-020-10878-4

2.5. Chapter V: Novel agar plate assay for screening of AAO mutant libraries

Title	Agar plate assay for rapid screening of aryl-alcohol oxidase mutant libraries in *Pichia pastoris*
Authors	Nina Jankowski, Katja Koschorreck
Contribution	Design, planning and conducting half of the experiments, evaluation of data, correction of the first draft of the manuscript. Relative contribution: 50 %
Published in	*Journal of Biotechnology,* 346, 47–51 (**2022**)
DOI	10.1016/j.jbiotec.2022.01.006
Publisher	Elsevier B.V.
Copyright	Copyright © 2022, Elsevier B.V

Journal of Biotechnology 346 (2022) 47–51

Contents lists available at ScienceDirect

Journal of Biotechnology

journal homepage: www.elsevier.com/locate/jbiotec

Short communication

Agar plate assay for rapid screening of aryl-alcohol oxidase mutant libraries in *Pichia pastoris*

Nina Jankowski, Katja Koschorreck [*,1]

Institute of Biochemistry, Heinrich-Heine University Düsseldorf, Universitätsstraße 1, 40225 Düsseldorf, Germany

ARTICLE INFO

Keywords:
Aryl-alcohol oxidase
Pichia pastoris
Agar plate-based assay
Hydrogen peroxide
Benzylic alcohols

ABSTRACT

Directed evolution is a powerful tool for developing biocatalysts with tailor-made properties for biocatalytic applications. High-throughput activity screening of large mutant libraries generated by e.g. means of directed evolution is usually performed in 96-well microtiter plates requiring, however, time-consuming and laborious enzyme expression, cell harvesting and activity measurements. In addition, automated liquid handling systems are needed to cope with the high number of colonies to be screened. Herein, we developed an agar plate-based assay for simple and fast screening of H_2O_2-producing aryl-alcohol oxidase (AAO) mutant libraries in *Pichia pastoris*. Buffered minimal methanol agar plates were supplemented with 2,2′-azino-bis(3-ethylbenzothiazoline-6-sulfonic acid) (ABTS), horseradish peroxidase (HRP) and the target substrate. AAO activity is visualized by formation of green zones around AAO-secreting *P. pastoris* colonies due to ABTS oxidation by HRP which is fueled with H_2O_2 by AAO in course of substrate oxidation. Colonies were screened within 24 h for AAO activity using different AAO substrates like veratryl alcohol, *p*-anisyl alcohol or *trans,trans*-2,4-hexadien-1-ol and even low AAO activity towards 5-hydroxymethylfurfural could be detected within 48 h. The developed agar plate-based assay can be extended to other substrates and might also be applied for fast and substrate-specific screening of other H_2O_2-producing oxidases in *P. pastoris*.

1. Main document

Biocatalysis has evolved as a promising tool for the production of chemicals, pharmaceuticals, flavors and fragrances over the last twenty years (Bell et al., 2021; Hauer, 2020). Enzymes used as biocatalysts can be produced from renewable resources, operate under environmentally friendly reaction conditions and are able to convert bio-based compounds with high activity and selectivity into valuable products (Wiltschi et al., 2020). Their scope of application was further broadened by the implementation of directed evolution for the development of tailored biocatalysts for biotechnological applications (Wu et al., 2021).

Aryl-alcohol oxidases (AAOs; EC 1.1.3.7) are FAD-containing oxidoreductases that belong to the glucose-methanol-choline (GMC) oxidoreductase superfamily and were assigned in 2013 to "Auxiliary Activities 3" subfamily 2 (AA3_2) in the Carbohydrate Active enZyme (CAZy) database (Levasseur et al., 2013). These enzymes have emerged as promising biocatalysts during the last two decades. Predominantly found in fungi as secreted glycoproteins, AAOs oxidize a broad range of benzylic and aliphatic allylic primary alcohols to the corresponding aldehydes while reducing O_2 to H_2O_2 (Guillén et al., 1992). Hydrated aldehydes (*gem*-diols) are also accepted as substrates and oxidized to the corresponding acids, but at much lower efficiencies (Ferreira et al., 2010). Potential fields of application of AAOs comprise the synthesis of pharmaceuticals, building blocks, and flavor and fragrance compounds, as well as delignification and decolorization of dyes by fueling peroxidases with H_2O_2, which has been summarized in recent reviews (Serrano et al., 2020; Urlacher and Koschorreck, 2021). However, production of AAOs at high levels is still a crucial challenge. Several directed evolution campaigns of the well-studied *Pe*AAO1 from *Pleurotus eryngii* were conducted using *Saccharomyces cerevisiae* as host to improve its demanding expression, to enhance its activity and to broaden its substrate scope (Viña-Gonzalez and Alcalde, 2020; Viña-Gonzalez et al., 2015, 2019, 2020). Thereby, several improved *Pe*AAO1 variants have been generated, but their expression levels in *S. cerevisiae* and *Pichia pastoris (Komagataella phaffii)* remained low, reaching only 4.5 and 4.3 mg/L in shaking flasks cultures, respectively (Viña-Gonzalez et al., 2018). Recently, we showed that AAOs can be expressed in *P. pastoris* under control of the methanol-inducible *AOX1* promoter at high levels

* Corresponding author.
E-mail address: Katja.Koschorreck@hhu.de (K. Koschorreck).
[1] ORCID ID 0000-0001-9689-9863

https://doi.org/10.1016/j.jbiotec.2022.01.006
Received 29 October 2021; Received in revised form 17 January 2022; Accepted 30 January 2022
Available online 2 February 2022

(Jankowski et al., 2020, 2021; Lappe et al., 2021). Two mutations introduced to *Pe*AAO1, K583E and Q584R (ER), enabled its expression in *P. pastoris* at 116 mg per liter culture medium (Jankowski et al., 2021). In addition, *Pe*AAO2 from *P. eryngii* P34 and *Ma*AAO from *Moesziomyces antarcticus* were expressed at several hundred milligrams per liter (Jankowski et al., 2020; Lappe et al., 2021) which is a good starting point for directed evolution campaigns of AAOs in *P. pastoris* to develop tailor-made biocatalysts.

Screening of enzyme libraries for improved variants is usually performed in 96-well microtiter plates, requiring, however, time-consuming pre-culturing, enzyme expression, cell harvesting and eventually high-throughput activity testing. Moreover, automated liquid handling systems are usually required to enable high-throughput screening of thousands of generated variants but are not available in every lab. Agar plate-based activity assays, on the other hand, can be performed in short time without lots of laborious work, high costs or the need for special equipment and represent a simple tool for fast screening of enzyme or metagenomic libraries (Alexeeva et al., 2002; Carlina et al., 2016; Weiß et al., 2018). These assays are based on conversion of agar-embedded substrates by the target enzyme. The formation of clear or colored zones around colonies indicate expression of the target enzyme in its catalytically active form. While for other secreted fungal oxidases like laccases or peroxidases agar plate assays based on chromogenic substrates like 2,2′-azino-bis(3-ethylbenzothiazoline-6-sulfonic acid) (ABTS) or guaiacol have been applied for screening purposes in *P. pastoris* or *S. cerevisiae* (Karnaouri et al., 2021; Kiiskinen et al., 2004; Mate et al., 2013), up to now no agar plate-based assays for rapid screening of AAOs or mutant libraries thereof in *P. pastoris* or other hosts have been described.

Here, we report on the development of a multi-functional agar plate-based assay for fast screening of AAO mutant libraries in *P. pastoris* towards a broad range of substrates.

For assay development the coupled horseradish peroxidase (HRP)-ABTS assay applied for screening of AAOs in liquid medium (Viña-Gonzalez et al., 2015) was transferred to agar plates. Thereby, the AAO-catalyzed substrate oxidation and H_2O_2 production is coupled with the oxidation of ABTS to the greenish ABTS radical cation by H_2O_2-dependent HRP (Scheme 1). Expression of AAO in *P. pastoris* was conducted under control of the methanol-inducible *AOX1* promoter. Buffered minimal methanol (BMM; 0.5% methanol) agar plates were used to induce AAO expression and were supplemented with ABTS, HRP and veratryl alcohol or *p*-anisyl alcohol, two typical AAO substrates (Couturier et al., 2016; Guillén et al., 1992; Jankowski et al., 2020), for activity screening. AAOs with different expression levels in *P. pastoris* (Table S1), namely *Pe*AAO1 variants K583E, ER (K583E/Q584R), AER (V367A/K583E/Q584R) and NER (D361N/K583E/Q584R) (Jankowski et al., 2021) as well as *Pe*AAO2 (Jankowski et al., 2020), were used for assay validation. Although in shaking flasks experiments secretion of these enzymes from recombinant *P. pastoris* transformants into the medium is difficult to detect by SDS-PAGE analysis (Fig. S1A), AAO secretion was confirmed after fed-batch fermentation and enzyme purification from culture supernatants (Fig. S1B). *P. pastoris* colonies containing non-expressible *Pe*AAO1 or empty vector pPICZαA were used as negative controls to exclude background activity of *P. pastoris*' alcohol oxidases AOX1 and AOX2 on BMM-screening agar plates.

Recombinant *P. pastoris* transformants with genomically integrated AAO encoding genes were transferred from yeast extract peptone dextrose (YPD) agar plates to BMM-veratryl alcohol agar plates and incubated at 30 °C for up to three days. Deep green zones appeared after 24 h incubation around *P. pastoris* colonies expressing *Pe*AAO1 ER, AER, NER and *Pe*AAO2 due to veratryl alcohol oxidation by the secreted AAOs accompanied by production of H_2O_2, which was used by HRP for oxidation of ABTS (Table 1). As expected, *P. pastoris* colonies containing empty vector or non-expressible *Pe*AAO1 showed no color development and only a slightly greenish zone appeared around *P. pastoris* colonies expressing *Pe*AAO1 K583E. This is in good agreement with the results obtained in shaking flasks experiments where volumetric activity in BMMY medium was only 1.2 U/L for *Pe*AAO1 K583E, but reached up to 62.1 U/L for NER after 24 h of expression at 25 °C using veratryl alcohol as substrate. *Pichia* transformants with very intense green zones (*Pe*AAO2, ER, AER and NER) after 24 h, indicating high AAO activity, but with different volumetric activity (Table S1) could be distinguished on BMM-screening agar plates as well. For instance, already after 4 h of incubation a slightly greenish zone appeared around *P. pastoris* transformants expressing *Pe*AAO1 variants AER and NER while almost no activity of *Pe*AAO2 and *Pe*AAO1 ER (both with around two times lower volumetric activity than NER) on BMM-veratryl alcohol agar plates was detectable at that time (Table 1). Thus, the developed assay enables fast identification of AAO variants with improved expression or activity in *P. pastoris* and competes with screening of AAO libraries in *S. cerevisiae* in microtiter plates (Viña-Gonzalez et al., 2015). In addition, even at low expression levels of ~4–6 U/L in shaking flasks after 48 h, differences of ~20% in volumetric activity of the respective colonies could be visualized on agar plate as was shown for *Pe*AAO1 variant NE (D361N/K583E). Four different *P. pastoris* colonies containing *Pe*AAO1 NE, with volumetric activities of 4.3–5.5 U/L in shaking flasks experiments after 48 h, were spread on BMM agar plates containing *p*-anisyl alcohol as substrate. After 48 h of incubation colony #4 with an ~20% increase in volumetric activity in liquid culture showed the most intense color formation compared to the other ones (Table 2). The high sensitivity of this assay allows to identify AAO variants with slightly enhanced expression levels or low enzymatic activity towards a target

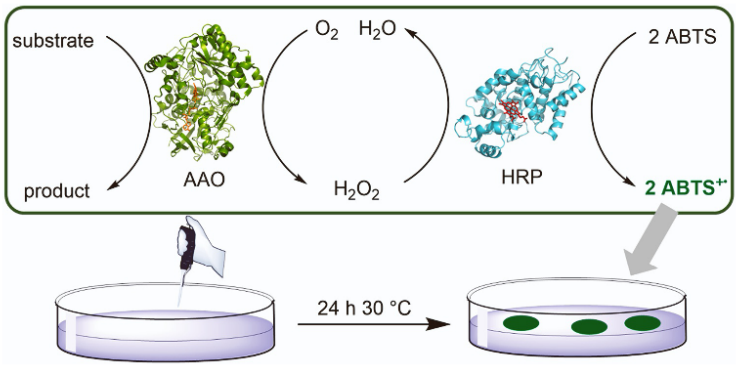

Scheme 1. Principle of agar plate-based screening assay for AAO-expressing *P. pastoris* transformants.

Table 1
Development of green zones around *P. pastoris* transformants expressing *Pe*AAO1, *Pe*AAO2 and *Pe*AAO1 variants K583E, ER, AER and NER, respectively, on BMM-screening agar plates containing veratryl alcohol as substrate. Agar plates were incubated for up to 24 h at 30 °C. *P. pastoris* X-33 transformed with empty vector (pPICZαA) was used as negative control.

Incubation time	Empty vector	*Pe*AAO1	*Pe*AAO1 K583E	*Pe*AAO1 ER	*Pe*AAO1 AER	*Pe*AAO1 NER	*Pe*AAO2
4 h	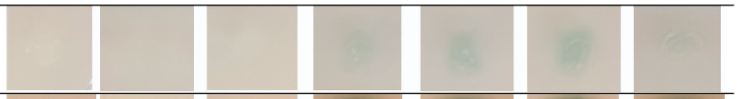						
24 h	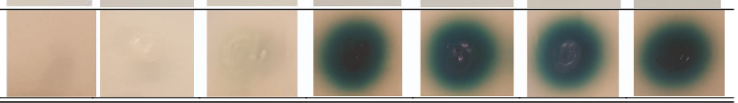						

Table 2
Development of green zones around four different *P. pastoris* colonies expressing *Pe*AAO1 variant NE on BMM-*p*-anisyl alcohol agar plates after 48 h at 30 °C.

*Pe*AAO1 NE#1	*Pe*AAO1 NE#2	*Pe*AAO1 NE#3	*Pe*AAO1 NE#4
			

substrate. An estimation of the volumetric activity (U/L) of the agar plate-screened enzymes in liquid culture based on the strength of ABTS oxidation on agar plate is, however, difficult, because of the different expression conditions on agar plate and in liquid culture (medium composition, oxygen supply, cell mass) and the dependence of coloration on colony size. Moreover, as with liquid screening assays, it is not possible to distinguish enzyme variants with improved specific activity from those with improved expression level. However, at similar expression, differences in specific activities can be detected with the developed assay. When we applied increasing concentrations of purified *Pe*AAO2 on BMM-*p*-anisyl alcohol and BMM-veratryl alcohol agar plates we observed a stronger ABTS oxidation on *p*-anisyl alcohol plates (Fig. S2) which is due to the higher specific activity of *Pe*AAO2 towards *p*-anisyl alcohol (60 U/mg) than towards veratryl alcohol (43 U/mg) (Jankowski et al., 2021).

Next, we investigated whether other AAO substrates could also be used as screening compounds. Besides a broad range of benzylic primary alcohols, AAOs were shown to oxidize aliphatic allylic primary alcohols

Table 3
Development of green zones around *P. pastoris* transformants expressing *Pe*AAO2 and *Pe*AAO1 variant K583E, respectively, on BMM-screening agar plates containing different substrates. Agar plates were incubated at 25 °C or 30 °C for up to 48 h.

Substrate		*Pe*AAO2	*Pe*AAO1 K583E		*Pe*AAO2	*Pe*AAO1 K583E
		24 h at 25 °C		48 h at 25 °C	24 h at 30 °C	
p-Anisyl alcohol	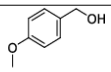	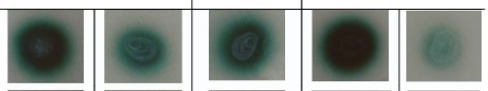				
Veratryl alcohol	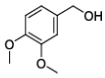					
trans,trans-2,4-Hexadien-1-ol	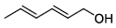	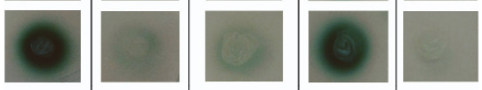				
2-Naphthalenemethanol	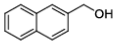	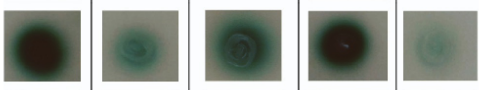				
Cinnamyl alcohol	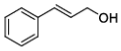	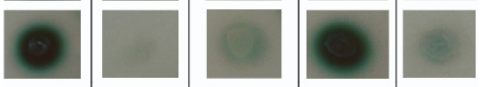				
HMF	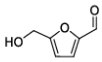	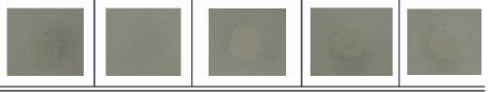				

and furan derivatives (Carro et al., 2015; Guillén et al., 1992; Jankowski et al., 2020). Therefore, besides veratryl alcohol and *p*-anisyl alcohol, we tested *trans,trans*-2,4-hexadien-1-ol, 2-naphthalenemethanol, cinnamyl alcohol and 5-hydroxymethylfurfural (HMF) as screening compounds in BMM-screening agar plates. Well-expressed *Pe*AAO2 and low-expressed *Pe*AAO1 variant K583E were chosen for assay validation. *P. pastoris* transformants were incubated on BMM-screening agar plates at both, 25 °C and 30 °C, for up to 96 h to determine the influence of incubation temperature on assay performance. Deep green zones appeared around *P. pastoris* colonies expressing *Pe*AAO2 on all BMM-screening agar plates at both temperatures already after 24 h, except for agar plates containing HMF (Table 3). This correlates with the high activity of purified *Pe*AAO2 towards 2-naphthalenemethanol, *trans,trans*-2,4-hexadien-1-ol and *p*-anisyl alcohol, while HMF was poorly oxidized by this enzyme (Jankowski et al., 2020). However, after 48 h of incubation at 25 °C a slightly green zone around *Pe*AAO2-expressing *P. pastoris* colonies appeared (Fig. S3). These results show that the developed assay can be used for screening towards different AAO substrates and is even suitable for screening towards less good substrates like HMF. The latter one is oxidized by many AAOs mainly to 5-formyl-2-furancarboxylic acid (FFCA), while oxidation of FFCA to 2,5-furandicarboxylic acid (FDCA), a building block for bioplastics, is rather low (Serrano et al., 2019). Identification of AAO variants with improved activity towards HMF and, in particular, FFCA will put development of an efficient biocatalyst for the production of FDCA from HMF a big step forward as was recently shown for an evolved *Pe*AAO1 variant (Viña-Gonzalez et al., 2020).

P. pastoris transformants expressing *Pe*AAO1 K583E developed slightly greenish zones on BMM-screening agar plates containing *p*-anisyl alcohol, veratryl alcohol and 2-naphthalenemethanol after 24 h at 25 °C (Table 3). Color development was stronger at 25 °C than at 30 °C indicating improved enzyme expression or enzyme activity at lower temperatures on agar plates as it has been reported for heterologous expression of other proteins in *P. pastoris* in liquid medium (Anasontzis et al., 2014; Dragosits et al., 2009). After 48 h at 25 °C formation of green zones around *Pe*AAO1 K583E-expressing *P. pastoris* colonies on all BMM-screening agar plates was observed, except for HMF-containing plates (Table 3) which can be explained by the low expression of *Pe*AAO1 K583E accompanied by the generally lower activity of many AAOs towards HMF compared to benzylic primary alcohols (Jankowski et al., 2020; Kadowaki et al., 2020). Increased concentrations of methanol (up to 3%) in BMM-screening agar plates to enhance expression of *Pe*AAO2 and *Pe*AAO1 K583E did not improve AAO activity on e.g. HMF-containing BMM screening agar plates but resulted in formation of slightly greenish zones around negative controls. This might be due to enhanced cell lysis at increased methanol concentrations resulting in release of AOX1 and AOX2 from *Pichia* cells and formation of H_2O_2 from methanol by these enzymes which is then used by HRP for ABTS oxidation.

To further demonstrate the applicability of the developed agar plate assay for screening of AAO mutant libraries in *P. pastoris* a small library of *Pe*AAO1 double mutants, created by site-directed mutagenesis, was screened on BMM-*p*-anisyl alcohol agar plates for improved activity. Only *P. pastoris* transformants expressing *Pe*AAO1 variant ER developed deep green zones around colonies (Fig. 1). This corresponds to the results obtained in liquid culture where the constructed double mutants, except for variant ER, showed low activity (Jankowski et al., 2021). Our results demonstrate that the developed assay can be applied for fast screening of AAO mutant libraries and thus might be used as screening tool for directed evolution campaigns in *P. pastoris*. While *S. cerevisiae* has been established as a suitable host for directed evolution (Gonzalez-Perez et al., 2012), the use of *P. pastoris* for this purpose is rather limited (Mate et al., 2013; Sandström et al., 2009; Schmidt et al., 2019). This is due to the low transformation efficiency of *P. pastoris* when using integrative plasmids and the limited number of stable episomal *P. pastoris* expression vectors. Recently, Püllmann and colleagues developed a promoter and signal peptide shuffling system for episomal high throughput expression of unspecific peroxygenases (UPOs) in *P. pastoris* (Püllmann et al., 2021; Püllmann and Weissenborn, 2021). The system was successfully applied for construction and screening of error-prone PCR-based UPO libraries in *P. pastoris* and might thus enable directed evolution campaigns of other enzymes like AAO in *P. pastoris*.

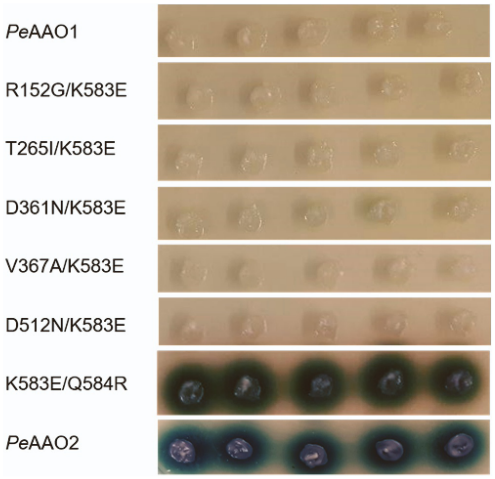

Fig. 1. Formation of green zones around different *P. pastoris* transformants expressing *Pe*AAO1, several *Pe*AAO1 double mutants and *Pe*AAO2, respectively, on BMM-agar plates containing *p*-anisyl alcohol as substrate after 24 h at 30 °C.

In conclusion, the developed agar plate-based assay can be applied for fast screening of AAOs and variants thereof in *P. pastoris* towards a broad range of substrates and is thus a promising tool for screening of AAO mutant libraries in *P. pastoris*. Improved AAO variants can be identified within 24 h by simple transfer to BMM-screening agar plates without time-consuming and laborious preculturing, cell harvesting and automated high-throughput activity testing. Finally, the agar plate-based assay described here is not restricted to AAOs and might also be applied for screening of other H_2O_2-producing enzymes like galactose oxidases or copper-radical oxidases in *P. pastoris*.

CRediT authorship contribution statement

Nina Jankowski and Katja Koschorreck conducted the experiments, analyzed the data and evaluated the results. Katja Koschorreck conceived and designed the study and drafted the manuscript. All authors read and approved the final manuscript.

Declaration of Competing Interest

The authors declare that they have no known competing financial interests or personal relationships that could have appeared to influence the work reported in this paper.

Acknowledgment

The financial support by the Bioeconomy Science Center (BioSC) through the Ministry of Innovation, Science and Research within the framework of the NRW-Strategieprojekt BioSC (No. 313/323-400-002 13) is gratefully acknowledged.

Appendix A. Supporting information

Supplementary data associated with this article can be found in the online version at doi:10.1016/j.jbiotec.2022.01.006.

References

Alexeeva, M., Enright, A., Dawson, M.J., Mahmoudian, M., Turner, N.J., 2002. Deracemization of a-methylbenzylamine using an enzyme obtained by in vitro evolution. Angew. Chem. Int. Ed. 41, 3177–3180. https://doi.org/10.1002/1521-3773(20020902)41:17<3177::Aid-Anie3177>3.0.Co;2-P.

Anasontzis, G.E., Salazar Penã, M., Spadiut, O., Brumer, H., Olsson, L., 2014. Effects of temperature and glycerol and methanol-feeding profiles on the production of recombinant galactose oxidase in *Pichia pastoris*. Biotechnol. Prog. 30, 728–735. https://doi.org/10.1002/btpr.1878.

Bell, E.L., Finnigan, W., France, S.P., Green, A.P., Hayes, M.A., Hepworth, L.J., Lovelock, S.L., Niikura, H., Osuna, S., Romero, E., Ryan, K.S., Turner, N.J., Flitsch, S. L., 2021. Biocatalysis. Nat. Rev. Methods Prim. 1, 46. https://doi.org/10.1038/s43586-021-00044-z.

Carlina, P.-G., Mónica, M.-M., Dolores, R.-D., Manuel, F., 2016. High throughput screening of esterases, lipases and phospholipases in mutant and metagenomic libraries: a review. Comb. Chem. High Throughput Screen. 19, 605–615. https://doi.org/10.2174/1386207319666151110123927.

Carro, J., Ferreira, P., Rodriguez, L., Prieto, A., Serrano, A., Balcells, B., Arda, A., Jimenez-Barbero, J., Gutierrez, A., Ullrich, R., Hofrichter, M., Martinez, A.T., 2015. 5-hydroxymethylfurfural conversion by fungal aryl-alcohol oxidase and unspecific peroxygenase. FEBS J. 282, 3218–3229. https://doi.org/10.1111/febs.13177.

Couturier, M., Mathieu, Y., Li, A., Navarro, D., Drula, E., Haon, M., Grisel, S., Ludwig, R., Berrin, J.G., 2016. Characterization of a new aryl-alcohol oxidase secreted by the phytopathogenic fungus *Ustilago maydis*. Appl. Microbiol. Biotechnol. 100, 697–706. https://doi.org/10.1007/s00253-015-7021-3.

Dragosits, M., Stadlmann, J., Albiol, J., Baumann, K., Maurer, M., Gasser, B., Sauer, M., Altmann, F., Ferrer, P., Mattanovich, D., 2009. The effect of temperature on the proteome of recombinant *Pichia pastoris*. J. Proteome Res. 8, 1380–1392. https://doi.org/10.1021/pr8007623.

Ferreira, P., Hernandez-Ortega, A., Herguedas, B., Rencoret, J., Gutierrez, A., Martinez, M.J., Jimenez-Barbero, J., Medina, M., Martinez, A.T., 2010. Kinetic and chemical characterization of aldehyde oxidation by fungal aryl-alcohol oxidase. Biochem. J. 425, 585–593. https://doi.org/10.1042/Bj20091499.

Gonzalez-Perez, D., Garcia-Ruiz, E., Alcalde, M., 2012. *Saccharomyces cerevisiae* in directed evolution: an efficient tool to improve enzymes. Bioeng. Bugs 3, 172–177. https://doi.org/10.4161/bbug.19544.

Guillén, F., Martinez, A.T., Martinez, M.J., 1992. Substrate-specificity and properties of the aryl-alcohol oxidase from the ligninolytic fungus *Pleurotus eryngii*. Eur. J. Biochem. 209, 603–611. https://doi.org/10.1111/j.1432-1033.1992.tb17326.x.

Hauer, B., 2020. Embracing nature's catalysts: a viewpoint on the future of biocatalysis. ACS Catal. 10, 8418–8427. https://doi.org/10.1021/acscatal.0c01708.

Jankowski, N., Koschorreck, K., Urlacher, V.B., 2020. High-level expression of aryl-alcohol oxidase 2 from *Pleurotus eryngii* in *Pichia pastoris* for production of fragrances and bioactive precursors. Appl. Microbiol. Biotechnol. 104, 9205–9218. https://doi.org/10.1007/s00253-020-10878-4.

Jankowski, N., Urlacher, V.B., Koschorreck, K., 2021. Two adjacent C-terminal mutations enable expression of aryl-alcohol oxidase from *Pleurotus eryngii* in *Pichia pastoris*. Appl. Microbiol. Biotechnol. https://doi.org/10.1007/s00253-021-11585-4.

Kadowaki, M.A.S., Higasi, P.M.R., de Godoy, M.O., de Araujo, E.A., Godoy, A.S., Prade, R.A., Polikarpov, I., 2020. Enzymatic versatility and thermostability of a new aryl-alcohol oxidase from *Thermothelomyces thermophilus* M77. Biochim. Biophys. Acta, Gen. Subj. 1864, 129681 https://doi.org/10.1016/j.bbagen.2020.129681.

Karnaouri, A., Zerva, A., Christakopoulos, P., Topakas, E., 2021. Screening of recombinant lignocellulolytic enzymes through rapid plate assays. In: Labrou, N.E. (Ed.), Protein Downstream Processing: Design, Development, and Application of High and Low-resolution Methods. Springer, New York, NY, pp. 479–503.

Kiiskinen, L.-L., Rättö, M., Kruus, K., 2004. Screening for novel laccase-producing microbes. J. Appl. Microbiol. 97, 640–646. https://doi.org/10.1111/j.1365-2672.2004.02348.x.

Lappe, A., Jankowski, N., Albrecht, A., Koschorreck, K., 2021. Characterization of a thermotolerant aryl-alcohol oxidase from *Moesziomyces antarcticus* oxidizing 5-hydroxymethyl-2-furancarboxylic acid. Appl. Microbiol. Biotechnol. https://doi.org/10.1007/s00253-021-11557-8.

Levasseur, A., Drula, E., Lombard, V., Coutinho, P.M., Henrissat, B., 2013. Expansion of the enzymatic repertoire of the CAZy database to integrate auxiliary redox enzymes. Biotechnol. Biofuels 6. https://doi.org/10.1186/1754-6834-6-41.

Mate, D.M., Gonzalez-Perez, D., Kittl, R., Ludwig, R., Alcalde, M., 2013. Functional expression of a blood tolerant laccase in *Pichia pastoris*. BMC Biotechnol. 13, 38. https://doi.org/10.1186/1472-6750-13-38.

Püllmann, P., Knorrscheidt, A., Münch, J., Palme, P.R., Hoehenwarter, W., Marillonnet, S., Alcalde, M., Westermann, B., Weissenborn, M.J., 2021. A modular two yeast species secretion system for the production and preparative application of unspecific peroxygenases. Commun. Biol. 4, 562. https://doi.org/10.1038/s42003-021-02076-3.

Püllmann, P., Weissenborn, M.J., 2021. Improving the heterologous production of fungal peroxygenases through an episomal *Pichia pastoris* promoter and signal peptide shuffling system. ACS Synth. Biol. 10, 1360–1372. https://doi.org/10.1021/acssynbio.0c00641.

Sandström, A.G., Engström, K., Nyhlén, J., Kasrayan, A., Bäckvall, J.-E., 2009. Directed evolution of *Candida antarctica* lipase A using an episomaly replicating yeast plasmid. Protein Eng. Des. Sel. 22, 413–420. https://doi.org/10.1093/protein/gzp019.

Schmidt, A., Shvetsov, A., Soboleva, E., Kil, Y., Sergeev, V., Surzhik, M., 2019. Thermostability improvement of *Aspergillus awamori* glucoamylase via directed evolution of its gene located on episomal expression vector in *Pichia pastoris* cells. Protein Eng. Des. Sel. 32, 251–259. https://doi.org/10.1093/protein/gzz048.

Serrano, A., Calvino, E., Carro, J., Sanchez-Ruiz, M.I., Canada, F.J., Martinez, A.T., 2019. Complete oxidation of hydroxymethylfurfural to furandicarboxylic acid by aryl-alcohol oxidase. Biotechnol. Biofuels 12, 217. https://doi.org/10.1186/s13068-019-1555-z.

Serrano, A., Carro, J., Martinez, A.T., 2020. Reaction mechanisms and applications of aryl-alcohol oxidase. Enzymes 47, 167–192. https://doi.org/10.1016/bs.enz.2020.05.005.

Urlacher, V.B., Koschorreck, K., 2021. Peculiarities and applications of aryl-alcohol oxidases from fungi. Appl. Microbiol. Biotechnol. 105, 4111–4126. https://doi.org/10.1007/s00253-021-11337-4.

Viña-Gonzalez, J., Alcalde, M., 2020. Directed evolution of the aryl-alcohol oxidase: beyond the lab bench. Comput. Struct. Biotechnol. J. 18, 1800–1810. https://doi.org/10.1016/j.csbj.2020.06.037.

Viña-Gonzalez, J., Elbl, K., Ponte, X., Valero, F., Alcalde, M., 2018. Functional expression of aryl-alcohol oxidase in *Saccharomyces cerevisiae* and *Pichia pastoris* by directed evolution. Biotechnol. Bioeng. 115, 1666–1674. https://doi.org/10.1002/bit.26585.

Viña-Gonzalez, J., Gonzalez-Perez, D., Ferreira, P., Martinez, A.T., Alcalde, M., 2015. Focused directed evolution of aryl-alcohol oxidase in *Saccharomyces cerevisiae* by using chimeric signal peptides. Appl. Environ. Microbiol. 81, 6451–6462. https://doi.org/10.1128/Aem.01966-15.

Viña-Gonzalez, J., Jimenez-Lalana, D., Sancho, F., Serrano, A., Martinez, A.T., Guallar, V., Alcalde, M., 2019. Structure-guided evolution of aryl alcohol oxidase from *Pleurotus eryngii* for the selective oxidation of secondary benzyl alcohols. Adv. Synth. Catal. 361, 2514–2525. https://doi.org/10.1002/adsc.201900134.

Viña-Gonzalez, J., Martinez, A.T., Guallar, V., Alcalde, M., 2020. Sequential oxidation of 5-hydroxymethylfurfural to furan-2,5-dicarboxylic acid by an evolved aryl-alcohol oxidase. Biochim. Biophys. Acta, Proteins Proteom. 1868, 140293 https://doi.org/10.1016/j.bbapap.2019.140293.

Weiß, M.S., Bornscheuer, U.T., Höhne, M., 2018. Solid-phase agar plate assay for screening amine transaminases. In: Bornscheuer, U.T., Höhne, M. (Eds.), Protein Engineering: Methods and Protocols. Springer, New York, NY, pp. 283–296.

Wiltschi, B., Cernava, T., Dennig, A., Galindo Casas, M., Geier, M., Gruber, S., Haberbauer, M., Heidinger, P., Herrero Acero, E., Kratzer, R., Luley-Goedl, C., Muller, C.A., Pitzer, J., Ribitsch, D., Sauer, M., Schmolzer, K., Schnitzhofer, W., Sensen, C.W., Soh, J., Steiner, K., Winkler, C.K., Winkler, M., Wriessnegger, T., 2020. Enzymes revolutionize the bioproduction of value-added compounds: from enzyme discovery to special applications. Biotechnol. Adv. 40, 107520 https://doi.org/10.1016/j.biotechadv.2020.107520.

Wu, S., Snajdrova, R., Moore, J.C., Baldenius, K., Bornscheuer, U.T., 2021. Biocatalysis: enzymatic synthesis for industrial applications. Angew. Chem. Int. Ed. 60, 88–119. https://doi.org/10.1002/anie.202006648.

2.5.1. Supplemental Information

SUPPLEMENTAL INFORMATION

Agar plate assay for rapid screening of aryl-alcohol oxidase mutant libraries in *Pichia pastoris*

Nina Jankowski [1] and Katja Koschorreck [1,*]

[1] Institute of Biochemistry, Heinrich-Heine University Düsseldorf, Universitätsstraße 1, 40225 Düsseldorf, Germany

[*] Corresponding Author

Tel. +49 211 81-10749

Fax +49 211 81-13117

Katja.Koschorreck@hhu.de

ORCID ID 0000-0001-9689-9863

SUPPLEMENTAL MATERIAL AND METHODS

Strains and enzymes

Construction of *P. pastoris* X-33 transformants with genomically integrated pPICZA_*Pe*AAO1, pPICZA_*Pe*AAO2 and pPICZA_*Pe*AAO1 variants NE (D361N/K583E), ER (K583E/Q584R), AER (V367A/K583E/Q584R), NER (D361N/K583E/Q584R), R152G/K583E, T265I/K583E, V367A/K583E and D512N/K583E, respectively, has been described elsewhere (Jankowski et al., 2020; Jankowski et al., 2021). Purification of *Pe*AAO2, ER, AER and NER was conducted as previously described (Jankowski et al., 2021).

Agar plate assay

Agar plate-based assays were conducted on Buffered Minimal Methanol (BMM, 1.34 % yeast nitrogen base without amino acids, 100 mM potassium phosphate buffer pH 6.0, 4 x 10^{-5} % biotin, 0.5 %

methanol, 2 % agar) screening agar plates supplemented with 0.5 mM 2,2'-azino-bis(3-ethylbenzothiazoline-6-sulphonic acid (ABTS), 6 µg/ml horseradish peroxidase (HRP, Type VI, Sigma-Aldrich, Schnelldorf, Germany) and 2 mM substrate (*p*-anisyl alcohol, veratryl alcohol, *trans,trans*-2,4-hexadien-1-ol, 2-naphthalenemethanol, cinnamyl alcohol and 5-hydroxymethyl furfural (HMF), respectively). Agar plates were prepared by autoclaving ddH_2O with agar and adding filter sterilized stock solutions of supplements after cooling. Recombinant *P. pastoris* X-33 cells were transferred from YPD agar plates (1 % yeast extract, 2 % peptone, 2 % dextrose, 2 % agar) with 100 µg/ml zeocin™ to BMM-screening plates using sterile pipette tips and incubated at 25 °C or 30 °C for up to 4 days.

Expression of AAO in shaking flasks

For expression of recombinant *P. pastoris* X-33 transformants in shaking flasks 10 ml Buffered Glycerol Complex medium (BMGY; 1 % yeast extract, 2 % peptone, 100 mM potassium phosphate buffer pH 6.0, 1.34 % yeast nitrogen base without amino acids, 4 x 10^{-5} % biotin, 1 % glycerol) was inoculated with *P. pastoris* transformants from YPD agar plates with zeocin and incubated at 30 °C and 200 rpm overnight. Ten ml Buffered Methanol Complex medium (BMMY, composition like BMGY, but with 0.5 % (v/v) methanol instead of glycerol) was inoculated with the overnight cultures to an optical density (OD_{600}) of 1. Cells were incubated for 3 days at 25 °C and 200 rpm and methanol (0.5 % (v/v)) was added daily. Volumetric activity of the cell-free supernatants was measured in 100 mM sodium phosphate buffer pH 6.0 using veratryl alcohol (5 mM) as substrate. Measurements were conducted on an Ultrospec 7000 photometer (GE Healthcare, Chicago, USA) by following formation of veratraldehyde (ε_{310}=9,300 M^{-1} cm^{-1}) (Guillén et al., 1992) at 310 nm. One Unit is defined as the amount of enzyme that converts 1 µmol substrate per minute.

Screening of a small AAO library

A library of six *Pe*AAO1 double mutants (R152G/K583E, T265I/K583E, D361N/K583E, V367A/K583E, D512N/K583E and K583E/Q584R) has been constructed as described elsewhere (Jankowski et al., 2021). Five randomly selected *P. pastoris* colonies each were transferred from YPD

agar plates to BMM-*p*-anisyl alcohol plates using sterile pipette tips and incubated at 30 °C for 24 h. *P. pastoris* transformants with integrated *Pe*AAO1 and *Pe*AAO2, respectively, were used as control.

SUPPLEMENTAL TABLES

Table S1 Volumetric activity of *Pe*AAO2 and *Pe*AAO1 variants in shaking flasks after 24 h and 48 h of expression at 25 °C and 200 rpm in BMMY medium, respectively. Volumetric activity was measured using veratryl alcohol as substrate.

Enzyme variant	Volumetric activity (U/L)	
	24 h	48 h
*Pe*AAO1 K583E	1.2 ± 0.3	3.7 ± 0.4
*Pe*AAO1 NE #1	2.2 ± 0.4	4.3 ± 0.5
*Pe*AAO1 NE #2	1.6 ± 0.1	4.7 ± 0.1
*Pe*AAO1 NE #3	2.3 ± 0.5	4.6 ± 0.2
*Pe*AAO1 NE #4	2.5 ± 0.2	5.5 ± 0.1
*Pe*AAO1 ER	31.5 ± 0.9	63.1 ± 0.1
*Pe*AAO1 AER	51.0 ± 2.4	103.7 ± 0.5
*Pe*AAO1 NER	62.1 ± 2.2	134.7 ± 1.7
*Pe*AAO2	23.6 ± 0.3	48.2 ± 0.2

SUPPLEMENTAL FIGURES

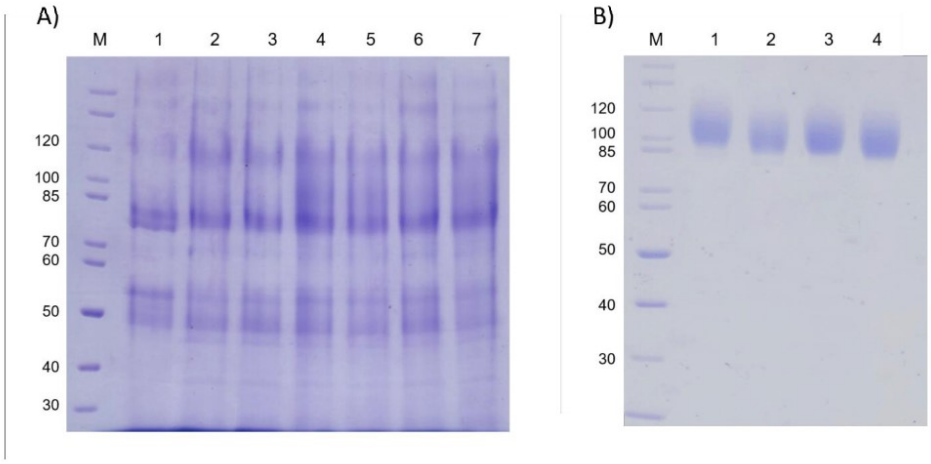

Fig. S1 SDS-PAGE analysis of AAO expression in *P. pastoris*. A) Trichloroacetic acid precipitated supernatants of *P. pastoris* cultures expressing empty vector pPICZαA (1), *Pe*AAO1 V367A/K583E (2 and 3), AER (4 and 5) and *Pe*AAO2 (6 and 7) after 3 d of cultivation in BMMY medium at 25 °C and 200 rpm. B) Purified *Pe*AAO2 (1), *Pe*AAO1 ER (2), NER (3) and AER (4) (Jankowski et al., 2021). Five µg of purified proteins were loaded onto the gel.

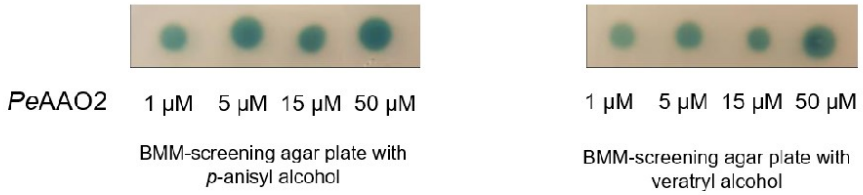

Fig. S2 Color development by purified *Pe*AAO2 on BMM-screening agar plates containing *p*-anisyl alcohol or veratryl alcohol as substrate. Increasing concentrations of purified *Pe*AAO2 (1 µL) were applied on BMM-screening agar plates. One µM of purified *Pe*AAO2 corresponds to a volumetric activity of 3.4 U/mL towards *p*-anisyl alcohol and 2.4 U/ml towards veratryl alcohol (measured spectrophotometrically). Pictures were taken after 30 min of reaction at RT.

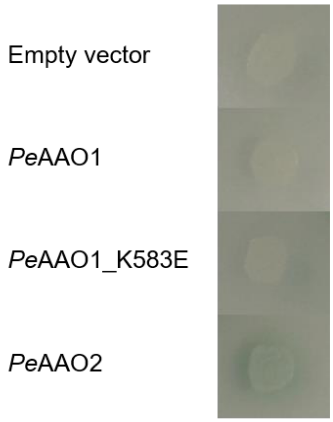

Fig. S3 Formation of green zones around *P. pastoris* transformants expressing *Pe*AAO1, *Pe*AAO1 variant K583E and *Pe*AAO2, respectively, on BMM-HMF agar plates after 48 h at 25 °C. *P. pastoris* X-33 transformed with empty vector (pPICZαA) was used as negative control.

SUPPLEMENTAL REFERENCES

Guillén, F., Martinez, A.T., Martinez, M.J., 1992. Substrate-specificity and properties of the aryl-alcohol oxidase from the ligninolytic fungus *Pleurotus eryngii*. Eur. J. Biochem. 209, 603-611. https://doi.org/10.1111/j.1432-1033.1992.tb17326.x.

Jankowski, N., Koschorreck, K., Urlacher, V.B., 2020. High-level expression of aryl-alcohol oxidase 2 from *Pleurotus eryngii* in *Pichia pastoris* for production of fragrances and bioactive precursors. Appl. Microbiol. Biotechnol. 104, 9205-9218. https://doi.org/10.1007/s00253-020-10878-4.

Jankowski, N., Urlacher, V.B., Koschorreck, K., 2021. Two adjacent C-terminal mutations enable expression of aryl-alcohol oxidase from *Pleurotus eryngii* in *Pichia pastoris*. Appl Microbiol Biotechnol. https://doi.org/10.1007/s00253-021-11585-4.

2.6. Chapter VI: Biocatalytic applicability of *Pe*AAO2

Title Aryl-alcohol-oxidase-mediated synthesis of piperonal and other valuable aldehydes

Authors Nina Jankowski, Katja Koschorreck, Vlada B. Urlacher

Contribution Design, planning and conduction of all experiments, evaluation of all data, drafting of the manuscript. Relative contribution: 90 %

Published in *Advanced Synthesis & Catalysis,* 364, 2364–2372 (**2022**)

DOI 10.1002/adsc.202200381

Publisher Wiley-VCH

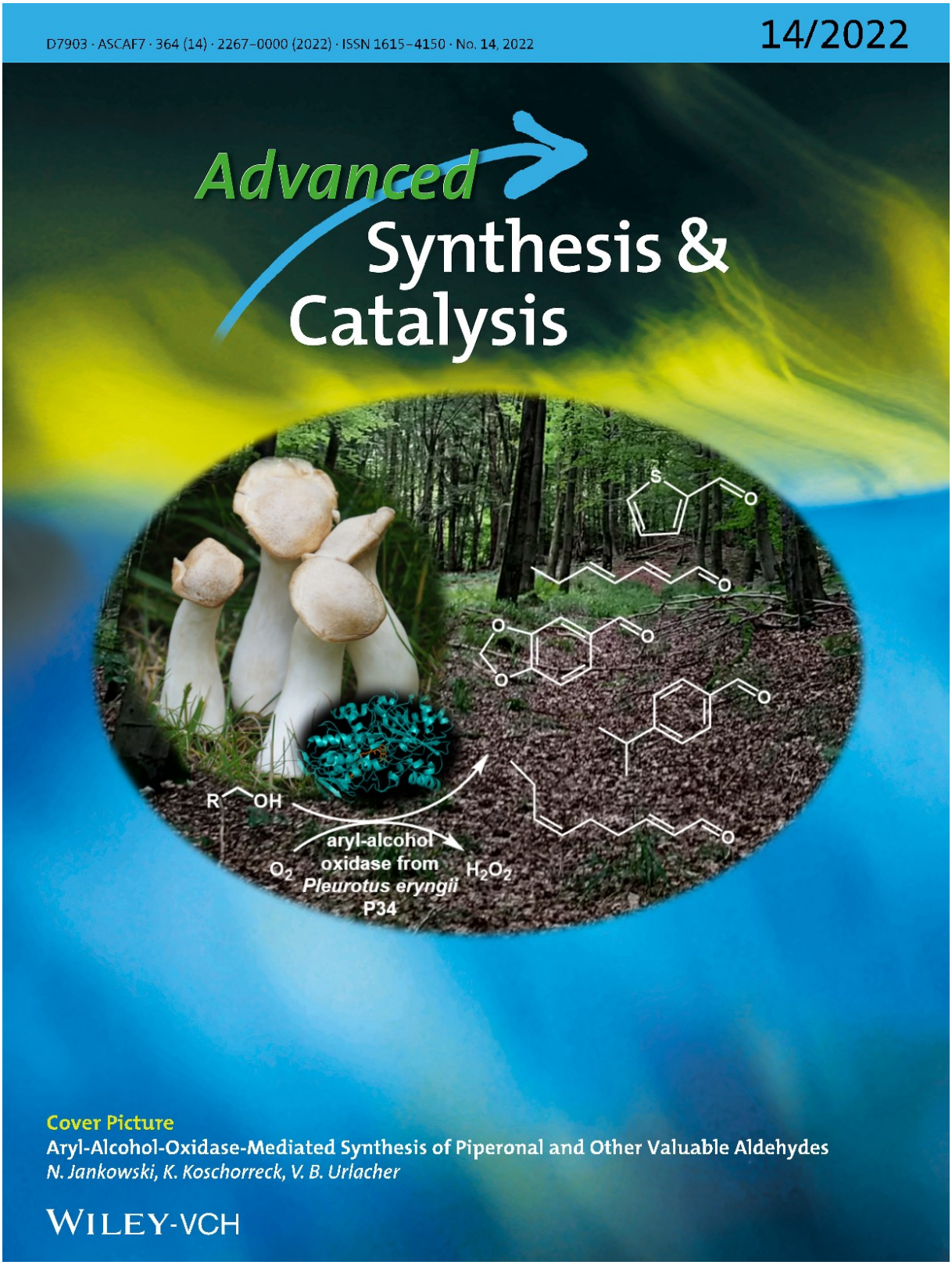
D7903 · ASCAF7 · 364 (14) · 2267–0000 (2022) · ISSN 1615–4150 · No. 14, 2022
14/2022
Advanced Synthesis & Catalysis
R OH
O2
aryl-alcohol oxidase from Pleurotus eryngii P34
H2O2
Cover Picture
Aryl-Alcohol-Oxidase-Mediated Synthesis of Piperonal and Other Valuable Aldehydes
N. Jankowski, K. Koschorreck, V. B. Urlacher
WILEY-VCH

COVER

Aryl-Alcohol-Oxidase-Mediated Synthesis of Piperonal and Other Valuable Aldehydes

Adv. Synth. Catal. **2022**, *364*, 1–2

N. Jankowski, K. Koschorreck, V. B. Urlacher*

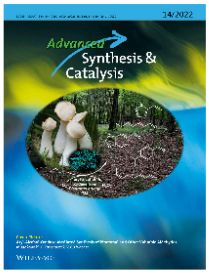

The front cover image illustrates the oxidation of primary aromatic and aliphatic allylic alcohols to valuable aldehydes catalyzed by a recombinant aryl-alcohol oxidase of *Pleurotus eryngii* P34. This versatile enzyme demonstrates high stability against the by-product of the reaction, H_2O_2, and in the presence of organic solvents. After reaction optimization, a space-time-yield of 9.5 g piperonal/l/h was achieved on a preparative scale. The produced aldehydes are of great interest as fragrances or building blocks in the synthesis of pharmaceuticals. Further details can be found in the Research Article by Urlacher and co-workers (N. Jankowski, K. Koschorreck, V. B. Urlacher, *Adv. Synth. Catal.* **2022**, *364*, XXXX–XXXX; DOI: 10.1002/adsc.202200381)

RESEARCH ARTICLE doi.org/10.1002/adsc.202200381 Advanced Synthesis & Catalysis

Very Important Publication

Aryl-Alcohol-Oxidase-Mediated Synthesis of Piperonal and Other Valuable Aldehydes

Nina Jankowski,[a] Katja Koschorreck,[a] and Vlada B. Urlacher[a,*]

[a] Institute of Biochemistry, Heinrich-Heine University Düsseldorf, Universitätsstraße 1, 40225 Düsseldorf, Germany
E-mail: Vlada.Urlacher@uni-duesseldorf.de

Manuscript received: April 7, 2022; Revised manuscript received: June 3, 2022;
Version of record online: June 21, 2022

Dedicated to Professor Rolf D. Schmid on the occasion of his 80th birthday.

Supporting information for this article is available on the WWW under https://doi.org/10.1002/adsc.202200381

Abstract: The use of fungal aryl-alcohol oxidases in biocatalysis is still modest, despite their advantageous capability to produce valuable aldehydes via oxidation of the respective alcohols without the need for costly external cofactors. For biocatalytic application, enzyme stability in the presence of organic solvents used for substrate solubilization has to be investigated, and process limitations due to low oxygen supply and the accumulation of the by-product H_2O_2 must be addressed. In this study, we showed that the aryl-alcohol oxidase *Pe*AAO2 from *Pleurotus eryngii* P34 remained active and stable in the presence of up to 30% (*v/v*) various organic solvents and up to 500 mM H_2O_2. The potential of this biocatalyst was explored based on conversion of piperonyl alcohol to the fragrance compound piperonal. After reaction optimization, product titers of up to 245 mM were achieved within 3 h. Addition of catalase was imperative to re-introduce O_2 as co-substrate into the reaction, thereby diminishing oxygen limitation. On a preparative scale, space-time-yield of 9.5 g/l/h was achieved and 244.6 mg piperonal (85% yield) with >99% purity were isolated via simple crystallization from *n*-hexane extract. Under optimized reaction conditions four other substrates, cumic alcohol, 2-thiophenemethanol, *trans,trans*-2,4-heptadienol and *trans*-2-*cis*-6-nonadienol, at concentrations of up to 300 mM were converted to the corresponding aldehydes within 20 h. Our results demonstrate that *Pe*AAO2 is a versatile and promising biocatalyst for the production of valuable aldehydes.

Keywords: Biocatalysis; Aryl-alcohol oxidase; Enzymes; Hydrogen peroxide; Aldehydes; Piperonal; Flavors

Introduction

Selective oxidations of primary and secondary alcohols leading to aldehydes, acids or ketones are reactions that are relevant for the pharmaceutical and the flavor and fragrance industries but still challenging for chemical catalysts.[1] These reactions often require harsh conditions, hazardous reactants and yield toxic waste.[2] The switch towards more sustainable and environmentally friendly processes with emphasis on waste prevention and avoidance of hazardous compounds paved the way for the use of biocatalysts under mild reaction conditions.[3]

The application of fungal aryl-alcohol oxidases (AAOs, EC 1.1.3.7) in biocatalysis has gained increasing interest over the last years. These flavoenzymes catalyze the oxidation of a variety of primary aromatic and aliphatic allylic alcohols, do not require costly external cofactors, and are active under mild reaction conditions with O_2 as terminal electron acceptor yielding H_2O_2 as the only by-product.[4] The major research attention regarding the use of AAOs as biocatalysts has been laid on conversion of the bio-

RESEARCH ARTICLE asc.wiley-vch.de Advanced Synthesis & Catalysis

based substrate 5-hydroxymethylfurfural into the polymer-precursor 2,5-furandicarboxylic acid, either applied as a single enzyme or in conjunction with other oxidizing enzymes.[5] More recently, protein engineering was employed to switch the substrate preference of AAOs towards secondary alcohols to produce the corresponding ketones, enabling kinetic resolution of racemic mixtures of alcohols.[6]

The substrates of AAOs, benzylic and aliphatic unsaturated alcohols, are oxidized to aldehydes which quite often have unique sensory features and are of value as flavors and fragrances to a wide variety of industrial products including food and beverages, cosmetics and household items.[7] An AAO from the fungus *Pleurotus eryngii* ATCC 90787 (*Pe*AAO) was applied for the synthesis of the flavor and fragrance compound *trans*-2-hexenal ("leaf aldehyde"[8]) in a two-liquid-phase-system and in a continuous-flow microreactor, reaching catalytic turnovers of over two millions.[9] However, after expression in *Escherichia coli* recombinant *Pe*AAO has to be purified from inclusion bodies, which necessitates *in vitro* refolding and yields around 45 mg of active enzyme per liter of cell culture.[10,9b] Directed evolution campaigns enabled expression of *Pe*AAO variant FX9 in *Pichia pastoris* at 25.5 mg/l,[11] which is still insufficient for application as biocatalyst at larger scales. In our previous work, we showed that *Pe*AAO2 from *P. eryngii* P34 is produced in *P. pastoris* at one of the highest reported yields for an AAO (315 mg/l).[12] Its broad substrate scope, high pH and thermal stability along with high expression levels make this enzyme a promising AAO for the production of valuable aldehydes like e.g. piperonal, the oxidation product of piperonyl alcohol **1a**. Catalytic efficiency of *Pe*AAO2 during **1a** oxidation is more than 25-fold higher than in the reaction with benzyl alcohol, a typical AAO substrate.[12,13] Piperonal **1b** (also termed as "heliotropin") is a valuable flavor and fragrance compound and can serve as intermediate in the synthesis of pharmaceutical and agrochemical compounds.[14] On an industrial scale, the production of **1b** occurs via oxidative cleavage of isosafrole using oxidants like chromium(VI) salts, or via electrochemical procedures starting with either isosafrole or **1a**.[15] More recently, production of **1b** through a whole-cell biotransformation of isosafrole or piperonylic acid **1c** by utilizing a *trans*-anethole oxygenase or carboxylate reductase has been reported.[16]

Here, we assessed the biotechnological potential of *Pe*AAO2 during the oxidation of **1a** to **1b** as a model reaction. The influence of organic solvents and H_2O_2 on enzyme activity and stability was investigated followed by optimization of the reaction conditions regarding substrate concentration, O_2 supply and temperature. Oxidation of **1a** was scaled up to 300 mg-scale. Finally, production of other valuable aldehydes, namely cuminal **2b**, 2-thiophenecarboxaldehyde **3b**, *trans,trans*-2,4-heptadienal **4b** and *trans*-2-*cis*-6-nonadienal **5b** was investigated under the optimized reaction conditions.

Results and Discussion

In order to develop efficient biocatalytic processes relying on AAOs, some issues like the stoichiometric production of H_2O_2, particularly at high substrate concentrations, oxygen limitation in aqueous media and low solubility of hydrophobic substrates in water have to be addressed. Moreover, if the formed aldehyde (piperonal **1b** in our model reaction, Scheme 1) is present in its hydrated form (*gem*-diol), it might serve as a substrate for AAO and result in formation of the over-oxidation product (piperonylic acid **1c**) and thus reduce product yields. For aromatic substrates, the presence of electron-withdrawing or electron-donating ring substituting groups seems to stabilize or destabilize the *gem*-diol intermediate.

Addition of organic solvents usually enhances availability of hardly water-soluble substrates for biocatalytic conversions but can negatively influence enzyme stability and activity. Thus, optimization of reaction conditions like reaction time, substrate concentration and the choice of organic solvent are essential for effective enzyme performance.

Regarding the negative effect of high H_2O_2 concentration on enzyme activity/stability, addition of catalase was shown to retain oxidases' activity and therefore enhance product yield.[5b,16a] On the one hand, catalase decomposes deleterious H_2O_2 to O_2 and H_2O and, on

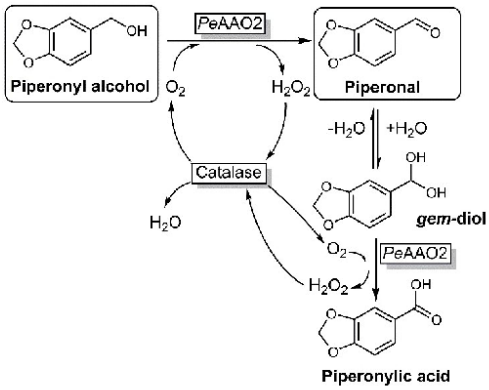

Scheme 1. Oxidation of **1a** to **1b** catalyzed by *Pe*AAO2 at the expense of molecular O_2. The by-product H_2O_2 is decomposed by catalase to H_2O and O_2 which fuels the AAO reaction. If the aldehyde product is hydrated to form the *gem*-diol, it may be further oxidized to **1c**.

RESEARCH ARTICLE asc.wiley-vch.de Advanced Synthesis & Catalysis

the other hand, re-introduces O_2 into the system. In order to address all these issues and elucidate *Pe*AAO2's potential for biotechnological applications, we investigated, at first, the influence of H_2O_2 and organic solvents on the enzyme's activity and stability.

Influence of H_2O_2

External H_2O_2 of up to 100 mM had a low impact on *Pe*AAO2's performance with a relative activity towards piperonyl alcohol **1a** of 97% compared to a control without external H_2O_2 (Figure S1). Even with 500 mM H_2O_2, enzyme activity remained above 90% and still reached 48% after addition of 4 M H_2O_2. Likewise, the stability of *Pe*AAO2 was hardly affected by incubation in the presence of H_2O_2. Relative activities of around 90% were recorded after 24 h incubation in up to 200 mM H_2O_2 and 74% of its initial activity remained after incubation with 500 mM H_2O_2 (Figure S2). After 96 h incubation, above 80% of the initial activity remained in the presence of up to 100 mM H_2O_2, and activity still reached 42% after incubation with 500 mM H_2O_2. For comparison, *Ma*AAO from *Moesziomyces antarcticus* lost all its activity after 24 h incubation at 500 mM H_2O_2,[5d] and the FAD-dependent 5-hydroxymethylfurfural oxidase (HMFO) from *Methylovorus sp.* MP688 retained only 20% of its initial activity after 72 h in the presence of 30 mM H_2O_2.[17] High stability of *Pe*AAO2 can be due to its high degree of glycosylation. It contains 8 potential *N*-glycosylation sites, and *N*-deglycosylation revealed 30% *N*-glycosylation extent,[12] while *Ma*AAO possesses 6 potential *N*-glycosylation sites with an *N*-glycosylation extent of 11%.[5d] Additionally, a cysteine residue located on the surface of *Ma*AAO can be oxidized by H_2O_2, which would negatively affect the enzyme's stability. On the surface of *Pe*AAO2 there are two cysteine residues forming a disulfide bridge, which can also contribute to the observed high stability against H_2O_2.

Influence of Organic Solvents

Further, the influence of organic solvents on activity and stability of *Pe*AAO2 was evaluated. The enzyme activity was tested in presence of up to 50% (*v*/*v*) of the following organic solvents: acetone, acetonitrile, methanol, ethanol, 2-propanol, dimethylformamide (DMF), dimethyl sulfoxide (DMSO) and tetrahydrofuran (THF). Methanol, ethanol, 2-propanol and DMSO had the lowest impact on *Pe*AAO2's activity with relative activities of around 80 to 90% at volume percentages of 30% (*v*/*v*), and at 50% (*v*/*v*) organic solvent the highest relative activity of 72% was measured with 2-propanol (Figure 1). THF at concentrations of 30 or 50% (*v*/*v*) had a slightly stronger effect as compared to methanol and ethanol, with

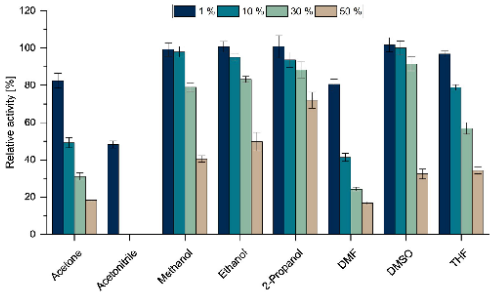

Figure 1. Effect of organic solvents on *Pe*AAO2 activity. The enzyme was incubated for 5 min with 1, 10, 30 or 50% (*v*/*v*) of organic solvents in 100 mM sodium phosphate buffer pH 6, before measuring the activity towards 5 mM **1a**. A control reaction without organic solvents was set as 100%. All reactions were carried out in triplicate.

relative activities of 57 and 34%, respectively. Acetone and DMF had a strong negative effect leading to 49% and 41% remaining activity at only 10% (*v*/*v*), respectively, while with 1% (*v*/*v*) acetonitrile relative activity was halved and with 10% (*v*/*v*) the enzyme completely lost its activity.

Next, enzyme stability in the investigated organic solvents was evaluated. At up to 30% (*v*/*v*) of most of the tested solvents, *Pe*AAO2 remained stable for 96 h with relative activities of around 90% (Figure 2). Acetonitrile had the most severe effect; after 24 h in the presence of 30% (*v*/*v*) the activity dropped to 17% and further declined to 5% after 96 h.

In general, only scarce information about activity and stability of AAOs in the presence of organic solvents is available, although their evaluation is essential for application of the respective enzymes in biotechnological processes, where organic solvents are applied to achieve high substrate concentrations. *Ma*AAO from *M. antarcticus* was reported to possess a similar high stability in the presence of up to 20% (*v*/*v*) DMSO after 24 h, with a remaining activity of almost 100%.[5d] However, at 30% DMSO around 30% relative activity of *Ma*AAO was registered, while *Pe*AAO2 retained 90% of its original activity under these conditions. As mentioned above, the higher degree of *N*-glycosylation of *Pe*AAO2 compared to *Ma*AAO might contribute to the higher stability of *Pe*AAO2 in organic solvents.

Long-term storage stability of purified *Pe*AAO2 was evaluated as well. The enzyme was stored in 50 mM potassium phosphate buffer pH 6 at 4 °C for 388 days and still reached 96% of its initial activity measured directly after purification (Figure S3). Even though the flavin cofactor FAD is non-covalently

RESEARCH ARTICLE asc.wiley-vch.de Advanced Synthesis & Catalysis

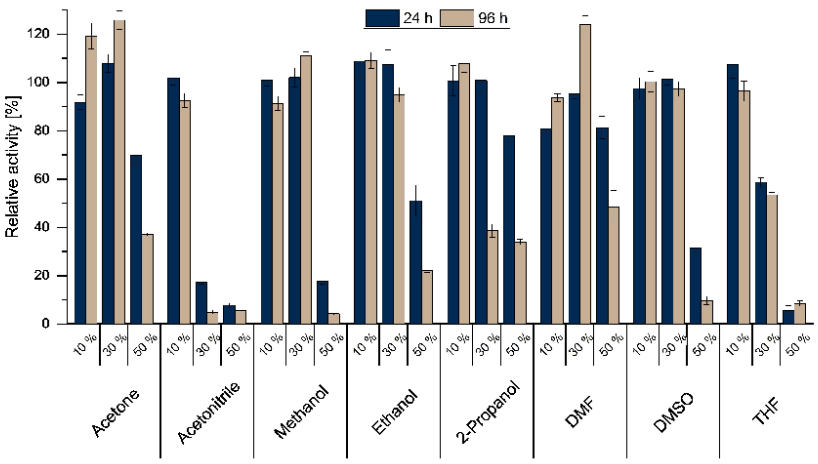

Figure 2. Stability of *Pe*AAO2 in the presence of organic solvents at 25 °C. The enzyme was incubated with the respective volume percentage (*v/v*) of solvents for the indicated time periods. Remaining activity towards 5 mM **1 a** was measured in 100 mM sodium phosphate buffer pH 6, containing finally 1/100 of the solvent volume percentage. Activity immediately after enzyme addition to the respective organic solvent was set as 100%. All reactions were carried out in triplicate.

bound to AAOs,[18] the holoenzyme stays intact for a long period of time under storage conditions.

High activity of *Pe*AAO2 in the presence of organic solvents along with its high tolerance towards these solvents and high storage stability are clearly advantageous properties that render this AAO a promising biocatalyst for biotechnological applications.

Reaction Optimization

Due to the high stability of *Pe*AAO2 in the presence of DMSO, the latter was chosen as co-solvent in the experiments on **1 a** oxidation. For reaction optimization, different reaction parameters were investigated including substrate concentration, amount of catalase, conversion time, temperature and shaking speed (Figure 3). Reactions were conducted in 100 mM potassium phosphate buffer pH 6. Activity of *Pe*AAO2 towards **1 a** was hardly influenced by the type of buffer system and pH value in the range from 4 to 7 (Figure S4).

Up to 70 mM **1 a** were completely converted to **1 b** but to some extent further oxidized to **1 c** under the starting conditions (1 μM *Pe*AAO2, 25 °C, 600 rpm for 20 h) with 100 U/ml catalase (entry E1 to E4 in Figure 3). At 100 mM substrate, no over-oxidation occurred, and 97% conversion was reached (E5). Without catalase, a two-times lower conversion of 100 mM **1 a** was observed (ES5 in Figure S5).

By further increasing the catalase concentration to 1000 U/ml, full conversion of 100 mM substrate was achieved but again **1 c** (3%) was detected (E6). Whereas under the same reaction conditions, 150 mM **1 a** were completely converted to **1 b** without further over-oxidation to **1 c** (E7), at substrate concentrations ranging from 200 to 300 mM conversion was incomplete (E8 to E10). Increased concentrations of catalase (2000 U/ml) in reaction with 300 mM substrate resulted in 53% conversion (E11), which is only slightly higher compared to reactions with 1000 U/ml catalase (51% conversion).

Due to this marginal increase in product content, we concluded that 1000 U/ml catalase was sufficient to boost the conversion of **1 a** to **1 b** by *Pe*AAO2 mainly by re-introducing molecular O_2 into the reaction mixture since H_2O_2 had a marginal effect on the enzyme's activity and stability (shown above).

At 300 mM **1 a**, only 53% were converted to **1 b** after 20 h under the conditions used (25 °C, 600 rpm, 1000 U/ml catalase). To achieve higher product concentration, the reaction time was prolonged to 44 h, which increased conversion to 79% (E12). When switching to 30 °C, conversion was further increased to 83% (E13). Finally, the shaking speed was varied and instead of 600 rpm, both 1000 and 1500 rpm were tested: At 1000 rpm, 91% and at 1500 rpm even 97% conversion of 300 mM **1 a** was achieved (E14 and E15). Obviously, the availability of O_2 was the limiting factor in conversion of **1 a** and has to be addressed to achieve high productivities, especially at high substrate concentrations. The solubility of gaseous O_2 from air in aqueous medium is rather low (0.268 mM, 25 °C,

RESEARCH ARTICLE asc.wiley-vch.de Advanced Synthesis & Catalysis

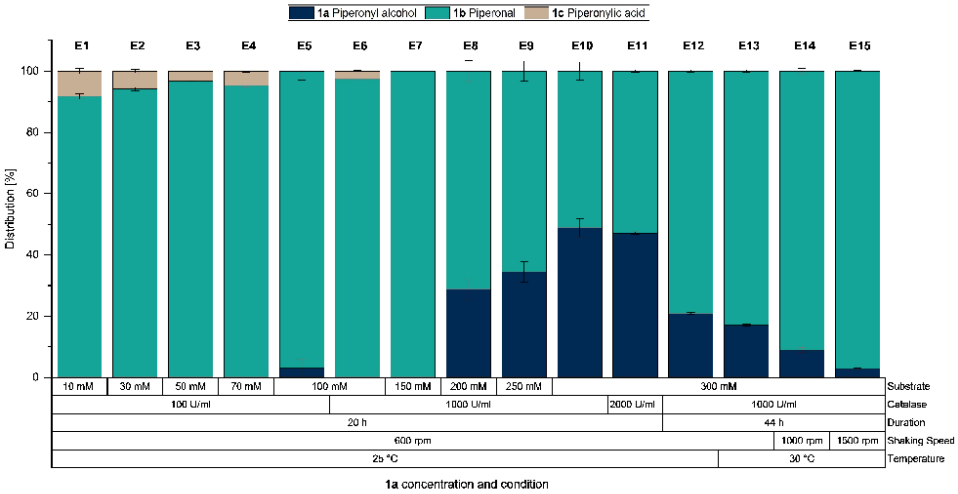

Figure 3. Optimization of **1 a** oxidation. Conditions: 10 to 300 mM **1 a**, 1 µM *Pe*AAO2 in 100 mM potassium phosphate buffer pH 6. Variation of the following parameters: Catalase was added at 100, 1000 or 2000 U/ml, reaction time was 20 h or 44 h, shaking speed was 600, 1000 or 1500 rpm and temperature was 25 °C or 30 °C. Each entry is named with E1 to E15. Content of DMSO varied from 8 to 24% (*v/v*). Substrate/product distribution (%) was calculated based on peak area. All reactions were carried out in duplicate.

1 atm pressure).[19] It was reported that the use of pure oxygen instead of air increased the maximum O_2 solubility five-fold in water,[20] but is expensive and requires specialized equipment.

Other strategies to enhance O_2 concentration and thereby process productivity include benchtop continuous-flow reaction systems to easily improve O_2 availability in reactions without the need for specialized equipment or pressurized gas.[21] A similar approach has already been applied in a continuous-flow microreactor during the oxidation of *trans*-2-hexenol to the corresponding *trans*-2-hexenal catalyzed by aryl-alcohol oxidase *Pe*AAO.[9a]

Under the optimized reaction condition (30 °C, 1500 rpm, 1000 U/ml catalase, 1 µM *Pe*AAO2), conversion of 300 mM **1 a** was followed over 48 h. 245 mM **1 b** were produced within 3 h and product concentration further increased to 274 mM after 6 h of reaction (Figure S6). After 48 h, the substrate was almost completely converted to 292 mM **1 b**, while no over-oxidation to **1 c** was observed (Figure S16). With this setup, a turnover number of 292.000 and a space-time yield of 12.3 g/l/h was achieved. A higher turnover number in AAO-catalyzed reactions was only reported in production of *trans*-2-hexenal from *trans*-2-hexenol employing *Pe*AAO in a biphasic system.[9b]

Piperonal Production on a Preparative Scale

Next, **1 a** conversion was conducted at three hundred milligram scale (304.3 mg). 2-Propanol instead of DMSO was used as co-solvent to simplify product isolation and to substitute for DMSO, that is hard to get rid of.[22] In an initial experiment on a small scale, 0.5 µM of *Pe*AAO2 were sufficient to convert around 96% of 200 mM substrate within 3 h to **1 b** (data not shown). Furthermore, reactions in baffled Erlenmeyer flasks resulted in a higher conversion than in non-baffled flasks, most likely due to better aeration and thus better O_2 supply (data not shown).

Baffled flasks with 0.5 µM *Pe*AAO2 were chosen for the preparative scale production of **1 b**. Within 3 h, 95% of the substrate **1 a** were converted to **1 b**. After extraction by *n*-hexane and evaporation, the clear residue crystallized to a white solid as **1 b** with > 99% purity (GC). 244.6 mg **1 b** were isolated at 85% yield (Figure S7 - S15 and Table S2 - S4). This corresponds to a space-time yield of 9.5 g/l/h and a turnover number of the enzyme of 380.000. Schwendenwein *et al.* reported on biocatalytic production of **1 b** using a fungal carboxylate reductase and **1 c** as substrate.[16a] Productivity was around 1.5 g/l/h with 30 mM substrate in 200 ml reaction volume, but instead of isolated enzyme, a recombinant *E. coli* whole-cell biocatalyst was used.

RESEARCH ARTICLE asc.wiley-vch.de Advanced Synthesis & Catalysis

Extension to Other Substrates

To demonstrate the versatility of *Pe*AAO2 for biocatalytic applications, four other substrates, namely cumic alcohol **2a**, 2-thiophenemethanol **3a**, *trans,-trans*-2,4-heptadienol **4a** and *trans*-2-*cis*-6-nonadienol **5a**, were chosen for conversion under the optimized reaction conditions. The expected aldehydes are of great interest to various medical fields, and the flavor and fragrance industry. Cuminal **2b**, the reaction product of **2a** oxidation, possesses among others antibiofilm, anticancer, antidiabetic, antifungal and neuroprotective properties.[23] The heterocyclic thiophene moiety is present in many pharmacologically active compounds, predominantly showing anticancer, anti-inflammatory and antidepressant effects.[24] 2-Thiophenecarboxaldehyde **3b** itself was used as building block for the synthesis of various anticancer- and apoptosis inducing compounds as well as in the production of thiophene–chitosan hydrogels, which facilitate removal of toxic heavy metal ions such as mercury from contaminated water with high efficiency.[25] *Trans*-2-*cis*-6-nonadienal **5b** (also termed as "violet leaf aldehyde" or "cucumber aldehyde") is among the most potent fragrance compounds and is found in aroma of various fruits and flower scents.[8,26]

10 and 100 mM of each **2a**, **3a** and **4a** were completely converted to the corresponding aldehydes within 20 h (Table 1, Figure S17–S19). Only in the reaction with 100 mM **4a**, 6% of the product *trans,-trans*-2,4-heptadienal **4b** were further oxidized to *trans,trans*-2,4-heptadienoic acid **4c** (Table 1 and Figures S19–S22). Within 20 h, 10 mM **5a** was completely converted to **5b**, while 100 mM were converted to 87% (Figures S23 and S24). In reactions with 300 mM substrate, conversions reached more than 80% within 20 h, except for substrate **5a**, which was converted to 49.7%. **5a** is the "poorest" *Pe*AAO2 substrate with a relative activity of only 0.7% as compared to **1a** (set as 100%).[12]

As mentioned above, over-oxidation to the corresponding acid was only observed with 100 mM **4a**, which is the "best" substrate in this study with a relative activity of 163% compared to **1a**.[12] At 10 mM **4a** the over-oxidation product was not detected but its concentration can be lower than the detection limit. An excess of **4a** (300 mM) in the reaction mixture might protect the aldehyde product **4b** from over-oxidation. The absence of the over-oxidation product in the reactions with **2a** and **3a** may be due to the absence or low stability of *gem*-diols of the respective aldehydes, or the enzyme's affinity to the formed *gem*-diols is low and therefore no over-oxidation was observed.

Our results emphasize the high potential of *Pe*AAO2 for biocatalytic application, as it can achieve

Table 1. Conversion of further primary alcohols. Conditions: 10 to 300 mM substrates **2–5a**, 1 μM *Pe*AAO2, 1000 U/ml catalase, 30 °C, 1500 rpm for 20 h in 100 mM potassium phosphate buffer pH 6. Conversion (%) of substrate was calculated by comparing to a control without enzyme and by calculating the substrate/internal standard 2-naphthol ratio. Product distribution (%) was calculated based on peak areas. All reactions were carried out in duplicate.

Compound		Rel. activity [%][a]	Time [h]	2-5a [mM]	Conv. [%]	Product distribution [%]	
						Aldehyde 2–5b	Acid 2–5c
2a	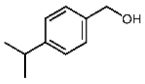	49	20	10	100	100	–
				100	100	100	–
				300	97.9	100	–
3a		5.2	20	10	100	100	–
				100	100	100	–
				300	85.6	100	–
4a	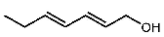	163	20	10	100	100	n.d.[b]
				100	100	94.0	6.0
				300	99.8	100	–
5a	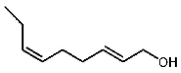	0.7	20	10	100	100	–
				100	87.0	100	–
				300	49.7	100	–

[a] Relative activity as compared to **1a** (set to 100%); values taken and calculated new from [12].
[b] Not detectable.

RESEARCH ARTICLE asc.wiley-vch.de Advanced Synthesis & Catalysis

high product amounts in a short time under optimized reaction conditions even with less "good" substrates.

Conclusion

Here, we demonstrated the potential of aryl-alcohol oxidase *Pe*AAO2 from *P. eryngii* P34 for the production of flavor and fragrance compounds and substances with diverse beneficial medicinal properties. *Pe*AAO2 demonstrates high robustness and tolerates high concentrations of several organic solvents and H_2O_2.

After optimization of reaction conditions, a space-time-yield of 9.5 g/l/h was achieved on a 300 mg preparative scale in the conversion of piperonyl alcohol **1a** to the flavor and fragrance compound piperonal **1b**. Product isolation via simple crystallization yielded **1b** at high purity of > 99%.

The versatility of this biocatalyst was underlined by the conversion of other chemically diverse substrates at concentrations of up to 300 mM to industrially relevant aldehydes. This makes *Pe*AAO2 a promising enzyme for application in biocatalysis.

Experimental Section

Materials

All reagents were of analytical grade. Catalase from bovine liver (EC 1.11.1.6), piperonal (99.9%), 2-thiophenemethanol (98%) and *trans*-2-*cis*-6-nonadien-1-ol (98.6%) were purchased from Sigma-Aldrich (Schnelldorf, Germany). Piperonyl alcohol (98%), cuminal (98%), cumic acid (98%) and 2-thiophenecarboxaldehyde (98%) were obtained from J&K Scientific (Lommel, Belgium), cumic alcohol (97%) and piperonylic acid (99%) from Acros Organics (Geel, Belgium). *trans,trans*-2,4-Heptadien-1-ol and 2-thiophenecarboxylic acid (98%) were purchased from Alfa Aesar (Kandel, Germany) and 2-naphthol (99%) from TCI Chemicals (Eschborn, Germany).

Production and Purification of *Pe*AAO2

The aryl-alcohol oxidase 2 (*Pe*AAO2) from the fungus *P. eryngii* P34 was produced in a fed-batch fermentation process using the methylotrophic yeast *Pichia pastoris* and purified to homogeneity in three consecutive chromatographic purification steps as described previously.[12]

Activity and Stability in the Presence of H_2O_2 and Organic Solvents

The effect of H_2O_2 and organic solvents on the activity of *Pe*AAO2 was evaluated in a spectrophotometric assay with different concentrations of H_2O_2 (100 mM to 4 M) and organic solvents (1 to 50% (*v/v*)). The following solvents were investigated: acetone, acetonitrile, methanol, ethanol, 2-propanol, dimethylformamide (DMF), dimethyl sulfoxide (DMSO) and tetrahydrofuran (THF). Different amounts of H_2O_2 and organic solvents were mixed with an appropriately diluted sample of *Pe*AAO2 in sodium phosphate buffer (100 mM, pH 6) and incubated for 5 min at room temperature prior the addition of the substrate piperonyl alcohol **1a** (5 mM). The oxidation to piperonal **1b** was followed at 317 nm in a 96-well micro plate using an Infinite M200 Pro plate reader (Tecan, Männedorf, Switzerland). The molar extinction coefficient of **1b** ($\varepsilon_{317} = 8{,}680\ M^{-1}\ cm^{-1}$)[12] was used to calculate volumetric activities from the initial reaction rate according to Lambert-Beer's law. The relative activities were calculated related to a control without added H_2O_2 or organic solvent.

For stability analysis, *Pe*AAO2 was incubated in potassium phosphate buffer (50 mM, pH 6) with different H_2O_2 concentrations (10 to 500 mM) or with organic solvents (10, 30 or 50% (*v/v*)) over a period of 96 h at 25 °C. After certain time points, samples were taken and the relative activity towards **1a** (5 mM) was determined as described above. For H_2O_2 stability determination, samples were diluted 1:10, and for organic solvent stability determination samples were diluted 1:100, resulting in final percentages of 0.1 to 0.5% of the solvents in the spectrophotometric assay.

Initial Conversion Experiments

All biocatalytic conversions of **1a** were carried out in 1.5 ml safe-lock reaction tubes with a total reaction volume of 125 µl in potassium phosphate buffer (100 mM, pH 6) for 20 h at 25 °C and 600 rpm (Thermomixer C, Eppendorf). All reactions were done in duplicate. In the initial experiments, *Pe*AAO2 (1 µM) was used to convert **1a** (10 to 100 mM) prepared from a stock solution (500 mM in DMSO), resulting in final DMSO concentration of up to 20% (*v/v*). Conversion products were analyzed via GC/MS (see below).

Optimization of Reaction Conditions

The same reactions mixtures as stated above in potassium phosphate buffer (100 mM, pH 6) were supplemented with catalase from bovine liver (100, 1000 or 2000 U/ml dissolved in 100 mM potassium phosphate buffer pH 6) to remove produced H_2O_2. The concentration of **1a** was further increased to 300 mM (from 500 mM stock solution in 40% DMSO/potassium phosphate buffer, to give a final DMSO concentration of 24% (*v/v*)). During conversion of **1a** (300 mM), catalase (1000 U/ml) was added, and the reaction time was extended to 44 h. To investigate the effect of increased temperature and shaking speed, both parameters were varied: 25 vs. 30 °C and 600 rpm vs. 1000 and 1500 rpm, respectively.

Time Course

Conversion of **1a** (300 mM) was carried out under the optimized conditions in potassium phosphate buffer (100 mM, pH 6), containing *Pe*AAO2 (1 µM) and catalase (1000 U/ml) at 30 °C, 1500 rpm for 48 h. Substrate and product concentrations were determined after 1, 3, 6, 24 and 48 h of reaction. For each time point, separate reaction tubes were used and analyzed at respective time points.

Product Analysis via GC/MS

The reactions were stopped by addition of HCl (5 µl of 6 N). In case of time course analysis of **1a** conversion, 2-naphthol (40 mM from 500 mM stock in DMSO) was added as internal

standard (IS) and for conversion of other substrates, 2 mM 2-naphthol (at substrate concentrations of 10 and 100 mM) and 40 mM (at substrate concentration of 300 mM) was added, respectively. The mixtures were extracted twice with ethyl acetate (100 µl) by vigorous vortexing (1 min), followed by centrifugation for phase separation (12.300 × *g*, 2 min). The combined organic phases were dried over magnesium sulfate. In case of **1a** conversion, the organic phase was evaporated to dryness and the residue was dissolved in *N,O*-bis(trimethylsilyl)-trifluoroacetamide with trimethylchlorosilane (50 µl) and transferred to a GC glass vial for derivatization at 80 °C for 15 min. For conversion of other substrates, the dried organic phase after addition of magnesium sulfate was directly injected on the GC column.

A FS-Supreme-5 column (30 m × 0.25 mm × 0.25 µm, CS-Chromatographie Service GmbH, Langerwehe, Germany) connected to a GC/MS-QP2010 (Shimadzu, Germany, Duisburg) was used for GC/MS analysis. For detailed GC/MS methods, see Table S1.

For **1a** conversion, the qualitative analysis to evaluate distribution of components was calculated on the basis of relative peak area (%) and relative sensitivities of substrate and product peaks were considered. The quantitative analysis for the time course experiment was carried out with calibration curves using known concentrations of **1a**, of products piperonal **1b** and piperonylic acid **1c**, and 40 mM 2-naphthol as internal standard (IS). Conversion of cumic alcohol **2a**, 2-thiophenemethanol **3a**, *trans,trans*-2,4-heptadienol **4a** and *trans*-2-*cis*-6-nonadienol **5a** was calculated from substrate depletion (control set to 100%) and product distribution based on relative peak area (%) in relation to internal standard 2-naphthol. Products were identified via comparison with authentic standards (for **2a** and **3a** conversion) or with mass spectrometric data in the NIST08 database (for **4a** and **5a** conversion).

Piperonal Production on a Preparative Scale

Scale-up of **1b** production was conducted in two 100 ml baffled Erlenmeyer flasks with 10 ml reaction volume each (100 mM potassium phosphate buffer pH 6) at 30 °C and 220 rpm on a horizontal shaker. **1a** (304.3 mg or 200 mM from 1 M stock in 2-propanol) was mixed with *Pe*AAO2 (0.5 µM), converted over 3 h in the presence of catalase (1000 U/ml) and the reaction was stopped with HCl (200 µl of 6 N). For determination of conversion, one flask was extracted with ethyl acetate (3x 10 ml) and analyzed via GC/MS, while the other flask was used for product isolation and **1b** was extracted with *n*-hexane (3 × 10 ml). The *n*-hexane extract was dried under vacuum. The crystallization of the clear residue was initiated with storage at −20 °C (10 min). Product identity was confirmed by comparison of GC peaks and mass fragmentation patterns of the isolated **1b** and of a **1b** standard, as well as by comparing the chemical shifts in ^{1}H-NMR and ^{13}C-NMR to those of published data (Figure S9–S15 and Tables S2–S4).

Piperonal **1b** (white solid, from *n*-hexane): ^{1}H NMR (600 MHz, $CDCl_3$): 9.84 (s, 1H), 7.44 (dd, J = 7.9, 1.6 Hz, 1H), 7.36 (d, J = 1.6 Hz, 1H), 6.96 (d, J = 7.9 Hz, 1H), 6.10 (s, 2H); ^{13}C-NMR (151 MHz, $CDCl_3$): δ 190.29, 153.12, 148.72, 131.89, 128.67, 108.36, 106.90, 102.13.

Conversion of Other Substrates

To investigate the applicability of *Pe*AAO2 for conversion of chemically diverse substrates, a set of different AAO substrates was tested: cumic alcohol **2a**, 2-thiophenemethanol **3a**, *trans,-trans*-2,4-heptadienol **4a** and *trans*-2-*cis*-6-nonadienol **5a**. Each substrate (10, 100 and 300 mM from stocks in DMSO) were converted for 20 h under optimized conditions (30 °C, 1500 rpm, 1000 U/ml catalase) with *Pe*AAO2 (1 µM) in potassium phosphate buffer (100 mM, pH 6). Content of DMSO in reaction mixture was 10, 25 or 30% (*v/v*) for 10, 100 and 300 mM of substrates, respectively.

Acknowledgements

The financial support by the Bioeconomy Science Center (BioSC, Germany) through the Ministry of Innovation, Science and Research within the framework of the NRW-Strategieprojekt BioSC (No. 313/323-400-00213) is gratefully acknowledged. Open Access funding enabled and organized by Projekt DEAL.

References

[1] R. A. Sheldon, *Front. Chem.* **2020**, *8*, 132.
[2] A. Lorente-Arevalo, M. Ladero, J. M. Bolivar, *Curr. Opin. Green Sustain. Chem.* **2021**, *32*, 100544.
[3] R. A. Sheldon, J. M. Woodley, *Chem. Rev.* **2018**, *118*, 801–838.
[4] V. B. Urlacher, K. Koschorreck, *Appl. Microbiol. Biotechnol.* **2021**, *105*, 4111–4126.
[5] a) A. Karich, S. Kleeberg, R. Ullrich, M. Hofrichter, *Microorganisms* **2018**, *6*, 5; b) A. Serrano, E. Calviño, J. Carro, M. I. Sánchez-Ruiz, F. J. Cañada, A. T. Martínez, *Biotechnol. Biofuels* **2019**, *12*, 217; c) J. Viña-Gonzalez, A. T. Martinez, V. Guallar, M. Alcalde, *Biochim. Biophys. Acta* **2020**, *1868*, 140293; d) A. Lappe, N. Jankowski, A. Albrecht, K. Koschorreck, *Appl. Microbiol. Biotechnol.* **2021**, *105*, 8313–8327.
[6] A. Serrano, F. Sancho, J. Viña-González, J. Carro, M. Alcalde, V. Guallar, Á. T. Martínez, *Catal. Sci. Technol.* **2019**, *9*, 833–841.
[7] D. Ribeaucourt, B. Bissaro, F. Lambert, M. Lafond, J. G. Berrin, *Biotechnol. Adv.* **2021**, 107787.
[8] H. Surburg, J. Panten, *Common Fragrance and Flavor Materials*, 6th ed., Wiley-VCH, Weinheim, **2016**.
[9] a) M. M. C. H. van Schie, T. P. de Almeida, G. Laudadio, F. Tieves, E. Fernández-Fueyo, T. Noël, I. W. C. E. Arends, F. Hollmann, *Beilstein J. Org. Chem.* **2018**, *14*, 697–703; b) T. P. de Almeida, M. M. C. H. van Schie, A. Ma, F. Tieves, S. H. H. Younes, E. Fernández-Fueyo, I. W. C. E. Arends, A. Riul, F. Hollmann, *Adv. Synth. Catal.* **2019**, *361*, 2668–2672.
[10] F. J. Ruiz-Dueñas, P. Ferreira, M. J. Martínez, A. T. Martínez, *Protein Expression Purif.* **2006**, *45*, 191–199.
[11] J. Viña-Gonzalez, K. Elbl, X. Ponte, F. Valero, M. Alcalde, *Biotechnol. Bioeng.* **2018**, *115*, 1666–1674.
[12] N. Jankowski, K. Koschorreck, V. B. Urlacher, *Appl. Microbiol. Biotechnol.* **2020**, *104*, 9205–9218.

[13] F. Guillén, Á. T. Martínez, M. J. Martínez, *Eur. J. Biochem.* **1992**, *209*, 603–611.

[14] a) A. S. Santos, N. Pereira, I. M. Da Silva, M. I. M. Sarquis, O. A. C. Antunes, *Appl. Biochem. Biotechnol.* **2003**, *105–108*, 649–657; b) A. S. Santos, N. Pereira, I. M. Da Silva, M. I. M. Sarquis, O. A. C. Antunes, *Process Biochem.* **2004**, *39*, 2269–2275; c) M. Bellardita, V. Loddo, G. Palmisano, I. Pibiri, L. Palmisano, V. Augugliaro, *Appl. Catal. B* **2014**, *144*, 607–613; d) J. D. O. C. Brum, D. C. F. Neto, J. S. F. D. de Almeida, J. A. Lima, K. Kuca, T. C. C. França, J. D. Figueroa-Villar, *Int. J. Mol. Sci.* **2019**, *20*, 3944; e) S. Wang, L. Bao, D. Song, J. Wang, X. Cao, *Bioorg. Med. Chem. Lett.* **2019**, *29*, 126661; f) J. Akash, C. Dushyant, C. Jasmine, *Mini-Rev. Med. Chem.* **2020**, *20*, 1846–1856.

[15] a) J. R. Holum, *J. Org. Chem.* **1961**, *26*, 4814–4816; b) F. Cortés-Salazar, E. Avella-Moreno, M. T. Cortés, M. F. Suárez-Herrera, *J. Electroanal. Chem.* **2007**, *606*, 1–7.

[16] a) D. Schwendenwein, G. Fiume, H. Weber, F. Rudroff, M. Winkler, *Adv. Synth. Catal.* **2016**, *358*, 3414–3421; b) P. Wen, D. Wu, P. Zheng, P. Chen, S. Liu, Y. Fu, *J. Agric. Food Chem.* **2019**, *67*, 14121–14128.

[17] M. I. Sanchez-Ruiz, A. T. Martinez, A. Serrano, *Microb. Cell Fact.* **2021**, *20*, 1–13.

[18] I. S. Fernández, F. J. Ruiz-Dueñas, E. Santillana, P. Ferreira, M. J. Martínez, Á. T. Martínez, A. Romero, *Acta Crystallogr. Sect. D* **2009**, *65*, 1196–1205.

[19] A. Toftgaard Pedersen, W. R. Birmingham, G. Rehn, S. J. Charnock, N. J. Turner, J. M. Woodley, *Org. Process Res. Dev.* **2015**, *19*, 1580–1589.

[20] J. M. Woodley, *Top. Catal.* **2019**, *62*, 1202–1207.

[21] M. R. Chapman, S. C. Cosgrove, N. J. Turner, N. Kapur, A. J. Blacker, *Angew. Chem. Int. Ed.* **2018**, *57*, 10535–10539; *Angew. Chem.* **2018**, *130*, 10695–10699.

[22] D. Prat, J. Hayler, A. Wells, *Green Chem.* **2014**, *16*, 4546–4551.

[23] a) H. S. Lee, *J. Agric. Food Chem.* **2005**, *53*, 2446–2450; b) D. Morshedi, F. Aliakbari, A. Tayaranian-Marvian, A. Fassihi, F. Pan-Montojo, H. Pérez-Sánchez, *J. Food Sci.* **2015**, *80*, H2336–H2345; c) K. D. Tsai, Y. H. Liu, T. W. Chen, S. M. Yang, H. Y. Wong, J. Cherng, K. S. Chou, J. M. Cherng, *Nutrients* **2016**, *8*, 318; d) Z. Zhang, W. Zhang, Y. Bi, Y. Han, Y. Zong, D. Prusky, *Microorganisms* **2020**, *8*; e) S. Chatterjee, P. Paul, P. Chakraborty, S. Das, R. K. Sarker, S. Sarkar, A. Das, P. Tribedi, *3 Biotech* **2021**, *11*, 485.

[24] a) Archna, S. Pathania, P. A. Chawla, *Bioorg. Chem.* **2020**, *101*, 104026; b) R. Mishra, N. Kumar, I. Mishra, N. Sachan, *Mini Rev. Med. Chem.* **2020**, *20*, 1944–1965.

[25] a) N. K. Duddukuri, S. Thatikonda, C. Godugu, R. A. Kumar, N. Doijad, *ChemistrySelect* **2018**, *3*, 6859–6864; b) S. Maity, N. Naskar, B. Jana, S. Lahiri, J. Ganguly, *Carbohydr. Polym.* **2021**, *251*, 116999.

[26] a) W. Grosch, J. Schwarz, *Lipids* **1971**, *6*, 351–352; b) W. Schmid, W. Grosch, *Z. Lebensm.-Unters. Forsch.* **1986**, *183*, 39–44; c) P. Schieberle, S. Ofner, W. Grosch, *J. Food Sci.* **1990**, *55*, 193–195; d) J. A. Pino, J. Mesa, *Flavour Fragrance J.* **2006**, *21*, 207–213.

2.6.1. Supplemental Information

Advanced Synthesis & Catalysis

Supporting Information

Aryl-Alcohol-Oxidase-Mediated Synthesis of Piperonal and Other Valuable Aldehydes

Nina Jankowski, Katja Koschorreck, and Vlada B. Urlacher*

Supplemental Information

Aryl-alcohol oxidase-mediated synthesis of piperonal and other valuable aldehydes

Nina Jankowski [a], Katja Koschorreck [a], Vlada B. Urlacher [a,*]

[a] Institute of Biochemistry, Heinrich-Heine-University Düsseldorf, Universitätsstraße 1, 40225 Düsseldorf, Germany

[*] Address correspondence to

Vlada B. Urlacher

E-mail: Vlada.Urlacher@uni-duesseldorf.de

1 **Content**

26

Supplemental Experimental Section

Activity and stability in the presence of H_2O_2

The effect of different H_2O_2 concentrations on the activity and stability of the biocatalyst *Pe*AAO2 was evaluated in a spectrophotometric assay. Different amounts of H_2O_2 (yielding 100 mM to 4 M) were mixed with an appropriate diluted sample of *Pe*AAO2 in sodium phosphate buffer (100 mM, pH 6) and incubated for 5 min at room temperature prior the addition of the substrate piperonyl alcohol **1a** (5 mM). The oxidation to piperonal **1b** was followed at 317 nm in a 96-well micro plate using an Infinite M200 Pro plate reader (Tecan, Männedorf, Switzerland). The molar extinction coefficient of **1b** (ε_{317} = 8,680 M^{-1} cm^{-1})[1] was used to calculate volumetric activities from the initial reaction rate according to Lambert-Beer's law. The relative activities were calculated related to a control without added H_2O_2.

For stability analysis, *Pe*AAO2 was incubated in potassium phosphate buffer (50 mM, pH 6) with different H_2O_2 concentrations (10 to 500 mM) over a period of 96 h at 25 °C. After certain time points, samples were taken and the relative activity towards **1a** (5 mM) was determined as described above. For H_2O_2 stability determination, samples were diluted 1:10 in the spectrophotometric assay.

Storage stability of *Pe*AAO2

Purified *Pe*AAO2 was stored at 4 °C in potassium phosphate buffer (50 mM, pH 6) without addition of any protectants for over one year. At irregular intervals, samples were taken and the volumetric activity towards the standard substrate veratryl alcohol was determined. For this, a photometric assay using veratryl alcohol (5 mM) in sodium phosphate buffer (100 mM, pH 6) was used. The conversion to veratraldehyde was followed at 310 nm using an Infinite M200 Pro plate reader (Tecan, Männedorf, Switzerland) and the volumetric activity was calculated using the molar extinction coefficient of the product (ε_{310} = 9,300 M^{-1} cm^{-1}).[2]

Optimization of buffer system

Different buffer systems at varying pH values were investigated in order to find the best conditions for **1a** conversion. Purified *Pe*AAO2 was mixed with **1a** (5 mM) to an appropriate final concentration in micro titer plate in the following reactions buffers: potassium phosphate (KPi), sodium phosphate (NaP_i), Britton-Robinson, McIlvaine's (citrate-phosphate), potassium acetate (K-acetate) and sodium acetate (Na-acetate). Molarity was 100 mM and pH value was varied between pH 6 - 7 for KPi and NaP_i, pH 4 - 7 for Britton-Robinson and McIlvaine´s, and pH 4.5 - 5.5 for K- and Na-acetate buffers. The conversion of **1a** to **1b** was followed at 317 nm over 2 min using an Infinite M200 Pro plate reader. Volumetric activities were calculated using the molar extinction coefficient of piperonal (ε_{317} = 8,680 M^{-1} cm^{-1}) as described elsewhere.[1]

60 **Initial experiments on 1a conversion without added catalase**

61 For initial experiments on conversion of **1a** without added catalase, 1 µM of *Pe*AAO2 was used and **1a**
62 concentration was varied (10 to 100 mM from 500 mM stock solution in DMSO), resulting in final
63 DMSO percentages of up to 20 % (*v/v*). Each conversion was done in a 1.5 ml safe-lock reaction tube
64 with a total reaction volume of 125 µl in potassium phosphate buffer (100 mM, pH 6) for 20 h at 25 °C
65 and 600 rpm (Thermomixer C, Eppendorf). Conversion products were analyzed via GC/MS (see main
66 text). All reactions were done in duplicate.

67 **Product analysis by GC/MS**

68 All reaction mixtures were extracted and prepared as described in the main text and analyzed using the
69 respective GC/MS method in Table S1. Following parameters were the same for all measurements:
70 Column FS-Supreme-5 column (30 m x 0.25 mm x 0.25 µm, Chromatographic Service GmbH)
71 connected to GC/MS-QP2010 (Shimadzu, Germany, Duisburg), injection temperature: 250 °C, ion
72 source: 200 °C, interface temperature: 290 °C, helium as carrier gas at 30 cm/s, split mode and injection
73 of 0.5 µl of sample using an auto injector/auto sampler AOC-20i/s unit (Shimadzu, Germany, Duisburg).

74 **Table S1**. All GC/MS methods used in this study.

Method name	Rate [°C/min]	Final Temperature [°C]	Hold Time [min]
Piperonyl alcohol - optimization of reaction conditions	-	110	3
	4	150	0
	50	300	2
		Run time: 18:00 min	
Piperonyl alcohol N - time course analysis - preparative scale production	-	125	2
	3	160	0
	50	300	1
		Run time: 17:47 min	
Purity Check	-	50	5
	20	300	2
		Run time: 19:50 min	
Cumic alcohol	-	130	4
	5	180	0
	50	300	2
		Run time: 18:40 min	
2-Thiophenemethanol	-	90	3
	5	99	2
	2	110	0
	50	300	2
		Run time: 18:10 min	
Heptadienol / Nonadienol	-	90	4
	10	180	0
	50	300	2
		Run time: 17:40 min	

75

Supplemental Results

Influence of H_2O_2 on activity

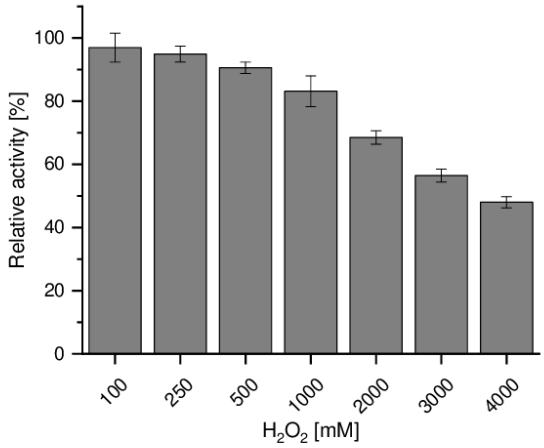

Figure S1. Effect of added H_2O_2 on *Pe*AAO2 activity. *Pe*AAO2 was incubated for 5 min with a set of H_2O_2 concentrations ranging from 100 mM to 4 M and the relative activity towards 5 mM **1a** in 100 mM sodium phosphate buffer pH 6 was determined. A control reaction without added H_2O_2 was set as 100 %. All reactions were carried out in triplicate.

Influence of H_2O_2 on stability

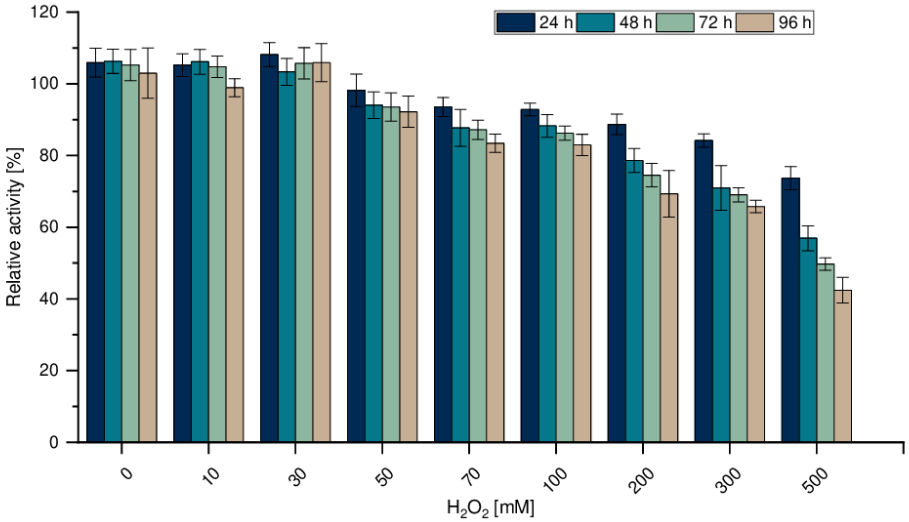

Figure S2. Stability of *Pe*AAO2 in the presence of increasing H_2O_2 concentrations over 96 h at 25 °C. The enzyme was incubated for the indicated time and an aliquot was withdrawn to determine the relative activity towards 5 mM **1a** in 100 mM sodium phosphate buffer pH 6. Time point "0 min" directly after mixing for each sample was set as 100 %. All reactions were carried out in triplicate.

Storage stability of *Pe*AAO2

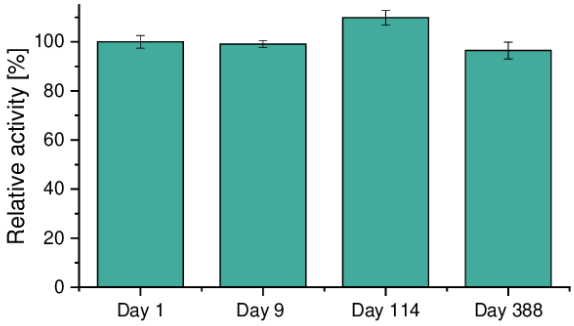

Figure S3. Storage stability of *Pe*AAO2. The purified enzyme was stored at 4 °C in 50 mM potassium phosphate buffer pH 6 for over one year. At irregular intervals, samples were taken and the volumetric activity towards 5 mM veratryl alcohol was determined. Relative activity [%] calculated in relation to initial activity after purification at day one (set as 100 %).

Optimization of buffer system

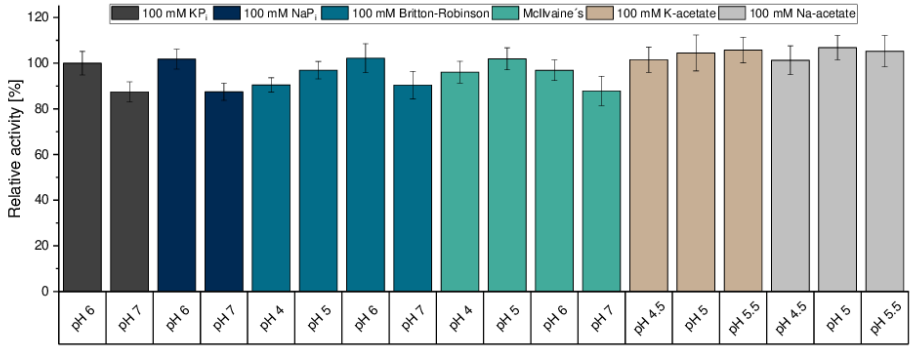

Figure S4. Optimization of reaction buffer for **1a** conversion. 5 mM of **1a** were used in a photometric assay with different reaction buffers to follow the conversion to **1b** at 317 nm. Following reaction buffers at 100 mM were used: potassium phosphate (KP_i), sodium phosphate (NaP_i), Britton-Robinson, McIlvaine's (citrate-phosphate), potassium acetate (K-acetate) and sodium acetate (Na-acetate). Relative activity [%] calculated in relation to 100 mM KP_i buffer (set as 100 %).

103 **Conversion of piperonyl alcohol without added catalase**

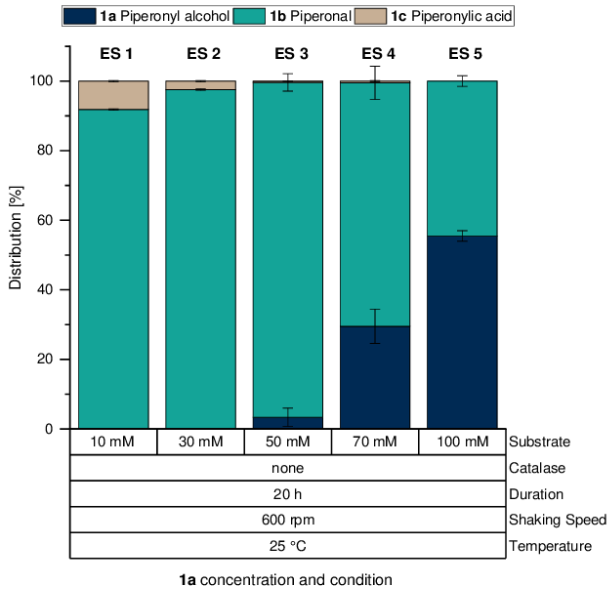

104

105 **Figure S5.** Initial optimization of **1a** conversions. Conditions: 10 to 100 mM **1a**, 1 µM *Pe*AAO2, 25 °C, 600 rpm for 20 h in
106 100 mM potassium phosphate buffer pH 6. Content of DMSO varied from 2 to 20 % (*v/v*). Distribution (%) was calculated on
107 basis of peak area. All reactions were carried out in duplicate. Each entry is named with ES1 to ES5 above the columns.

108

109 **Time course of reaction**

110

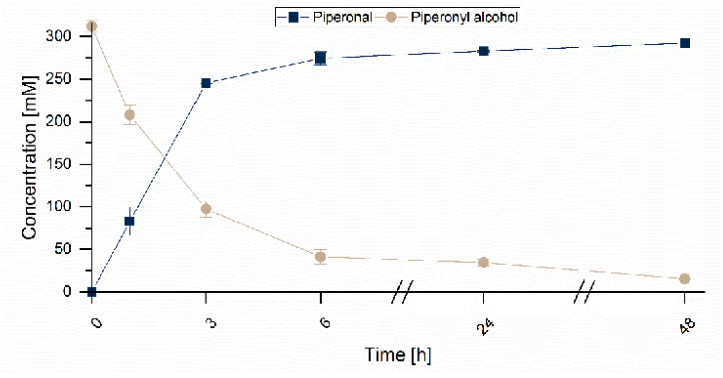

111

112 **Figure S6.** Time course of **1a** conversion. Conditions: 300 mM **1a**, 1 µM *Pe*AAO2, 1000 U/ml catalase, 30 °C,
113 1500 rpm for 48 h in 100 mM potassium phosphate buffer pH 6. Concentrations of substrate and product were
114 calculated from the calibration curves with 2-naphthol as internal standard. Content of DMSO was 24 % (*v/v*). All
115 reactions were carried out in duplicate.

Piperonal production on preparative scale

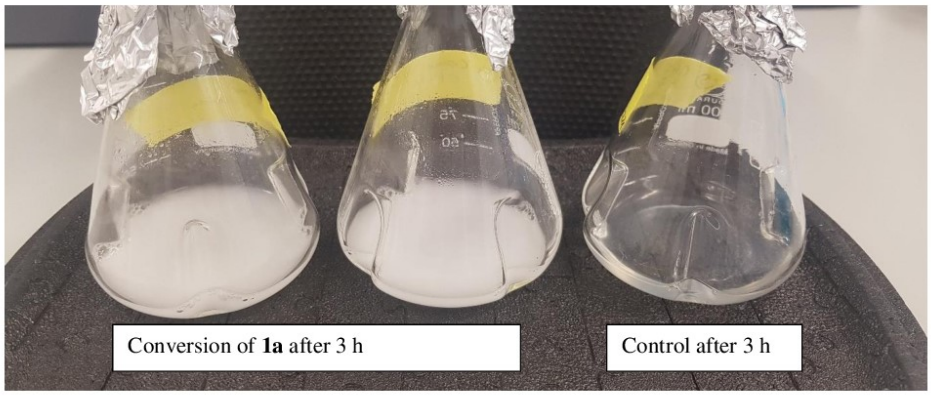

Figure S7. Conversion of 200 mM **1a** (304.3 mg from stock in 2-propanol) on preparative scale with 0.5 µM *Pe*AAO2 and 1000 U/ml catalase in baffled 100-ml flasks and control reaction without enzyme after 3 h (30 °C, 220 rpm).

Figure S8. Isolated **1b** from preparative scale production after evaporation of *n*-hexane.

Identification of the isolated piperonal

GC/MS

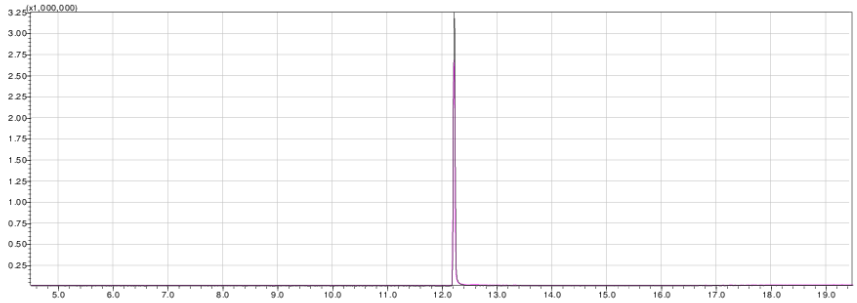

Figure S9. GC chromatogram of isolated piperonal **1b** from *n*-hexane extract (**pink**) and **1b** standard (**black**) at 12.21 min. Method used: purity check (Table S1).

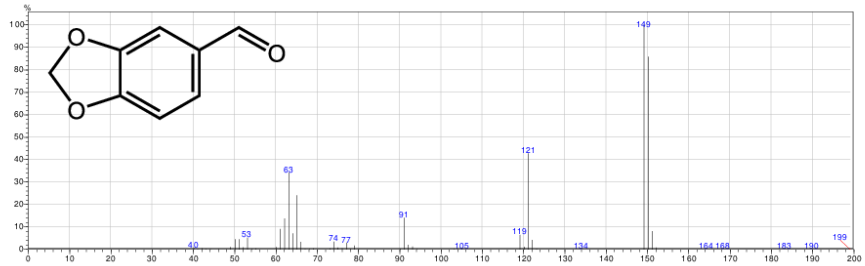

Figure S10. MS trace of isolated **1b** from *n*-hexane extract (12.21 min, **pink** in Figure S9).

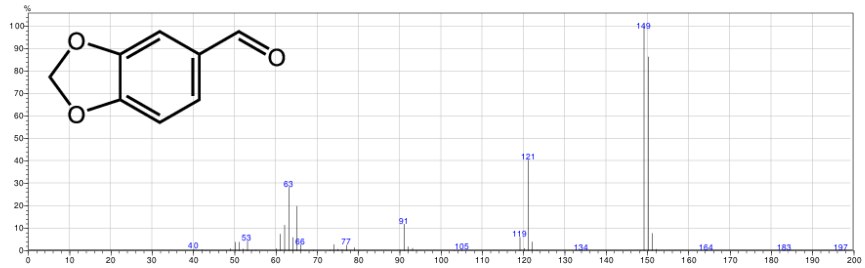

Figure S11. MS trace of **1b** standard (12.21 min, **black** in Figure S9).

134 **Table S2.** Comparison of relative intensities [%] of the mass fragments (*m/z*, cut-off above 10 % of relative intensity) in isolated
135 **1b** and in a **1b** standard (derived from Figure S10 and Figure S11).

	Relative intensity [%]	
m/z	Isolated **1b**	**1b** standard
149.15	100.00	100.00
150.15 [M⁺]	85.86	86.40
121.10	42.99	40.56
63.05	34.70	28.89
65.05	24.31	20.31
91.05	14.21	12.08
62.05	13.95	11.75

^{1}H-NMR

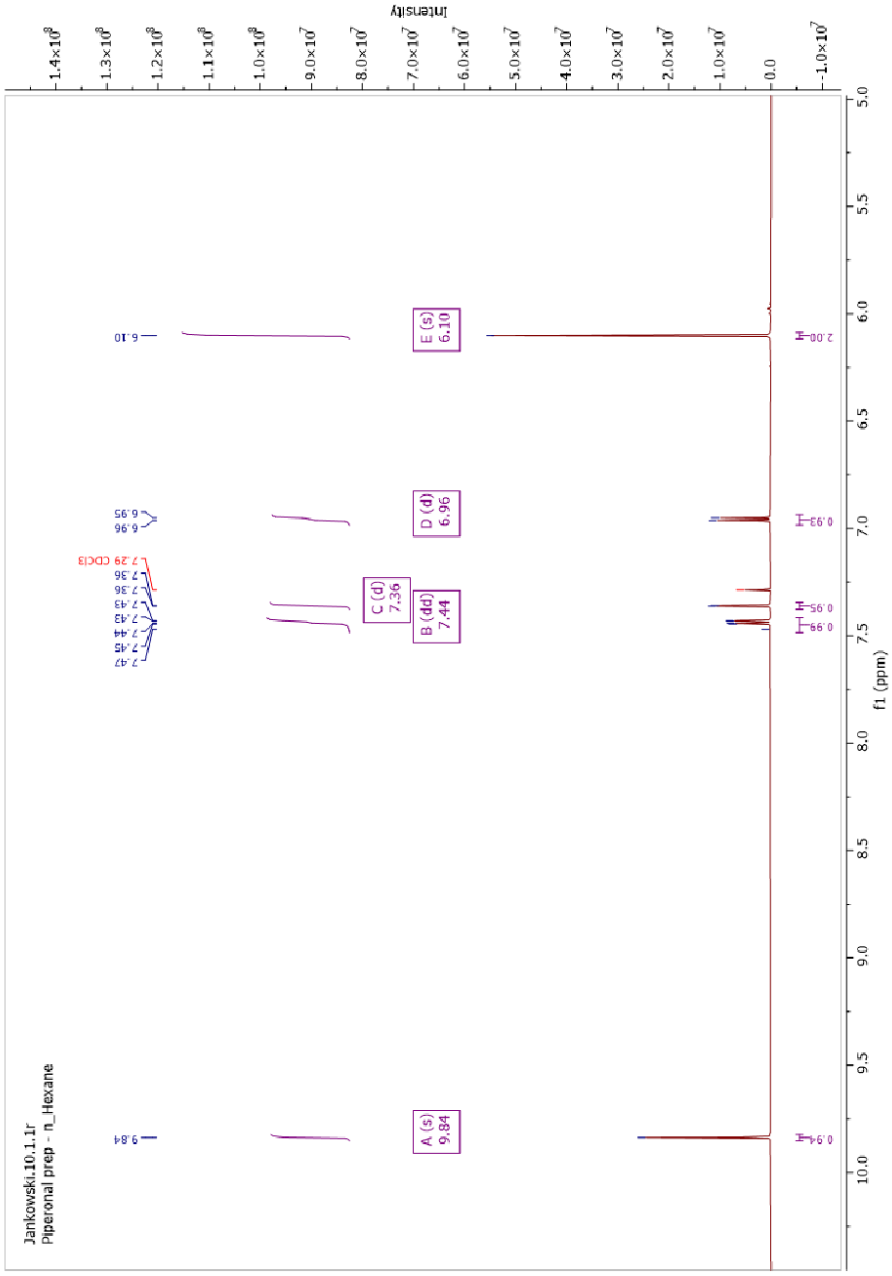

Figure S12. ^{1}H-NMR (600 MHz) spectrum of isolated piperonal **1b** ($CDCl_3$): δ 9.84 (s, 1H), 7.44 (dd, *J* = 7.9, 1.6 Hz, 1H), 7.36 (d, *J* = 1.6 Hz, 1H), 6.96 (d, *J* = 7.9 Hz, 1H), 6.10 (s, 2H).

140 **Table S3.** Comparison of observed signals in ^{1}H-NMR of isolated **1b** (Figure S12) to values from literature. Chemical shifts δ
141 [ppm], multiplicity, coupling constants [Hz] and integrals are given. For position of H-atoms see Figure S13. s: singlet, d:
142 doublet, dd: doublet of doublet.

	Observed signals			
H-Atom	**This study (600 MHz, $CDCl_3$)**	**Bellardita et al.[3] (250 MHz, $CDCl_3$)**	**Schwendenwein et al.[4] ($CDCl_3$)**	**Meriga et al.[5] (400 MHz, $CDCl_3$)**
1	9.84, s, 1H	9.82, s, 1H	9.83, s, 1H	9.82, s, 1H
2	7.44, dd, 7.9 and 1.6 Hz, 1H	7.44, dd, 8 and 2 Hz, 1H	7.44, d, 7.9 Hz, 1H	7.53, dd, 1H
3	7.36, d, 1.6 Hz, 1H	7.35, d, 2 Hz, 1H	7.36, s, 1H	7.32, s, 1H
4	6.96, d, 7.9 Hz, 1H	6.95, d, 8 Hz, 1H	6.95, d, 7.9 Hz, 1H	7.15, dd, 1H
5, 6	6.10, s, 2H	6.09, s, 2H	6.10, s, 2H	6.19, s, 2H

143

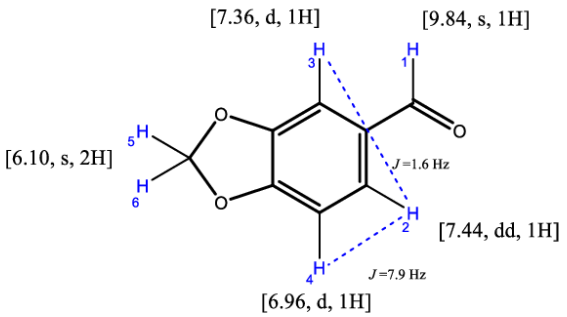

144

145 **Figure S13.** Structure of **1b** with assigned numbering to H-atoms and observed chemical shifts, multiplicity and integrals in
146 ^{1}H-NMR according to Figure S12 and Table S3.

^{13}C-NMR

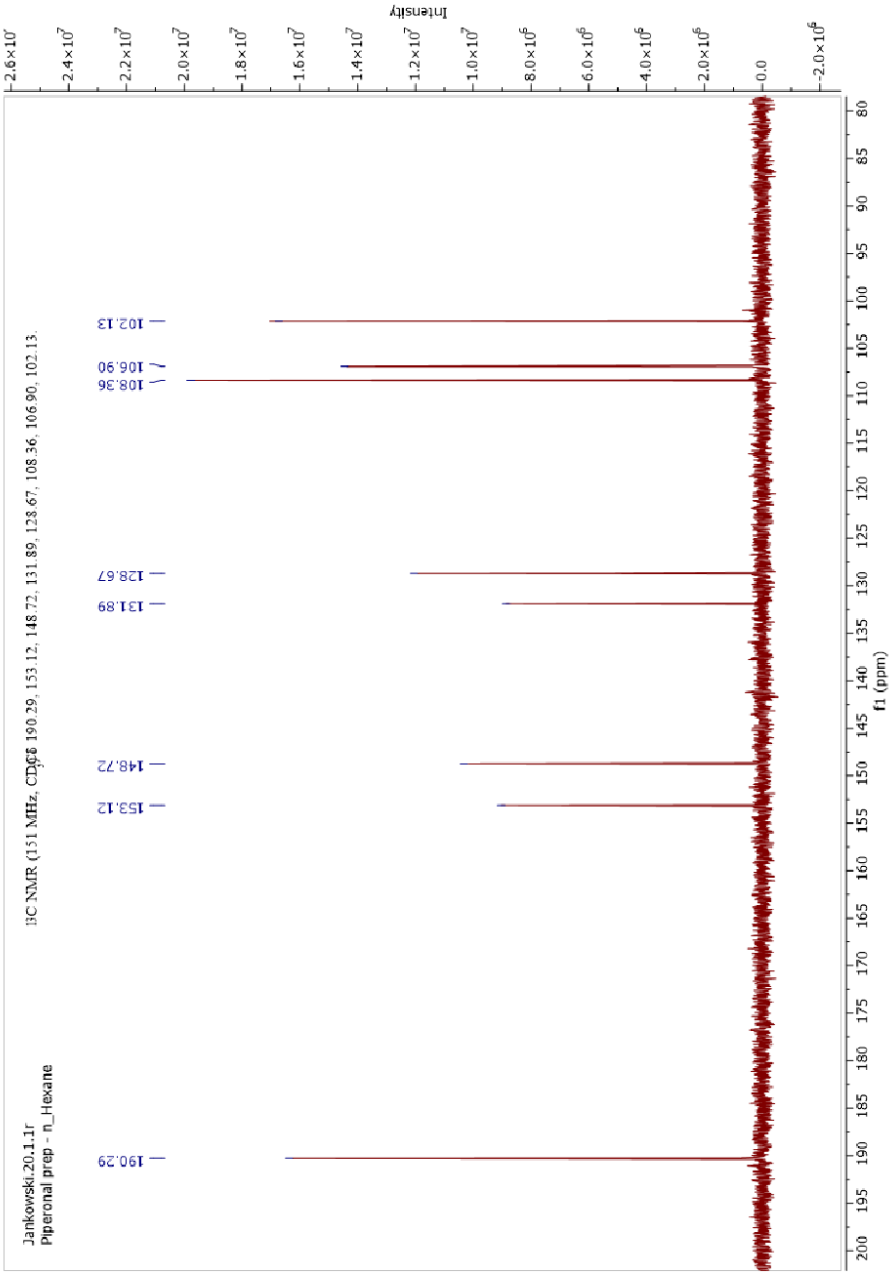

Figure S14. ^{13}C-NMR (151 MHz) spectrum of isolated piperonal **1b** ($CDCl_3$): δ 190.29, 153.12, 148.72, 131.89, 128.67, 108.36, 106.90, 102.13.

Table S4. Comparison of observed signals in ^{13}C-NMR of isolated **1b** (Figure S14) to values from literature. Chemical shifts δ [ppm] are given. For position of C-atoms see Figure S15.

	Observed signals		
C-Atom	**This work (151 MHz, $CDCl_3$)**	**Schwendenwein et al. [4] ($CDCl_3$)**	**Meriga et al. [5] (400 MHz, $CDCl_3$)**
1	190.29	190.3	190.72
2	131.89	131.9	131.3
3	128.67	128.7	128.6
4	108.36	108.4	108.7
5	153.12	153.1	152.6
6	102.13	102.1	102.0
7	148.72	148.7	148.2
8	106.90	106.9	105.9

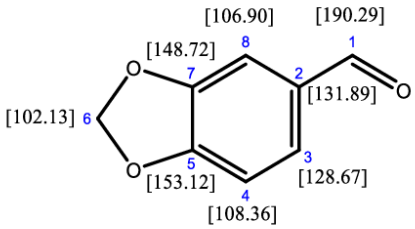

Figure S15. Structure of **1b** with assigned numbering to C-atoms and observed chemical shifts in ^{13}C-NMR according to Figure S14 and Table S4.

Identification of conversion products

Piperonyl alcohol 1a

Method name: Piperonyl alcohol N (Table S1)

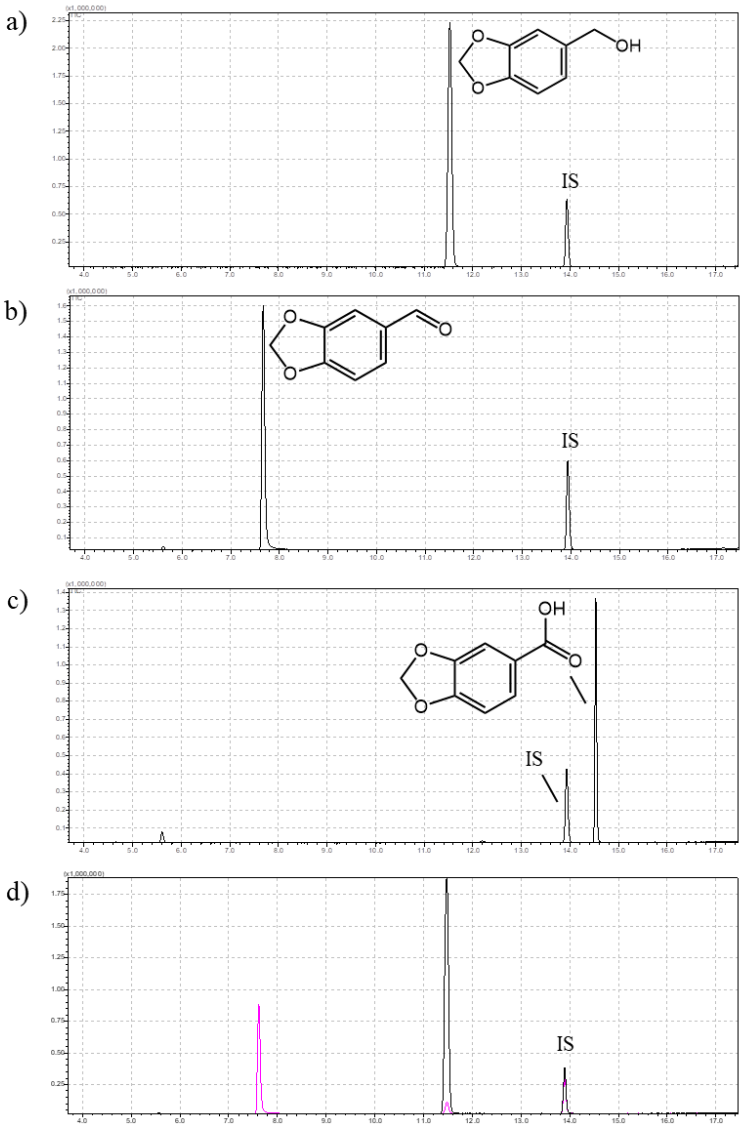

Figure S16 GC chromatogram of piperonyl alcohol **1a** and product standards as well as conversion products. **a)** piperonyl alcohol **1a** (11.47 min), **b)** piperonal **1b** (7.61 min), **c)** piperonylic acid **1c** (14.53 min); **d)** Conversion of 300 mM **1a** over 48 h with 1 µM *Pe*AAO2 under optimized conditions (30 °C, 1500 rpm, 1000 U/ml catalase), **black**: control without enzyme, **pink**: conversion with enzyme. Internal standard 2-naphthol (IS) at 13.9 min. Method used: piperonyl alcohol N (Table S1).

Cumic alcohol 2a

Method name: Cumic alcohol (Table S1)

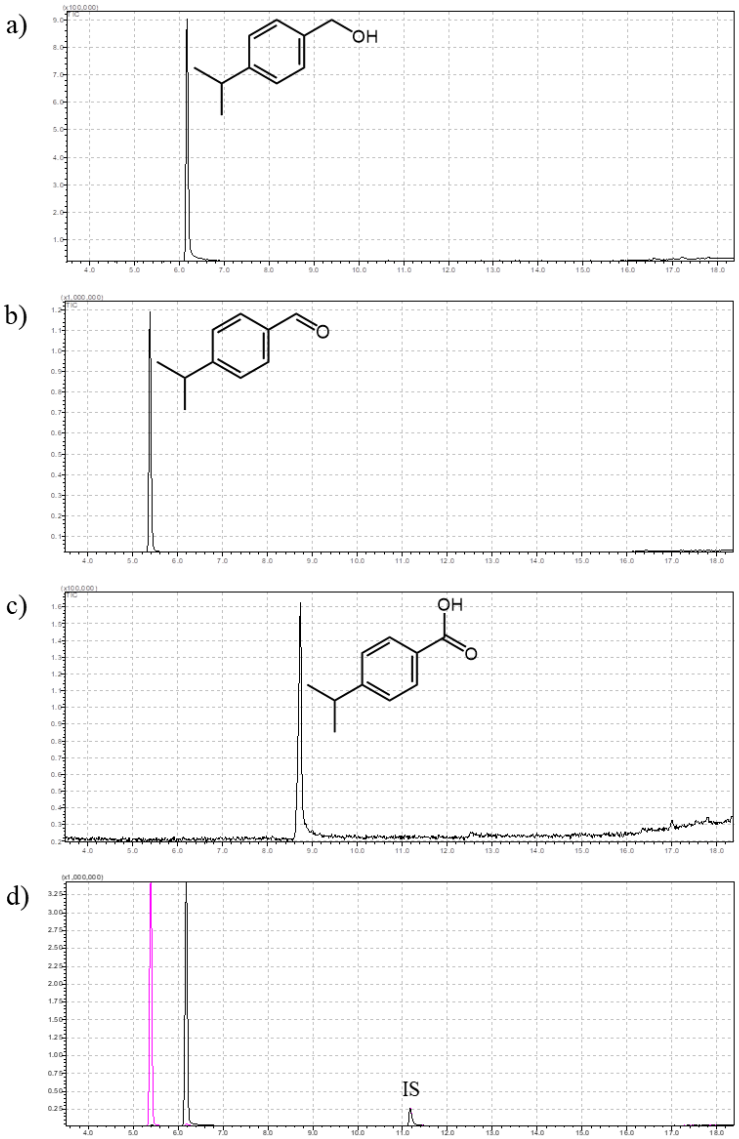

Figure S17. GC chromatogram of cumic alcohol **2a** and product standards as well as conversion products. **a)** cumic alcohol **2a** (6.18 min), **b)** cuminal **2b** (5.39 min), **c)** cuminic acid **2c** (8.70 min); **d)** Conversion of 100 mM **2a** over 20 h with 1 µM *Pe*AAO2 under optimized conditions (30 °C, 1500 rpm, 1000 U/ml catalase), **black**: control without enzyme, **pink**: conversion with enzyme. Internal standard 2-naphthol (IS) at 11.2 min. Method used: cumic alcohol (Table S1).

2-Thiophenemethanol 3a

Method name: 2-Thiophenemethanol (Table S1)

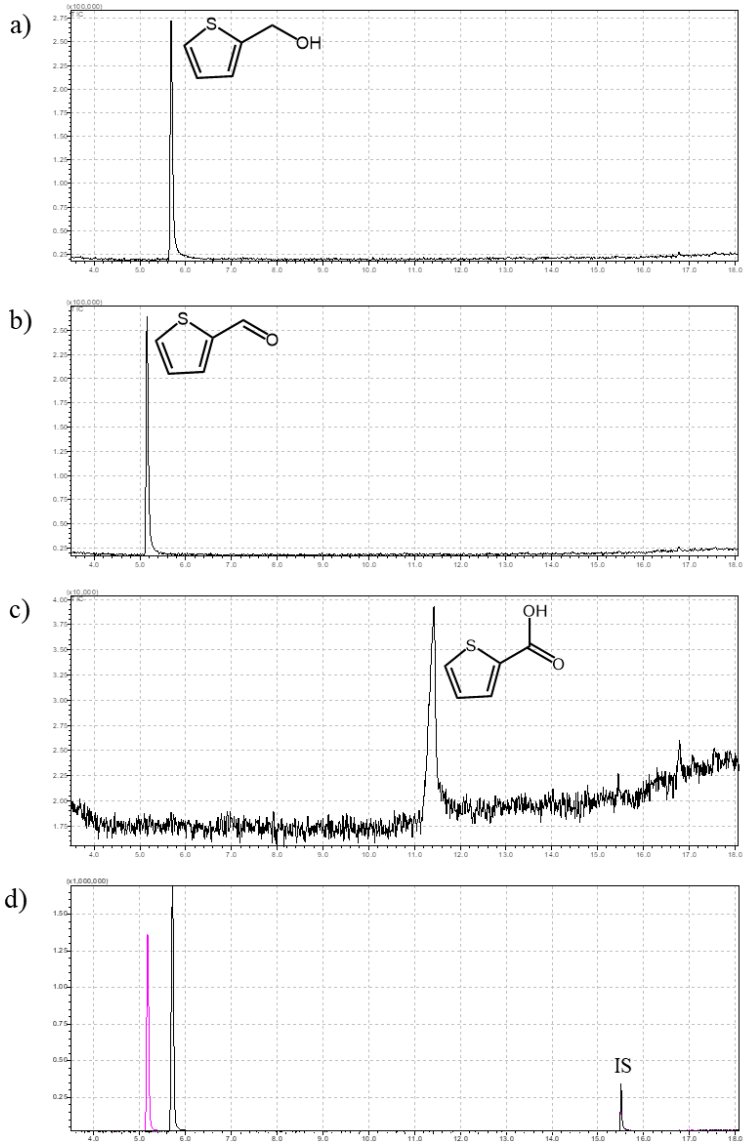

Figure S18: GC chromatogram of 2-thiophenemethanol **3a** and product standards as well as conversion products. **a)** 2-thiophenemethanol **3a** (5.69 min), **b)** 2-thiophenecarboxaldehyde **3b** (5.15 min), **c)** 2-thiophenecarboxylic acid **3c** (11.4 min); **d)** Conversion of 100 mM **3a** over 20 h with 1 µM *Pe*AAO2 under optimized conditions (30 °C, 1500 rpm, 1000 U/ml catalase), **black**: control without enzyme, **pink**: conversion with enzyme. Internal standard 2-naphthol (IS) at 15.5 min. Method used: 2-thiophenemethanol (Table S1).

***trans,trans*-2,4-Heptadienol 4a**

Method: Heptadienol / Nonadienol (Table S1)

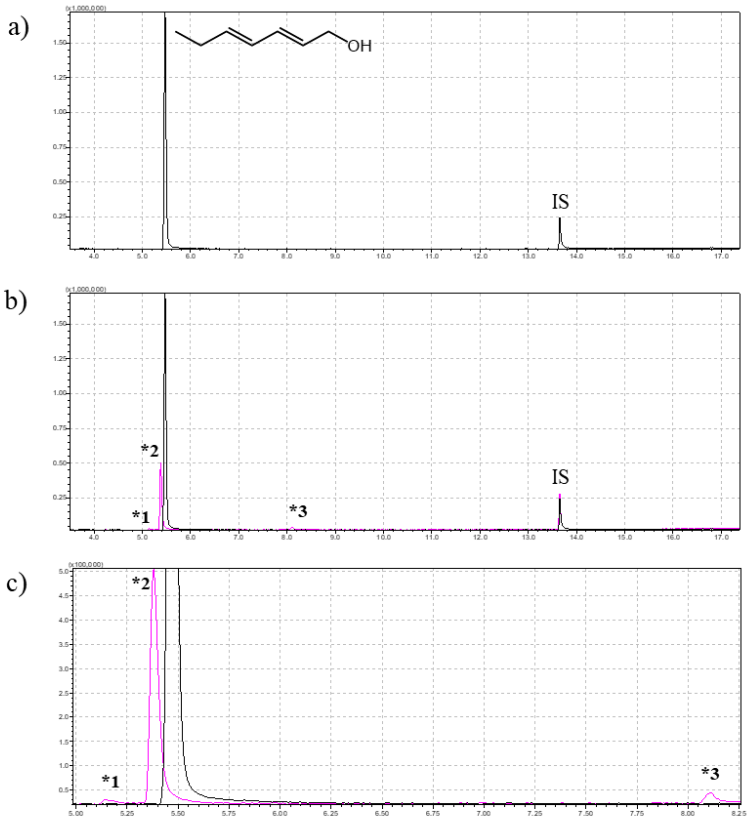

Figure S19. GC chromatogram of *trans,trans*-2,4-heptadienol **4a** standard and conversion products. **a)** *trans,trans*-2,4-heptadienol **4a** (5.45 min) and internal standard 2-naphthol (IS, at 13.6 min); **b)** Conversion of 100 mM **4a** over 20 h with 1 µM *Pe*AAO2 under optimized conditions (30 °C, 1500 rpm, 1000 U/ml catalase), **black**: control without enzyme, **pink**: conversion with enzyme with three product peaks (marked with *1 to *3) at 5.13 min, 5.38 min and 8.11 min; **c)** Zoom in on 5.25 to 8.25 min. Method used: Heptadienol / Nonadienol (Table S1).

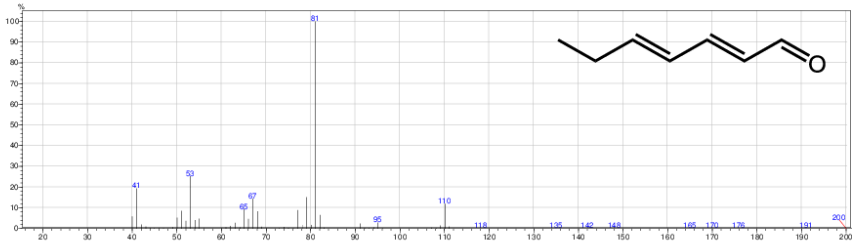

Figure S20. MS trace from main product peak at 5.38 min (*2 in Figure S19c) of **4a** conversion. Comparison with NIST08 database shows 95 % agreement with expected product *trans,trans*-2,4-heptadienal **4b**.

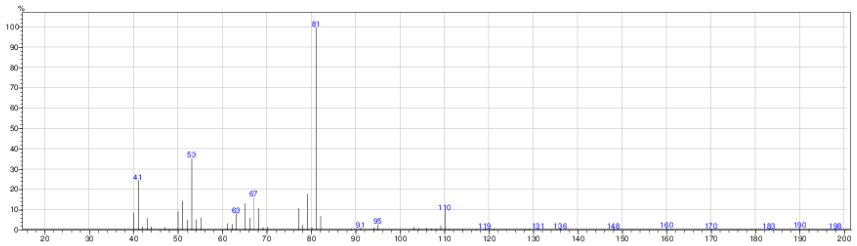

Figure S21. MS trace from minor product peak at 5.13 min (*1 in Figure S19c) of **4a** conversion. Comparison with NIST08 database did not reveal compounds with similar MS pattern. However, the main fragments (81, 53, 41, 67 and 110 *m/z*) are identical to the fragments in Figure S20 representing the aldehyde product *trans,trans*-2,4-heptadienal **4b**.

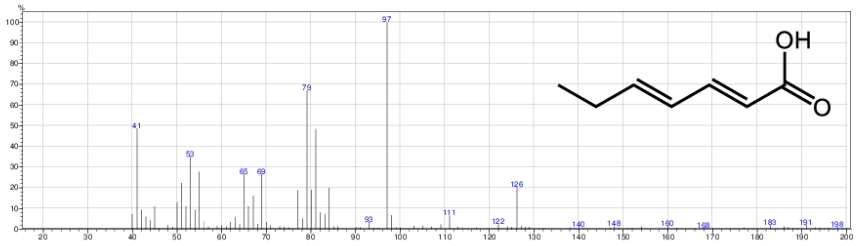

Figure S22. MS trace from minor product peak at 8.11 min (*3 in Figure S199c) of **4a** conversion. Comparison with NIST08 database did not reveal compounds with similar MS pattern. However, as the largest fragment with 126 *m/z* corresponds to the molecular ion [M$^+$] of *trans,trans*-2,4-heptadienoic acid **4c**, the third peak is presumably the product of the aldehyde oxidation to give the acid.

***trans*-2-*cis*-6-Nonadienol 5a**

Method: Heptadienol / Nonadienol (Table S1)

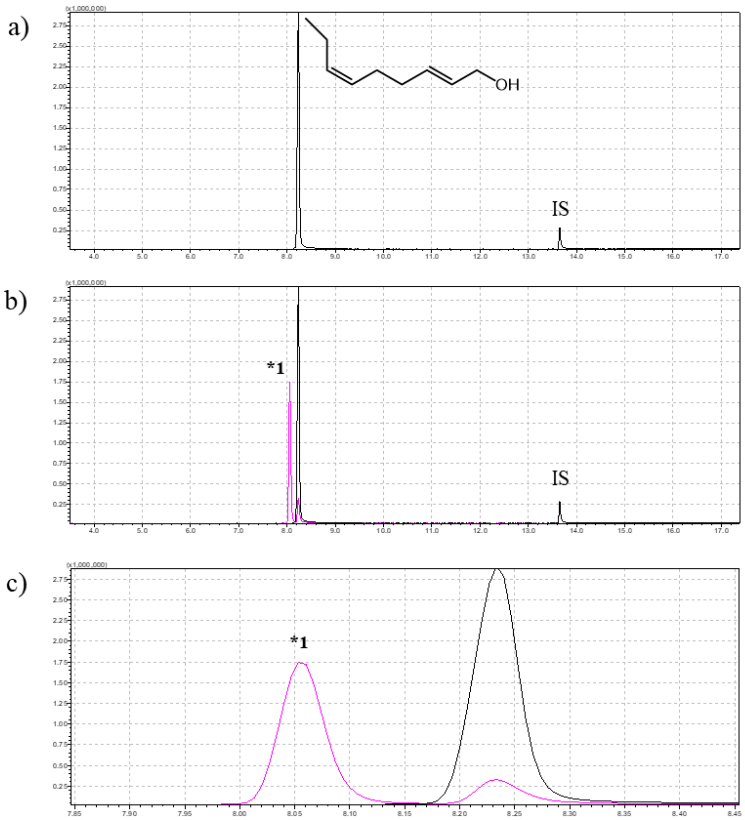

Figure S23. GC chromatogram of *trans*-2-*cis*-6-nonadienol **5a** standard and conversion products. **a)** *trans*-2-*cis*-6-nonadienol **5a** (8.21 min) and internal standard 2-naphthol (IS, at 13.6 min); **b)** Conversion of 100 mM **5a** over 20 h with 1 µM *Pe*AAO2 under optimized conditions (30 °C, 1500 rpm, 1000 U/ml catalase), **black**: control without enzyme, **pink**: conversion with enzyme and product peak *1 at 8.05 min; **c)** Zoom in on 7.85 to 8.45 min.

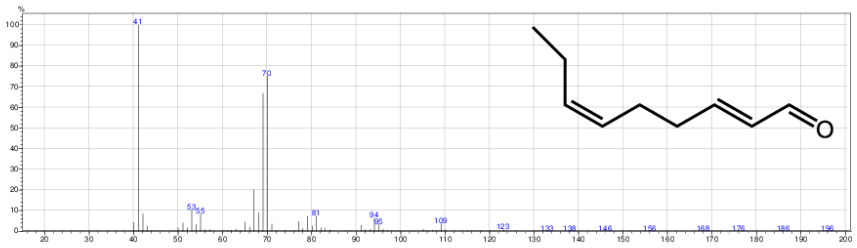

Figure S24. MS trace from product peak *1 at 8.05 min of **5a** conversion (Figure S23c). Comparison with NIST08 database shows 93 % agreement with expected product *trans*-2-*cis*-6-nonadienal **5b**.

210 **References**

211 [1] N. Jankowski, K. Koschorreck, V. B. Urlacher, *Appl. Microbiol. Biotechnol.* **2020**, *104*, 9205-9218.
212 [2] F. Guillén, Á. T. Martínez, M. J. Martínez, *Eur. J. Biochem.* **1992**, *209*, 603-611.
213 [3] M. Bellardita, V. Loddo, G. Palmisano, I. Pibiri, L. Palmisano, V. Augugliaro, *Appl. Catal. B* **2014**, *144*,
214 607-613.
215 [4] D. Schwendenwein, G. Fiume, H. Weber, F. Rudroff, M. Winkler, *Adv. Synth. Catal.* **2016**, *358*, 3414-
216 3421.
217 [5] B. Meriga, B. Parim, V. R. Chunduri, R. R. Naik, H. Nemani, P. Suresh, S. Ganapathy, V. V. Sathibabu
218 Uddandrao, *Nutr. Metab.* **2017**, *14*, 1-14.

3. Conclusion and Outlook

In this thesis, research on fungal aryl-alcohol oxidases was conducted to further advance their understanding and use as biocatalysts. As the implementation of enzymes in industrial settings requires large quantities of enzymes, a suitable expression system is one of the major prerequisites. The secretory production of fungal aryl-alcohol oxidases (AAOs) by the native fungal hosts is usually quite low and thus considered as insufficient for industrial applications. The first heterologous expression systems capable of producing AAOs, such as *Escherichia coli*[41], *Aspergillus nidulans*[40] and *Saccharomyces cerevisiae*[44,45], also did not provide high expression levels either (Table 4), but were sufficient for biochemical and structural studies. Only one report described an AAO produced at high concentration of 1 g/l,[72] which was achieved using the yeast *P. pastoris* and initiated our search for other candidate AAOs to be produced in the methylotrophic yeast *P. pastoris*.

The first three chapters of this thesis dealt with the search for and expression of several new genes encoding for AAOs in *P. pastoris.* The two most promising recombinant AAOs, namely *Ma*AAO (previously annotated as *Ma*GMC1) from *M. antarcticus*[84] and *Pe*AAO2[85] from *P. eryngii* P34, were produced in a bioreactor with yields of 750 mg/l and 315 mg/l, respectively. These yields are among the highest for recombinant AAOs up to date (Table 4), making these two enzymes potential candidates for industrial use and further highlighting the suitability of *P. pastoris* for the secretory production of AAOs. In the early 1990s, initial attempts to produce AAOs for biochemical characterization resulted in low levels of extracellularly detected activity, which would hardly be sufficient for their use as biocatalysts.[29,33] The emerge of heterologous expression hosts such as *E. coli*, *A. nidulans* and *P. pastoris* coupled with their easy genetic manipulation and the ability to induce gene

expression under optimal conditions upon the addition of an inducer, enabled the heterologous expression of AAOs.[40,41,72] Another benefit associated with heterologous expression using e.g. *E. coli*, *A. nidulans* or *P. pastoris* is the short cultivation time required to obtain sufficient amounts of recombinant enzyme. For *E. coli*, the heterologous intracellular expression can be completed in less than 24 h (overnight preculture, inoculation of main culture and 4-hour incubation from start of the induction), whereas for *A. nidulans* the heterologous extracellular production can take up to 72 h (preculture, washing of mycelia and 48-h incubation from start of the induction).[40,41] Similar durations are required for the production of secreted enzymes using *P. pastoris*: On a small scale, the expression can take up to 72 h (overnight preculture, inoculation of main culture and 48-h incubation), while production in a bioreactor can take up to 9 days.[85]

Table 4 Heterologously expressed fungal aryl-alcohol oxidases and selected variants thereof, their source and host organisms for expression and yield/activity. A brief commentary on the main purpose and introduced changes/mutations is included.

Enzyme	Variant	Commentary	Source organism	Host organism	Yield/Activity	Ref.
*Pe*AAO	Wild-type	Native signal peptide	*Pleurotus eryngii* ATCC 90787	*Aspergillus nidulans biA1, metG1, argB2*	400-500 U/l [a]	40
	Wild-type	Without signal peptide, intracellular production	*Pleurotus eryngii* ATCC 90787	*Escherichia coli* W3110	45 mg/l [b]	41
	FX7	Optimized chimeric signal peptide; H91N mutation	*Pleurotus eryngii* ATCC 90787	*Saccharomyces cerevisiae* BJ5465	2 mg/l	44
	FX9	Optimized chimeric signal peptide; based on FX7 variant, H91N/L170M mutations	*Pleurotus eryngii* ATCC 90787	*Saccharomyces cerevisiae* BJ5465	4,5 mg/l	45
	FX9	Optimized chimeric signal peptide; based on FX7 variant, H91N/L170M mutations	*Pleurotus eryngii* ATCC 90787	*Pichia pastoris* X-33	25,5 mg/l / 1378 U/l [c]	45

	LanDo	Enabled oxidation of secondary alcohols; based on FX9 variant, A77V/R80C/ V340A/I500M/F501W mutations	*Pleurotus eryngii* ATCC 90787	*Saccharomyces cerevisiae* BJ5465	4,6 mg/l	[54]
	Bantha	Optimized oxidation of 5-HMF; based on FX9 variant, F501W mutation	*Pleurotus eryngii* ATCC 90787	*Saccharomyces cerevisiae* BJ5465	n.d.	[56]
	ER	Native signal peptide, K583E/Q584R mutations; enhanced expression in *P. pastoris*	*Pleurotus eryngii* ATCC 90787	*Pichia pastoris* X-33	116 mg/l	[86] and this work
	NER	Native signal peptide, D361N/K583E/Q584R mutations	*Pleurotus eryngii* ATCC 90787	*Pichia pastoris* X-33	113 mg/l	[86] and this work
	AER	Native signal peptide, V367A/K583E/Q584R mutations	*Pleurotus eryngii* ATCC 90787	*Pichia pastoris* X-33	98 mg/l	[86] and this work
*Pe*AAO2	Wild-type	Native signal peptide	*Pleurotus eryngii* P34	*Pichia pastoris* X-33	315 mg/l	[85] and this work
*Um*AAO	Wild-type	α-factor signal peptide	*Ustilago maydis* BRFM 1093	*Pichia pastoris* X-33	1000 mg/l	[72]
*Ma*AAO	Wild-type	Native signal peptide	*Moesziomyces antarcticus* JCM 10317	*Pichia pastoris* X-33	750 mg/l	[84] and this work
r*Cc*AAO	Wild-type	Native signal peptide	*Coprinopsis cinerea* #326	*Pichia pastoris* KM71H	n.m.	[87]

[a] Activity towards veratryl alcohol as substrate.

[b] Yield after purification from inclusion bodies.

[c] Activity towards *p*-anisyl alcohol as substrate was measured with a coupled assay consisting of horseradish peroxidase (HRP) and 2,2′-azino-bis(3-ethylbenzothiazoline-6-sulphonic acid (ABTS).

n.m. = not measured

As can be seen, the reported recombinant AAOs (Table 4) were predominantly expressed in eukaryotic hosts, which have two distinct advantages over most prokaryotic hosts such as *E. coli*: the possibility of extracellular expression via secretion and the introduction of post-translational modifications such as disulfide bond formation and *N*- and *O*-glycosylation. In nature, AAOs are secreted from the mycelium of their native fungal hosts to participate in lignin degradation in conjunction with a consortium of other oxidative enzymes, and therefore the heterologous expression using the *P. pastoris* secretory pathway seems obvious, as fungal *aao*-genes already contain signal sequences for secretion. The secretion of the target enzyme also allows rapid and easy detection of activity by agar plate based assays[88] or liquid assays with cell-free supernatant, and usually facilitates the purification process by avoiding contamination with intracellular protein. In addition, the introduction of (over)glycosylation may lead to higher product stability and sometimes glycosylations are required for correct folding or biological function, especially of therapeutic proteins.[89] In summary, the yeast *P. pastoris* is a suitable expression host for secreted fungal AAOs, but the feasibility of expression for each *aao* gene needs to be investigated on a case-by-case basis. For example, *Pe*AAO1 from *P. eryngii* ATCC 90787[86] is not expressible in *P. pastoris*, whereas the closely related *Pe*AAO2 from another *P. eryngii* strain was shown to be well expressible in this work, and therefore other sequence-based differences may influence the success of heterologous expression.

During the biochemical characterization of *Ma*AAO and *Pe*AAO2, their substrate scopes were thoroughly investigated in the hope of exploring new potential applications of AAOs. A substrate library was constructed from known AAO substrates and complemented with structurally related compounds, and revealed piperonyl alcohol, cumic alcohol and 2-thiophenemethanol were well accepted by *Pe*AAO2.[84,85] The extension of the known substrate

scope was greatly aided by a simple and comparable activity assay for all compounds. For *Pe*AAO2, a colorimetric coupled assay based on the oxidation of ABTS was used and the added AAO substrates were the only components that varied in each measurement, resulting in comparable setups for all substrates tested. This alleviated the comparison of the substrates among each other. In this context, chapter V of this thesis dealt with the establishment of an agar plate based activity assay to easily visualize AAO activity without the need for laborious and time consuming liquid culture cultivation. The agar plate based assay utilizes the same coupled assay based on the oxidation of ABTS and therefore leads to color formation in the vicinity of *P. pastoris* transformants secreting active AAO. The rapidly detected and easily visualized activity helps to identify AAO enzyme variants generated by mutagenesis (rational design or directed evolution) with altered/improved activity towards a specific substrate. This type of assay has not been previously reported for *P. pastoris* and the expression of AAOs. It would also be plausible to extend the application of this assay to screen for activity towards new substrates such as aldehydes or secondary alcohols. Furthermore, this plate based assay is transferable to other expression systems that secrete active AAOs or other H_2O_2-producing enzymes, extending the significance of this new assay.

Chapter IV of this thesis dealt with the high amino acid similarity between well-expressed *Pe*AAO2 from *P. eryngii* P34 and the closely related but non-expressible *Pe*AAO1 from *P. eryngii* ATCC 90787.[86] Both enzymes differ in only seven amino acid positions, but heterologous expression of *Pe*AAO1 in *P. pastoris* was not observed. Several *Pe*AAO1 variants were created based on the amino acid sequence of *Pe*AAO2 to evaluate which amino acid enables the heterologous expression of *Pe*AAO2 in *P. pastoris*.[86] The two mutations introduced K583E/Q584R (*Pe*AAO1 variant ER), appear to have a positive synergistic effect on the expression of this variant and are located on the surface of the enzyme in a C-terminal α-helix,

and yielded similar high extracellular activity as *Pe*AAO2. Analysis of homology models indicated that a new complex salt bridge can form in the *Pe*AAO1 variant ER, as a new negative charge is introduced with Glu583, connecting different parts of the enzyme, which may contribute to improved protein folding and stability. However, it is important to note that these mutations were selected by comparing two closely related AAOs from two *P. eryngii* strains, and this approach is not necessarily feasible for AAOs without closely related and characterized enzymes, as the rational basis for successful expression in a given microbial host is unknown. Nevertheless, these results show that even minor changes with single introduced mutations can have large impact on the expression of recombinant enzymes. Several strategies can be used to optimize the expression of initially non-expressible enzymes: the use of codon-optimized genes, variation of signal peptides, choice of expression plasmids and promoters, introduction of purification tags, introduction/deletion of glycosylation sites, or evolutionary protein engineering approaches. However, these individual aspects have to be examined for the expression optimization of each new enzyme, and predicting the positive outcome is difficult.

The final chapter dealt with demonstrating the applicability of *Pe*AAO2 for the production of valuable fine chemicals. The obtained expression yield of 315 mg/l of *Pe*AAO2[85] using *P. pastoris* was among the highest of recombinant AAOs described to date (Table 4), paving the way for its use in industrial settings, which needs to be explored step by step, starting with small-scale bioconversion studies. Piperonal is a valuable flavor and fragrance compound with prospects as a building block for various pharmaceutical and agrochemical products and can be produced via oxidation of piperonyl alcohol using *Pe*AAO2.[85,90-95] The conversion was optimized on a small scale and was then scaled up to a space-time yield of 9.5 g piperonal/l/h at the 300-mg scale. To demonstrate that the optimized conversion conditions could be transferred to other substrates as well, the aldehyde and strong fruity fragrance *trans*-2-*cis*-6-

nonadienal was produced with 87 % conversion from 100 mM alcohol substrate under the same small scale conditions, highlighting the high potential of this AAO as biocatalyst for the synthesis of fragrance compounds.[96] In general, the activity of *Pe*AAO2 towards substrates of interest shows potential for industrial application settings and would enable the biocatalytic production of a range of valuable aldehydes. The optimization carried out for piperonal production is also applicable to optimizing the conversion of other substrates as well, where the strong dependence on oxygen availability can be assumed for all AAO-catalyzed reactions. The excellent transition from small scale to milligram scale, as demonstrated for piperonal production, renders upscaling to the gram range as highly feasible. In this context, a controlled and optimized O_2 supply on reactor scale could further increase the enzymatic productivity. Immobilization experiments are worth investigating to further improve the applicability of *Pe*AAO2, although the enzyme has been shown to be quite pH- and thermostable, as well as tolerant to organic solvents and H_2O_2[85,96]. This approach could lead to the reusability of AAO as a biocatalyst, as the immobilized AAO could be easily removed from reaction mixtures and reused. Furthermore, the establishment of reaction cascades with H_2O_2-dependent enzymes such as peroxidases and peroxygenases could increase the significance of AAO as biocatalyst.

In conclusion, the methylotrophic yeast *P. pastoris* is a well suited heterologous expression system for the production of fungal secreted AAOs and yields in the hundreds of milligrams range are achievable, thereby expanding the toolbox of recombinant AAOs for biotechnological applications. However, even minor sequence-based differences do play a role and can reduce the expression level accordingly. The prospects for the biotechnological application of AAOs are promising, as these enzymes have a broad substrate scope, high activities and stabilities, and initial efforts for optimizing conversion have been promising and further broaden the range of possible applications. Moreover, AAOs do not require expensive

cofactors, but only require sufficient amounts of O_2 and release H_2O_2 as by-product, which can be easily converted and re-introduced as O_2 by the action of catalase, generating a quasi-self-sufficient system.

VII. Bibliography

1 Worldometers.info. *World Population*, <https://www.worldometers.info/world-population/> (2022).

2 Sheldon, R. A. Atom utilisation, E factors and the catalytic solution. *Comptes Rendus de l'Académie des Sciences - Series IIC - Chemistry* **3**, 541-551, doi:10.1016/S1387-1609(00)01174-9 (2000).

3 Sheldon, R. A. & Woodley, J. M. Role of biocatalysis in sustainable chemistry. *Chem. Rev.* **118**, 801-838, doi:10.1021/acs.chemrev.7b00203 (2018).

4 Anastas, P. & Eghbali, N. Green Chemistry: Principles and Practice. *Chem. Soc. Rev.* **39**, 301-312, doi:10.1039/b918763b (2010).

5 Sheldon, R. A. & Brady, D. The limits to biocatalysis: pushing the envelope. *Chem. Commun.* **54**, 6088-6104, doi:10.1039/c8cc02463d (2018).

6 Liu, L. *et al.* How to achieve high-level expression of microbial enzymes: strategies and perspectives. *Bioengineered* **4**, 212-223, doi:10.4161/bioe.24761 (2013).

7 Dong, J. J. *et al.* Biocatalytic Oxidation Reactions: A Chemist's Perspective. *Angew. Chem. Int. Ed.* **57**, 9238-9261, doi:10.1002/anie.201800343 (2018).

8 Sheldon, R. A., Brady, D. & Bode, M. L. The Hitchhiker's guide to biocatalysis: recent advances in the use of enzymes in organic synthesis. *Chem. Sci.* **11**, 2587-2605, doi:10.1039/c9sc05746c (2020).

9 Damasceno, L. M., Huang, C. J. & Batt, C. A. Protein secretion in *Pichia pastoris* and advances in protein production. *Appl. Microbiol. Biotechnol.* **93**, 31-39, doi:10.1007/s00253-011-3654-z (2012).

10 *Protein Engineering. Methods and Protocols*. (Humana Press, 2018).

11 Bottcher, D. & Bornscheuer, U. T. Protein engineering of microbial enzymes. *Curr. Opin. Microbiol.* **13**, 274-282, doi:10.1016/j.mib.2010.01.010 (2010).

12 Porter, J. L., Rusli, R. A. & Ollis, D. L. Directed Evolution of Enzymes for Industrial Biocatalysis. *ChemBioChem* **17**, 197-203, doi:10.1002/cbic.201500280 (2016).

13 Savile, C. K. *et al.* Biocatalytic asymmetric synthesis of chiral amines from ketones applied to sitagliptin manufacture. *Science* **329**, 305-309, doi:10.1126/science.1188934 (2010).

14 nobelprize.org. *The Nobel Prize in Chemistry 2018* <https://www.nobelprize.org/prizes/chemistry/2018/arnold/facts/> (2018).

15 Woodley, J. M. Accelerating the implementation of biocatalysis in industry. *Appl. Microbiol. Biotechnol.* **103**, 4733-4739, doi:10.1007/s00253-019-09796-x (2019).

16 Schutyser, W. *et al.* Chemicals from lignin: an interplay of lignocellulose fractionation, depolymerisation, and upgrading. *Chem. Soc. Rev.* **47**, 852-908, doi:10.1039/C7CS00566K (2018).

17 Janusz, G. *et al.* Lignin degradation: microorganisms, enzymes involved, genomes analysis and evolution. *FEMS Microbiol Rev* **41**, 941-962, doi:10.1093/femsre/fux049 (2017).

18 Streffer, F. Lignocellulose to Biogas and other Products. *JSM Biotechnology & Biomedical Engineering* **2**, 1-8 (2014).

19 Pollegioni, L., Tonin, F. & Rosini, E. Lignin-degrading enzymes. *FEBS J.* **282**, 1190-1213, doi:10.1111/febs.13224 (2015).

20 Bertella, S. & Luterbacher, J. S. Lignin Functionalization for the Production of Novel Materials. *Trends in Chemistry* **2**, 440-453, doi:10.1016/j.trechm.2020.03.001 (2020).

21 Weng, C., Peng, X. & Han, Y. Depolymerization and conversion of lignin to value-added bioproducts by microbial and enzymatic catalysis. *Biotechnol. Biofuels* **14**, 84, doi:10.1186/s13068-021-01934-w (2021).

22 Urlacher, V. B. & Koschorreck, K. Pecularities and applications of aryl-alcohol oxidases from fungi. *Appl. Microbiol. Biotechnol.* **105**, 4111-4126, doi:10.1007/s00253-021-11337-4 (2021).

23 Singhvi, M. & Kim, B. S. Lignin valorization using biological approach. *Biotechnol. Appl. Biochem.* **68**, 459-468, doi:10.1002/bab.1995 (2021).

24 Lopes, A. M. M., Martins, M. & Goldbeck, R. Heterologous Expression of Lignocellulose-Modifying Enzymes in Microorganisms: Current Status. *Mol. Biotechnol.* **63**, 184-199, doi:10.1007/s12033-020-00288-2 (2021).

25 *Biorefineries*. Vol. 166 (Springer, 2019).

26 Silva, J. P., Ticona, A. R. P., Hamann, P. R. V., Quirino, B. F. & Noronha, E. F. Deconstruction of Lignin: From Enzymes to Microorganisms. *Molecules* **26**, doi:10.3390/molecules26082299 (2021).

27 Sharma, R. K., Mukhopadhyay, D. & Gupta, P. Microbial fuel cell-mediated lignin depolymerization: a sustainable approach. *J. Chem. Technol. Biotechnol.* **94**, 927-932, doi:10.1002/jctb.5841 (2019).

28 Kohlstedt, M. *et al.* From lignin to nylon: Cascaded chemical and biochemical conversion using metabolically engineered *Pseudomonas putida*. *Metab. Eng.* **47**, 279-293, doi:10.1016/j.ymben.2018.03.003 (2018).

29 Guillén, F., Martínez, Á. T. & Martínez, M. J. Substrate specificity and properties of the aryl-alcohol oxidase from the ligninolytic fungus *Pleurotus eryngii*. *Eur. J. Biochem.* **209**, 603-611, doi:10.1111/j.1432-1033.1992.tb17326.x (1992).

30 Henderson, M. E. K. Release of Aromatic Compounds from Birch and Spruce Sawdusts during Decomposition by White-Rot Fungi. *Nature* **175**, 634-635, doi:DOI 10.1038/175634b0 (1955).

31 Farmer, V. C., Henderson, M. E. & Russell, J. D. Aromatic-alcohol-oxidase activity in the growth medium of *Polystictus versicolor. Biochem. J.* **74**, 257-262, doi:10.1042/bj0740257 (1960).

32 Sannia, G. *et al.* Purification and characterization of a veratryl alcohol oxidase enzyme from the lignin degrading basidiomycete *Pleurotus ostreatus*. *Biochimica et Biophysica Acta* **1073**, 114-119, doi:10.1016/0304-4165(91)90190-R (1991).

33 Guillén, F., Martínez, A. T. & Martínez, M. J. Production of hydrogen peroxide by aryl-alcohol oxidase from the ligninolytic fungus *Pleurotus eryngii*. *Appl. Microbiol. Biotechnol.* **32**, 465-469, doi:10.1007/BF00903784 (1990).

34 Bourbonnais, R. & Paice, M. G. Veratryl alcohol oxidases from the lignin-degrading basidiomycete *Pleurotus sajor-caju*. *Biochem. J.* **255**, 445-450, doi:10.1042/bj2550445 (1988).

35 Muheim, A., Waldner, R., Leisola, M. S. A. & Fiechter, A. An extracellular aryl-alcohol oxidase from the white-rot fungus *Bjerkandera adusta*. *Enzyme and Microbial Technology* **12**, 204-209, doi:10.1016/0141-0229(90)90039-S (1990).

36 Kimura, Y., Asada, Y. & Kuwahara, M. Screening of Basidiomycetes for Lignin Peroxidase Genes Using a DNA Probe. *Appl. Microbiol. Biotechnol.* **32**, 436-442, doi:Doi 10.1007/Bf00903779 (1990).

37 Muheim, A., Leisola, M. S. A. & Schoemaker, H. E. Aryl-alcohol oxidase and lignin peroxidase from white-rot fungus *Bjerkandera adusta*. *J. Biotechnol.* **13**, 159-167, doi:10.1016/0141-0229(90)90039-S (1990).

38 Varela, E., Martínez, A. T. & Martínez, M. J. Molecular cloning of aryl-alcohol oxidase from the fungus *Pleurotus eryngii*, an enzyme involved in lignin degradation. *Biochem. J.* **341**, 113, doi:10.1042/0264-6021:3410113 (1999).

39 Varela, E., Martínez, M. J. & Martínez, A. T. Aryl-alcohol oxidase protein sequence: A comparison with glucose oxidase and other FAD oxidoreductases. *Biochim. Biophys. Acta* **1481**, 202-208, doi:10.1016/S0167-4838(00)00127-8 (2000).

40 Varela, E., Guillén, F., Martínez, Á. T. & Martínez, M. J. Expression of *Pleurotus eryngii* aryl-alcohol oxidase in *Aspergillus nidulans*: Purification and characterization of the recombinant enzyme. *Biochim. Biophys. Acta* **1546**, 107-113, doi:10.1016/S0167-4838(00)00301-0 (2001).

41 Ruiz-Dueñas, F. J., Ferreira, P., Martínez, M. J. & Martínez, A. T. In vitro activation, purification, and characterization of *Escherichia coli* expressed aryl-alcohol oxidase, a unique H_2O_2-producing enzyme. *Protein Expr. Purif.* **45**, 191-199, doi:10.1016/j.pep.2005.06.003 (2006).

42 Fernández, I. S. *et al.* Novel structural features in the GMC family of oxidoreductases revealed by the crystal structure of fungal aryl-alcohol oxidase. *Acta Crystallogr. Sect. D. Biol. Crystallogr.* **65**, 1196-1205, doi:10.1107/S0907444909035860 (2009).

43 Ferreira, P., Hernández-Ortega, A., Herguedas, B., Martínez, Á. T. & Medina, M. Aryl-alcohol oxidase involved in lignin degradation. A mechanistic study based on steady and pre-steady state kinetics and primary and solvent isotope effects with two alcohol substrates. *J. Biol. Chem.* **284**, 24840-24847, doi:10.1074/jbc.M109.011593 (2009).

44 Viña-Gonzalez, J., Gonzalez-Perez, D., Ferreira, P., Martínez, Á. T. & Alcalde, M. Focused directed evolution of aryl-alcohol oxidase in *Saccharomyces cerevisiae* by using chimeric signal peptides. *Appl. Environ. Microbiol.* **81**, 6451-6462, doi:10.1128/AEM.01966-15 (2015).

45 Viña-Gonzalez, J., Elbl, K., Ponte, X., Valero, F. & Alcalde, M. Functional expression of aryl-alcohol oxidase in *Saccharomyces cerevisiae* and *Pichia pastoris* by directed evolution. *Biotechnol. Bioeng.* **115**, 1666-1674, doi:10.1002/bit.26585 (2018).

46 Ferreira, P. *et al.* Kinetic and chemical characterization of aldehyde oxidation by fungal aryl-alcohol oxidase. *Biochem. J.* **425**, 585-593, doi:10.1042/BJ20091499 (2010).

47 Hernández-Ortega, A. *et al.* Role of active site histidines in the two half-reactions of the aryl-alcohol oxidase catalytic cycle. *Biochemistry* **51**, 6595-6608, doi:10.1021/bi300505z (2012).

48 Hernandez-Ortega, A. *et al.* Substrate diffusion and oxidation in GMC oxidoreductases: an experimental and computational study on fungal aryl-alcohol oxidase. *Biochem. J.* **436**, 341-350, doi:10.1042/BJ20102090 (2011).

49 Hernández-Ortega, A. *et al.* Stereoselective hydride transfer by aryl-alcohol oxidase, a member of the GMC superfamily. *ChemBioChem* **13**, 427-435, doi:10.1002/cbic.201100709 (2012).

50 Ferreira, P. *et al.* Aromatic stacking interactions govern catalysis in aryl-alcohol oxidase. *FEBS J.* **282**, 3091-3106, doi:10.1111/febs.13221 (2015).

51 Carro, J., Martínez, M., Medina, M., Martínez, Á. T. & Ferreira, P. Protein dynamics promote hydride tunnelling in substrate oxidation by aryl-alcohol oxidase. *Phys. Chem. Chem. Phys.* **19**, 28666-28675, doi:10.1039/C7CP05904C (2017).

52 Carro, J. *et al.* Multiple implications of an active site phenylalanine in the catalysis of aryl-alcohol oxidase. *Sci. Rep.*, 1-12, doi:10.1038/s41598-018-26445-x (2018).

53 Carro, J., Ferreira, P., Martínez, Á. T. & Gadda, G. Stepwise hydrogen atom and proton transfers in dioxygen reduction by aryl-alcohol oxidase. *Biochemistry* **57**, 1790−1797, doi:10.1021/acs.biochem.8b00106 (2018).

54 Viña-Gonzalez, J. *et al.* Structure-guided evolution of aryl alcohol oxidase from *Pleurotus eryngii* for the selective oxidation of secondary benzyl alcohols. *Adv. Synth. Catal.* **361**, 2514-2525, doi:10.1002/adsc.201900134 (2019).

55 Serrano, A. *et al.* Switching the substrate preference of fungal aryl-alcohol oxidase: towards stereoselective oxidation of secondary benzyl alcohols. *Catal. Sci. Technol.* **9**, 833-841, doi:10.1039/C8CY02447B (2019).

56 Viña-Gonzalez, J., Martinez, A. T., Guallar, V. & Alcalde, M. Sequential oxidation of 5-hydroxymethylfurfural to furan-2,5-dicarboxylic acid by an evolved aryl-alcohol oxidase. *Biochim. Biophys. Acta* **1868**, 140293, doi:10.1016/j.bbapap.2019.140293 (2020).

57 Drula, E. *et al.* The carbohydrate-active enzyme database: functions and literature. *Nucleic Acids Res.* **50**, D571-D577, doi:10.1093/nar/gkab1045 (2022).

58 Levasseur, A., Drula, E., Lombard, V., Coutinho, P. M. & Henrissat, B. Expansion of the enzymatic repertoire of the CAZy database to integrate auxiliary redox enzymes. *Biotechnol. Biofuels* **6**, doi:10.1186/1754-6834-6-41 (2013).

59 Cavener, D. R. GMC oxidoreductases. A newly defined family of homologous proteins with diverse catalytic activities. *J. Mol. Biol.* **223**, 811-814, doi:10.1016/0022-2836(92)90992-S (1992).

60 Sützl, L., Foley, G., Gillam, E. M. J., Bodén, M. & Haltrich, D. The GMC superfamily of oxidoreductases revisited: Analysis and evolution of fungal GMC oxidoreductases. *Biotechnol. Biofuels* **12**, 1-18, doi:10.1186/s13068-019-1457-0 (2019).

61 Serrano, A., Carro, J. & Martínez, Á. T. in *The Enzymes* Vol. 47 *Flavin-Dependent Enzymes: Mechanisms, Structures and Applications* (eds Pimchai Chaiyen & Fuyuhiko Tamanoi) 167-192 (Elsevier, 2020).

62 Ferreira, P., Ruiz-Dueñas, F. J., Martínez, M. J., Van Berkel, W. J. H. & Martínez, A. T. Site-directed mutagenesis of selected residues at the active site of aryl-alcohol oxidase, an H_2O_2-producing ligninolytic enzyme. *FEBS J.* **273**, 4878-4888, doi:10.1111/j.1742-4658.2006.05488.x (2006).

63 Hernandez-Ortega, A. *et al.* Modulating O2 reactivity in a fungal flavoenzyme: involvement of aryl-alcohol oxidase Phe-501 contiguous to catalytic histidine. *J. Biol. Chem.* **286**, 41105-41114, doi:10.1074/jbc.M111.282467 (2011).

64 Ferreira, P. *et al.* Spectral and catalytic properties of aryl-alcohol oxidase, a fungal flavoenzyme acting on polyunsaturated alcohols. *Biochem. J.* **389**, 731-738, doi:10.1042/BJ20041903 (2005).

65 Wu, S., Snajdrova, R., Moore, J. C., Baldenius, K. & Bornscheuer, U. T. Biocatalysis: Enzymatic Synthesis for Industrial Applications. *Angew Chem Int Ed Engl* **60**, 88-119, doi:10.1002/anie.202006648 (2021).

66 Cheetham, P. S. J. in *Biotechnology of Aroma Compounds* Vol. 55 *Advances in Biochemical Engineering/Biotechnology* (eds R. G. Berger *et al.*) 1-49 (Springer, 1997).

67 van Schie, M. M. C. H. *et al.* Biocatalytic synthesis of the green note *trans*-2-hexenal in a continuous-flow microreactor. *Beilstein J. Org. Chem.* **14**, 697-703, doi:10.3762/bjoc.14.58 (2018).

68 de Almeida, T. P. *et al.* Efficient aerobic oxidation of *trans*-2-hexen-1-ol using the aryl alcohol oxidase from *Pleurotus eryngii*. *Adv. Synth. Catal.* **361**, 2668-2672, doi:10.1002/adsc.201801312 (2019).

69 Serrano, A. *et al.* Complete oxidation of hydroxymethylfurfural to furandicarboxylic acid by aryl-alcohol oxidase. *Biotechnol. Biofuels* **12**, 217, doi:10.1186/s13068-019-1555-z (2019).

70 de Jong, E., Visser, H. R. A., Dias, A. S., Harvey, C. & Gruter, G. M. The Road to Bring FDCA and PEF to the Market. *Polymers (Basel)* **14**, doi:10.3390/polym14050943 (2022).

71 Carro, J. *et al.* 5-Hydroxymethylfurfural conversion by fungal aryl-alcohol oxidase and unspecific peroxygenase. *FEBS J.* **282**, 3218-3229, doi:10.1111/febs.13177 (2014).

72 Couturier, M. *et al.* Characterization of a new aryl-alcohol oxidase secreted by the phytopathogenic fungus *Ustilago maydis*. *Appl. Microbiol. Biotechnol.* **100**, 697-706, doi:10.1007/s00253-015-7021-3 (2016).

73 Varela, E., Böckle, B., Romero, A., Martínez, A. T. & Martínez, M. J. Biochemical characterization, cDNA cloning and protein crystallization of aryl-alcohol oxidase from *Pleurotus pulmonarius*. *Biochim. Biophys. Acta* **1476**, 129-138, doi:10.1016/S0167-4838(99)00227-7 (2000).

74 Grote, A. *et al.* JCat: A novel tool to adapt codon usage of a target gene to its potential expression host. *Nucleic Acids Res.* **33**, 526-531, doi:10.1093/nar/gki376 (2005).

75 Laemmli, U. K. Cleavage of structural proteins during assembly of head of bacteriophage-T4. *Nature* **227**, 680-685, doi:10.1038/227680a0 (1970).

76 Guillén, F., Martínez, A. T., Martínez, M. J. & Evans, C. S. Hydrogen-peroxide-producing system of *Pleurotus eryngii* involving the extracellular enzyme aryl-alcohol oxidase. *Appl. Microbiol. Biotechnol.* **41**, 465-470, doi:10.1007/BF00939037 (1994).

77 Bronikowski, A., Koschorreck, K. & Urlacher, V. B. Redesign of a new manganese peroxidase highly expressed in *Pichia pastoris* towards a lignin-degrading versatile peroxidase. *ChemBioChem*, doi:10.1002/cbic.201800500 (2018).

78 Bronikowski, A., Hagedoorn, P. L., Koschorreck, K. & Urlacher, V. B. Expression of a new laccase from *Moniliophthora roreri* at high levels in *Pichia pastoris* and its potential application in micropollutant degradation. *AMB Express* **7**, doi:10.1186/s13568-017-0368-3 (2017).

79 Kukuruzinska, M. A., Bergh, M. L. E. & Jackson, B. J. Protein glycosylation in yeast. *Annu. Rev. Biochem.* **56**, 915-944, doi:10.1146/annurev.bi.56.070187.004411 (1987).

80 Teufel, F. *et al.* SignalP 6.0 predicts all five types of signal peptides using protein language models. *Nat. Biotechnol.* **40**, 1023-1025, doi:10.1038/s41587-021-01156-3 (2022).

81 Gasteiger, E. *et al.* in *The Proteomics Protocols Handbook Springer Protocols Handbooks* (ed John M. Walker) 571-607 (Humana Press, 2005).

82 Gupta, R. & Brunak, S. Prediction of glycosylation across the human proteome and the correlation to protein function. *Pac. Symp. Biocomput.*, 310-322, doi:10.1142/9789812799623_0029 (2002).

83 Madeira, F. *et al.* Search and sequence analysis tools services from EMBL-EBI in 2022. *Nucleic Acids Res.*, doi:10.1093/nar/gkac240 (2022).

84 Lappe, A., Jankowski, N., Albrecht, A. & Koschorreck, K. Characterization of a thermotolerant aryl-alcohol oxidase from *Moesziomyces antarcticus* oxidizing 5-hydroxymethyl-2-furancarboxylic acid. *Appl. Microbiol. Biotechnol.* **105**, 8313-8327, doi:10.1007/s00253-021-11557-8 (2021).

85 Jankowski, N., Koschorreck, K. & Urlacher, V. B. High-level expression of aryl-alcohol oxidase 2 from *Pleurotus eryngii* in *Pichia pastoris* for production of fragrances and bioactive precursors. *Appl. Microbiol. Biotechnol.* **104**, 9205-9218, doi:10.1007/s00253-020-10878-4 (2020).

86 Jankowski, N., Urlacher, V. B. & Koschorreck, K. Two adjacent C-terminal mutations enable expression of aryl-alcohol oxidase from *Pleurotus eryngii* in *Pichia pastoris*. *Appl. Microbiol. Biotechnol.* **105**, 7743-7755, doi:10.1007/s00253-021-11585-4 (2021).

87 Tamaru, Y., Umezawa, K. & Yoshida, M. Characterization of an aryl-alcohol oxidase from the plant saprophytic basidiomycete *Coprinopsis cinerea* with broad substrate specificity against aromatic alcohols. *Biotechnol. Lett.* **40**, 1077-1086, doi:10.1007/s10529-018-2534-3 (2018).

88 Jankowski, N. & Koschorreck, K. Agar plate assay for rapid screening of aryl-alcohol oxidase mutant libraries in *Pichia pastoris*. *J. Biotechnol.* **346**, 47-51, doi:10.1016/j.jbiotec.2022.01.006 (2022).

89 Cereghino, G. P., Cereghino, J. L., Ilgen, C. & Cregg, J. M. Production of recombinant proteins in fermenter cultures of the yeast *Pichia pastoris*. *Curr. Opin. Biotechnol.* **13**, 329-332, doi:10.1016/s0958-1669(02)00330-0 (2002).

90 Santos, A. S., Pereira, N., Da Silva, I. M., Sarquis, M. I. M. & Antunes, O. A. C. Peroxidase catalyzed microbiological oxidation of isosafrol into piperonal. *Process Biochem.* **39**, 2269-2275, doi:10.1016/j.procbio.2003.11.019 (2004).

91 Santos, A. S., Pereira, N., Da Silva, I. M., Sarquis, M. I. M. & Antunes, O. A. C. Microbiologic oxidation of isosafrole into piperonal. *Appl. Biochem. Biotechnol.* **105-108**, 649-657, doi:10.1385/abab:107:1-3:649 (2003).

92 Bellardita, M. *et al.* Photocatalytic green synthesis of piperonal in aqueous TiO2 suspension. *Appl. Catal. B* **144**, 607-613, doi:10.1016/j.apcatb.2013.07.070 (2014).

93 Brum, J. d. O. C. *et al.* Synthesis of new quinoline-piperonal hybrids as potential drugs against Alzheimer's disease. *Int. J. Mol. Sci.* **20**, 3944, doi:10.3390/ijms20163944 (2019).

94 Wang, S., Bao, L., Song, D., Wang, J. & Cao, X. Heterocyclic lactam derivatives containing piperonyl moiety as potential antifungal agents. *Bioorg. Med. Chem. Lett.* **29**, 126661, doi:10.1016/j.bmcl.2019.126661 (2019).

95 Akash, J., Dushyant, C. & Jasmine, C. Piperonal: The Journey so Far. *Mini-Rev. Med. Chem.* **20**, 1846-1856, doi:10.2174/1389557520666200711173149 (2020).

96 Jankowski, N., Koschorreck, K. & Urlacher, V. Aryl-alcohol-Oxidase-Mediated Synthesis of Piperonal and Other Valuable Aldehydes. *Adv. Synth. Catal.* **364**, 2364–2372, doi:10.1002/adsc.202200381 (2022).

VIII. Danksagung

An dieser Stelle möchte ich mich bei all denjenigen bedanken, ohne die die Anfertigung dieser Dissertation nicht möglich gewesen wäre.

Mein besonderer Dank gilt Prof. Dr. Vlada B. Urlacher für die Überlassung des interessanten Promotionsthemas, die fortwährende Betreuung und Unterstützung während meiner Promotion, sowie die Übernahme der ersten Begutachtung meiner Arbeit.

Apl. Prof. Martina Pohl danke ich für die freundliche Übernahme des Zweitgutachtens.

Ein großes Dankeschön gilt allen Mitarbeitern und Doktoranden des Instituts für Biochemie II, die sich zeitgleich den Weg zur Promotion mit mir geteilt haben und gemeinsam eine tolle und motivierende Arbeitsatmosphäre geschaffen haben: Thomas Hilberath, Ansgar Bokel, Davide Decembrino, Anna Olbrich, Arsenij Kokorin, Nikolas Ditz, Alessandra Raffaele, Stefan Wohlgemuth und Sebastian Hölzel. Besonders freut es mich, dass aus vielen von euch in den letzten Jahren gute Freunde mit vielen gemeinsamen Erlebnissen geworden sind und unsere gemeinsame Zeit auch weit abseits der Promotion noch lange nicht zu Ende ist.

Ein besonderer Dank gilt Agathe Bronikowski; zunächst als Praktikumsbetreuerin im Mastermodul, dann als Betreuerin meiner Masterarbeit am Institut für Biochemie II, und schließlich als sehr liebe Kollegin und Freundin. Vielen Dank für deine herzliche und immer muntere Art. Ebenso möchte ich mich bei Katja Koschorreck als sehr einfühlsame Kollegin bedanken, für die bekräftigende Unterstützung und dein immer offenes Ohr, besonders in den Zeiten, in denen das Projekt nicht immer rund lief.

Darüber hinaus möchte ich mich ganz besonders bei Fabian Schmitz bedanken, der mich nicht nur während der Promotion als Kollege, sondern auch als Partner in bereits vielen Lebenslagen unterstützt, motiviert und wieder aufgebaut hat, und immer für mich da gewesen ist. Es ist schön, dich in meinem Leben zu haben.

Ich möchte mich auch bei meinen lieben Freunden bedanken, die in all den Jahren meiner Promotion auf unterschiedlichste Art und Weise dazu beigetragen haben, dass ich viel Abwechslung abseits des Arbeitsalltags hatte und mir sehr dabei geholfen haben, den Kopf von

manchen Dingen frei zu bekommen und neue Kraft zu tanken. Es sind zu viele, um sie alle namentlich zu erwähnen, also fühlt euch alle gedrückt, ich habe euch lieb!

Ebenfalls möchte ich Dr. Michael Piontek und Dr. Melanie Piontek als meine Arbeitgeber danken, da sie es mir ermöglicht haben, neben der Aufnahme meiner Arbeit bei Artes Biotechnology auch weiterhin zeitlich flexibel an meiner Dissertation zu arbeiten. Vielen Dank für eure Geduld und Unterstützung.

Zuletzt und von ganzem Herzen möchte ich mich bei meiner Familie bedanken. Ohne euch und eure grenzenlose und liebevolle Unterstützung während meines gesamten Studiums wäre diese Arbeit nicht möglich gewesen. Vielen Dank für alles. Ich habe euch lieb!